



National Library
of Canada

Bibliothèque nationale
du Canada

Canadian Service Service des thèses canadiennes

Ottawa, Can
K1A 0N4

NOTICE

The quality of this microform is heavily dependent upon the quality of the original thesis submitted for microfilming. Every effort has been made to ensure the highest quality of reproduction possible.

If pages are missing, contact the university which granted the degree.

Some pages may have indistinct print especially if the original pages were typed with a poor typewriter ribbon or if the university sent us an inferior photocopy.

Previously copyrighted materials (journal articles, published tests, etc.) are not filmed.

Reproduction in full or in part of this microform is governed by the Canadian Copyright Act, R.S.C. 1970, c. C-30.

AVIS

La qualité de cette microforme dépend grandement de la qualité de la thèse soumise au microfilmage. Nous avons tout fait pour assurer une qualité supérieure de reproduction.

S'il manque des pages, veuillez communiquer avec l'université qui a conféré le grade.

La qualité d'impression de certaines pages peut laisser à désirer, surtout si les pages originales ont été dactylographiées à l'aide d'un ruban usé ou si l'université nous a fait parvenir une photocopie de qualité inférieure.

Les documents qui font déjà l'objet d'un droit d'auteur (articles de revue, tests publiés, etc.) ne sont pas microfilmés.

La reproduction, même partielle, de cette microforme est soumise à la Loi canadienne sur le droit d'auteur, SRC 1970, c. C-30.

THE UNIVERSITY OF ALBERTA

A THEORY OF

MOLECULAR-STATE-CLOSE-COUPLING

INCLUDING THE CONTINUUM

by

GUNADYA BANDARAGE

A THESIS SUBMITTED

TO THE FACULTY OF GRADUATE STUDIES AND RESEARCH

IN PARTIAL FULFILMENT OF THE REQUIREMENTS

FOR THE DEGREE OF DOCTOR OF PHILOSOPHY

DEPARTMENT OF CHEMISTRY

EDMONTON, ALBERTA

FALL 1987

Permission has been granted to the National Library of Canada to microfilm this thesis and to lend or sell copies of the film.

The author (copyright owner) has reserved other publication rights, and neither the thesis nor extensive extracts from it may be printed or otherwise reproduced without his/her written permission.

L'autorisation a été accordée à la Bibliothèque nationale du Canada de microfilmer cette thèse et de prêter ou de vendre des exemplaires du film.

L'auteur (titulaire du droit d'auteur) se réserve les autres droits de publication; ni la thèse ni de longs extraits de celle-ci ne doivent être imprimés ou autrement reproduits sans son autorisation écrite.

ISBN 0-315-41043-4

THE UNIVERSITY OF ALBERTA

RELEASE FORM

NAME OF AUTHOR Gunadya Bandarage

TITLE OF THESIS A Theory of Molecular-State
..... Close-Coupling Including
..... The Continuum

DEGREE FOR WHICH THESIS WAS PRESENTED Ph.D.

YEAR THIS DEGREE GRANTED 1987

Permission is hereby granted to the UNIVERSITY OF ALBERTA LIBRARY to reproduce single copies of this thesis and to lend or sell such copies for private, scholarly or scientific research purposes only.

The author reserves other publication rights, and neither the thesis nor extensive extracts from it may be printed or otherwise reproduced without the author's written permission.

(Signed) G. Bandarage

Permanent Address:

No. 65, Dibbedda Road,
Nalluruwa, Panadura,
Sri Lanka,

DATED 5/10/87

THE UNIVERSITY OF ALBERTA
FACULTY OF GRADUATE STUDIES AND RESEARCH

The undersigned certify that they have read, and recommend to the Faculty of
Graduate Studies and Research for acceptance, a thesis entitled

"A THEORY OF MOLECULAR-STATE CLOSE-COUPPLING
INCLUDING THE CONTINUUM"

submitted by G. Bandarage in partial fulfilment of the requirements for the degree
of Doctor of Philosophy.

Walter R. Thomas

Supervisor

W. D. ...

Ronald ...

M. J. ...

J. F. Reading

External Examiner

28/8/87

Date

To My Parents

ABSTRACT

A problem in describing impact ionization is properly accounting for the behavior of the electronic continuum; the ionized electrons must be allowed to leave the interaction region. Using the adiabatic basis a set of coupled integral equations relevant for slow atomic collisions in one-electron-two-nucleus systems is derived more formally than their previous derivation, using different assumptions. These equations allow the ionized probability amplitude to escape from the interaction region where it is represented by a set of localized wave packets.

Additional complications of the theory arise from the singular behavior of the nonadiabatic couplings between two continuum states. However, these are well behaved within the packet basis provided the coupling matrix elements have a certain structure. We derive this structure based upon a rigorous extension of the Hellmann-Feynman theorem to two adiabatic continuum states and use the theorem to compute relevant coupling matrix element properties and test assumptions made in the derivation of effective packet state couplings. These effective couplings can be used with the known bound-bound and bound-continuum couplings to solve the close-coupled integral equations.

We construct exact continuum states using the quantal momentum method, specifying radial wave functions in terms of smooth, slowly varying amplitude and phase functions. These can be computed rapidly and stored extremely efficiently, which permits much more rapid and accurate regeneration of wave functions for further calculations. This representation also offers important conceptual advantages.

We construct the wave packets by superposing continuum states with uniform amplitudes over packet widths. We show that packet states are localized

in a manner controlled by the packet widths, and propose a scheme to select them such that the resulting packets are localized within a specified interaction region. The packets (and the true continuum states) are centred at the centre of charge of the nuclei, a point not previously noted in the literature.

Although the numerical work presented in this thesis is done on the specific system H_2^+ , the conceptual and the analytical work is generally valid for any one-electron-two-nucleus collision system at low energies.

ACKNOWLEDGEMENT

I would like to thank my supervisor, Professor Walter R. Thorson, for his continuous guidance and encouragement. This work would not have been possible without his help.

I would like to thank the Killam Scholarship Committee at the University of Alberta for three years of financial support and the University of Alberta for granting me a Dissertation Fellowship.

Thanks are also due to my friends Balthz, Epa, Karen, Maria, Pancrasio and Shah of the theoretical-chemistry division for making a pleasant working environment.

TABLE OF CONTENTS

Chapter	Page
1. INTRODUCTION	1
1.1 An overview	1
1.2 Objectives of this work	4
1.3 Basic Theoretical Background	6
1.3.1 Context of this work	6
1.3.2 Classical Trajectory Formulation	6
1.3.3 "Slow" and "Fast" Collisions and basis states	12
1.4 Molecular States expansions and their Characteristics	17
1.4.1 Synopsis	17
1.4.2 The PSS formulation	17
1.4.3 Defects of PSS theory and ETF corrections	18
1.5 Problem of Including the Electronic Continuum	20
1.5.1 Synopsis	20
1.5.2 Space-Time discretization techniques	21
1.5.3 Explicit techniques	23
1.5.4 L^2 -discretization techniques	23
2. THEORY	30
2.1 Introduction	30
2.2 Physical Assumpt	33
2.3 Basis set assumpt	35
2.4 Derivation	35
2.5 The Disconnected form	37
2.6 The Decay in the Connected form	38
2.7 Discussion	48

3. ONE-ELECTRON-TWO-CENTRE CONTINUUM STATES	55
3.1 Introduction	55
3.1.1 Bound States	57
3.1.2 Continuum States	57
3.1.3 Phase-Amplitude form	58
3.2 Continuum Radial wave functions in phase-amplitude form	59
3.2.1 The General Solution of equation (3 - 4)	59
3.2.2 A General Solution to Milne's equation	61
3.2.3 Behavior of P_R , P_I and Θ near $\xi = 1$	62
3.2.4 The Physical solution	65
3.2.5 Summary of the Physical solution	65
3.2.6 The Phase Shift	65
3.2.7 Numerical Method	67
3.2.8 Numerical Details	68
3.2.9 Global representation of $\chi(\xi)$	69
3.3 Results	69
3.4 Discussion	76
4. ADIABATIC WAVE PACKETS	92
4.1 Introduction	92
4.2 Definition of Packets	92
4.3 An Approximate analytical form	92
4.4 A Unique Choice of Packet Widths	95
4.5 Calculation of $\Delta(lm; R; b_b; \epsilon)$	95
4.5.1 Theory	95
4.5.2 Numerical Method	99
4.5.3 Numerical Details	100

4.5.4 Results	101
4.6 Calculation of ϵ_j and Δ_j	101
4.7 Choice of b_j and the Energy Sampling	101
4.8 Explicit Construction of Wave Packets	108
4.9 Discussion	108
5. FORMAL PROPERTIES OF CONTINUUM	
NONADIABATIC COUPLINGS	118
5.1 Introduction	118
5.2 Radial and Angular Couplings	120
5.3 Translational Invariance and Translational Factor Corrections	123
5.4 Hellmann-Feynman Theorem	127
5.5 Extension of the Hellmann-Feynman Theorem to Continuum States	129
5.6 Properties of the Fundamental Integral	131
5.6.1 Summary of the Strength of singularities	134
5.7 Angular Coupling Matrix Elements	134
5.7.1 Summary of Continuum state angular couplings	138
5.8 Radial Coupling Matrix Elements	138
5.9 Discussion	139
6. EVALUATION OF NONADIABATIC COUPLING MATRIX	
ELEMENTS BETWEEN CONTINUUM STATES	140
6.1 Introduction	140
6.2 Evaluation of $\langle k'; R (\hat{L} + V) k; R \rangle$	141
6.2.1 Derivation of general expressions	141
6.2.2 Behavior of the integrand in equation (6 - 4) near $\xi = 1$	142
6.2.3 An Upper-bound to $ A_n^\pm(\xi_\infty, \infty) $	144
6.3 Generation of Gauss Hypergeometric Function	145

6.4	Evaluation of $\langle k'; R (\partial V / \partial R)_{\vec{r}} k; R \rangle$	146
6.5	Numerical Details	150
6.6	Analytic Coefficients of δ -function parts	151
6.6.1	Angular Couplings	151
6.6.2	Radial Couplings	152
6.7	Results	152
6.8	Discussion	170
7.	SUMMARY	172
	FOOTNOTES	177
	BIBLIOGRAPHY	180
	APPENDIX A	186
	APPENDIX B	189
	APPENDIX C	191
	APPENDIX D	193
	APPENDIX E	195

LIST OF TABLES

Table		Page
4 - 1	$\Delta(lm; R; b_b; \epsilon)$ at $b_b = 20.0$ a.u.	102
4 - 2	$\Delta(lm; R; b_b; \epsilon)$ at $b_b = 40.0$ a.u.	103
4 - 3	$\Delta(lm; R; b_b; \epsilon)$ at $b_b = 60.0$ a.u.	104
4 - 4	Energy Sampling	107

LIST OF FIGURES

Figure		Page
1 - 1	Classical Trajectory of B relative to A	7
2 - 1	A Binary Collision	34
2 - 2	$g(j'; nlm; \tau)$ vs. τ	42
2 - 3	$g(j'; nlm; \tau)$ vs. τ	43
2 - 4	$g(j'; nlm; \tau)$ vs. τ	44
2 - 5	$g^P(j'; j; \tau)$ vs. τ	49
2 - 6	$g^P(j'; j; \tau)$ vs. τ	50
2 - 7	$g^P(j'; j; \tau)$ vs. τ	51
2 - 8	$g^P(j; j; \tau)$ vs. τ	52
2 - 9	$g^\delta(j; \tau)$ vs. τ	53
3 - 1	Prolate Spheroidal Coordinates	56
3 - 2	P_R and Θ vs. ξ	70
3 - 3	P_R and Θ vs. ξ	71
3 - 4	P_R and Θ vs. ξ	72
3 - 5	P_R and Θ vs. ξ	73
3 - 6	P_R and Θ vs. ξ	74
3 - 7	P_R and Θ vs. ξ	75
3 - 8	Phase Shift λ vs. R	77
3 - 9	Phase Shift λ vs. R	78
3 - 10	Angular wave function vs. η	79
3 - 11	Angular wave function vs. η	80
3 - 12	Angular wave function vs. η	81
3 - 13	Angular wave function vs. η	82
3 - 14	Angular wave function vs. η	83

3 - 15	Angular wave function vs. η	84
3 - 16	Continuum states.....	85
3 - 17	Continuum states.....	86
3 - 18	Continuum States.....	87
3 - 19	Continuum States.....	88
3 - 20	Continuum States.....	89
3 - 21	Continuum States.....	90
4 - 1	$\partial\theta/\partial\epsilon$ vs. ξ	94
4 - 2	Packet Width vs. Continuum Energy.....	105
4 - 3	Packet Width vs. b_b	106
4 - 4	First Packet Energy vs. b_b	109
4 - 5	Wave Packets.....	110
4 - 6	Wave Packets.....	111
4 - 7	Wave Packets.....	112
4 - 8	Wave Packets.....	113
4 - 9	Wave Packets.....	114
4 - 10	Wave Packets.....	115
5 - 1	Molecule and Space-Fixed reference frames.....	121
6 - 1	Gauss Hypergeometric Function.....	143
6 - 2	$\langle \mathcal{P}^\theta \rangle$ vs. continuum energy.....	154
6 - 3	$\langle \mathcal{P}^\theta \rangle$ vs. continuum energy.....	155
6 - 4	$\langle \mathcal{P}^\theta \rangle$ vs. continuum energy.....	156
6 - 5	$\langle \mathcal{P}^\theta \rangle$ vs. continuum energy.....	157
6 - 6	$\langle \mathcal{P}^R \rangle$ vs. continuum energy.....	158
6 - 7	$\langle \mathcal{P}^R \rangle$ vs. continuum energy.....	159
6 - 8	$\langle \mathcal{P}^R \rangle$ vs. continuum energy.....	160

6 - 9	$\langle \mathcal{P}^R \rangle$ vs. continuum energy.....	161
6 - 10	$\langle \mathcal{D}^\theta \rangle$ and $\langle \mathcal{D}^R \rangle$ vs. continuum energy.....	162
6 - 11	$\langle \mathcal{P}^\theta \rangle$ vs. R	163
6 - 12	$\langle \mathcal{P}^\theta \rangle$ vs. R	164
6 - 13	$\langle \mathcal{P}^\theta \rangle$ vs. R	165
6 - 14	$\langle \mathcal{P}^\theta \rangle$ vs. R	166
6 - 15	$\langle \mathcal{P}^\theta \rangle$ vs. R	167
6 - 16	$\langle \mathcal{D}^\theta \rangle$ and $\langle \mathcal{D}^R \rangle$ vs. R	168
6 - 17	$\langle \mathcal{D}^\theta \rangle$ and $\langle \mathcal{D}^R \rangle$ vs. R	169

NOMENCLATURE AND ABBREVIATIONS

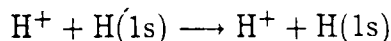
In the body of the text, references to bibliography and footnotes are indicated by numbers within square brackets and superscripted numbers, respectively.

1. INTRODUCTION

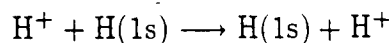
1.1 An overview

Many fundamental atomic collision phenomena are illustrated by processes occurring in one- and two-electron systems:

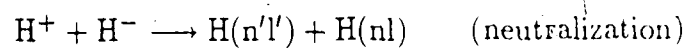
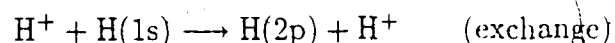
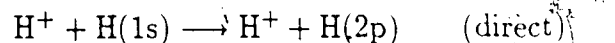
(a) Elastic Scattering.



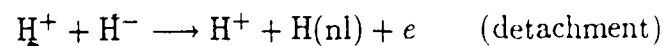
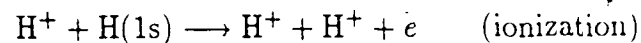
(b) Resonant charge transfer.



(c) Direct or Exchange excitation.



(d) Ionization and Detachment.



The work reported in this thesis forms my contribution to a continuing theoretical study of such prototype processes by Professor W.R.Thorson and coworkers at the University of Alberta. This thesis is concerned specifically with problems bearing on the description of ionization; similar considerations apply to detachment. Although computations have been carried out here only for the proton-hydrogen atom system, the results obtained are generally applicable to any one-electron-two-nucleus collision system.

In the past two decades substantial progress has been made, both experimentally and theoretically, in understanding the simpler processes listed above. Most theoretical work has focussed on one-electron prototype systems because

both atomic and molecular electronic basis states can be computed accurately. While experimental work on these systems is much more difficult than for systems with nonreactive or inert atoms, enough experimental information has been obtained to provide some critical tests of developing theory. Elastic scattering processes were the earliest to be studied and today these are generally well understood¹. More recently (since about 1977) considerable advance has also been made in the study of bound-state inelastic processes, although it is clear that reliable calculation of individual state excitation cross sections remains a difficult problem.

At the present time interest is turning to the study of ionization and detachment processes in which an unbound electron is produced by the collision. Theoretical description of these processes is fundamentally more difficult than for bound state excitations in which the excited electron remains localized in the neighbourhood of one or both of the original collision partners. Up to the present time, atomic collision processes have mostly been studied using the *coupled states* method, which describes the behavior of the electron system by expansion in a suitable finite set of " L^2 -type" (square-integrable) *basis states*. Heavy particle motion may be described quantum mechanically if necessary, but it is normally adequate [2,3] to use the *classical trajectory* method in which the nuclei move on a preset collision trajectory and the resulting time-dependent Schrödinger equation is to be solved for the electron system. Use of a coupled-states expansion then leads to a system of coupled first-order differential equations for the probability amplitudes associated with the basis states. *Such equations necessarily conserve probability of finding the electron within the subspace spanned by the basis set.* Basis states in coupled-state expansions are usually chosen to correspond to specific states of the system at the beginning/end of collision ("*channel states*"),

although sometimes additional basis states called *pseudostates* are included to represent the behavior not well described by channel states alone. This general scheme is adequate for describing many bound-state excitation processes, but there are fundamental conceptual problems for its extension to processes such as ionization or detachment in which the electronic continuum plays a major part. Electronic continuum states are not of L^2 -type, are not localized spatially and form a non-denumerably infinite set; an electron ejected to the continuum eventually propagates away from the localized region of configuration space ("interaction region") where initial excitation from a bound state occurs. While it is possible to "represent" electronic continuum states within a localized region by expansion in a suitably constructed set of L^2 -type pseudostates, the subsequent *escape* of the unbound electron from this region cannot be fully described. In particular the probability-conserving differential equations of conventional coupled states theory are in error since they fail to take such escape into account. This point was emphasized by Reading and Ford [4] in connection with the use of pseudostates locally representing the continuum in atomic states basis expansions for high energy collisions; they replaced the conventional differential equations of the coupled states method by a system of coupled *integral* equations in which effects of escape from a continuum pseudostates basis are represented by decaying amplitudes and the resulting formalism does *not* conserve probability within the close-coupled subspace. So far however most attempts to describe ionization using coupled states methods have used pseudostates to "represent" the continuum in the conventional formulation and do not take escape effects into account [5-9]. In some studies [10,11] the continuum is *formally* "fully included", and the integrations over continuum energy which result are performed by numerical quadrature. However, these approaches fail to appreciate that any quadrature involves sampling at a

finite number of points, equivalent to a truncation of the continuum to a localized region, and is therefore also in error by ignoring escape effects.

Further developments in the theory of collisional ionization or detachment must consider the problem posed by escape of unbound electrons from the region spanned by a finite basis and the problem of continuum evolution outside that region. The work presented in this thesis has a bearing on these issues.

1.2 Objectives of this work

Following an approach like that of Reading and Ford [4], Professor Thorson has developed a coupled states formulation for low to intermediate energy collisions, based on an expansion in molecular (adiabatic) states [12]. Transitions arise from "nonadiabatic couplings", i.e. from distortion of the adiabatic states as they follow the moving nuclei. The continuum is "represented" by a finite set of *packet states* (of L^2 -type) which span it locally, within a specified "interaction region", and are constructed explicitly from the exact adiabatic continuum states. Integral equations similar to those of Reading and Ford were derived, in which escape effects appear explicitly and probability is not conserved. Additional complications in the theory arise from the singularities in the nonadiabatic couplings of adiabatic continuum states.

An important part of this research was a careful study of these integral equations and their derivation as well as the background of exact continuum state properties and relations on which they are based. During this study it was realized that several versions of the integral equations result from the assumptions or approximations made in the derivation.

In Chapter 2 the formally most satisfactory version is derived. The rest of the thesis is concerned with proofs required as the background to the

new formulation and the computations involved in its application to the proton-hydrogen atom prototype system.

In Chapter 3 we construct a global "phase-amplitude" representation of exact adiabatic continuum states for H_2^+ . This form is conceptually and computationally efficient in constructing packet states.

In Chapter 4 we construct packet states, examine their physical properties, and show how packet widths and energies may be determined from assumptions about the size of the localized region within which the continuum is to be "represented". A significant property of the molecular continuum packet states which has not been appreciated previously is their strong localization at the centre of charge (rather than on the nuclei).

In Chapter 5 we derive the formal properties of nonadiabatic coupling among adiabatic continuum states, with particular attention to the structure of the singularities in these couplings when the coupled states are degenerate. The derivation is based on a rigorous extension of the Hellmann-Feynman theorem to adiabatic continuum states. The results provide a scheme for efficient computation of these couplings.

In Chapter 6 we outline computations of nonadiabatic coupling matrix elements and present representative results.

Appendices to the thesis contain auxiliary proofs or details of computational methods.

The remainder of this introductory chapter presents a summary of basic background theory of atomic collisions and leads up to the problems posed by inclusion of the continuum. The discussion focusses mainly on low to intermediate energies and problems limited to the one-electron prototype systems.

1 Basic Theoretical Background

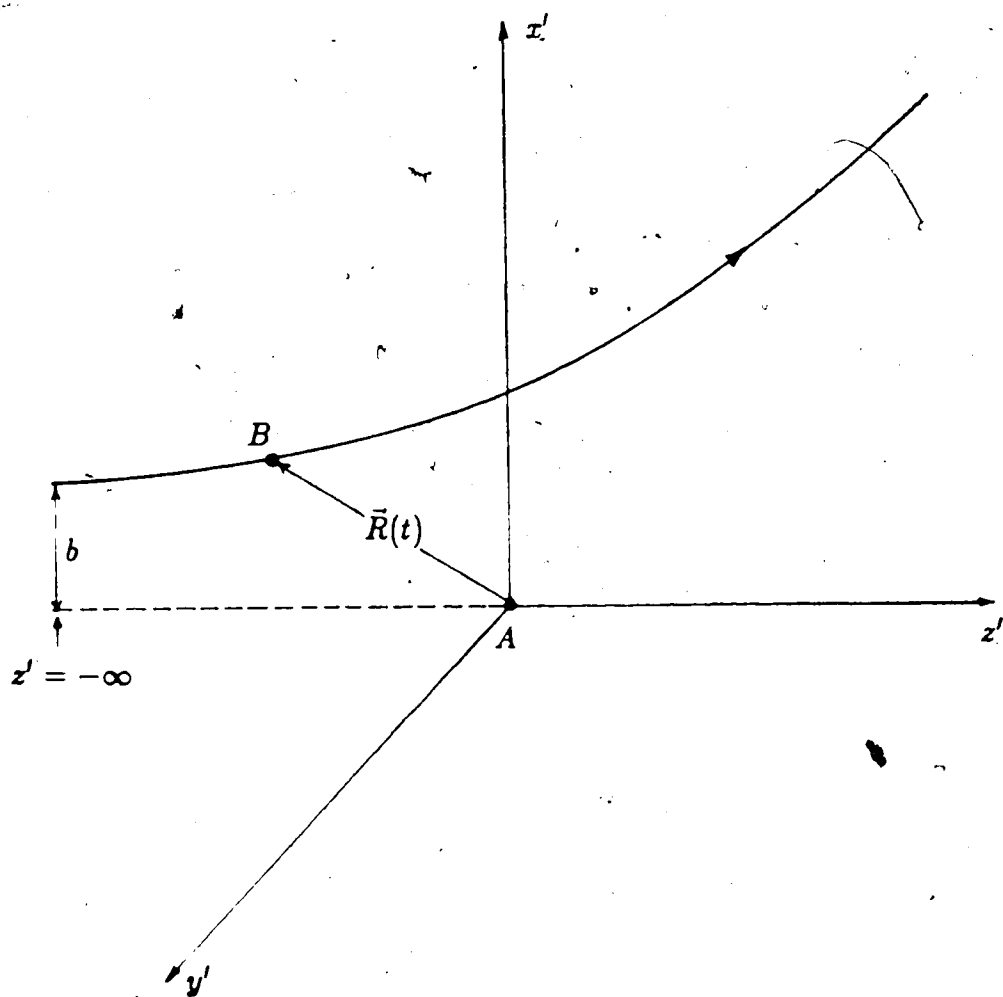
1.3.1 Context of this work

This work is concerned with collisional ionization or detachment in binary ion/atom collisions at low to intermediate energies, i.e. for collisional energies in the centre-of-mass (c.m.) system between 0.05 – 9.0 keV/amu. The *classical trajectory* method is used: the nuclei are assumed to move along a predetermined classical trajectory $\vec{R}(t)$ for given c.m. collision energy E and impact parameter b (see Fig. 1 - 1), and the evolution of the electronic system is determined by the resulting time-dependent Schrödinger equation. The electronic wave function is described by a coupled-state expansion in suitably defined *molecular* (adiabatic) basis functions. Particular attention is focussed on problems posed by the inclusion of electronic continuum states in such a formulation. This section gives a brief discussion of background assumptions and their context of validity in atomic collision theory.

1.3.2 Classical Trajectory Formulation

A binary atomic collision involves two nuclei A, B and one or more electrons, all initially bound to A and/or B; the prototypes treated explicitly in this thesis are one-electron systems. Since the centre of mass motion can be factored out, description of a collision is concerned only with relative motion. Many choices may be made for the relative coordinates [13]; for our purposes the most convenient is the *molecular* coordinates (\vec{R}, \vec{r}') , where \vec{R} is the position vector of B relative to A and \vec{r}' is the electron coordinate vector in a space fixed reference frame centred at the centre of mass of the nuclei. The essential problem in atomic collision processes of all types is the transfer of energy, momentum etc. between the heavy particle motion (here associated with \vec{R}) and the electronic degrees of freedom,

Figure 1 - 1 : Classical Trajectory of B relative to A



\vec{r}' . In principle, a complete account of this dynamical interaction requires a fully quantum mechanical treatment of the system: one must solve the time independent Schrödinger equation

$$H(\vec{r}', \vec{R}) \Psi(\vec{r}', \vec{R}) = E \Psi(\vec{r}', \vec{R}) \quad (1-1)$$

with the usual boundary conditions of an incident plane wave for the initial state plus outgoing scattered waves for final states. In molecular coordinates the total Hamiltonian (for a one-electron-two-nucleus system) is

$$H(\vec{r}', \vec{R}) = -\frac{\hbar^2}{2\mu} (\nabla_{\vec{R}}^2)_{\vec{r}'} + \frac{Z_A Z_B e^2}{R} + \hat{h}_e(\vec{r}'; \vec{R}) \quad (1-2)$$

where

$$\mu = M_A M_B / (M_A + M_B)$$

\hat{h}_e is the electronic Hamiltonian.

$$\hat{h}_e(\vec{r}'; \vec{R}) = -\frac{\hbar^2}{2m_e} (\nabla_{\vec{r}'}^2)_{\vec{R}} + V(\vec{r}'; \vec{R}) \quad (1-3)$$

with molecular electronic reduced mass m_e given by

$$m_e = m_0 (M_A + M_B) / (m_0 + M_A + M_B)$$

and $V(\vec{r}'; \vec{R})$ is the molecular electronic potential,

$$V(\vec{r}'; \vec{R}) = -\frac{Z_A e^2}{r_A} - \frac{Z_B e^2}{r_B} \quad (1-4)$$

It is well understood today [2,3,13] that a fully quantum mechanical treatment of atomic collision processes of the types which concern us here is unnecessary. The primary goal of the theory is the computation of probabilities/cross

sections for electronic excitation, ionization, and the *reaction* of the heavy-particle system to these actions is of relatively little interest. Furthermore, excitation of the electron system by the heavy particles is an inefficient process at very low energies. This feature of atomic collision theory is in sharp contrast with the more complex dynamical problems involved in translation-rotation or translation-vibration energy transfer processes in molecular collisions; it arises from the great disparity in nuclear and electronic masses. The general consequence is that while the electronic system must be treated quantum mechanically, the heavy particles often behave "classically".

In the much simpler and physically appealing *classical trajectory* formulation of atomic collision theory, the heavy particles are assumed to move on some classical trajectory $\vec{R}(t)$, with well-defined position and momentum at each instant. Within this classical picture, the molecular electronic potential becomes time-dependent; the electronic wave function $\Upsilon(\vec{r}', t)$ for the system must then satisfy the time-dependent *electronic* Schrödinger equation

$$i\hbar \frac{\partial \Upsilon(\vec{r}', t)}{\partial t} = \hat{h}_e(\vec{r}'; \vec{R}(t)) \Upsilon(\vec{r}', t) \quad (1-5)$$

Excitation probabilities per collision of given impact parameter are integrated over impact parameters to yield electronic excitation cross sections.

The utility and accuracy of the classical trajectory method was demonstrated in empirical practice and by computational comparison with quantal calculations well before clear theoretical justification was provided for its use². It is clear that one necessary criterion for the applicability of this description to an inelastic collision is that it be applicable for corresponding elastic scattering behavior. This is generally true if $k \gg 1.0$ a.u. and $\vartheta > 1/kr_0$ (shadow scattering), where k is the wave number for relative nuclear motion with energy E , ϑ is the

angle of scattering of the nuclei, and r_0 their distance of closest approach. For the proton-hydrogen atom system, $k > 1.0$ a.u. if $E > 1.5 \times 10^{-2}$ a.u. (≈ 0.4 eV). Depending on the process, this means the classical trajectory method might be applicable for all energies above thermal energies in this system; this is the case for elastic scattering and resonant charge transfer processes at these low energies in H_2^+ .

More rigorous justification of the classical trajectory formulation must rest upon its *derivation* from the fully quantum mechanical formulation of the problem. Within the general coupled states scheme, this is done by expanding the total wave function Ψ in eq (1 - 1) in an appropriate set of electronic basis states, $\{|\phi_n\rangle\}$, and simplifying the resulting set of coupled *second order* differential equations for the heavy particle wave functions $\{\chi_n(R)\}$. The objective of such simplification is reduction to the set of coupled *first-order* differential equations which are obtained when the solution $\Upsilon(\vec{r}', t)$ to the time-dependent electronic Schrödinger equation (1 - 5) is expanded in the same set of basis states,

$$\Upsilon(\vec{r}', t) = \sum_n a_n(t) \exp\left(-\frac{i}{\hbar} \int dt \epsilon_n(t')\right) |\phi_n(\vec{r}')\rangle \quad (1-6)$$

The essential point is that the "time" t which appears in the classical trajectory equations is merely a parametric variable connected in some average way to the dynamical variable \vec{R} of the quantum mechanical theory. Several authors have used the eikonal approximation for this reduction [14]. Some other derivations [15,16,17] are based on semiclassical approximations to the heavy particle wave functions $\{\chi_n(R)\}$. Such derivations give more specific conditions for the validity of the classical trajectory formulation. Though these depend on the particular approximations used in reduction, in all cases the following general conditions must be met:

(a) JWKB condition for the nuclear motion: the de Broglie length

$\lambda = h/\sqrt{2\mu(E - \epsilon_n(R))}$ must be small compared to the distance over which the elastic scattering potentials $\epsilon_n(R)$ associated with the electronic states $|\phi_n(\vec{r}', \vec{R})\rangle$ change appreciably.

(b) The electronic momentum and energy transfer involved in excitations must be small compared to the total momentum and energy of the collision.

An important result which follows from the semiclassical derivations is that the classical trajectory equations are valid more generally than the literal *classical picture* which gives them intuitive physical meaning [17]. Although these equations appear to describe the time dependence of probability amplitudes for the electronic basis states in the coupled states expansion (1 - 6) throughout the duration of a classical collision, they are in reality only a device for computing the final excitation probabilities, and the values of these amplitudes at intermediate "times" are not to be associated with actual measurables.

In order to solve the classical trajectory equations one must define the trajectory $\vec{R}(t)$ which provides the parametric connection between nuclear position variable and the "time" t . Since electronic transitions are probabilistic in nature this can be done in at most an average sense. Early discussions of the classical trajectory method were very concerned with the problem of defining this "trajectory" in an optimal way [18,19]. However derivations [17] both show that *any* reasonable average trajectory is adequate if the method is valid and that when the results from different trajectory choices vary widely the method as a whole is also likely to be inaccurate. The low energy limit cited above for the theoretical formulations we discuss here is that for which the classical trajectory method becomes seriously in error for electronic excitations in proton-H-atom collisions.

In many cases, for collision energies $E \geq 0.5 - 1.0 \text{ keV}/amu$, even simpler approximations may be used for the classical trajectory $\vec{R}(t)$. In the *impact parameter method*, a straight line, constant velocity trajectory is used. Kimura and Thorson [20] for example have shown that for collision energies in the laboratory frame greater than $1.0 \text{ keV}/amu$ the impact parameter method is accurate. Some exceptions may occur in cases where collisions at very small impact parameters have a dominant effect on the process of interest or when $Z_A Z_B$ is large [2]; under these circumstances it may be necessary to use Coulomb trajectories [18] taking into account the deflection of the nuclei.

In general, for energies above about $0.05 - 0.1 \text{ keV}/amu$ one may safely assume the validity of the classical trajectory method, and for somewhat higher energies the trajectory may be simply defined.

1.3.3 "Slow" and "Fast" Collisions and Basis States

In principle, the time-dependent Schrödinger equation (1 - 5) can be solved by a coupled state expansion (1 - 6) in a *complete* set of electronic basis states $\{|\phi_n(\vec{r}'; \vec{R})\rangle\}$. Some limiting possibilities are the total sets of atomic electronic states of A or of B, or the set of molecular states of AB system. In practice severely truncated basis sets are used, which are certainly far from complete and may in some cases even be partially redundant (as for example if atomic states on both A and B are included in the basis). The use of physical insight in the selection of basis states is therefore important.

With this in view a broad division of atomic collision processes may be made according to the collision energy E . A collision may be said to be *fast* if the relative heavy particle velocity v is much greater than the Bohr orbit velocity v_e for a relevant electronic level, and *slow* if it is much less. In the one-electron case $v_e = Z/n \text{ a.u.}$ where n is the principal quantum number and Z_A the nuclear

charge for the initial electronic state. The boundary between "slow" and "fast" regimes ("intermediate energy") occurs for $E = 25MZ_A^2/n^2 \text{ keV}$, where M is the nuclear reduced mass in amu . For $H^+ + H(1s)$ collisions this is 12.5 keV .

For *fast* collisions $v \gg v_e$, since the collision time is much less than the orbital period for the electronic states of interest, it is logical to think of the electron as being in an atomic state associated with one of the nuclei A, B, and to regard the time-dependent *interaction potential* arising from the presence of the other collision partner as the source of excitations. This may be called the *atomic state picture* of a collision; a truncated set of atomic orbitals centred on A and/or B then forms an appropriate basis for a coupled states expansion.

When on the other hand the collision speed is much lower than the electron speeds which concern us we may expect the electrons to adjust smoothly to the time-varying potential $V(\vec{r}'; \vec{R}(t))$. This idea is the basis of the Born-Oppenheimer approximation used in the theory of molecular bound states. In a collision one can imagine the formation of a "quasimolecule" and the transitions to be taking place among *molecular* electronic states. A set of molecular basis states is then an appropriate basis set to use in a slow collision³. These are the *adiabatic* eigenfunctions of the electron Hamiltonian \hat{h}_e at each nuclear configuration,

$$\hat{h}_e(\vec{r}'; \vec{R}) |\phi_n(\vec{r}'; \vec{R})\rangle = \epsilon_n(R) |\phi_n(\vec{r}'; \vec{R})\rangle \quad (1-7)$$

The eigenfunctions ϕ_n and their eigenvalues $\epsilon_n(R)$ depend parametrically on the nuclear coordinate \vec{R} .

The *adiabatic* approximation forms the rationale for the use of molecular state expansions in slow atomic collisions. It can be shown rigorously [23] that in a (hypothetical) infinitely slow collision, $v \rightarrow 0$, no transitions among non-degenerate molecular states could take place, and at the end of a collision the

system would remain in its initial molecular electronic states, with only elastic scattering (and possibly resonant charge exchange) occurring. At non-zero velocities, transitions can occur among the adiabatic molecular states, due to the fact that these undergo deformation at a finite rate. The couplings in this case are called *nonadiabatic couplings*; they are proportional to the nuclear velocity, and have a more significant effect, as the states coupled become more nearly degenerate. In a molecular system, the variation of the electronic energy eigenvalues (potential curves) $\epsilon_n(R)$ with internuclear distance may be considerable and there are specific regions where two or more states are degenerate or nearly degenerate; under these circumstances there may be strong coupling of such states due to the local breakdown of adiabatic behavior, even though the adiabatic approximation is generally valid. This point is expressed more precisely and practically in the *Massey adiabatic criterion* [24], which states that transitions are "improbable" unless

$$\frac{\Delta\epsilon d_0}{\hbar v} < 1$$

where $\Delta\epsilon$ is a (local) spacing of adiabatic energy levels and d_0 an estimate of the range over which such spacing is maintained (often taken to be 1 a.u.). This is just a restatement of the uncertainty principle, since d_0/v is just the time over which the two levels are separated by energy gap $\Delta\epsilon$; the probability of transitions between adiabatic levels with this separation is small if the time period over which they interact is much longer than $\hbar/\Delta\epsilon$. The Massey criterion gives a more detailed appreciation of the nature of slow atomic collision processes. Even when most of the molecular states are well separated in energy and therefore behave adiabatically for the most part, highly specific interactions among them may lead to substantial transition probabilities for particular excitation processes, while other events remain essentially improbable. For instance, the cross section for

exciting the 2p atomic level in $H^+ + H(1s)$ collisions at energies below about 5 keV is orders of magnitude larger than the corresponding 3p cross section. One may speak of such specific transitions as *mediated* by the local degeneracies among the relevant electronic potential curves, and these may be grouped in three categories: (a) those mediated by degeneracy in the united atom limit, $R \rightarrow 0$; (b) those mediated by asymptotic degeneracy, $R \rightarrow \infty$; (c) those mediated by "curve crossings" at finite R -values. Many simple early treatments [25] of atomic collision processes, especially for collision energies at 1 keV/amu or less, involve modelling these localized degeneracies and their effects within a basis spanned by a very few molecular states. It was recognized fairly early that the key to understanding electronic excitations in the low energy regime lies in the adiabatic potential curves and the identification of the crucial mediating degeneracies among them. Thus the dominant 2p excitation process in $H^+ + H(1s)$ collisions at low energies is mediated by the united atom degeneracy of the $2p\pi_u$ molecular state (which dissociates to the 2p level of atomic hydrogen) with the $2p\sigma_u$ molecular state which corresponds asymptotically to the initial state level $H(1s)$. One may therefore use the *energy correlation diagram* (which gives the curves $\epsilon_n(R)$ as functions of internuclear distance R) to select dominant events in a slow collision. As the collision energy increases, more and more states participate in significant "nonadiabatic coupling", until in the intermediate energy regime the processes which play a significant role overall are less specific, and the justification for a molecular state expansion is less evident. We note however that the domain of "slow" collision theory still covers most of the energy range of interest for a great deal of practical atomic physics and essentially all of chemistry above thermal energies. We have taken the value 6 - 9 keV/amu as the upper limit for practical utility of the molecular state expansion approach, based on the value 12.5 keV from the H_2^+ system cited above ⁴.

Impact ionization (in the one-electron systems) is a non-specific process and present evidence [20,26] suggests a "ladder climbing" mechanism, i.e. excitations from low lying bound states to higher bound states and then to the continuum. Continuum states as well as highly lying Rydberg states are very closely spaced in energy; hence they cannot behave nearly adiabatically. A moment's thought reveals the physical reason for the inadequacy of an adiabatic description of these states.

An ionized electron is in an aperiodic orbit and eventually goes to "infinity". On the one hand it is not clear whether a Born-Oppenheimer type argument is applicable to such an aperiodic continuum electron. On the other hand electromagnetic disturbances take a finite time to travel from one point to another; hence a distant electron cannot know the nuclear position instantaneously to adjust smoothly to its variations. Though bound, an electron in a highly lying Rydberg state can also move out to very large distances. Also, because of the long Coulomb tail of the potential, such an electron is slow ($v_e \simeq 0$) in most of its allowed region in physical space; hence it too cannot behave adiabatically.

This physical analysis suggests that a near adiabatic description over *all physical space* is inappropriate for continuum and highly lying Rydberg electrons. However in the interaction region, where their velocities are high, they may behave "adiabatically".

1.4 Molecular States expansions and their Characteristics

1.4.1 Synopsis

A molecular state expansion was first proposed and developed by Mott and Massey [27] to describe charge transfer and excitation in slow atomic collisions. In this section we describe and criticize their formulation, usually known as the *perturbed stationary states* (PSS) method; a classical trajectory description is used.

1.4.2 The PSS formulation

We expand $\Upsilon(\vec{r}', t)$ in a basis set of *bound* molecular orbitals.

$$\Upsilon(\vec{r}', t) = \sum_n a_n(b; t) \exp\left(-\frac{i}{\hbar} \int^t dt' \epsilon_n(R(t'))\right) |\phi_n(\vec{r}'; \vec{R})\rangle \quad (1-8)$$

where b is the impact parameter.

Substituting equation (1-8) in equation (1-5) and multiplying on the left by $\langle \phi_j |$ one obtains coupled equations for the probability amplitudes $\{a_n(t)\}$.

$$i\hbar \frac{\partial a_j(b; t)}{\partial t} = \sum_n \vec{v} \cdot \vec{P}_{jn}(\vec{R}(t)) a_n(b; t) \exp\left(-\frac{i}{\hbar} \int^t dt' (\epsilon_j(R(t')) - \epsilon_n(R(t')))\right) \quad (1-9)$$

where $\vec{v} = d\vec{R}(t)/dt$ and

$$\vec{P}_{jn}(\vec{R}(t)) = \langle \phi_j(\vec{r}'; \vec{R}(t)) | -i\hbar (\vec{\nabla}_R)_{\vec{r}'} | \phi_n(\vec{r}'; \vec{R}(t)) \rangle \quad (1-10)$$

The initial condition on equation (1-9) is $a_j(b; t \rightarrow -\infty) = \delta_{ij}$ where $|\phi_i\rangle$ is the initial molecular states of the system.

There is a one-to-one correspondence between *bound* molecular states and the *bound* atomic states of A and B⁵ [28]; as $R \rightarrow \infty$ molecular states become atomic states. Therefore $a_j(b; t \rightarrow +\infty)$ is interpreted as a charge transfer

or excitation probability amplitude depending on whether the electron has changed the nucleus to which it was bound, or not.

The transitions among molecular states are caused by the *nonadiabatic* couplings \vec{P}_{jn} . In general

$$\vec{v} \cdot \vec{P}_{jn} = v^R P_{jn}^R + v^\vartheta P_{jn}^\vartheta + v^\varphi P_{jn}^\varphi \quad (1-11)$$

where (R, ϑ, φ) are spherical polar coordinates of \vec{R} (with respect to space fixed axes) and

$$P_{jn}^R = \langle \phi_j | -i\hbar (\partial/\partial R)_{\vec{r}} | \phi_n \rangle \quad (1-12a)$$

$$P_{jn}^\vartheta = \frac{1}{R} \langle \phi_j | -i\hbar (\partial/\partial \vartheta)_{\vec{r}} | \phi_n \rangle \quad (1-12b)$$

$$P_{jn}^\varphi = \frac{1}{R \sin \vartheta} \langle \phi_j | -i\hbar (\partial/\partial \varphi)_{\vec{r}} | \phi_n \rangle \quad (1-12c)$$

The nuclei move classically in a plane taken to be the xz -plane; hence $v^\varphi = 0$ and P_{jn}^φ does not concern us.

Molecular basis functions are "locked in" to the internuclear axis which rotates as the collision progresses. This rotation of the molecular orbitals leads to the *angular coupling*,⁶ P_{jn}^ϑ .

Radial coupling, P_{jn}^R , represents transitions due to "deformation" of the molecular orbitals associated with the changes in R .⁷

1.4.3 Defects of PSS theory and ETF corrections

An electron in a bound atomic state moves with the nucleus; hence the initial and final conditions of (1-9) must be expressed in terms of moving atomic orbitals. Molecular basis functions do not contain any information about the nuclear *motion* and become static (with respect to the molecular reference origin) atomic orbitals at $t \rightarrow \pm\infty$; the interpretation of $a_n(b; t \rightarrow +\infty)$ as the probability amplitude of a particular channel state breaks down.

Formally this is not a problem if one uses the total adiabatic set (including the continuum) and takes the projection onto *moving* atomic states at $t \rightarrow \pm\infty$. In practice we always truncate the basis and would like to retain the one-to-one correspondence.

The lack of translational information in the molecular basis manifests itself in the PSS theory by giving rise to a number of physically unacceptable properties of $\vec{P}(\vec{R}(t))$.

- (a) On physical grounds, there cannot be any electronic transitions when the atoms are far apart; we expect \vec{P} to vanish as $R \rightarrow \infty$. On the contrary, the radial couplings between some states (eg. $1s\sigma_g \rightarrow 2s\sigma_g$ in H_2^+) tend to non-vanishing constants [29].
- (b) Ionization from a low-lying bound state involves a large momentum and energy transfer, and one expects such transitions to occur when the two nuclei are close to each other. It has been observed [30] that the bound-continuum couplings extend to unrealistically large R ($R \sim 50$ a.u.).
- (c) In (1 - 10) one must perform the operation $\vec{\nabla}_R$ keeping \vec{r}' fixed (in a space fixed reference frame). The result of an operation depends on the molecular reference origin. This makes the calculated cross sections origin-dependent [13,31]. The results of a correct theory must be invariant to a Galilean transformation of reference frame. In our work we use the *Geometric Centre (GC)* as the conventional reference origin.

Bates and McCarroll [32] were the first to propose the use of travelling molecular states to overcome the difficulties in PSS theory. They were constructed by multiplying $\phi_n(\vec{r}', \vec{R})$ by a plane wave factor $F_n(\vec{r}', \vec{R})$ which represented the movement of the electron with the nucleus⁸. Conventionally F_n is called the electron translational factor (ETF) or momentum transfer factor.

Later Schneiderman and Russek [33], and Thorson and coworkers [19,34] refined these ideas and in 1978 Thorson and Delos [31] reformulated the PSS theory including ETF's. What is important for this thesis work is the major result of Thorson and Delos: "The corrected PSS theory can be obtained by replacing \bar{P} in PSS theory by $\bar{P} + \bar{A}$ where \bar{A} is a correction matrix depending on the ETF".

At each R the adiabatic basis undergoes distortion and rotation which causes electronic transitions. At the same time they undergo a certain "simple displacement" which cannot cause transitions. The role of \bar{A} is to identify the effects of this translation in \bar{P} and to subtract it, leaving the "deformation" effects. (A more complete technical discussion of \bar{A} is given in Chapter 5)

1.5 Problem of Including Electronic Continuum

1.5.1 Synopsis

The electronic continuum must be included in a theory of ionization and detachment. Moreover the continuum can play an important role even when such channels are unimportant. For example Gallaher and Willets [35] and Cheshire *et al.* [36] noted the importance of the hydrogenic continuum in charge transfer in $H^+ + H(1s)$ collisions. The important point is that a small set of atomic bound states (centred on target and projectile) is not flexible enough to represent the dynamical changes in the wave function when the nuclei are close to each other. One may categorize such effects of the continuum as *virtual* (or *indirect*) in contrast to the *direct* effects such as ionization and detachment. The virtual effects of the atomic continuum become increasingly important with decreasing impact parameter and relative nuclear velocity because of the increasing molecular nature of the collision [37].

Direct inclusion of the continuum in the coupled states expansion leads to a number of difficulties.

- (a) In the case of atomic expansions, continua of A and B, together with the bound states, form an overcomplete basis.
- (b) The resulting coupled states equations are nonenumerably infinite.
- (c) In contrast to couplings of bound states, coupling between continuum states can be singular.

Therefore one has to resort to special techniques in handling the effects of the continuum in an atomic collision. It is convenient to group these techniques, within the classical trajectory formulation, under three headings.

- (1) Space-Time discretization techniques.
- (2) Explicit techniques.
- (3) L^2 -discretization techniques.

This thesis research involves an L^2 -discretization of the molecular continuum. A very brief survey of the first and second type techniques are given for the reader to appreciate some of the difficulties in handling the continuum. The emphasis will be on one-electron systems, in particular $H^+ + H(1s)$.

1.5.2 Space-time discretization techniques

These are techniques where the time dependent Schrödinger equation is numerically integrated on a finite space-time grid; they can be viewed as alternatives to coupled states techniques. Such a method was originally proposed by Weiner and coworkers [38]. There are very few published applications to atomic collisions, some of which are listed in reference 39. The basic philosophy of the method can be understood by following the calculation of Grün *et al.* [39a] on the $H^+ + H(1s)$ system.

The wave function is expanded in a truncated set of magnetic substates,

$$\Upsilon(\vec{r}'; t) = \sum_{m=0}^n f_m(\rho, z, t) \exp(im\phi) ,$$

where (ρ, z, t) are the cylindrical polar coordinates of \vec{r}' with z along the internuclear axis (in a molecular fixed reference frame). Substitution in (1 - 5) leads to a finite set of coupled *partial differential equations* for f_m which are numerically integrated on a space-time grid using a finite difference technique. Appropriate boundary conditions on f_m are imposed at the surface of the space grid. The resulting wave function can then be *projected* on to the final scattering states.

Space-time discretization techniques can account for the *virtual* effects of the continuum. However a serious difficulty arises in the choice of proper boundary conditions for f_m ; Grün *et al.* have imposed $f_m = 0$. This prevents the truly ionized electrons from *escaping* the region of space spanned by the grid. They have *suggested* using a complex potential to make the boundary transparent to the ionized electron.

To overcome the same problem in solving a 1-dimensional Schrödinger equation Horbatsch [40] has used the coordinate transformation $r = \tan \theta$ so that the infinite coordinate r is mapped onto a finite variable θ . This enables the discretization of the total physical space. Application of this idea to a realistic atomic collision is yet to be seen.

Disregarding the above problem of *flux trapping*, (and using a different method than projecting on to the final scattering states) Terlecki *et al.* [39b] have calculated the total ionization cross section in $H^+ + H(1s)$. At present one cannot calculate *differential* ionization cross sections.

Though not very appealing physically, these techniques are very general and are applicable to both fast and slow collisions. An advantage over basis set expansion methods is that there is no problem of selecting an optimal basis and appropriate ETFs. The price one pays for this advantage is the enormous amount of computer time required.

1.5.3 Explicit techniques

Here the full continuum is explicitly included in the expansion basis but with some drastic assumptions on the nature of the coupling matrix elements and/or expansion coefficients to avoid the difficulties (b) and (c) mentioned in section (1 - 5 - 1). Examples of such techniques are the First Born approximation [1], Thorson and Levy's theory of impact ionization [41] and the dynamical complex potential method of Delos and coworkers [42]. The physical assumptions and the technology are very different from one theory to another. A common feature of all these techniques is the *neglect* of coupling among continuum states, so that these are not really close-coupling methods.

Because of the explicit inclusion of the true continuum these techniques are capable of accounting for the direct effects of the continuum; in particular they can, in principle, give differential ionization (detachment) cross sections and the question of flux trapping is absent. However the nature of the assumptions seriously limits their applicability to very specific systems.

1.5.4 L^2 -discretization techniques

One may be tempted to avoid the "problem-causing" continuum by replacing the atomic or molecular basis by an entirely discrete, L^2 -type basis. Galaher and Willets [35] used a truncated set of Sturmian functions¹⁰,

$\{S_{nl}(\epsilon; r) \cdot Y_{lm}(\theta, \phi)\}$, centred on each nucleus, to describe low to medium energy $H^+ + H(1s)$ collisions.

A serious problem with such a non-physical basis is that the expansion coefficients do not approach definite limits as $t \rightarrow \pm\infty$, but oscillate. Asymptotic channel states cannot be reconstructed from a finite set of Sturmians; hence the resulting transition amplitudes also oscillate indefinitely¹¹.

Cheshire *et al.* [36] took the point of view that it is more important to represent the physical wave function as closely as possible than to satisfy the formal completeness of the *non-truncated* basis. To avoid poor asymptotic behavior they included some unmodified hydrogenic bound states for which they wished to calculate cross sections. To this set they added some additional functions, orthogonal to those already present, chosen to overlap well with the lower bound states of He^+ (united atom). These additional states were assumed to represent the hydrogenic continuum (and account for the virtual effects) since it was known that He^+ states have a large overlap with it.

Shakeshaft [5,43] further developed the Sturmian function method and calculated the total ionization cross section [5] in $\text{H}^+ + \text{H}(1s)$ collisions. The truncated (Sturmian) basis was chosen in such a way that when the atomic Hamiltonian is diagonalized, the resulting eigenvalues (almost) coincide with the most important bound states and overlap the low energy part of the atomic continuum. The positive energy states, called *pseudostates*, were assumed to "represent" the (lower energy part of the) continuum in a "discretized" manner, which is the basis of all traditional pseudostates methods. The probability that the electron is found in pseudostates at $t \rightarrow +\infty$ was interpreted as ionization probability¹².

Instead of Sturmian functions one can use any reasonable Hilbert basis, e.g. Slater-type functions [9], or harmonic oscillator functions [44], to construct pseudostates. The key requirement is that they have high density in the *physically important region*.

Several attempts have been made to use the united atom bound states as pseudostates. Fritsch and Lin [45] placed them on atomic nuclei. Anderson *et al.* [46] have suggested placing them on the centre of charge. Coupled states calculations with such "triple centre" bases have been performed for $\text{H}^+ + \text{H}(1s)$ collisions by Lin *et al.* [47].

So far we have discussed the discretization of the atomic continuum. Very little work has been done on the discretization of the molecular continuum in collisions. In their work on Penning ionization [10] and impact ionization [11] Micha and coworkers have used molecular wave packets as pseudostates. They are obtained by integrating the true molecular continuum states, with a weight function, over energy. The wave packets are of L^2 -type and (automatically) orthogonal to all the molecular bound states. In this thesis work we use such adiabatic packet states and show (Chapter 4) that they have high density in the physically important region (around the centre of charge of the nuclei) for ionization in slow collisions.

Lüdde and Dreizler [48] have replaced the total molecular basis set by a non-physical "molecular" basis; the wave function in $H^+ + H(1s)$ collisions is expanded in a Hylleraas type basis¹³ (they have calculated only bound-bound transition cross sections).

At present there appear to be no strict guidelines to choose an adequate set of pseudostates. Atomic pseudostates are chosen on the general criterion that they should have high density in an "interaction region" (which is not defined) and low electronic energies. In the case of wave packets Micha *et al.* [11] have suggested changing the weight function until convergence (of the cross sections) is established, but such a procedure is not physically very illuminating.

A conventional coupled states calculation, with pseudostates representing the continuum, always gives the ionization probability as a discrete function in ejected electron energy. However one may use various projection techniques [9] to deduce the differential cross section.

By definition an L^2 -function cannot satisfy the usual scattering boundary condition; hence even with a complete L^2 -basis one may not be able to

represent the continuum *fully*. This formal deficiency leads to a physically unacceptable feature of the conventional coupled states calculations; ionized electrons are trapped within the region of space where the pseudostates are "concentrated". Such calculations (with few pseudostates) are bound to fail when ionization is a significant open channel.

Though the physical meaning of a positive energy L^2 -eigenstate of a Hamiltonian is somewhat unclear it is known that good pseudostates closely resemble the continuum states in a limited region of physical space [49,50];

$$|\tilde{\phi}_j(\vec{r}')\rangle \approx w_j |\phi_{\epsilon_j}(\vec{r}')\rangle \quad \text{for small } |\vec{r}'|$$

where $|\tilde{\phi}_j\rangle$ and $|\phi_{\epsilon_j}\rangle$ are the pseudostate and the continuum state of the same energy respectively. On physical grounds, the electronic transitions must take place within the interaction region. Hence one can certainly represent the continuum *locally*, in an atomic collision, with L^2 -pseudostates.

A formal analysis of coupled states expansion methods, as was done by Reading and Ford [4], reveals a way out of the dilemma of the L^2 -representation of the continuum.

Consider a fast atomic collision where the charge exchange is negligible. The electronic transitions, including ionization, take place in the physical space immediately surrounding the target (A) and a target centred basis (including pseudostates) is sufficient to "describe" the collision. Denote the projection operator onto this finite Hilbert basis, $\{\tilde{\phi}_{nlm}(\vec{r}'_A)\}$, by \hat{P} . Then we have

$$\Upsilon_P(\vec{r}'_A, t) = \hat{P} \Upsilon(\vec{r}'_A, t) = \sum_{nlm} C_{nlm}(t) \tilde{\phi}_{nlm}(\vec{r}'_A) \quad (1-13)$$

Note that we have not expanded the true wave function Υ in the limited basis and Υ_P describes it *only* within the interaction region. Υ satisfies

$$i\hbar \frac{\partial \Upsilon(\vec{r}'_A, t)}{\partial t} = [H_A + V(\vec{r}'_A, t)] \Upsilon(\vec{r}'_A, t) \quad (1-14)$$

with

$$H_A = -\frac{\hbar^2}{2m_0} \nabla_{\vec{r}'_A}^2 - \frac{Z_A e^2}{r_A}$$

and

$$V(\vec{r}'_A, t) = -\frac{Z_B e^2}{r_B}$$

Then the *correct* equation for the coupled states expansion, Υ_P , is obtained by projecting (1-14) onto the particular basis.

$$i\hbar \frac{\partial \Upsilon_P}{\partial t} = \hat{P} [H_A + V] \Upsilon$$

Note that the Hamiltonian (and V) operates on the total wave function and *not* on Υ_P . In a conventional coupled states calculation H_A and V are replaced by their *representatives* in the limited basis.

$$H_A \rightarrow \hat{P} H_A \hat{P} \quad (1-15a)$$

$$V \rightarrow \hat{P} V \hat{P} \quad (1-15b)$$

to obtain

$$i\hbar \frac{\partial \Upsilon_P}{\partial t} = \hat{P} [\hat{P} H_A \hat{P} + \hat{P} V \hat{P}] \Upsilon_P \quad (1-16)$$

(In deriving (1-16) we have used the idempotency of \hat{P})

It is reasonable to assume that the electronic transitions take place when nucleus B is close to A; hence the perturbing potential $V(\vec{r}'_A, t)$ may be assumed

to be "localized" within the interaction region. Since this region is adequately described by $\{\tilde{\phi}_{nlm}\}$, (1 - 15b) is reasonable.

On the other hand H_A includes the electronic kinetic energy operator which is *non-local* and cannot be fully represented with our basis. Hence (1 - 15a) is not valid and leads to non-physical flux trapping which concerns us here.

Reading and Ford avoided (1 - 15a) and derived coupled equations for $C_{nlm}(t)$ using the equation

$$i\hbar \frac{\partial \Upsilon_P}{\partial t} = \hat{P} \left[H_A + \hat{P} V \hat{P} \right] \Upsilon \quad (1 - 17)$$

Here we only quote their results.

$$\begin{aligned} C_{n'l'm'}(t) = & \exp\left(-\frac{i\epsilon_{jlm}t}{\hbar}\right) \delta_{n'l'm',jlm} \\ & - \frac{i}{\hbar} \sum_{nlm} \int_{-\infty}^t dt' \left\{ \exp\left(\frac{i\epsilon_{n'l'}(t'-t)}{\hbar}\right) \frac{\sin(\Delta_{n'l'}(t'-t)/2\hbar)}{(\Delta_{n'l'}(t'-t)/2\hbar)} \right. \\ & \left. \times \langle \tilde{\phi}_{n'l'm'} | V(\vec{r}'_A, t') | \tilde{\phi}_{nlm} \rangle C_{nlm}(t') \right\} \end{aligned} \quad (1 - 18)$$

Here $\Delta_{n'l'}$ is zero if $\tilde{\phi}_{n'l'm'}$ is a bound state and a positive constant if it is a pseudostate and $\tilde{\phi}_{jlm}$ represents the initial atomic state.

Equation (1 - 18) differs from the conventional coupled states equations by the factor $\sin(x)/x$ which is not equal to unity for pseudostates; it rapidly decays as $t' - t \rightarrow \infty$. Also $\langle \tilde{\phi}_{n'l'm'} | V(\vec{r}'_A, t') | \tilde{\phi}_{nlm} \rangle$ vanishes as $t \rightarrow \infty$ keeping $t' - t$ finite. Hence for pseudostates $|C_{n'l'm'}(t \rightarrow \infty)| = 0$; the probability has escaped at the end of collision.

Such a theory is not probability-conserving and does not describe the propagation of the electron outside the interaction region; hence it cannot give differential cross sections. However the total ionization probability is given by

$$\left[1 - \sum_{nlm} |C_{nlm}(t \rightarrow \infty)|^2\right].$$

In Chapter 2 we derive similar coupled equations, appropriate for slow atomic collisions, by projecting the full Schrödinger equation on a molecular basis.

2. THEORY

2.1 Introduction

Using the adiabatic basis, with wave packets representing the continuum, Professor Thorson [12] has derived two different sets of integral equations which we call the *connected* and the *disconnected* forms. In this chapter we derive the *connected* form in a more formal manner; the full Schrödinger equation is *projected* on to the L^2 -basis using different physical assumptions. Closed form expressions are also derived for the decay factors appearing in the propagator.

In the classical trajectory formulation we have to solve the time dependent Schrödinger equation

$$i\hbar \left(\frac{\partial}{\partial t} \right) |\Upsilon(t)\rangle = \hat{h}_e(\vec{R}(t)) |\Upsilon(t)\rangle \quad (2-1)$$

with some initial condition $|\Upsilon(t_0)\rangle$. The operator \hat{h}_e is the molecular electronic Hamiltonian given by equation (1 - 3). One can construct a formal solution to Equation (2 - 1) using a *complete* basis set.

The following facts can be deduced from the general formalism of quantum mechanics.

(1) Adiabatic basis set.

At each internuclear separation the infinite set of solutions, $\{|k; \vec{R}(t)\rangle\}$, (including the continuum) of the time independent Schrödinger equation

$$\hat{h}_e(\vec{R}(t)) |k; \vec{R}(t)\rangle = \epsilon_k(R) |k; \vec{R}(t)\rangle \quad (2-2)$$

forms a complete set. For bound states there is a one-to-one mapping [28]; $|k; \vec{R}(t)\rangle \rightarrow |k; \vec{R}(t')\rangle$ as $t \rightarrow t'$ and we can take $k \equiv (nlm)$ where (nlm) are

the united atom quantum numbers. For continuum states we take $k \equiv (\epsilon l n)$ and the mapping is defined to be $|\epsilon l m; \vec{R}(t)\rangle \rightarrow |\epsilon l m; \vec{R}(t')\rangle$; the *continuum energy*, $\epsilon_k = \epsilon$, is kept constant as \vec{R} changes. Adiabatic states have the following orthogonality properties.

$$\langle n'l'm'; \vec{R}(t) | nlm; \vec{R}(t) \rangle = \delta_{n'n} \delta_{l'l} \delta_{m'm}$$

$$\langle \epsilon'l'm'; \vec{R}(t) | nlm; \vec{R}(t) \rangle = 0$$

$$\langle \epsilon'l'm'; \vec{R}(t) | \epsilon l m; \vec{R}(t) \rangle = \delta(\epsilon' - \epsilon) \delta_{l'l} \delta_{m'm}$$

(See Appendix E for a proof of the last relation)

- (2) The propagator, $\hat{U}(t; t_0)$, of the system is defined to have the following properties [23]

$$(a) |\Upsilon(t)\rangle = \hat{U}(t; t_0) |\Upsilon(t_0)\rangle$$

$$(b) i\hbar(\partial/\partial t)\hat{U}(t; t_0) = \hat{h}_e(\vec{R}(t))\hat{U}(t; t_0)$$

$$(c) \hat{U}(t_0; t_0) = 1$$

$\hat{U}(t; t_0)$ takes the wave function from time t_0 (initial condition) to any time t (the general solution).

Using these facts one can rigorously derive the following equation [12]

$$\hat{U}(t; t_0) = \hat{\chi}(t; t_0) - \frac{i}{\hbar} \int_{t_0}^t dt' \hat{G}(t; t') \hat{U}(t'; t_0) \quad (2-3)$$

where

$$\hat{\chi}(t; t_0) = \sum_k |k; \vec{R}(t)\rangle \exp\left(-\frac{i}{\hbar} \int_{t_0}^t dt \epsilon_k(\vec{R}(t))\right) \langle k; \vec{R}(t_0) | \quad (2-4)$$

$$\hat{G}(t; t') = \hat{\chi}(t; t') \hat{K}(t') \quad (2-5)$$

$$\hat{K}(t') = \sum_{k', k} |k'; \vec{R}(t')\rangle K_{k'k}(t') \langle k; \vec{R}(t') | \quad (2-6)$$

$$K_{k'k}(t) = \langle k'; \vec{R}(t) | -i\hbar(\partial/\partial t) | k; \vec{R}(t) \rangle \quad (2-7)$$

Here \sum_k implies summation over all discrete quantum numbers and integration over continuum energy.

$\hat{\chi}(t; t')$ is called the *adiabatic propagator*. To see the meaning of this term, expand any wave function, at time t' , in terms of the adiabatic set and propagate under $\hat{\chi}(t; t')$. We then have

$$|\Upsilon(t')\rangle = \sum_k |k; \vec{R}(t')\rangle a_k(t')$$

$$\begin{aligned} |\Upsilon_{ad}(t)\rangle &= \hat{\chi}(t; t') |\Upsilon(t')\rangle \\ &= \sum_k |k; \vec{R}(t)\rangle b_k(t) \end{aligned}$$

with

$$b_k(t) = a_k(t') \exp\left(-\frac{i}{\hbar} \int_{t'}^t dt \epsilon_k(R(t))\right)$$

Since $\epsilon_k(R(t))$ is real we have $|b_k(t)| = |a_k(t')|$. Hence $\hat{\chi}(t; t')$ propagates wave functions adiabatically.

$\hat{K}(t)$ is the *non-adiabatic coupling operator* at time t , which causes transitions among adiabatic components propagating under $\hat{U}(t; t')$.

Non-adiabatic coupling matrix elements have the following form (Chapter 5); when at least one of the states is discrete

$$K_{k'k}(t) = \frac{\langle k'; \vec{R}(t) | \hat{N} | k; \vec{R}(t) \rangle}{\epsilon_k - \epsilon_{k'}};$$

when both states are unbound

$$K_{k'k}(t) = \mathcal{P} \left[\frac{\langle k'; \vec{R}(t) | \hat{N} | k; \vec{R}(t) \rangle}{\epsilon - \epsilon'} \right] + \delta(\epsilon' - \epsilon) \langle k'; \vec{R}(t) | \hat{M} | k; \vec{R}(t) \rangle$$

Operators \hat{N} and \hat{M} include both radial and angular couplings and \mathcal{P} means that one must take the Cauchy principal part when integrating over ϵ or ϵ' .

$\hat{G}(t; t')$ may be called the *non-adiabatic propagator* in this theory.

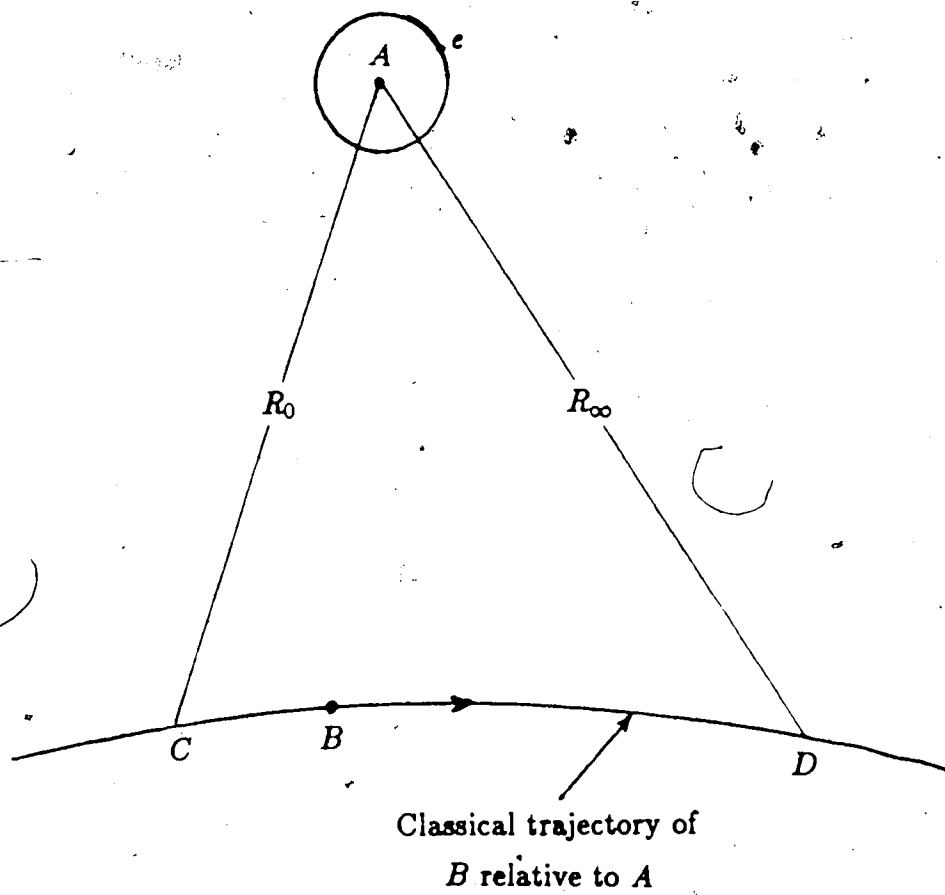
Equation (2 - 3) represents a denumerably infinite set of coupled integral equations. For a practical calculation one must discretize this set, which is achieved in the connected (or the disconnected) form of the equation. It enables one to calculate the *excitation, charge transfer* and *total ionization* probabilities.

2.2 Physical Assumptions

(1) Initially the electron is in a bound state of nucleus A. Transitions take place only when B is *within CD* (See Fig. 2 - 1) of the classical trajectory. Of course, to calculate the cross sections of transitions to each state in an asymptotically degenerate atomic manifold one has to consider the point collision long-range couplings which extend up to $R \rightarrow \infty$. We propose to handle this by analytical models [20,51]. As far as the present theory is concerned we assume the collision to be "over" when $R > R_\infty$. R_0 (point where the collision begins) and R_∞ are parameters of the theory which must be found computationally.

(2) Define a sufficiently large spherical region in physical space, centred at the centre of charge of the nuclei, as the *interaction region*. We designate the space inside the sphere as P' -space, and outside Q' -space. P' -space must include all the important bound molecular states throughout the collision. We assume that once an *ionized* electron gets out of the sphere it will never be recaptured. Implicit in this assumption is the fact that we neglect the contribution coming from Q' -space to the non-adiabatic couplings between continuum and highly Rydberg states. Lower angular momentum molecular states die down (Figures 3 - 15 \rightarrow 20) as the distance from the centre of charge increases. Hence, keeping P' -space large enough, in principle we can make the above mentioned couplings negligibly small for important continuum states. The radius of the sphere is a parameter of this theory (see Chapter 3).

Figure 2 - 1 : A binary collision



2.3 Basis Set Assumption

To evaluate the *charge transfer* and *excitation* cross sections it is sufficient to know the wave function within P' -space. The total set of adiabatic bound states can form a part of a basis describing the P' -space.

To describe the continuum we use a set of packet states defined by

$$|\bar{\phi}(jlm; \bar{R}(t))\rangle = \frac{1}{\sqrt{\Delta_j}} \int_{\epsilon_j - \frac{1}{2}\Delta_j}^{\epsilon_j + \frac{1}{2}\Delta_j} d\epsilon |elm; \bar{R}(t)\rangle \quad (2-8)$$

where

$$\epsilon_j = \frac{1}{2}\Delta_1; \quad \epsilon_{j+1} - \epsilon_j = \frac{1}{2}(\Delta_{j+1} + \Delta_j) \quad \text{for } j \geq 1$$

One can choose Δ_j so that the packets are fairly well localized in P' -space (see Chapter 4). They have the following properties.

$$\langle \bar{\phi}(j'l'm'; \bar{R}(t)) | \bar{\phi}(jlm; \bar{R}(t)) \rangle = \delta_{j'j} \delta_{l'l} \delta_{m'm} \quad (2-9a)$$

$$\langle \bar{\phi}(j'l'm'; \bar{R}(t)) | nlm; \bar{R}(t) \rangle = 0 \quad (2-9b)$$

We assume the total set of adiabatic bound states and the packet states is *complete* to describe the electronic wave function within the P' -space.

2.4 Derivation

We call the portion of the Hilbert space spanned by the above described basis, the P -space and the remainder, the Q -space. The Q -space corresponds to an ionized electron in physical Q' -space.

At any instant of time the projection operator for P -space is given by

$$\begin{aligned} \hat{P}(t) &= \hat{P}_D(t) + \hat{P}_C(t) \\ &= \sum_{nlm} |nlm; \bar{R}(t)\rangle \langle nlm; \bar{R}(t)| + \sum_{jlm} |\bar{\phi}(jlm; \bar{R}(t))\rangle \langle \bar{\phi}(jlm; \bar{R}(t))| \end{aligned} \quad (2-10)$$

At the beginning of the collision the electron is in a *bound state*; hence

$$|\Upsilon(t_0)\rangle \equiv |\Upsilon_P(t_0)\rangle \equiv \hat{P}(t_0)|\Upsilon(t_0)\rangle \quad (2-11)$$

Multiplication of equation (2-3) on the left by $\hat{P}(t)$ and on the right by $|\Upsilon(t_0)\rangle$ and, using equation (2-11) leads to the P-space projection of the wave function.

$$\begin{aligned} |\Upsilon_P(t)\rangle &= \hat{U}_{PP}(t; t_0)|\Upsilon(t_0)\rangle \\ &= \hat{\chi}_{PP}(t; t_0)|\Upsilon(t_0)\rangle - \frac{i}{\hbar} \int_{t_0}^t dt' \left(\hat{P}(t)\hat{G}(t; t')\hat{U}(t'; t_0)\hat{P}(t_0) \right) |\Upsilon(t_0)\rangle \end{aligned} \quad (2-12)$$

where the P-space projections of the operators are defined by

$$\hat{U}_{PP}(t; t') = \hat{P}(t)\hat{U}(t; t')\hat{P}(t')$$

$$\hat{\chi}_{PP}(t; t') = \hat{P}(t)\hat{\chi}(t; t')\hat{P}(t')$$

The first term in equation (2-12) takes into account the zero order adiabatic propagation of the wave function within P-space. The integrand of the second term can be interpreted as follows. It takes in the P-space portion of the wave function at time t_0 (which is equivalent to $|\Upsilon(t_0)\rangle$ itself) and propagates under \hat{U} to get the *exact* wave function at time t' . This is then "subjected" to nonadiabatic transitions and the resultant is then propagated from $t' \rightarrow t$ adiabatically. Then at time t the P-space projection is taken. According to the second physical assumption the portion of the wave function in the Q-space at any time, t' cannot give rise to a contribution to the wave function in P-space at a later time t . Hence one can insert $\hat{P}(t')$ in between $\hat{K}(t')$ and $\hat{U}(t'; t_0)$ in equation (2-12). Using the idempotency of the projection operators, we then obtain the

connected form of the coupled equations.

$$\hat{U}_{PP}(t; t_0) = \hat{\chi}_{PP}(t; t_0) - \frac{i}{\hbar} \int_{t_0}^t dt' \hat{G}_{PP}(t, t') \hat{U}_{PP}(t'; t_0) \quad (2 - 13)$$

where

$$\hat{G}_{PP}(t, t') = \hat{P}(t) \hat{G}(t, t') \hat{P}(t')$$

In equation (2 - 13) we have achieved the discretization of the adiabatic continuum allowing the ionized electrons to move out to "infinity". The truncation of the basis needs a second set of assumptions based mainly on computational experience.

- (a) The lowest few bound adiabatic states are sufficient to describe the bound manifold.
- (b) Only low "angular momentum" continuum states are important.
- (c) Only the low energy ionized electrons are important; hence a few packet states above the ionization threshold are sufficient to span the continuum manifold.

With a basis set truncation one must take into account the effects of electron translational factors which can be done by modifying the nonadiabatic coupling matrix elements [31]. (see also Chapter 5)

2.5 The Disconnected Form

Professor Thorson has further simplified $[\mathcal{G}]_{PP}$ using different assumptions in place of what is described in sections (2 - 2) and (2 - 3) and *disconnecting* $\hat{\chi}$ and \hat{K} . The disconnected form is given by [12]

$$\hat{U}_{PP}(t; t_0) = \hat{\chi}_{PP}(t; t_0) - \frac{i}{\hbar} \int_{t_0}^t dt' \hat{\chi}_{PP}(t; t') \hat{G}_{PP}(t') \hat{U}_{PP}(t'; t_0)$$

where

$$\hat{K}_{PP}(t) = \hat{P}(t)\hat{K}(t)\hat{P}(t)$$

Note that the propagation is done solely by $\hat{\chi}_{PP}(t; t')$; hence the decay factor is of the form $\sin(x)/x$ (see below). A consequence of the assumptions is that there are no packet→same packet couplings; they just strengthen the near neighbour couplings.

2.6 The Decay in the Connected form

It can be shown that

$$\begin{aligned} \hat{\chi}_{PP}(t; t') = & \sum_{nlm} |nlm; \vec{R}(t)\rangle \exp\left(-\frac{i}{\hbar} \int_{t'}^t dt \epsilon_{nlm}(R(t))\right) \langle nlm; \vec{R}(t')| \\ & + \sum_{jlm} |\tilde{\phi}(jlm; \vec{R}(t))\rangle \frac{\sin(\Delta_j \tau/2\hbar)}{(\Delta_j \tau/2\hbar)} \exp(-i\epsilon_j \tau/\hbar) \langle \tilde{\phi}(jlm; \vec{R}(t'))| \end{aligned} \quad (2-14)$$

with $\tau = t - t'$.

As τ increases the $\sin(x)/x$ factor decays rapidly which implies the probability escape from the packets during the adiabatic propagation; in zero order \hat{U}_{PP} allows the ionized electrons to move out of the P' -space. As expected a probability escape is not seen in bound state propagation.

Since the electron is in a bound state initially, what is more important is the probability loss during the non-adiabatic propagation. In deriving the expressions for these decay factors we use the following auxiliary assumptions.

- (a) ϵ_j and Δ_j are independent of (l, m) (Chapter 4).
- (b) The matrix elements of \hat{N} and \hat{M} are slowly varying functions of continuum energy so that over packet width Δ_j , they can be approximated by their values at $\epsilon = \epsilon_j$ (Chapter 6).

It is convenient to decompose $\hat{G}(t; t')$ into four components depending on the states they connect.

$$\hat{G}(t; t') = \hat{G}_{DD}(t, t') + \hat{G}_{DC}(t, t') + \hat{G}_{CD}(t, t') + \hat{G}_{CC}(t, t') \quad (2-15)$$

For example $\hat{G}_{DD}(t, t')$ propagates *discrete* states at time t' to *discrete* states at time t . Since the actual propagation in $\hat{G}(t; t')$ is done by $\hat{\chi}(t; t')$ one should anticipate that there is no probability loss from $[\hat{G}_{DD}(t, t')]_{PP}$ and $[\hat{G}_{DC}(t, t')]_{PP}$.

One can easily show that

$$[\hat{G}_{DD}(t, t')]_{PP} = \hat{P}_D(t)\hat{G}(t; t')\hat{P}_D(t') = \hat{G}_{DD}(t, t')$$

$$[\hat{G}_{DD}(t, t')]_{PP} = \sum_{n'l'm'} \sum_{nlm} \left\{ |n'l'm'; \vec{R}(t)\rangle \exp\left(-\frac{i}{\hbar} \int_{t'}^t dt \epsilon_{n'l'm'}(R(t))\right) \right. \\ \left. \times \frac{\langle n'l'm'; \vec{R}(t') | \hat{N} | nlm; \vec{R}(t') \rangle}{\epsilon_{nlm} - \epsilon_{n'l'm'}} \langle nlm; \vec{R}(t') | \right\} \quad (2-16)$$

$$[\hat{G}_{DC}(t, t')]_{PP} = \hat{P}_D(t)\hat{G}(t; t')\hat{P}_C(t')$$

It is straightforward to obtain

$$[\hat{G}_{DC}(t, t')]_{PP} = \sum_{n'l'm'} \sum_{jlm} \left\{ |n'l'm'; \vec{R}(t)\rangle \exp\left(-\frac{i}{\hbar} \int_{t'}^t dt \epsilon_{n'l'm'}(R(t))\right) \right. \\ \left. \times \frac{1}{\sqrt{\Delta_j}} \langle n'l'm'; \vec{R}(t') | \hat{N} | \epsilon_j lm; \vec{R}(t') \rangle g(n'l'm'; j) \langle \tilde{\phi}(jlm; \vec{R}(t')) | \right\}, \quad (2-17)$$

where

$$\begin{aligned}
 g(n'l'm'; j) &= \int_{-\frac{1}{2}\Delta_j}^{\frac{1}{2}\Delta_j} \frac{dx}{\epsilon_j - \epsilon_{n'l'm'} + x} \\
 &= \ln \left| \frac{\epsilon_j - \epsilon_{n'l'm'} + \frac{1}{2}\Delta_j}{\epsilon_j - \epsilon_{n'l'm'} - \frac{1}{2}\Delta_j} \right|
 \end{aligned} \tag{2-18}$$

Note that we have used the auxiliary assumption (b) in taking the nonadiabatic coupling matrix element out of the integral. The t dependence of these propagators are in the exponential factor; hence the probability is unaltered during propagation.

To see physically how the probability is lost let us examine the CD part carefully.

$$\begin{aligned}
 [\hat{G}_{CD}(t, t')]_{PP} &= \sum_{nlm} \left\{ \sum_{jlm} \langle \tilde{\phi}(j'l'm'; \vec{R}(t)) \right. \\
 &\quad \left. \times \langle \tilde{\phi}(j'l'm'; \vec{R}(t)) | \hat{\chi}(t, t') \hat{K}(t') | nlm; \vec{R}(t') \rangle \right\} \langle nlm; \vec{R}(t') |
 \end{aligned} \tag{2-19}$$

The interpretation of the operation within the curly brackets is as follows: $\hat{K}(t')$ mixes $|nlm; \vec{R}(t')\rangle$ with other states at t' and the resultant is propagated adiabatically. Then at time t , the projection is taken onto the packet states. Note that the propagation of the continuum states is done using the true continuum states. Hence, on physical grounds, we expect a probability loss; similar considerations apply for $[\hat{G}_{CC}(t, t')]_{PP}$.

One can show that

$$[\hat{G}_{CD}(t, t')]_{PP} = \hat{P}_C(t) \hat{G}(t, t') \hat{P}_D(t')$$

$$\begin{aligned} [\hat{G}_{CD}(t, t')]_{PP} = & \sum_{j'l'm'} \sum_{nlm} \left\{ |\bar{\phi}(j'l'm'; \vec{R}(t))\rangle \exp(-i\epsilon_{j'}\tau/\hbar) \right. \\ & \left. \times \frac{1}{\sqrt{\Delta_{j'}}} \langle \epsilon_{j'}l'm'; \vec{R}(t') | \hat{N} | nlm; \vec{R}(t') \rangle g(j'; nlm; \tau) \langle nlm; \vec{R}(t') | \right\} \end{aligned} \quad (2-20)$$

$$g(j'; nlm; \tau) = - \int_{-\frac{1}{2}\Delta_{j'}}^{\frac{1}{2}\Delta_{j'}} dx \frac{[\cos(\tau x/\hbar) - i \sin(\tau x/\hbar)]}{\epsilon_{j'} - \epsilon_{nlm} + x} \quad (2-21)$$

In deriving equation (2 - 20) we have used the auxiliary assumption (b) and the fact that the continuum state energies are independent of R .

Using the formulae given on page 187 of Ref. 52, one can evaluate the integrals in equation (2 - 21) to obtain the following expression for the decay factor.

$$\begin{aligned} g(j'; nlm; \tau) = & \exp(i(\epsilon_{j'} - \epsilon_{nlm})\tau/\hbar) \left\{ Ci \left((\epsilon_{j'} - \epsilon_{nlm} - \frac{1}{2}\Delta_{j'})\tau/\hbar \right) \right. \\ & - Ci \left((\epsilon_{j'} - \epsilon_{nlm} + \frac{1}{2}\Delta_{j'})\tau/\hbar \right) - i \left[Si \left((\epsilon_{j'} - \epsilon_{nlm} - \frac{1}{2}\Delta_{j'})\tau/\hbar \right) \right. \\ & \left. \left. - Si \left((\epsilon_{j'} - \epsilon_{nlm} + \frac{1}{2}\Delta_{j'})\tau/\hbar \right) \right] \right\} \end{aligned} \quad (2-22)$$

Mathematical properties of $Si(x)$ and $Ci(x)$ are listed in Chapter 5 of Ref. 53.

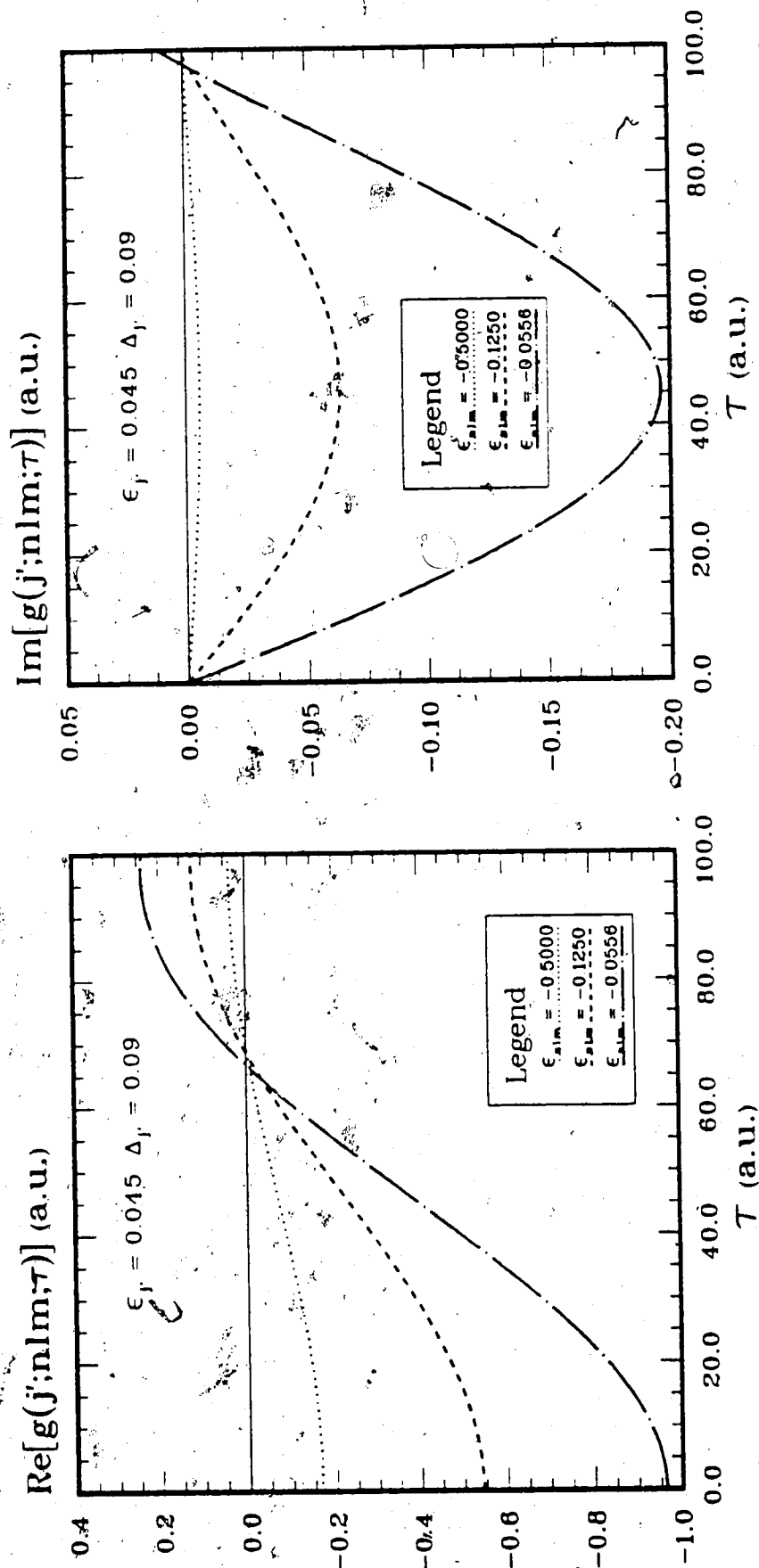
Using

$$\lim_{x \rightarrow -\infty} Si(x) = \frac{\pi}{2} \quad \lim_{x \rightarrow -\infty} Ci(x) = 0$$

we obtain

$$\lim_{\tau \rightarrow \infty} g(j'; nlm; \tau) = 0$$

For finite τ we have displayed $g(j'; nlm; \tau)$ for a number of ϵ_{nlm} ($= 1/2, -1/8, -1/18$) and $(\epsilon_{j'}, \Delta_{j'})$ (taken from table 4 - 4) in Figures 2 - 2→4. Though the imaginary parts increase in magnitude initially, they are small compared to the real parts and the overall effect is a general decay.

Figure 2 - 2 : $g(j';nlm;\tau)$ vs. τ

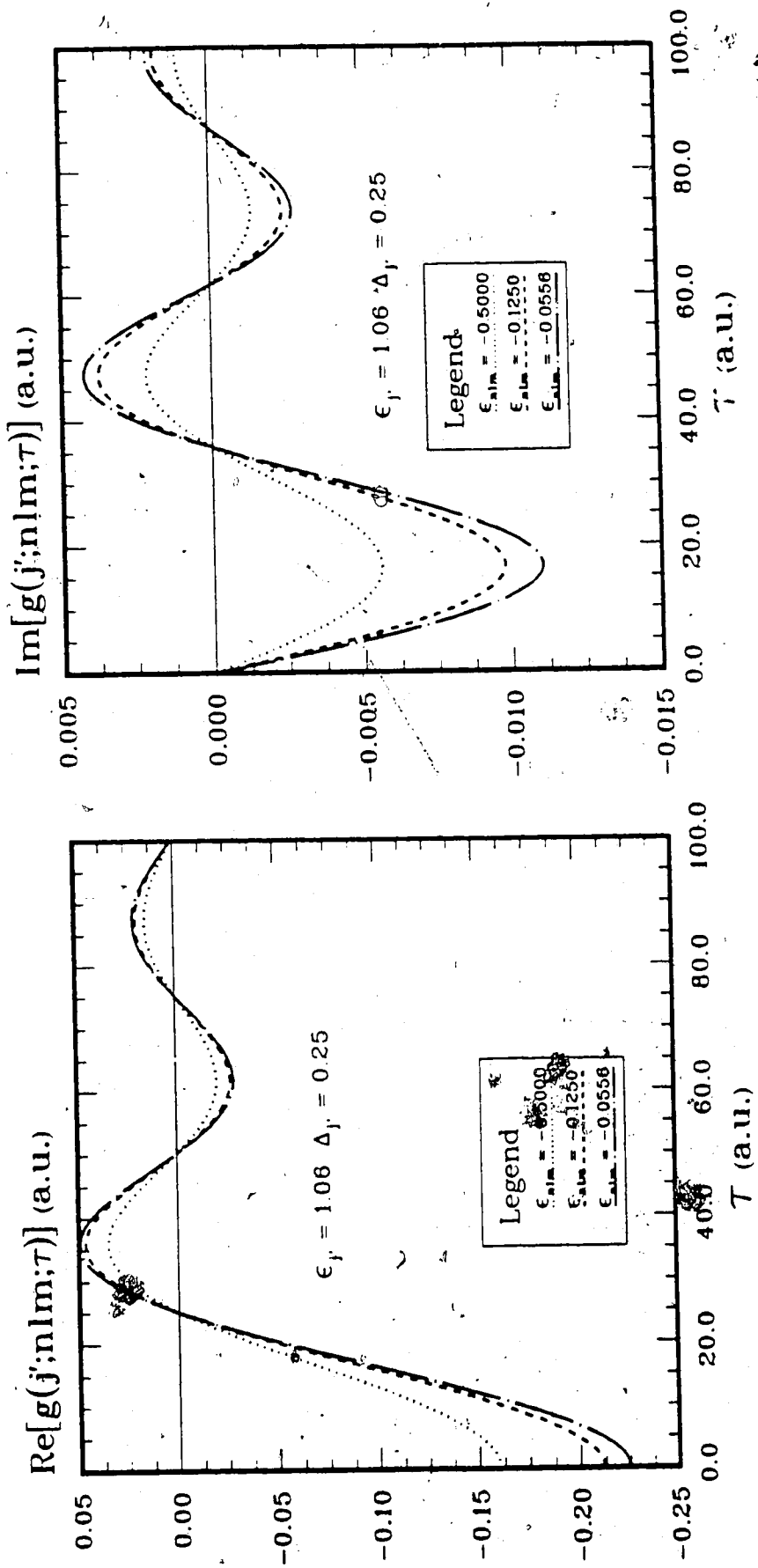


Figure 2 - 3 : $g(j';nlm;\tau)$ vs. τ

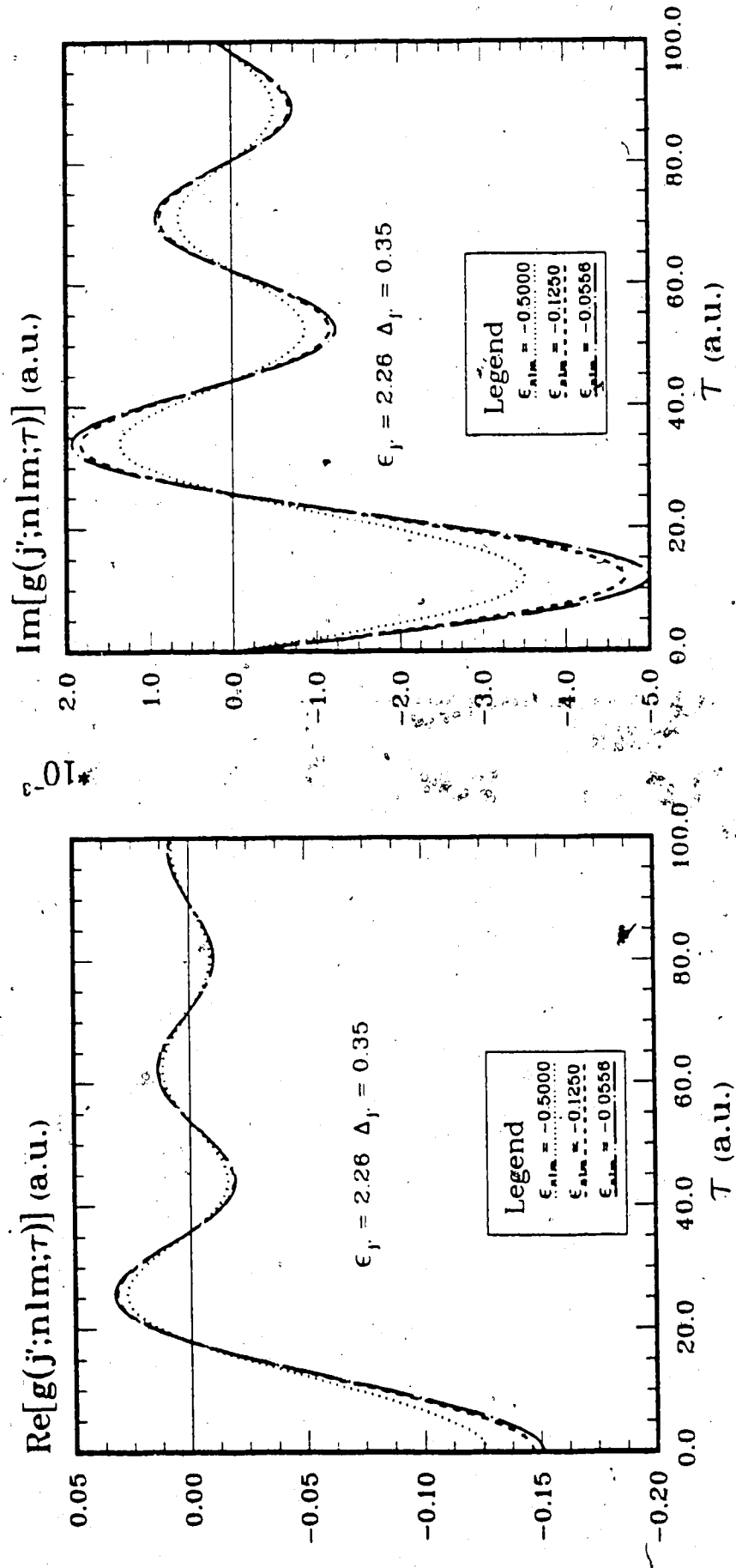


Figure 2 - 4: $g(j';nlm;\tau)$ vs. τ

Projection of the CC part can be done as follows.

$$\left[\hat{G}_{CC}(t, t') \right]_{PP} = \hat{P}_C(t) \hat{G}(t; t') \hat{P}_C(t')$$

Using the auxiliary assumptions (a) and (b) we then have

$$\begin{aligned} \left[\hat{G}_{CC}(t, t') \right]_{PP} &= \sum_{l'm'} \sum_{lm} \sum_{j'j} \left\{ \langle \tilde{\phi}(j'l'm'; \vec{R}(t)) \rangle \exp(-i\epsilon_j \tau / \hbar) \right. \\ &\quad \times \frac{1}{\sqrt{\Delta_{j'} \Delta_j}} \left[\langle \epsilon_j l' m'; \vec{R}(t') | \hat{N} | \epsilon_j l m; \vec{R}(t') \rangle g^P(j'; j; \tau) \right. \\ &\quad \left. \left. + \delta_{jj'} \langle \epsilon_j l' m'; \vec{R}(t') | \hat{M} | \epsilon_j l m; \vec{R}(t') \rangle g^\delta(j; \tau) \right] \langle \tilde{\phi}(jlm; \vec{R}(t')) \rangle \right\} \end{aligned} \quad (2-23)$$

It is straight forward to perform the integration over $\delta(\epsilon' - \epsilon)$ to obtain

$$\begin{aligned} g^\delta(j; \tau) &= \int_{-\frac{1}{2}\Delta_j}^{\frac{1}{2}\Delta_j} dy \exp(-iy\tau/\hbar) \int_{-\frac{1}{2}\Delta_j}^{\frac{1}{2}\Delta_j} dx \delta(x-y) \\ &= \frac{\Delta_j}{2} \left(\frac{\sin(\Delta_j \tau / 2\hbar)}{(\Delta_j \tau / 2\hbar)} \right) \end{aligned} \quad (2-24)$$

We have

$$g^P(j'; j; \tau) = \mathcal{P} \left[\int_{-\frac{1}{2}\Delta_{j'}}^{\frac{1}{2}\Delta_{j'}} dy \exp(-iy\tau/\hbar) \int_{-\frac{1}{2}\Delta_j}^{\frac{1}{2}\Delta_j} \frac{-dx}{\epsilon_j - \epsilon_{j'} - y + x} \right] \quad (2-25)$$

One can show that if $g^P = \alpha + i\beta$ for $(\epsilon_j - \epsilon_{j'}) > 0$, where α and β are real, then $g^P = -\alpha + i\beta$ for $\epsilon_j - \epsilon_{j'} < 0$. Hence we work out the expressions only for the former and $j = j'$ cases.

Case-1: $j > j' + 1$

Here $(\epsilon_j - \epsilon_{j'} - y + x)$ is never zero and equation (2-25) becomes an ordinary double integral. Performing the integral over x we obtain

$$g^P(j'; j; \tau) = X_+ - X_- \quad (2-26)$$

$$X_{\pm} = \int_{-\frac{1}{2}\Delta_{j'}}^{\frac{1}{2}\Delta_{j'}} dy \exp(-i\tau y/\hbar) \ln|\alpha_{\pm} - y| \quad (2-27)$$

$$\alpha_{\pm} = \epsilon_j - \epsilon_{j'} \pm \frac{1}{2}\Delta_j \quad (2-28)$$

Integration by parts gives

$$X_{\pm} = \frac{i\hbar}{\tau} \left\{ \left[\exp(-i\tau y/\hbar) \ln|\alpha_{\pm} - y| \right]_{-\frac{1}{2}\Delta_{j'}}^{\frac{1}{2}\Delta_{j'}} + \int_{-\frac{1}{2}\Delta_{j'}}^{\frac{1}{2}\Delta_{j'}} dx \frac{\exp(-i\tau y/\hbar)}{\alpha_{\pm} - y} \right\} \quad (2-29)$$

The remaining integral in equation (2-29) similar to the one in equation (2-21).

In addition using $Ci(-x) = Ci(x) + \pi/2$ and $Si(-x) = Si(x)$ we obtain

$$\begin{aligned} g^P(j'; j; \tau) = & \frac{i\hbar}{\tau} \left\{ \exp(-i\Delta_{j'}\tau/2\hbar) \ln \left| \frac{\alpha_+ - \frac{1}{2}\Delta_{j'}}{\alpha_- - \frac{1}{2}\Delta_{j'}} \right| - \exp(i\Delta_{j'}\tau/2\hbar) \ln \left| \frac{\alpha_+ + \frac{1}{2}\Delta_{j'}}{\alpha_- + \frac{1}{2}\Delta_{j'}} \right| \right. \\ & + \exp(-i\alpha_+\tau/\hbar) \left[Ci \left((\alpha_+ + \frac{1}{2}\Delta_{j'})\tau/\hbar \right) - Ci \left((\alpha_+ - \frac{1}{2}\Delta_{j'})\tau/\hbar \right) \right] \\ & - \exp(-i\alpha_-\tau/\hbar) \left[Ci \left((\alpha_- + \frac{1}{2}\Delta_{j'})\tau/\hbar \right) - Ci \left((\alpha_- - \frac{1}{2}\Delta_{j'})\tau/\hbar \right) \right] \\ & + i \exp(-i\alpha_+\tau/\hbar) \left[Si \left((\alpha_+ + \frac{1}{2}\Delta_{j'})\tau/\hbar \right) - Si \left((\alpha_+ - \frac{1}{2}\Delta_{j'})\tau/\hbar \right) \right] \\ & \left. - i \exp(-i\alpha_-\tau/\hbar) \left[Si \left((\alpha_- + \frac{1}{2}\Delta_{j'})\tau/\hbar \right) - Si \left((\alpha_- - \frac{1}{2}\Delta_{j'})\tau/\hbar \right) \right] \right\} \quad (2-30) \end{aligned}$$

Case-2: $j = j' + 1$

Here we have $\epsilon_j - \epsilon_{j'} - \frac{1}{2}(\Delta_j + \Delta_{j'}) = 0$. By taking this limit in (2-30)

we obtain

$$\begin{aligned}
 g^P(j'; j; \tau) = & \frac{i\hbar}{\tau} \left\{ \exp(-i\Delta_{j'}\tau/2\hbar) \ln \left| \left(\alpha_+ - \frac{1}{2}\Delta_{j'} \right) \right| \right. \\
 & - \exp(i\Delta_{j'}\tau/2\hbar) \ln \left| \frac{\alpha_+ + \frac{1}{2}\Delta_{j'}}{\alpha_- + \frac{1}{2}\Delta_{j'}} \right| \\
 & + \exp(-i\alpha_+\tau/\hbar) \left[Ci \left(\left(\alpha_+ + \frac{1}{2}\Delta_{j'} \right) \tau/\hbar \right) - Ci \left(\left(\alpha_+ - \frac{1}{2}\Delta_{j'} \right) \tau/\hbar \right) \right] \\
 & - \exp(-i\alpha_-\tau/\hbar) \left[Ci \left(\left(\alpha_- + \frac{1}{2}\Delta_{j'} \right) \tau/\hbar \right) - \gamma - \ln|\tau/\hbar| \right] \\
 & + i \exp(-i\alpha_+\tau/\hbar) \left[Si \left(\left(\alpha_+ + \frac{1}{2}\Delta_{j'} \right) \tau/\hbar \right) - Si \left(\left(\alpha_+ - \frac{1}{2}\Delta_{j'} \right) \tau/\hbar \right) \right] \\
 & \left. - i \exp(-i\alpha_-\tau/\hbar) \left[Si \left(\left(\alpha_- + \frac{1}{2}\Delta_{j'} \right) \tau/\hbar \right) \right] \right\}
 \end{aligned} \tag{2-31}$$

In deriving equation (2 - 31) we have used the relation

$$Ci(x) \rightarrow \gamma + \ln(x) + O(x^2) \quad \text{as } x \rightarrow 0$$

where $\gamma = 0.577215\dots = \text{Euler's Constant}$

Case-3: $j = j'$

In this case $\epsilon_j - \epsilon_{j'} = 0$ and we have

$$\begin{aligned}
 g^P(j; j; \tau) &= \lim_{\delta \rightarrow 0^+} \int_{-\frac{1}{2}\Delta_j + \delta}^{\frac{1}{2}\Delta_j - \delta} dy \exp(-iy\tau/\hbar) \left[\mathcal{P} \int_{-\frac{1}{2}\Delta_j}^{\frac{1}{2}\Delta_j} \frac{dx}{x-y} \right] \\
 &= \lim_{\delta \rightarrow 0^+} \int_{-\frac{1}{2}\Delta_j + \delta}^{\frac{1}{2}\Delta_j - \delta} dy \exp(-iy\tau/\hbar) \left[\ln \left| \frac{1}{2}\Delta_j - y \right| - \ln \left| \frac{1}{2}\Delta_j + y \right| \right]
 \end{aligned} \tag{2-32}$$

It is clear that $g^P(j; j; \tau)$ can be obtained from equation (2 - 30) by substituting

$\epsilon_j - \epsilon_{j'} = 0$ and $\frac{1}{2}\Delta_j = \frac{1}{2}\Delta_{j'} - \delta$ and, taking the limit $\delta \rightarrow 0^+$.

$$g^P(j; j; \tau) = \frac{2i\hbar}{\tau} \left\{ \cos(\Delta_j \tau / 2\hbar) [Ci(\Delta_j \tau / \hbar) - \gamma - \ln(\Delta_j \tau / \hbar)] + \sin(\Delta_j \tau / 2\hbar) Si(\Delta_j \tau / \hbar) \right\} \quad (2-33)$$

In all cases one can show that

$$\lim_{\tau \rightarrow \infty} g^P(j'; j; \tau) = 0$$

We have displayed $g^P(j'; j; \tau)$ for $j' \neq j$ in Figures 2-5→7. Overall decay is apparent.

The function $g^P(j; j; \tau)$, which is shown in Figure 2-8 is purely imaginary. It increases at the beginning. For near-neighbour packets it is reasonable to assume that the matrix elements of \hat{N} are approximately equal. The decay is apparent when $g^P(j; j; \tau)$ and $g^P(j; j \pm 1; \tau)$ are taken together.

Probability escape in g^δ is shown in Figure 2-9.

2.7 Discussion

\hat{U}_{PP} computed from equations (2-13) generates a *P-subspace* state vector, $|\Upsilon_P(t)\rangle$, from a *P-subspace* state vector at time t_0 . Since the *P'*-space is localized such an operator cannot describe a system with an initial state having an unbound electron.

Because of the probability escape, \hat{U}_{PP} is non-unitary; probability amplitude for a given basis state at time t depend, in principle, on the amplitudes on all basis states at *all previous times* t' . Hence the integral equation for \hat{U}_{PP} cannot be converted into an equivalent differential equation.

\hat{U}_{PP} allows one to calculate the total probability of finding the electron in a bound state at time t . The discrepancy between this number and unity

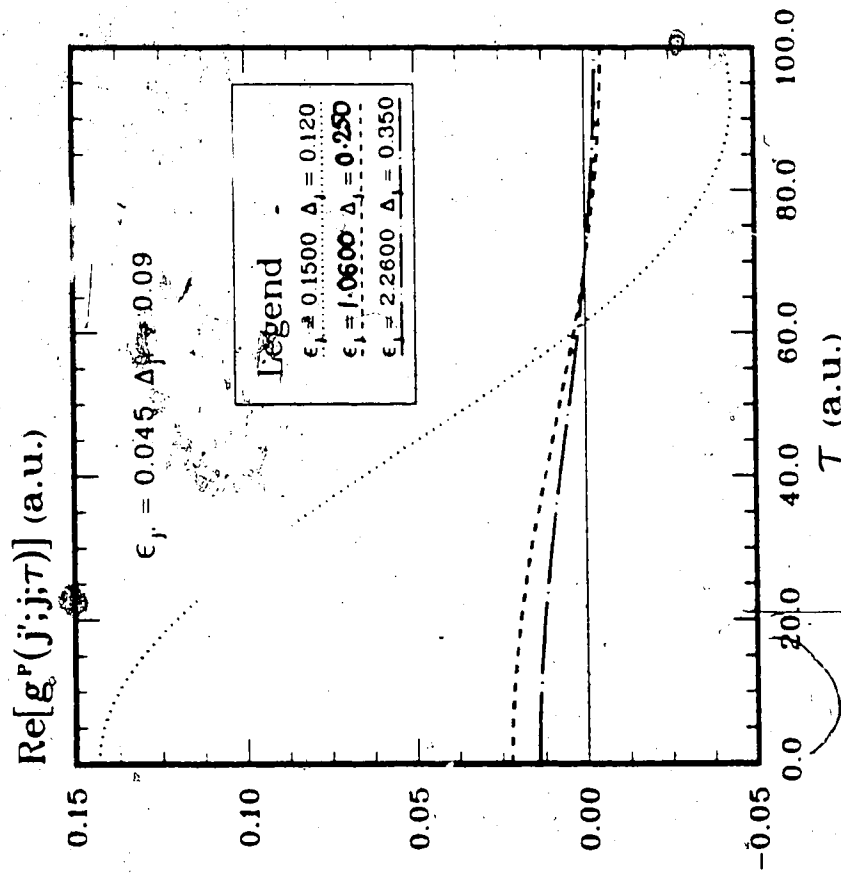
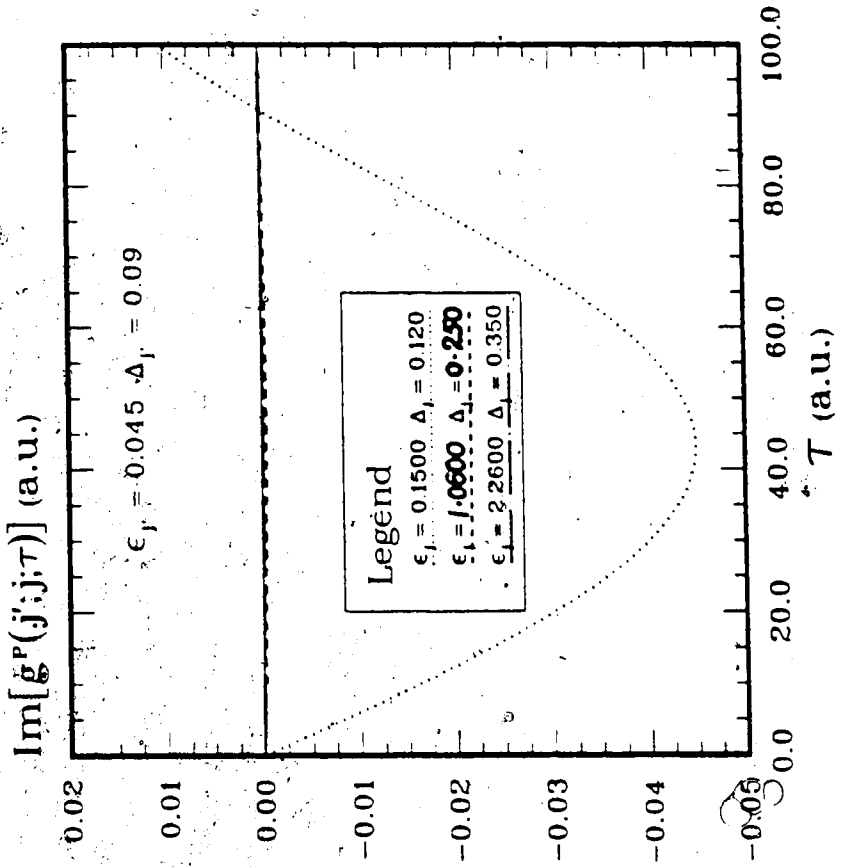


Figure 2 - 5 : $g^P(j';j;\tau)$ vs. τ

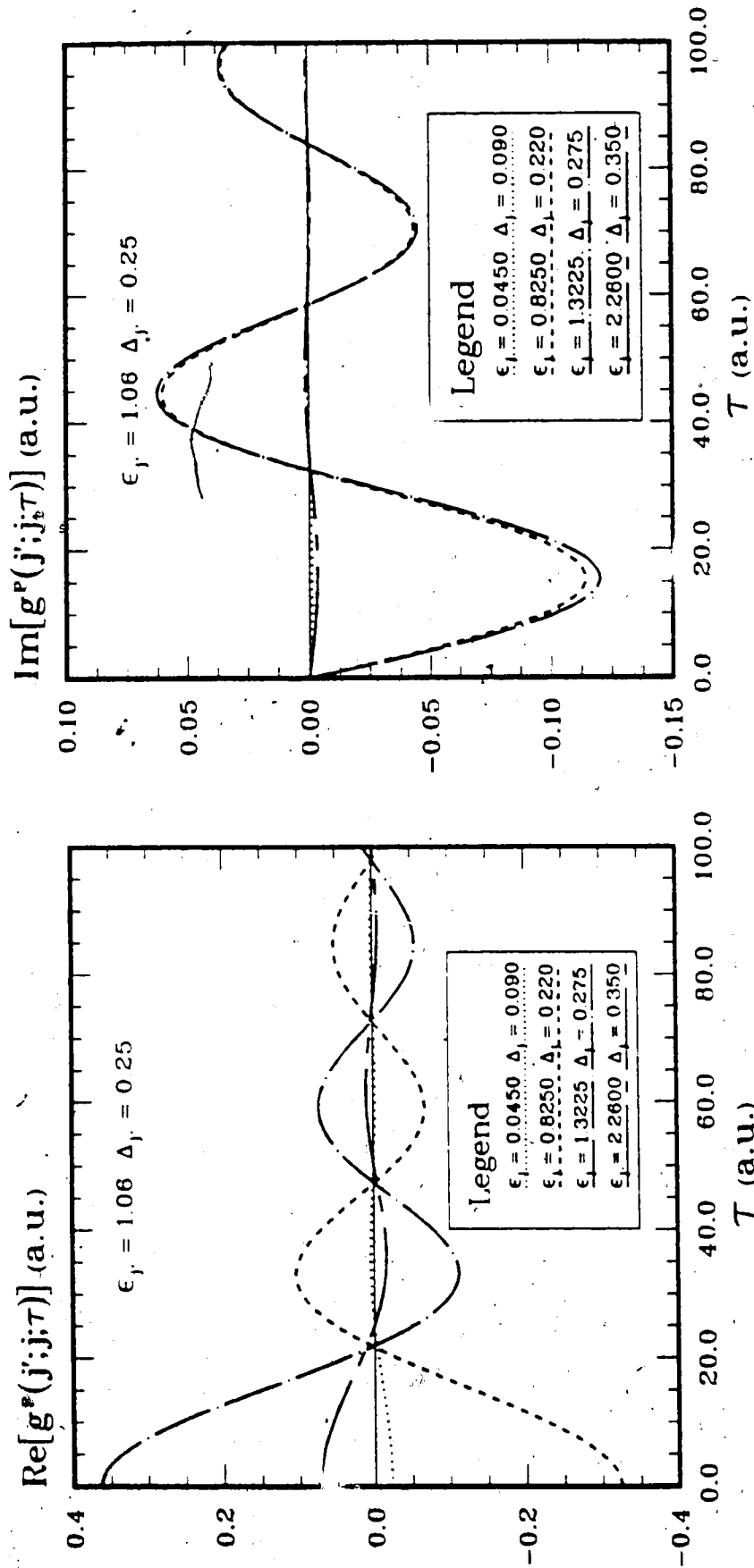


Figure 2 - 6 : $g^P(j; j; \tau)$ vs. τ

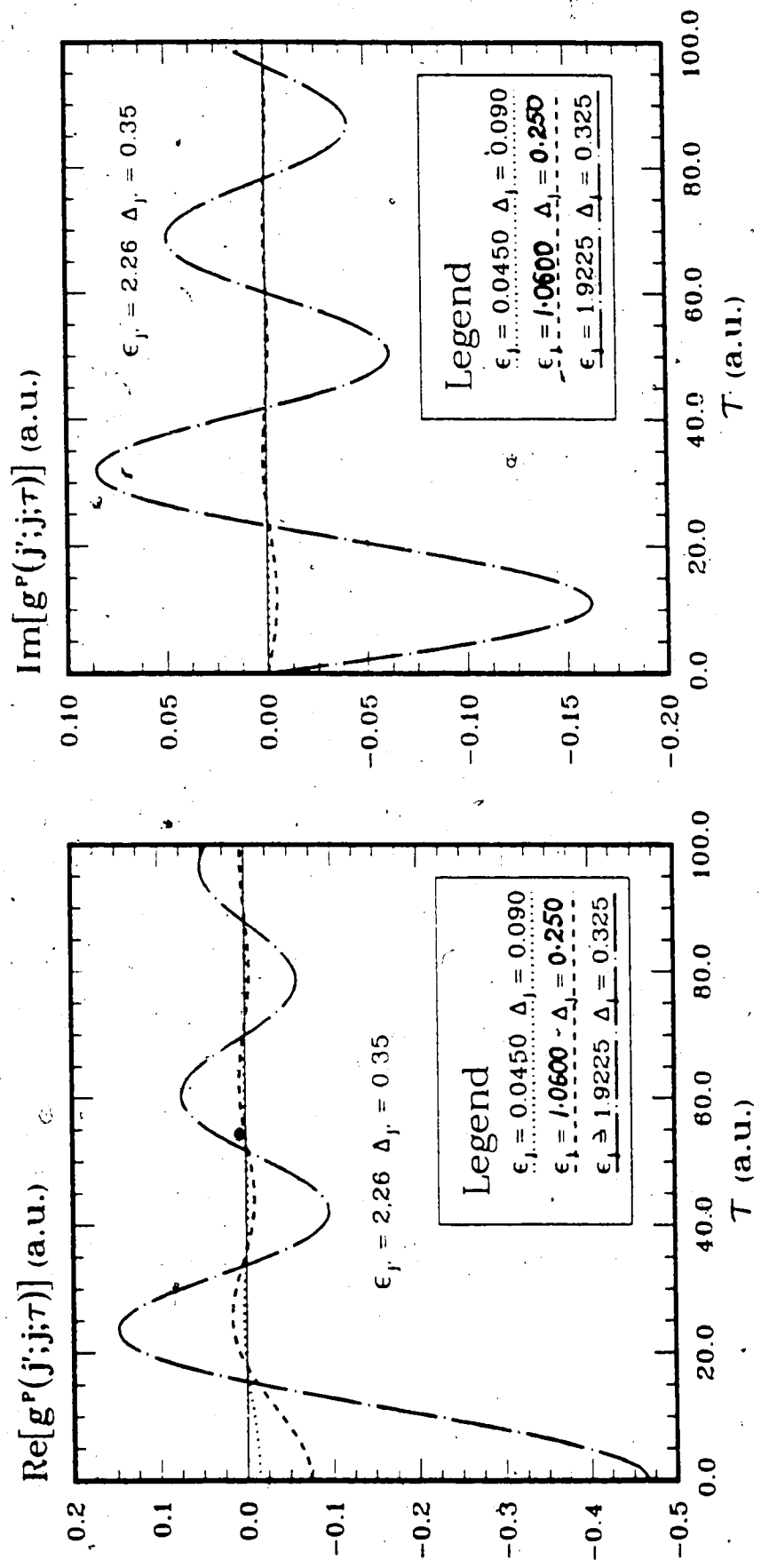
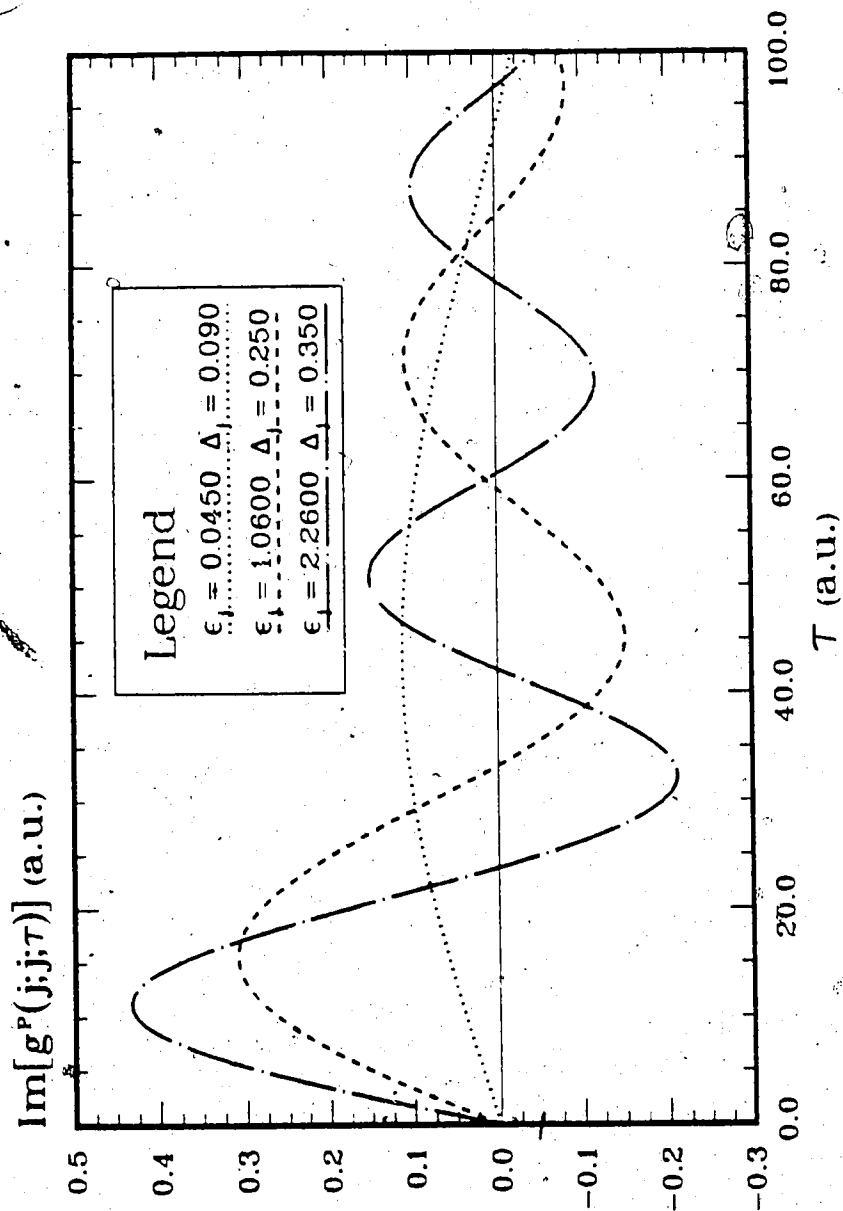
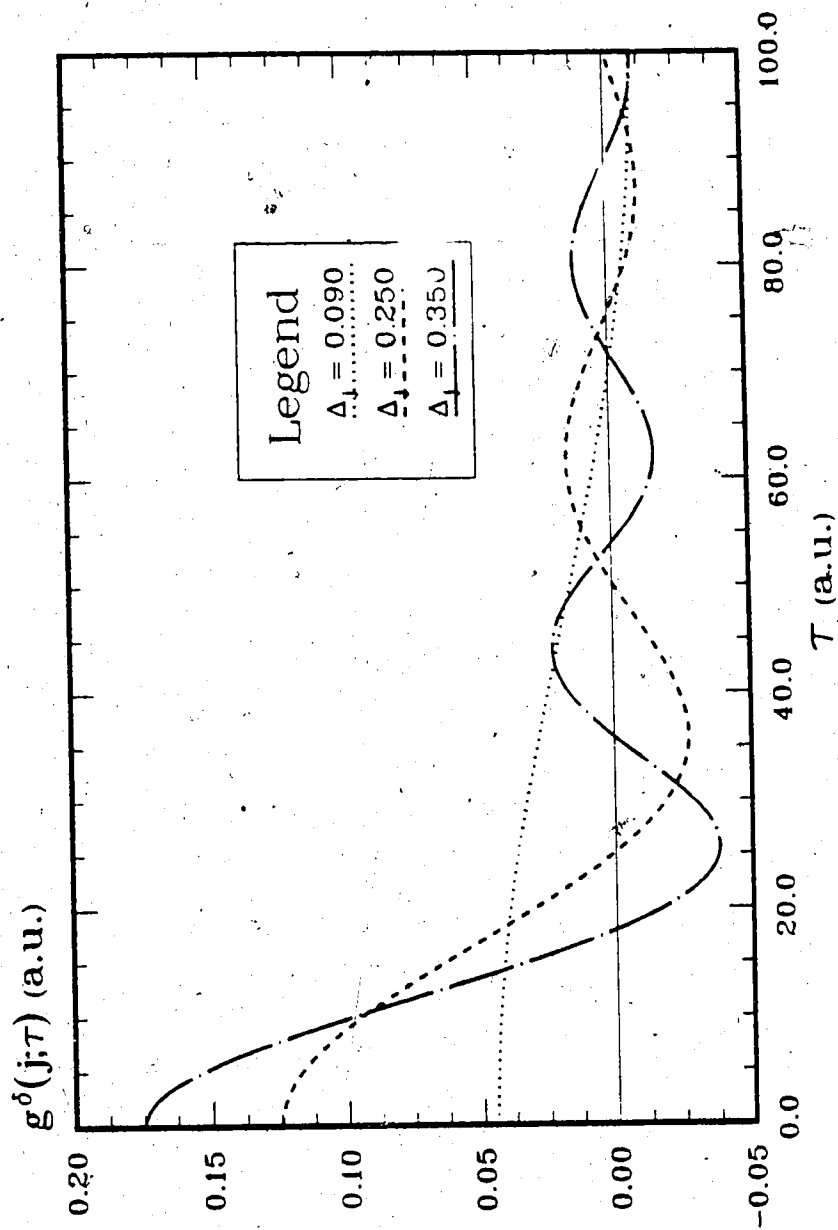


Figure 2 - 7 : $g^P(j';j;\tau)$ vs. τ

Figure 2 - 8 : $g^P(j;j;\tau)$ vs. τ

Figure 2 - 9 : $g^\delta(j;\tau)$ vs. τ

at the "end" of the collision, i.e. when $R = R_\infty$, can be interpreted as the total ionization probability. Note that this is not equal to the total probability of finding the electron in packet states at that time.

At $R = R_\infty$, there will be some *non-zero* amplitudes in packet states. We assume that there are no significant packet \rightarrow bound state transitions in spite of the fact that there may be packet \rightarrow packet state transitions. Using the spatial distributions of packet states, we will show in Chapter 4 that this assumption is self consistent with the use of packet states to span the continuum.

3. ONE - ELECTRON - TWO - CENTRE CONTINUUM STATES

3.1 Introduction

Born - Oppenheimer or *adiabatic* states, $\psi(\vec{r})$, for a given internuclear separation, are obtained by solving the time independent Schrödinger equation in a molecule fixed reference frame (see Figure 3-1). In atomic units we have

$$\left[-\frac{1}{2} \nabla_{\vec{r}}^2 - \frac{Z_A}{r_A} - \frac{Z_B}{r_B} \right] \psi(\vec{r}) = \epsilon \psi(\vec{r}) \quad (3-1)$$

For efficient evaluation of nonadiabatic coupling matrix elements and for the study of the spatial distributions of the functions themselves (or wave packets) it is desirable to generate $\psi(\vec{r})$ in a global representation. In this chapter we develop such a representation for continuum states.

It is well known [55] that equation (3-1) is separable in prolate spheroidal coordinates (see Figure 3-1).

$$\psi(\vec{r}) = \chi(\xi) S(\eta) \frac{\exp(im\phi)}{\sqrt{2\pi}} \quad (3-2)$$

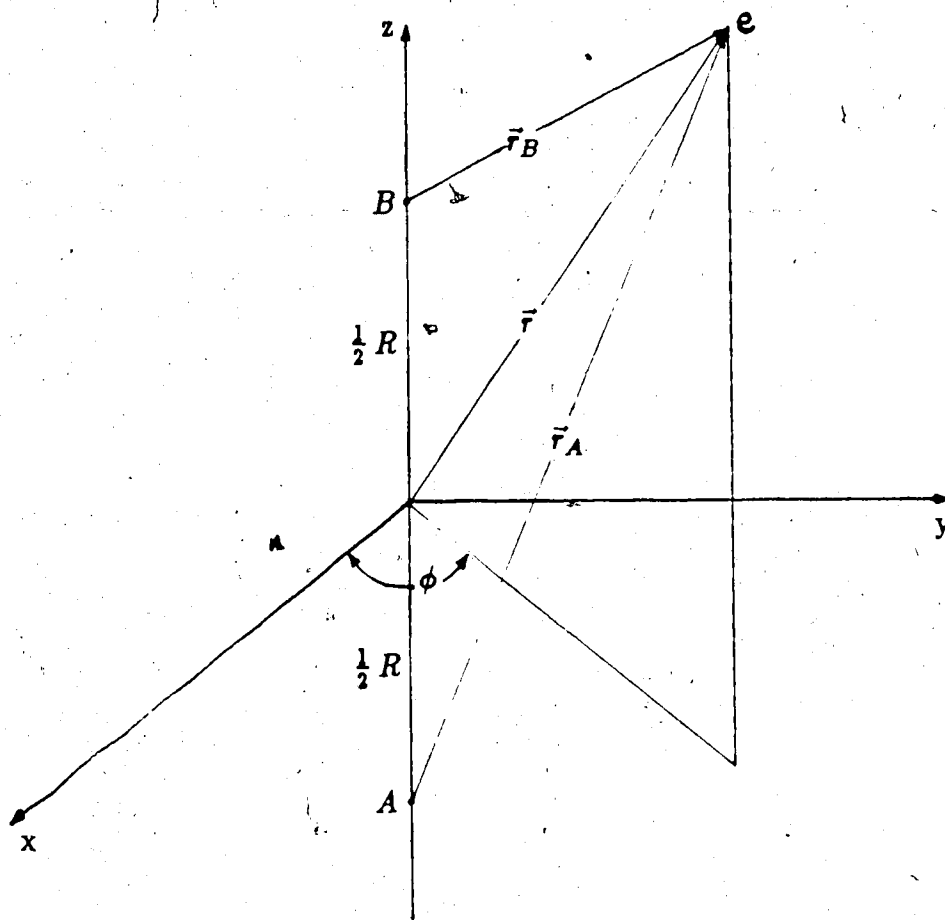
$$\frac{d}{d\eta} \left[(1-\eta^2) \frac{dS}{d\eta} \right] + \left[p\eta - c^2\eta^2 + A - \frac{m^2}{1-\eta^2} \right] S = 0 \quad (3-3)$$

$$\frac{d}{d\xi} \left[(\xi^2 - 1) \frac{d\chi}{d\xi} \right] + \left[q\xi + c^2\xi^2 - A - \frac{m^2}{\xi^2 - 1} \right] \chi = 0 \quad (3-4)$$

$$p = R(Z_B - Z_A) \quad q = R(Z_B + Z_A) \quad c^2 = \frac{\epsilon R^2}{2} \quad (3-5)$$

Equations (3-3) and (3-4) are known as the *angular* and *radial* equations. A and c^2 are separation constants; c^2 is negative for bound states and positive for continuum states.

Figure 3 - 1 : Prolate Spheroidal Coordinates



$$\xi = (r_A + r_B)/R$$

$$1 \leq \xi < \infty$$

$$\eta = (r_A - r_B)/R$$

$$-1 \leq \eta \leq +1$$

$$\phi = \text{azimuthal angle}$$

$$0 \leq \phi < 2\pi$$

In the united atom limit each $\psi(\vec{r})$ becomes an atomic state with good angular momentum quantum numbers (l, m) [28]. Based on this correlation the indices (l, m) may be used also as part of the molecular state label.

3.1.1 Bound States

Both c^2 and A are unknowns; one has to solve equations (3 - 3) and (3 - 4) as coupled equations to evaluate them. Using the method of Bates and Carson [56], Rankin [30b] has developed a computer code to generate bound state adiabatic states. The angular wave function is generated in two representations.

$$S(\eta) = \sum_{j=M}^{\infty} \alpha_j P_j^M(\eta) \quad (3-6)$$

$$S(\eta) = (1 - \eta^2)^{\frac{M}{2}} \sum_{j=0}^{\infty} \beta_j \eta^j \quad (3-7)$$

where $M = |m|$ and P_j^M are *Associated Legendre Polynomials*. The radial wave function is generated in the form

$$\chi(\xi) = \exp(-|c|\xi) (\xi^2 - 1)^{\frac{M}{2}} (\xi + 1)^{\sigma} \sum_{j=0}^{\infty} \gamma_j \left(\frac{\xi - 1}{\xi + 1} \right)^j \quad (3-8)$$

where $\sigma = q/(2|c|) - M - 1$.

Equations (3 - 6) or (3 - 7) plus equation (3 - 8) gives a *global* representation of a bound state. (Reference 57 gives some other formal representations)

3.1.2 Continuum States

In this case c^2 is not an unknown; we specify it by fixing the energy. Solving the eigenvalue problem for equation (3 - 3), one then determines A and $S(\eta)$ [58]. $S(\eta)$ can be generated in either of the forms (3 - 6) or (3 - 7); we calculated it in the latter form using Rankin's programs [30b]. The form in equation (3 - 8) is *not* useful for $\chi(\xi)$.

Bates *et al.* [59], Ponomarev and Somov [58] and Rankin and Thorson [60] have generated $\chi(\xi)$ by numerically integrating a second order differential equation related to equation (3 - 4). Cayford *et al.* [61] have integrated equation (3 - 4) using a finite difference technique. All these methods yield $\chi(\xi)$ in a point wise representation. Greenland and Greiner [62] have have constructed $\chi(\xi)$ as an expansion in Associated Legendre functions of the first kind. Though a global representation, it is not very useful for a practical calculation.

3. 1. 3 Phase-Amplitude Form

Milne [63] has shown that *bound state* solutions to a one-dimensional Schrödinger equation can be represented in the *phase - amplitude* form

$$\Psi(x) = a \omega(x) \sin\left(\int^x \left(\frac{dx}{\omega^2(x)}\right) + b\right) \quad (3 - 9)$$

where a and b are constants,

Milne's Function $\omega(x)$ is a solution of the second order differential equation (3 - 23), called *Milne's equation*. It is known [64,65] that one can obtain a *slowly varying* function $\omega(x)$ by choosing proper boundary conditions for equation (3 - 23). This slowly varying character of $\omega(x)$ greatly enhances the speed of numerical computation of $\Psi(x)$ in comparison to direct numerical integration of the radial Schrödinger equation. This representation was used for continuum states by Wheeler [66] for the determination of scattering phase shifts.

We have opted to calculate the radial part of the wave function in the phase amplitude form for the following reasons:

- (1) computational efficiency.
- (2) the method proposed to choose the *packet widths* (see Chapter 4) is based on the form given in equation (3 - 9) for adiabatic continuum radial wave functions.

(3) we may obtain an *accurate* and *practical* global representation for $\chi(\xi)$ by fitting the slowly varying $\omega^{-2}(\xi)$ with a simple algebraic function.

3.2 Continuum radial wave functions in Phase-Amplitude form

3.2.1 The General Solution of equation (3 - 4)

Define the function $f(\xi)$ by

$$\chi(\xi) = \frac{1}{\sqrt{\xi^2 - 1}} f(\xi) \quad (3-10)$$

Then $f(\xi)$ satisfies

$$\frac{d^2 f}{d\xi^2} + k^2(\xi) f = 0 \quad (3-11)$$

where

$$k^2(\xi) = \frac{1}{\xi^2 - 1} \left[c^2 \xi^2 + q\xi - A + \frac{1 - m^2}{\xi^2 - 1} \right] \quad (3-12)$$

k^2 is real since the separation constant A is real [58].

We seek solutions of equation (3 - 11) in the form

$$f^\pm(\xi) = \exp\left(\pm i \int^\xi d\xi P_\pm(\xi)\right) \quad (3-13)$$

The *quantal momentum*, P_\pm , will in general be complex. Substitution in equation (3 - 11) gives

$$P_+^2 - i \frac{dP_+}{d\xi} = k^2 \quad (3-14)$$

$$P_-^2 + i \frac{dP_-}{d\xi} = k^2 \quad (3-15)$$

Since k^2 is real P_+ and P_- can have the relation

$$P_- = P_+^* \quad (3-16)$$

where P_+^* is the complex conjugate of P_+ . Since any pair of linearly independent solutions, $\{P_+, P_-\}$, gives two linearly independent solutions of equation (3 - 11), without loss of generality we can impose the condition in equation (3 - 16).

Define the real functions $P_R(\xi)$ and $P_I(\xi)$ by

$$P_{\pm}(\xi) = P_R(\xi) \pm iP_I(\xi) \quad (3 - 17)$$

Substitution in equation (3 - 14) gives

$$P_I = \frac{1}{2P_R} \left(\frac{dP_R}{d\xi} \right) \quad (3 - 18)$$

Then it follows that

$$f^{\pm}(\xi) = \frac{\exp\left(\pm i \int^{\xi} d\xi P_R(\xi)\right)}{\sqrt{P_R(\xi)}} \quad (3 - 19)$$

Two real linearly independent solutions of equation (3 - 4) can now be written as

$$\chi(\xi) = \frac{a \sin(\Theta(\xi))}{\sqrt{(\xi^2 - 1) P_R(\xi)}} \quad (3 - 20a)$$

$$\tilde{\chi}(\xi) = \frac{a \cos(\Theta(\xi))}{\sqrt{(\xi^2 - 1) P_R(\xi)}} \quad (3 - 20b)$$

$$\Theta(\xi) = \int_1^{\xi} d\xi P_R(\xi) + b \quad (3 - 21)$$

where a and b are real constants.

Note that since we assume P_R to be integrable in the domain $1 \leq \xi < \infty$ without loss of generality we can introduce a lower limit to the integral.

Using the equations (3 - 14), (3 - 17) and (3 - 18) it can easily be verified that

$$\omega(\xi) = \frac{1}{\sqrt{P_R(\xi)}} \quad (3 - 22)$$

satisfies Milne's equation

$$\frac{d^2\omega(\xi)}{d\xi^2} + k^2(\xi)\omega(\xi) = \frac{1}{\omega^3(\xi)} \quad (3 - 23)$$

3.2.2 A General Solution to Milne's equation

A general solution to the equation (3 - 23) which is useful in determining the behavior of P_R (and P_I) near the *origin* can be derived as follows.

Denote the two real linearly independent solutions of equation (3 - 11) by $\psi_1(\xi)$ and $\psi_2(\xi)$. Then using equations (3 - 20) we have

$$\alpha\psi_1 = \frac{\sin \Theta}{\sqrt{P_R}} \quad (3 - 24a)$$

$$\alpha(\beta\psi_1 + \gamma\psi_2) = \frac{\cos \Theta}{\sqrt{P_R}} \quad (3 - 24b)$$

where α , β and γ are constants. Note that because of the linear independence of the functions appearing on the right hand side of equations (3 - 24) $\gamma \neq 0$. The Wronskian of the equations (3 - 24) gives

$$\alpha^2\gamma\varrho = 1 \quad (3 - 25a)$$

$$\varrho = \psi_2 \frac{d\psi_1}{d\xi} - \psi_1 \frac{d\psi_2}{d\xi} \quad (3 - 25b)$$

Then it follows from equations (3 - 24) that

$$P_R = \frac{\varrho\gamma}{\psi_1^2 + (\beta\psi_1 + \gamma\psi_2)^2} \quad (3 - 26)$$

$$\Theta(\xi) = \tan^{-1} \left[\frac{\psi_1}{\beta\psi_1 + \gamma\psi_2} \right] \quad (3 - 27)$$

Equation (3 - 26) gives a *general* solution ¹⁴ to Milne's equation via equation (3 - 22). Using equations (3 - 18) and (3 - 26) one can deduce an expression for P_I in terms of ψ_1 , ψ_2 , $d\psi_1/d\xi$ and $d\psi_2/d\xi$.

3.2.3 Behavior of P_R , P_I and Θ near $\xi = 1$

Near $\xi = 1$, one can present ψ_1 and ψ_2 in power series [68].

$$\psi_1(\xi) = (\xi - 1)^{n_+} \sum_{j=0}^{\infty} a_j (\xi - 1)^j \quad (3-28)$$

$$\psi_2(\xi) = D \psi_1(\xi) \ln(\xi - 1) + (\xi - 1)^{n_-} \sum_{j=0}^{\infty} b_j (\xi - 1)^j \quad (3-29)$$

$$n_{\pm} = \frac{1}{2} \pm \frac{M}{2}$$

The recursion relations for the coefficients are as follows.

$$a_j = 0 \quad \text{for } j < 0 \quad a_0 \neq 0$$

$$\begin{aligned} a_j = - \left\{ [(2j + M - 1)(2j + M - 3) + 2(c^2 + q - A)] a_{j-1} \right. \\ \left. + \left[\frac{1}{4}(2j + M - 3)(2j + M - 5) + 5c^2 + 3q - A \right] a_{j-2} \right. \\ \left. + (4c^2 + q)a_{j-3} + c^2 a_{j-4} \right\} / 4j(j + M) \quad \text{for } j \geq 1 \end{aligned} \quad (3-30)$$

$$b_j = 0 \quad \text{for } j < 0 \quad b_0 \neq 0 \quad \text{for } M \neq 0 \quad b_M = 0 \quad \text{for } M \neq 0$$

$$\begin{aligned} b_j = - \left\{ [(2j - M - 1)(2j - M - 3) + 2(c^2 + q - A)] b_{j-1} \right. \\ \left. + \left[\frac{1}{4}(2j - M - 3)(2j - M - 5) + 5c^2 + 3q - A \right] b_{j-2} \right. \\ \left. + [4c^2 + q] b_{j-3} + c^2 b_{j-4} + D \left[(2j - M - 4)a_{j-2-M} \right. \right. \\ \left. \left. + 4(2j - M - 2)a_{j-1-M} + 4(2j - M)a_{j-M} \right] \right\} / 4j(j - M) \end{aligned} \quad (3-31)$$

for $j > 0$ and $j \neq M$

$D \neq 0$, but is otherwise arbitrary for $M = 0$. For all other values of M , D is given by

$$D = - \left\{ [(M-1)(M-3) + 2(c^2 + q - A)] b_{M-1} \right. \\ \left. + \left[\frac{1}{4}(M-3)(M-5) + 5c^2 + 3q - A \right] b_{M-2} \right. \\ \left. + [4c^2 + q] b_{M-3} + c^2 b_{M-4} \right\} / 4M a_0 \quad (3-32)$$

The Wronskian of ψ_1 and ψ_2 is given by

$$\varrho = M a_0 b_0 - D a_0 \delta_{M0}. \quad (3-33)$$

Formally, the power series converge in the domain $1 \leq \xi < 3$. Using them we can deduce the behavior of P_R and P_I near $\xi = 1$.

$M = 0$:

$$P_R \xrightarrow{\xi \rightarrow 1} \left(\frac{\varrho}{\gamma D^2 a_0^2} \right) \frac{1}{(\xi-1) \ln^2(\xi-1)} \quad (3-34a)$$

$$P_I \xrightarrow{\xi \rightarrow 1} -\frac{1}{2} \frac{1}{(\xi-1)} \quad (3-34b)$$

$$\Theta \xrightarrow{\xi \rightarrow 1} - \left(\frac{\varrho}{\gamma D^2 a_0^2} \right) \frac{1}{\ln(\xi-1)} + b \quad (3-34c)$$

$M = 1$:

$$P_R \xrightarrow{\xi \rightarrow 1} \frac{\rho}{\gamma b_0^2 + 2D\gamma a_0 b_0 (\xi - 1) \ln(\xi - 1)} \quad (3 - 35a)$$

$$P_I \xrightarrow{\xi \rightarrow 1} -\frac{a_0 D}{b_0} \ln(\xi - 1) \quad (3 - 35b)$$

$$\Theta \xrightarrow{\xi \rightarrow 1} \left(\frac{\rho}{\gamma b_0^2} \right) \xi + b \quad (3 - 35c)$$

$M > 1$:

$$P_R \xrightarrow{\xi \rightarrow 1} \left(\frac{\rho}{\gamma b_0^2} \right) (\xi - 1)^{M-1} \quad (3 - 36a)$$

$$P_I \xrightarrow{\xi \rightarrow 1} \left(\frac{M-1}{2} \right) \frac{1}{(\xi - 1)} \quad (3 - 36b)$$

$$\Theta \xrightarrow{\xi \rightarrow 1} \left(\frac{\rho}{\gamma b_0^2} \right) \frac{(\xi - 1)^M}{M} + b \quad (3 - 36c)$$

When $M = 0$, P_R has a singularity at $\xi = 1$ which is less strong than $(\xi - 1)^{-1}$.

3.2.4 The Physical Solution

We use the form given in equation (3 - 20a) to represent the physical solution $\chi(\xi)$, which must be *bounded* at $\xi = 1$. Since P_R is less singular than $(\xi - 1)^{-1}$ at $\xi = 1$ we must have $\sin(\Theta(\xi = 1)) = 0$. Hence $b = n\pi$, $n = 0, 1, 2, \dots$

We define

$$b = 0$$

in equations (3 - 21), (3 - 34c), (3 - 35c) and (3 - 36c). To generate P_R we use the *first order* differential equation (3 - 14) instead of the *second order* Milne's equation. The theory does not dictate the boundary conditions for P_R and P_I .

We impose the semiclassical boundary conditions,

$$\lim_{\xi \rightarrow \infty} P_R = \lim_{\xi \rightarrow \infty} k = c \quad (3 - 37a)$$

$$\lim_{\xi \rightarrow \infty} P_l = \lim_{\xi \rightarrow \infty} \frac{1}{2k} \left(\frac{dk}{d\xi} \right) = 0 \quad (3-37b)$$

The constant a can be deduced from the normalization (see Appendix E).

$$a = \frac{2}{\sqrt{\pi R}}$$

3.2.5 Summary of the physical solution

$$\chi(\xi) = \frac{2}{\sqrt{\pi R}} \frac{\sin \Theta(\xi)}{\sqrt{(\xi-1)P_R(\xi)}} \quad (3-38a)$$

$$\Theta(\xi) = \int_1^{\xi} d\xi P_R(\xi) \quad (3-38b)$$

$$\lim_{\xi \rightarrow \infty} P_R(\xi) = c \quad (3-38c)$$

$$\lim_{\xi \rightarrow \infty} \frac{dP_R(\xi)}{d\xi} = 0 \quad (3-38d)$$

3.2.6 The Phase Shift

The physical solution has the following asymptotic form [30b,58]

$$\chi(\xi) \xrightarrow{\xi \rightarrow \infty} \frac{1}{\xi \sqrt{c}} \sin [c\xi + (q/2c) \ln \xi + \Lambda] \quad (3-39)$$

where Λ is the phase shift. Define the quantity λ by

$$\lambda = \Lambda - (q/2c) \ln(c) \quad (3-40)$$

which has the following limiting values [30b,69]

$$\lim_{R \rightarrow 0} \lambda = \sigma_l - \frac{l\pi}{2} + \frac{q}{2c} \ln 2 \quad (3-41a)$$

$$\sigma_l = \text{Arg} [\Gamma(l+1 - i(q/2c))] \quad (3-41b)$$

$$\lambda \xrightarrow{R \rightarrow \infty} -\frac{q}{2c} \ln(c/2) - \frac{l\pi}{2} + O(c^{-1}) \quad (3-42)$$

Here σ_l is the Coulomb phase shift. Now define a function $G(\xi)$ such that

$$G(\xi) = \Theta(\xi) - c\xi - (q/2c) \ln(\xi) - \Lambda \quad (3-43a)$$

Then from equation (3-39) we have

$$\lim_{\xi \rightarrow \infty} G(\xi) = 0 \quad (3-43b)$$

One can evaluate Λ by evaluating $G(\xi)$ and Θ .

When $c \neq 0$, one can represent (the "physical") P_+ by an *asymptotic series*, for sufficiently large ξ ,

$$P_+(\xi) = \sum_{j=0}^{\infty} \frac{C_j}{\xi^j} \quad (3-44)$$

where

$$C_0 = c \quad \left| \quad C_1 = q/2c \quad (3-45a)$$

For $j \geq 3$ and *odd*

$$C_j = \frac{1}{2C_0} \left[q - i(j-1)C_{j-1} - \sum_{n=1}^{j-1} C_n C_{j-n} \right] \quad (3-45b)$$

For $j \geq 4$ and *even*

$$C_j = \frac{1}{2C_0} \left[c^2 - A - \frac{1}{2}(j-2)(M^2 - 1) - i(j-1)C_{j-1} - \sum_{n=1}^{j-1} C_n C_{j-n} \right] \quad (3-45c)$$

Asymptotically P_R is given by

$$P_R(\xi) = c + \left(\frac{q}{2c}\right) \frac{1}{\xi} + \sum_{j=2}^{\infty} \frac{\text{Re}(C_j)}{\xi^j} \quad (3-46)$$

One can integrate this asymptotic series [70]. Hence

$$\int^{\xi} d\xi P_R(\xi) = c\xi + \left(\frac{q}{2c}\right) \ln(\xi) + \sum_{j=2}^{\infty} \frac{\text{Re}(C_j)}{(1-j)} \frac{1}{\xi^{j-1}} \quad (3-47)$$

One can deduce from the equations (3 - 43), (3 - 44) and (3 - 47) that

$$G(\xi) = \sum_{j=2}^{\infty} \frac{\text{Re}(C_j)}{(1-j)} \frac{1}{\xi^{j-1}} \quad (3-48)$$

when the asymptotic series is sufficiently accurate.

3.2.7 Numerical Method

Numerical work was done for the prototype system H_2^+ for which $p = 0$. In this case, the angular separation constant A for a state with a given (l, m) , is a function only of c^2 . The generated A values may be easily fitted, to a high accuracy (absolute error of about 1.0×10^{-7}) with a rational polynomial in c^2 . These fits were then used for radial and angular wave function calculations.

Following is an outline of the steps we performed to generate a *point-wise* representation of $\chi(\xi)$ (in fact of P_R and Θ) and to evaluate Λ

- (1) Generate $P_+(\xi)$ and $G(\xi)$ at $\xi = \xi_{\infty}$ using the asymptotic series.
- (2) Integrate the equation (3 - 14) towards $\xi = 1$. Simultaneously integrate $P_R(\xi)$ to obtain a function $\Theta_T(\xi)$ with $\Theta_T(\xi_{\infty}) = 0$.
- (3) At $\xi = \xi_0$ smoothly connect P_R to the form given in equation (3 - 26) to evaluate β and γ .

$$\gamma = \frac{1}{e} \left[\frac{(\psi_1' + P_I \psi_1)^2}{P_R} + P_R \psi_1^2 \right] \quad (3-49)$$

$$\beta = \frac{\psi_1'}{P_R \psi_1} + \frac{P_I}{P_R} - \frac{\gamma \psi_2}{\psi_1} \quad (3-50)$$

Here ' implies differentiation with respect to ξ . Use the power series to evaluate ψ_j and ψ'_j .

- (4) Resume step (2) and continue up to ξ_{00} where ξ_{00} is within the first node of the wave function $\chi(\xi)$. Generate $\Theta(\xi_{00})$ using equation (3 - 27).
- (5) Adjust $\Theta(\xi)$ to obtain $\Theta(\xi)$
- (6) Evaluate Λ using equation (3 - 43) at $\xi = \xi_{\infty}$.

3.2.8 Numerical Details

- (a) We have set

$$a_0 = 1$$

$$b_0 = \begin{cases} 1 & \text{if } M = 0 \\ 1/M & \text{if } M \neq 0 \end{cases}$$

$$D = -1 \quad \text{when } M = 0$$

This choice makes $\rho = 1$.

- (b) ρ was also evaluated at each point where ψ_1 and ψ_2 were evaluated, as a check on the accuracy of the function calculations.
- (c) We have set $\xi_{00} = 1.001$ and $\xi_0 = 1.5$.
- (d) When ξ_{∞} was greater than $(80/R)$, instead of equation (3 - 14), we integrated the differential equation for the function $g(\xi)$ defined by

$$g(\xi) = P_+(\xi) c\xi - \left(\frac{q}{2c}\right) \frac{1}{\xi}$$

up to $(80/R)$. Simultaneously we integrated $Re(g(\xi))$ with the initial condition $Re(g(\xi_{\infty}))$. To increase the efficiency we used the integration variable $u = 1/\xi$ in this part of the calculation.

- (e) We fixed the number of asymptotic series coefficients at 20. Then ξ_{∞} is determined by the required accuracy of P_+ . As expected, ξ_{∞} increases with decreasing c^2 .

- (f) All the numerical integrations were performed by the efficient algorithm of Bulirsch and Stoer [86].

The following checks were done to assess the accuracy/precision of the results.

- (i) Stability of the results was checked against changes in ξ_{00} , ξ_0 and ξ_∞ .
 (ii) The phase shifts were compared with those reported in reference 71.

3.2.9 Global Representation of $\chi(\xi)$

$\chi(\xi)$ can be evaluated by calculating $P_R(\xi)$ and $\Theta(\xi)$.

- (1) $1 \leq \xi \leq \xi_0$:

It can easily be shown that ψ_1 (together with a state dependent normalization constant) can be used to represent the physical solution $\chi(\xi)$.

- (2) $\xi_0 < \xi < \xi_\infty$:

Divide this interval into a number of subintervals. In each subinterval least squares fit P_R to the algebraic form given in equation (3 - 46). Integration of this fit determines $\Theta(\xi)$ up to a constant which can be determined using any calculated value of $\Theta(\xi)$.

- (3) $\xi_\infty \leq \xi < \infty$:

P_R can be evaluated using equation (3 - 46). $\Theta(\xi)$ can be represented using equation (3 - 43a) with $G(\xi)$ given by the equation (3 - 48).

3.3 Results

Representative examples of P_R and Θ are displayed in Figures 3-2 → 7. There we have used the notation $P_R(\epsilon l m; R; \xi)$ and $\Theta(\epsilon l m; R; \xi)$ which explicitly shows the state identification quantum numbers and the internuclear separation.

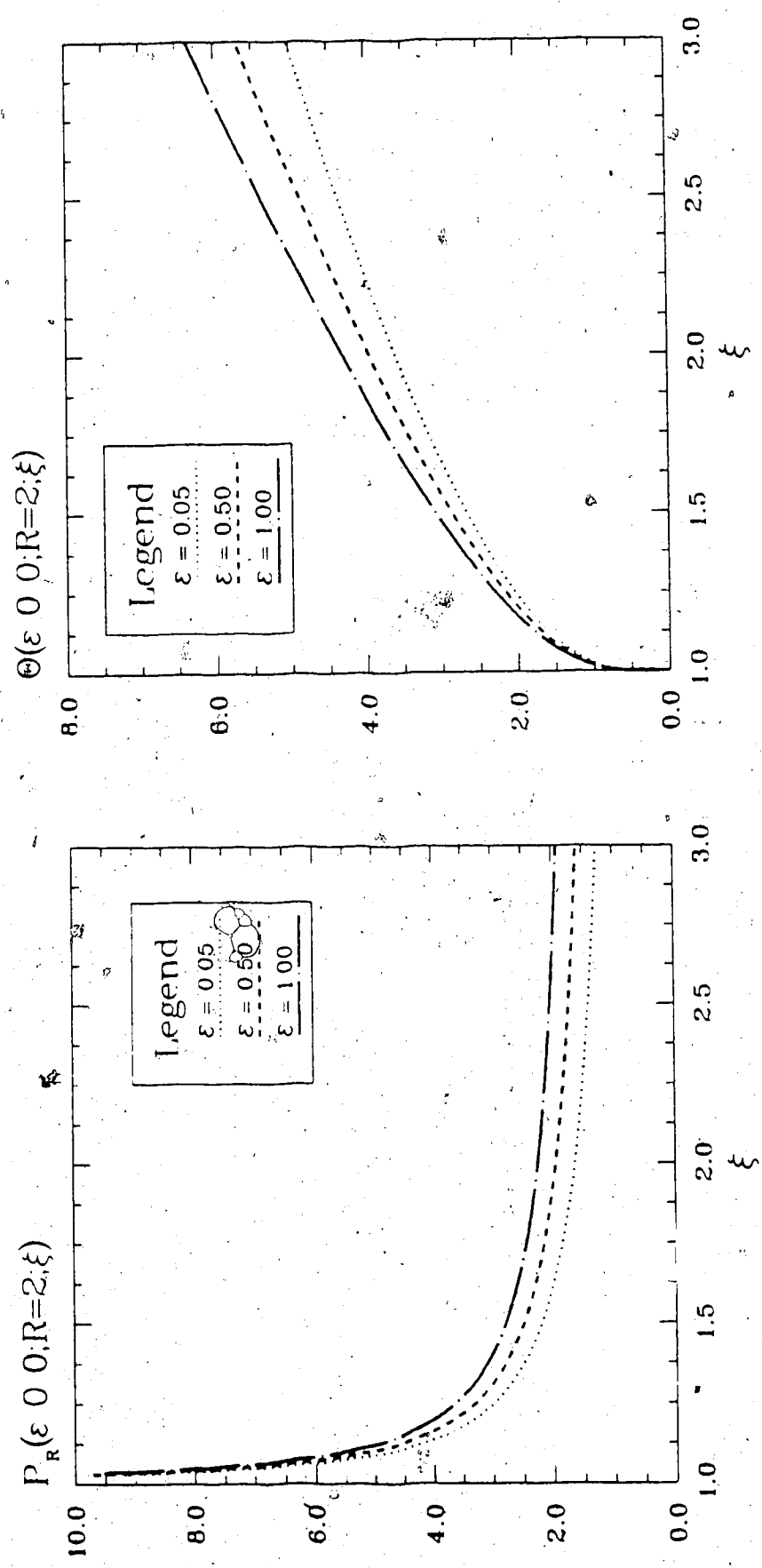


Figure 3 - 2 : P_R and Θ vs. ξ

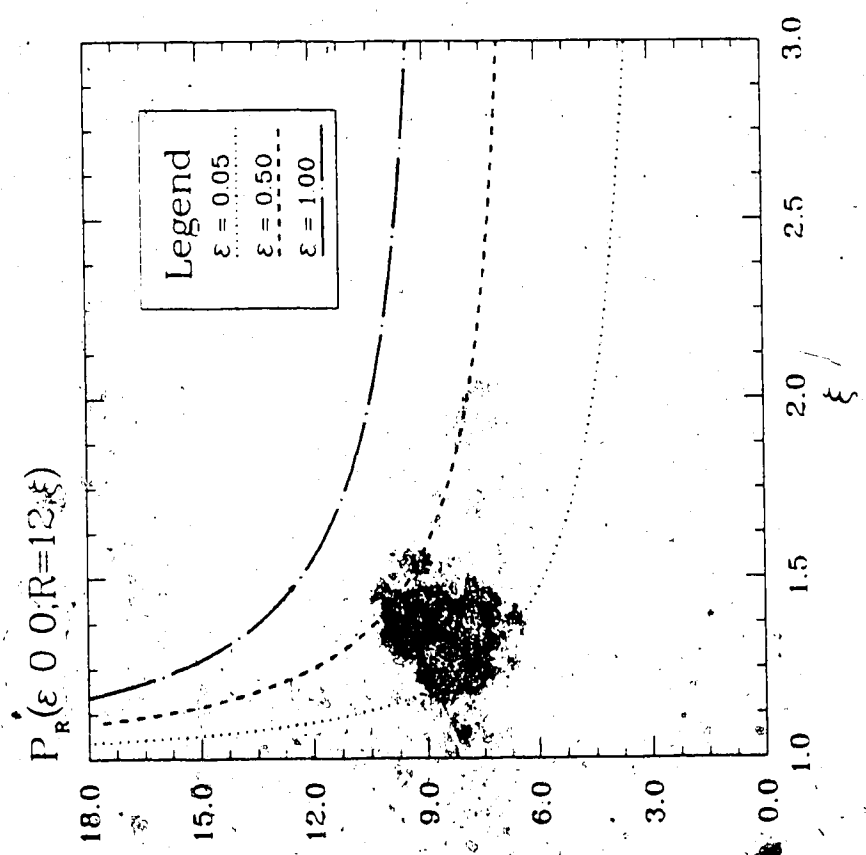
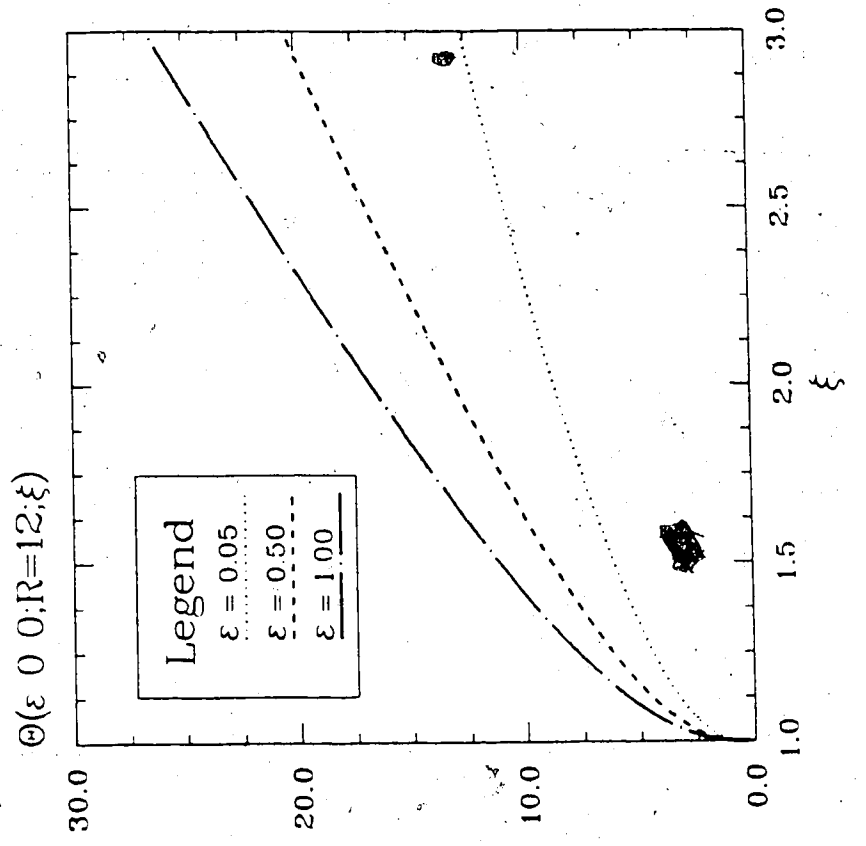


Figure 3 - 3 : P_R and Θ vs. ξ

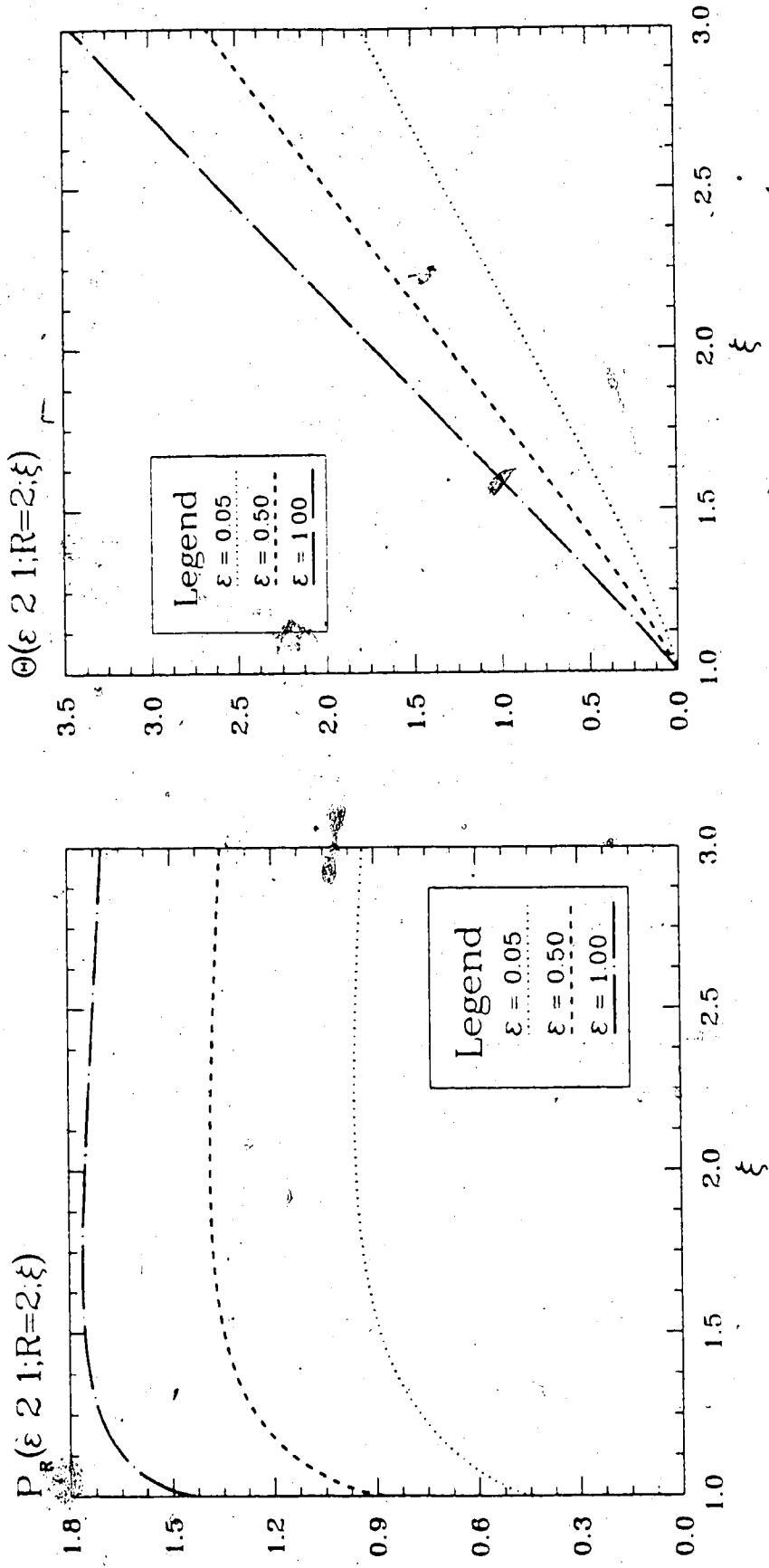


Figure 3 - 4 : P_R and Θ vs. ξ

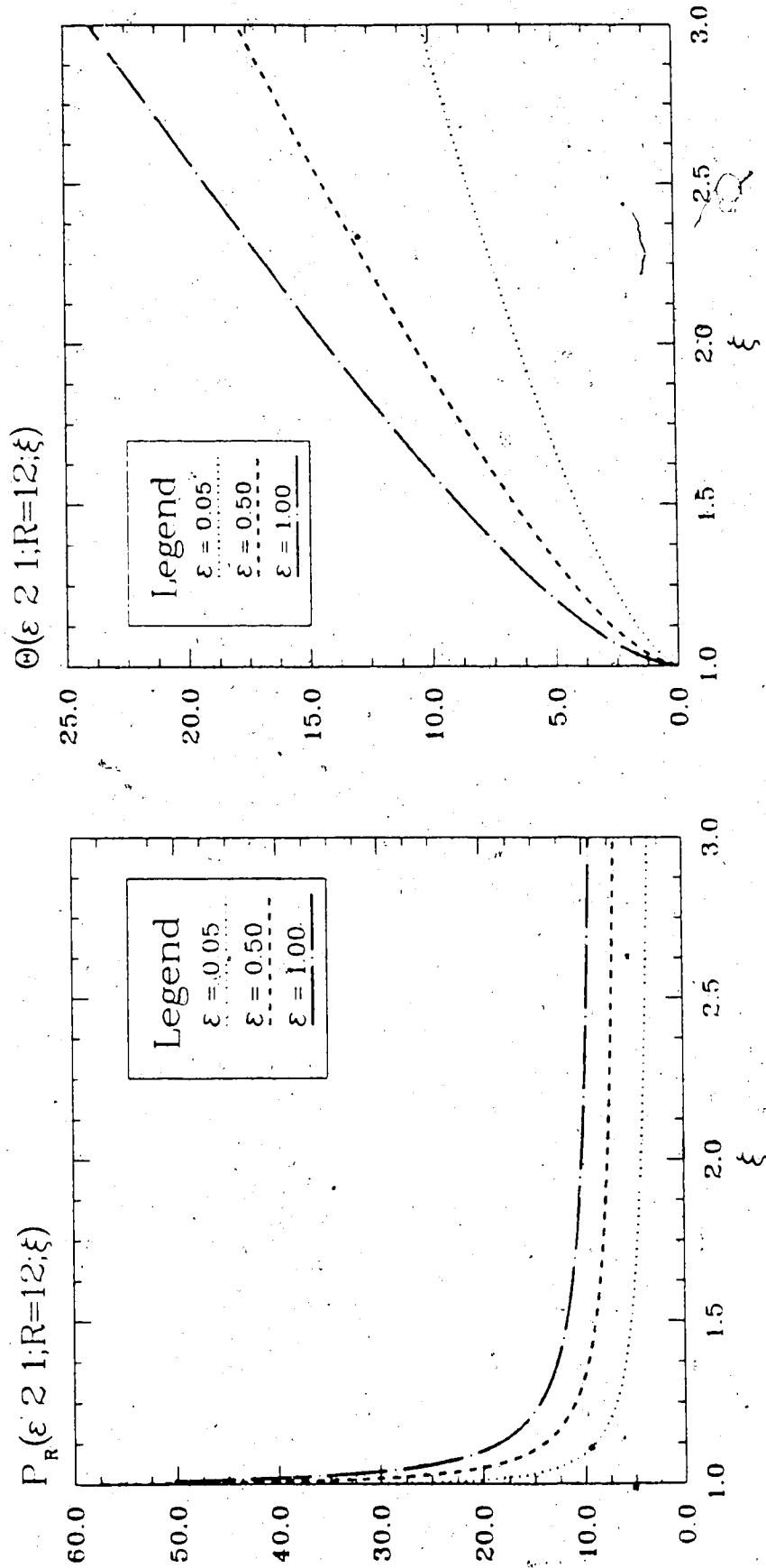


Figure 3 - 5 : P_R and Θ vs. ξ

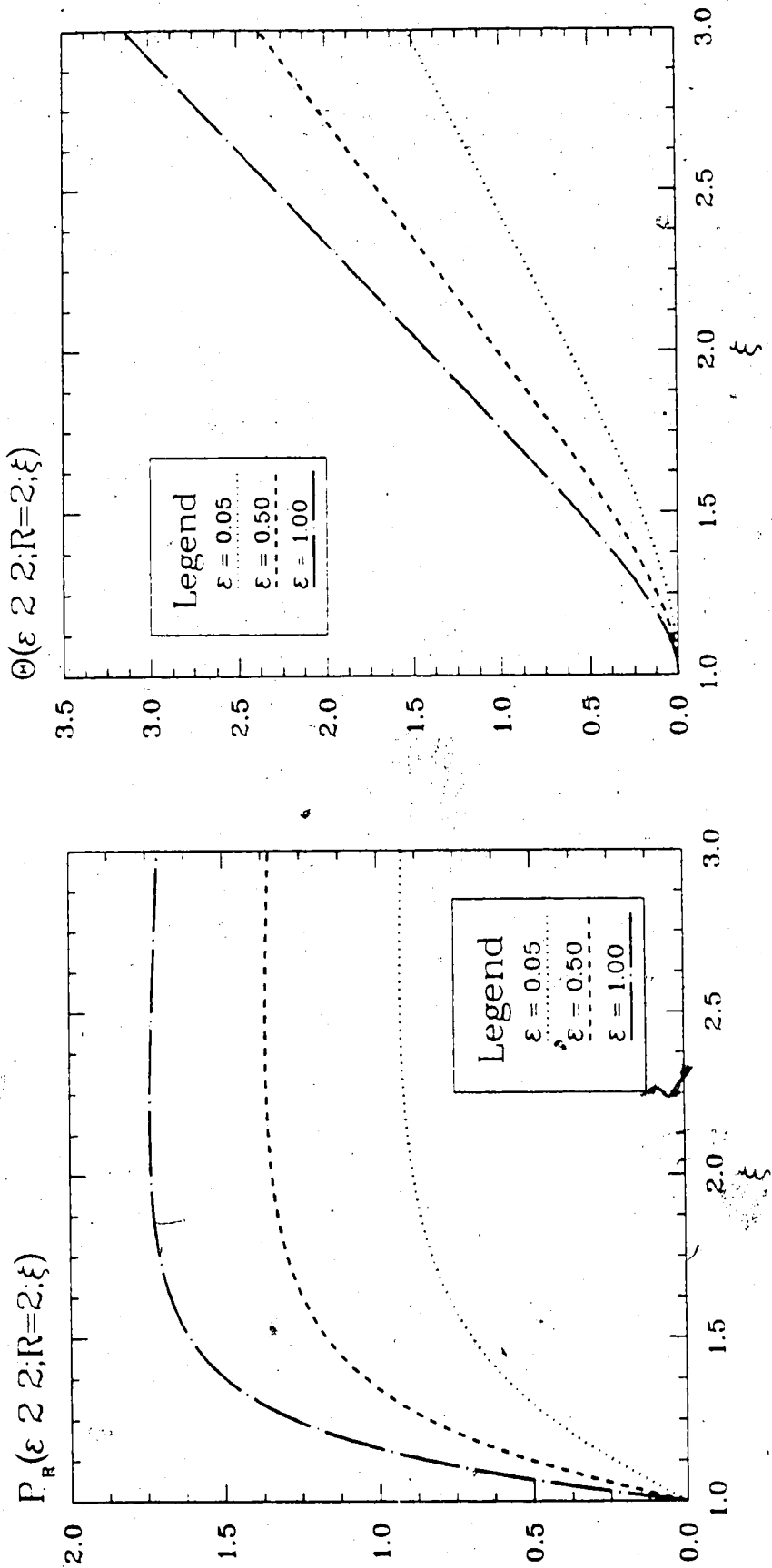


Figure 3 - 6 : P_R and Θ vs. ξ

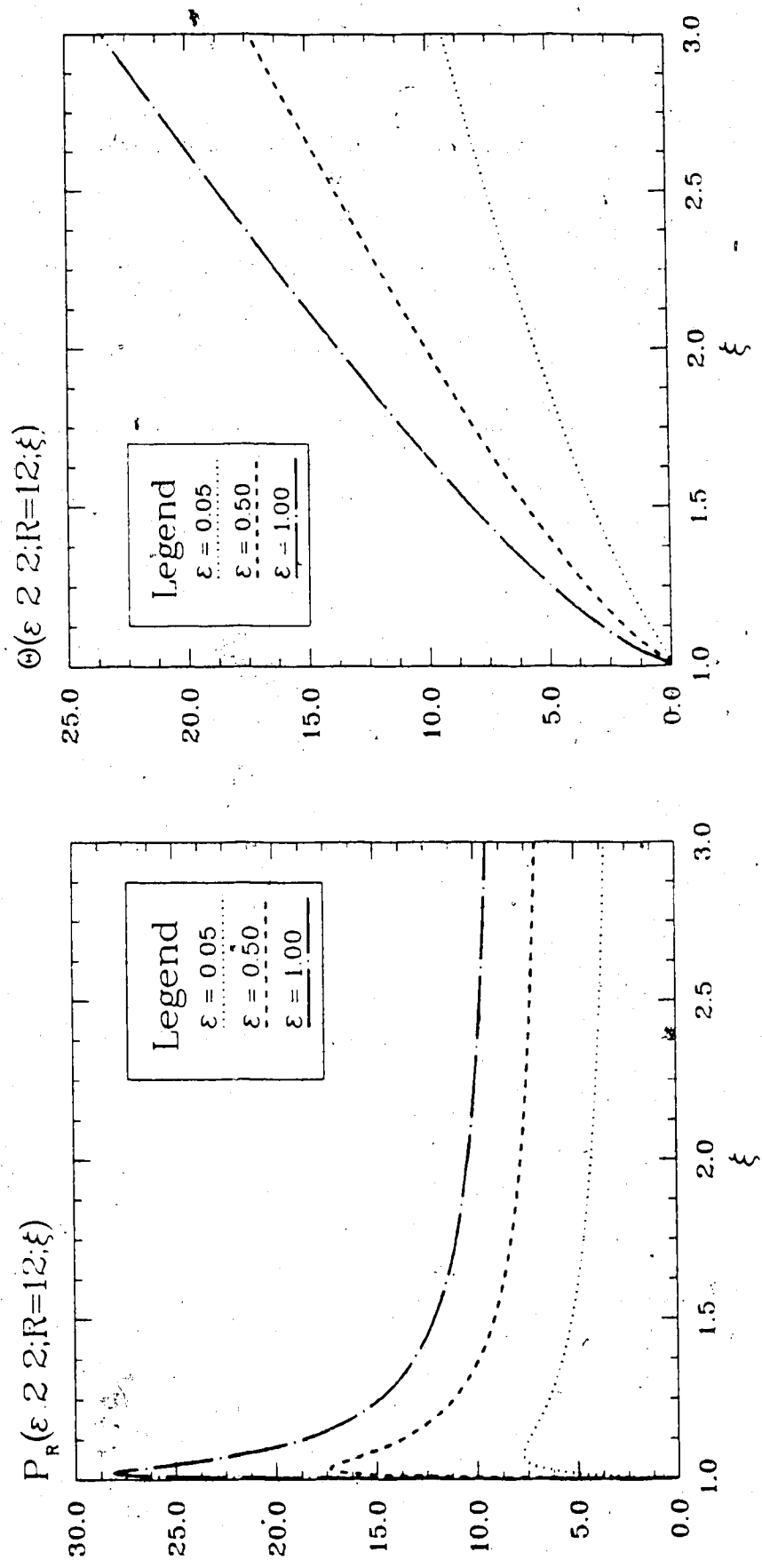


Figure 3 - 7 : P_R and Θ vs. ξ .

Beyond about $\xi \simeq 2$ the qualitative behavior of P_R and Θ is practically independent of ϵ, l, m and R ; they are monotonic smooth functions of ξ . As suggested by the equations (3 - 34) \rightarrow (3 - 36), their behavior near the origin is strongly m -dependent. Except within this region, P_R is a slowly varying function of ξ as well as ϵ ; this is a property we are going to use in deriving an approximate analytical form for packet states in Chapter 4.

In Figures 3 - 8 and 3 - 9 we have displayed the phase shift, λ , (equation (3 - 40)) for states with $l \leq 4$ at two different continuum energies.

We have shown a sample of the angular wave function $S(\epsilon l m; R; \eta)$ in Figures 3 - 10 \rightarrow 15. The number of nodes within $-1 < \eta < +1$ is equal to $(l - m)$. These functions are not very sensitive to changes in ϵ .

Figures 3 - 16 \rightarrow 21 are relief plots of total continuum wave functions in the xz - plane on an 80×80 a.u. grid. Continuum energy and the internuclear separation for each state is indicated (in a.u.) on each plot. It can be seen that they are centred at the centre of charge of the nuclei, a property which has not been appreciated in the past. This effect is more pronounced at higher energies.

3.4 Discussion

Mainly, our study was on the states $l = 0, 1, 2$ with all possible m . c^2 was limited to $0.005 \text{ a.u.} < c^2 < 200.0 \text{ a.u.}$

We have used the semiclassical boundary conditions for P_R . This leads to a smooth function for P_R (and P_I). Also we can represent P_R with the asymptotic series given in equation (3 - 46) which is of great computational utility. The asymptotic series is not valid when $c = 0$. This is not a major problem; to evaluate the propagator we only have to calculate the continuum states at the average packet energies ϵ_j which are non-zero.

Figure 3 - 8 : Phase shift λ vs. R

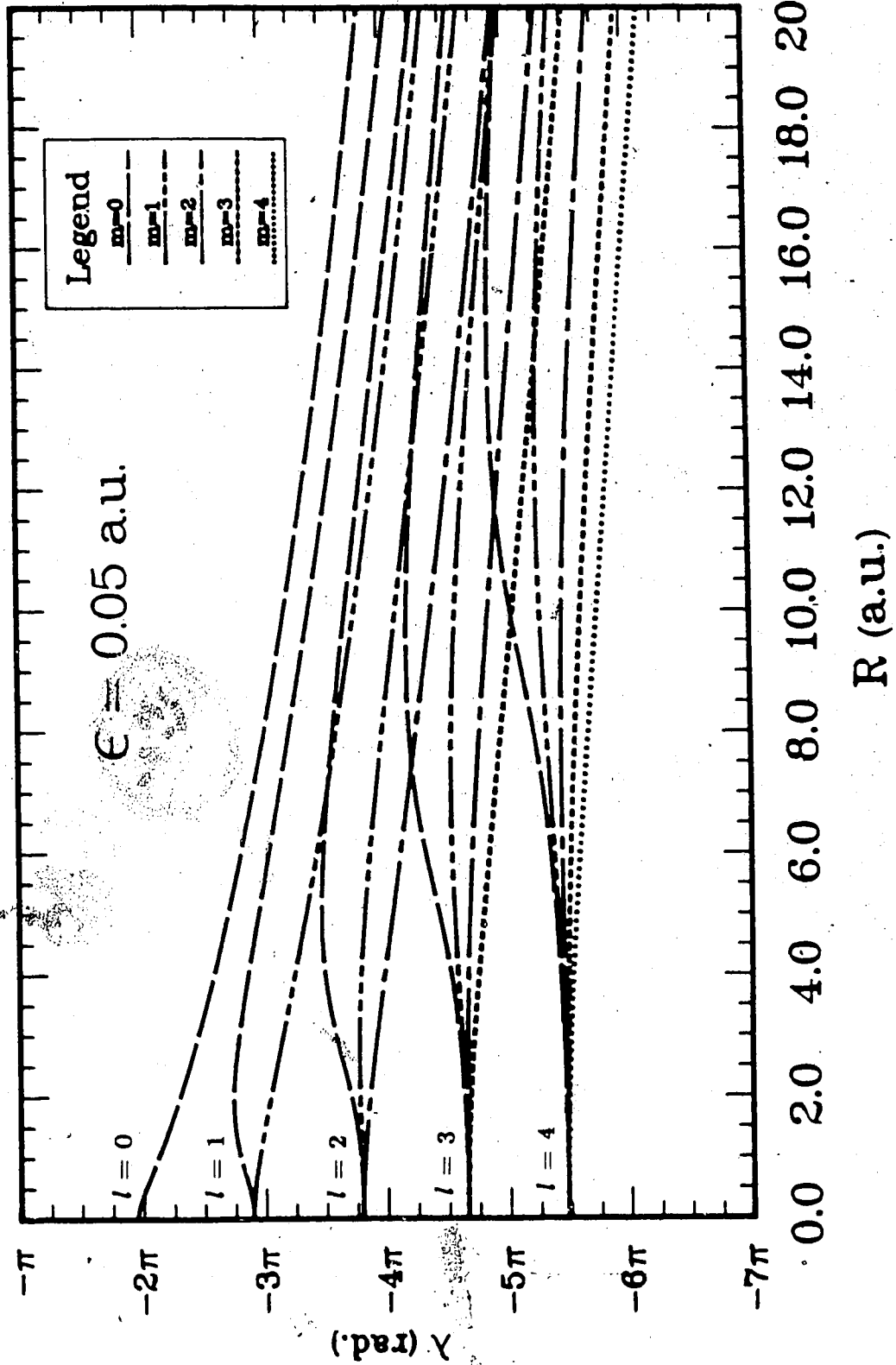
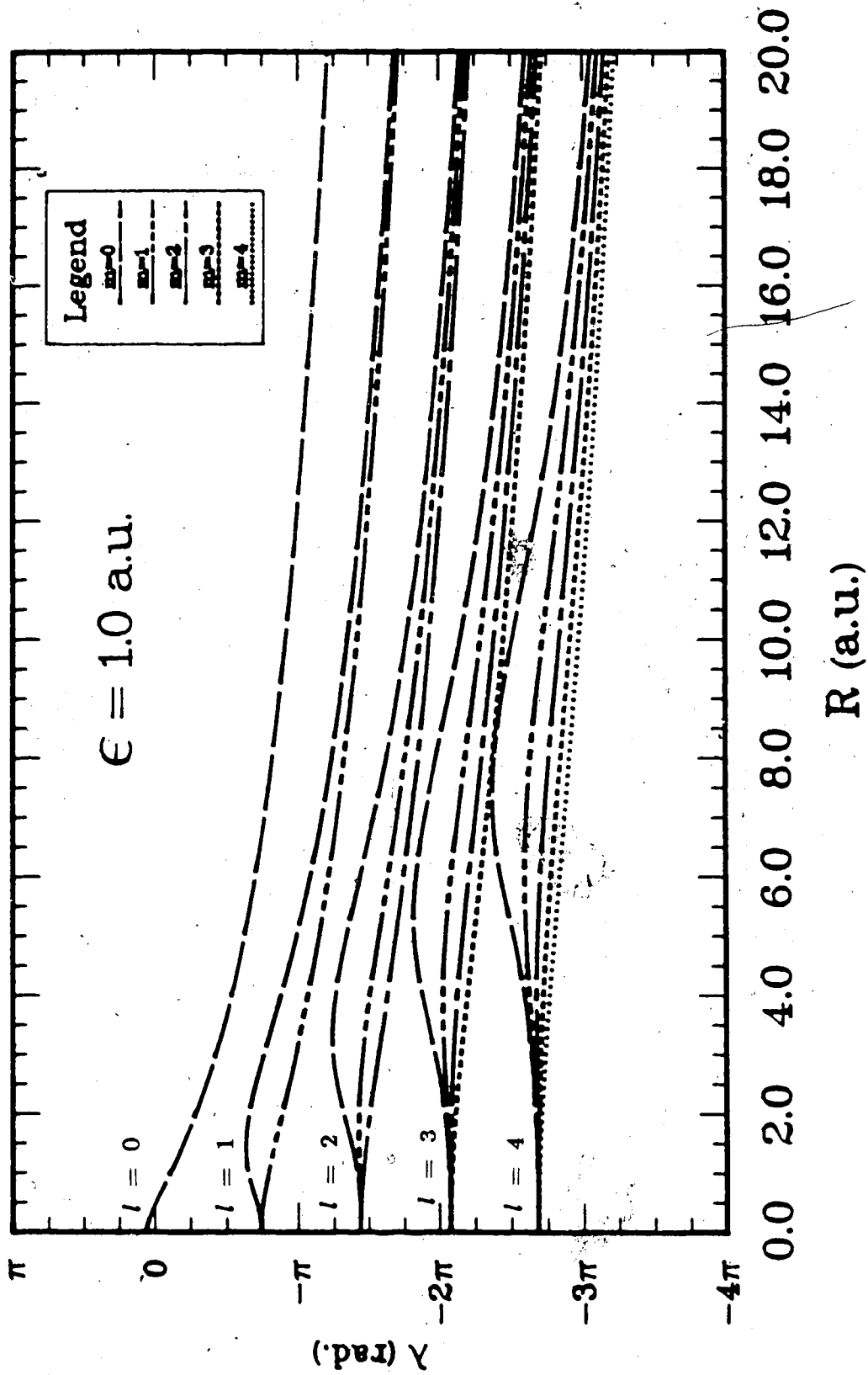


Figure 3 - 9 : Phase shift λ vs. R 

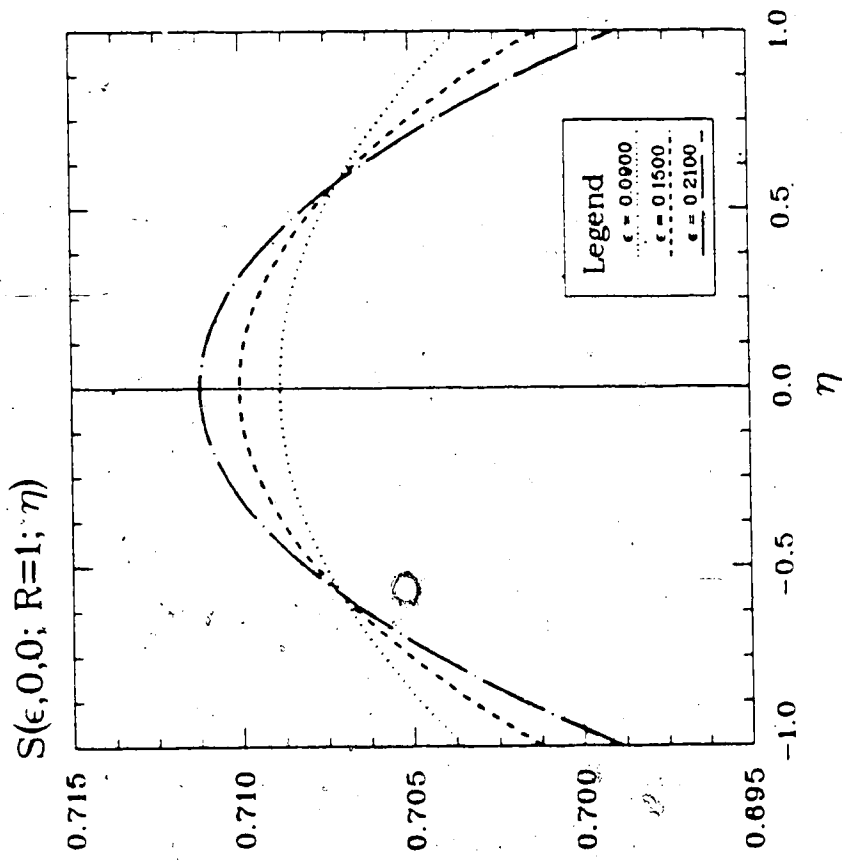
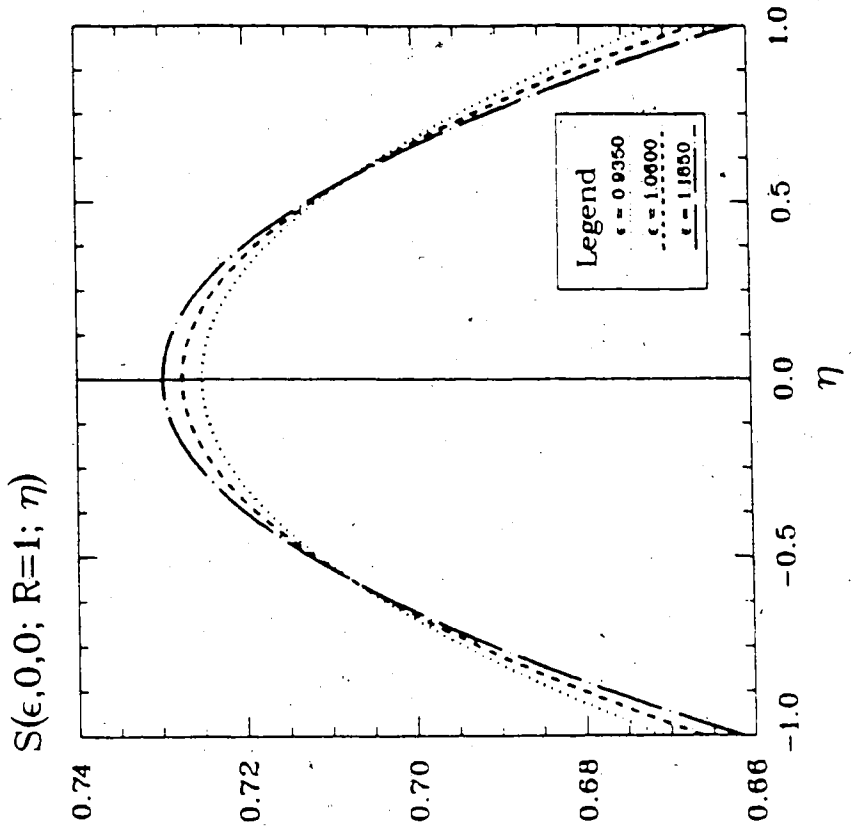


Figure 3 - 10 : Angular Wave Function vs. η

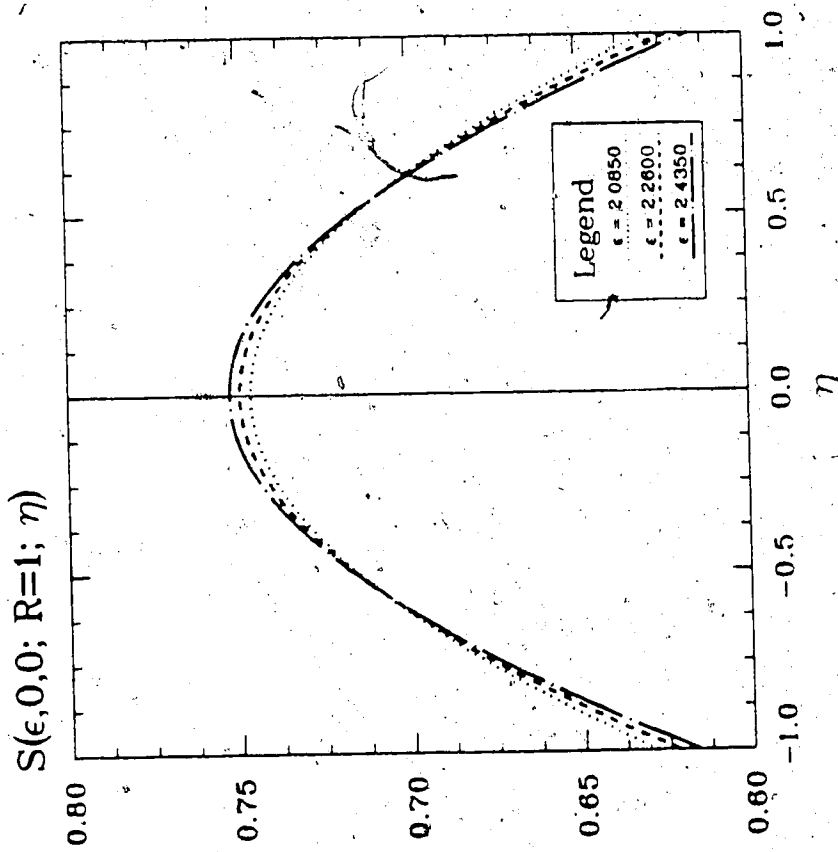
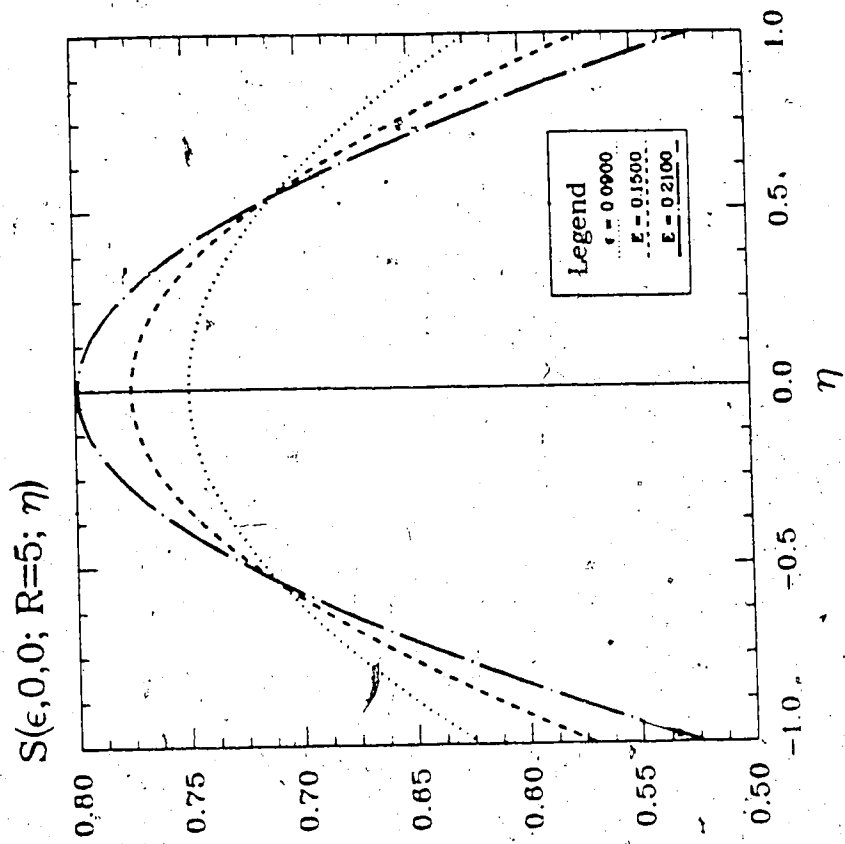


Figure 3 - 11 : Angular Wave Function vs. η

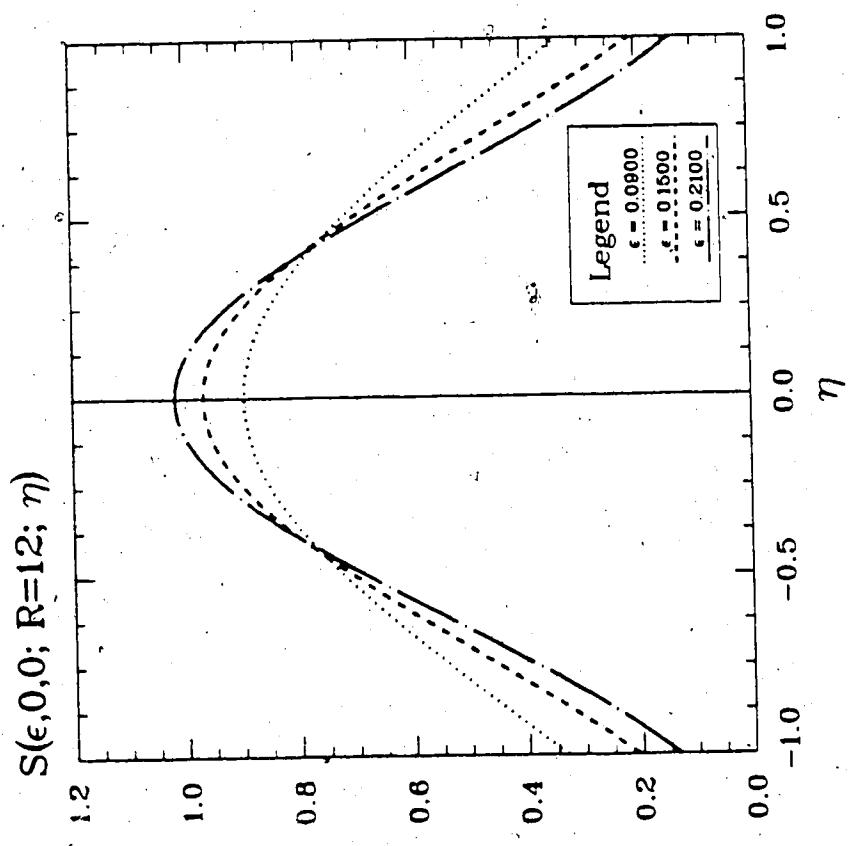
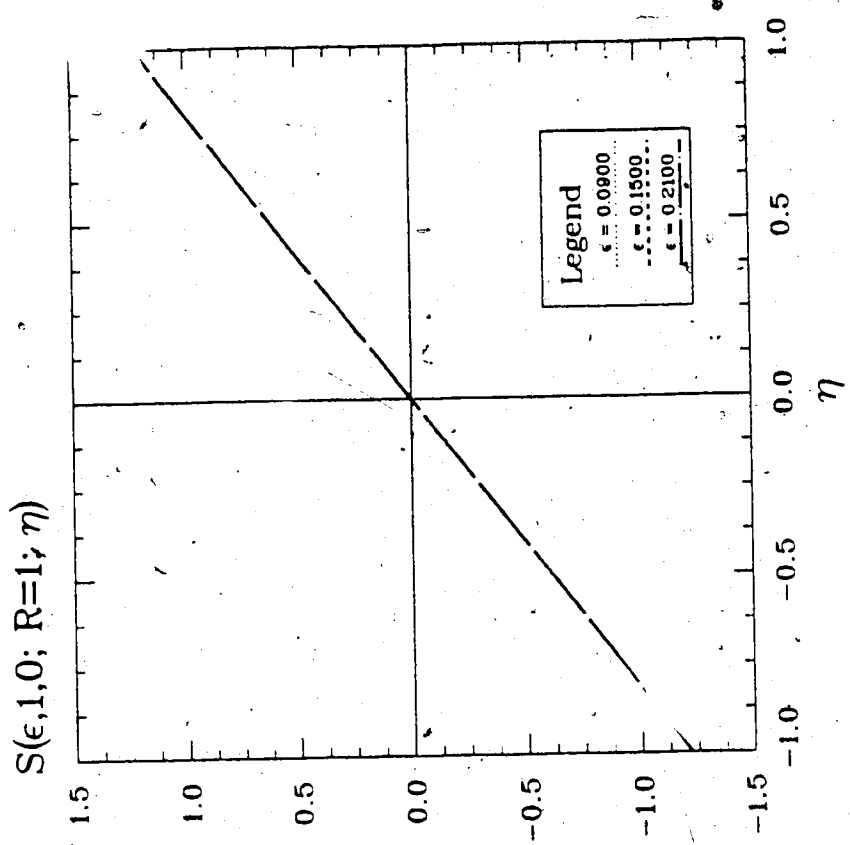


Figure 3 - 12: Angular Wave Function vs. η

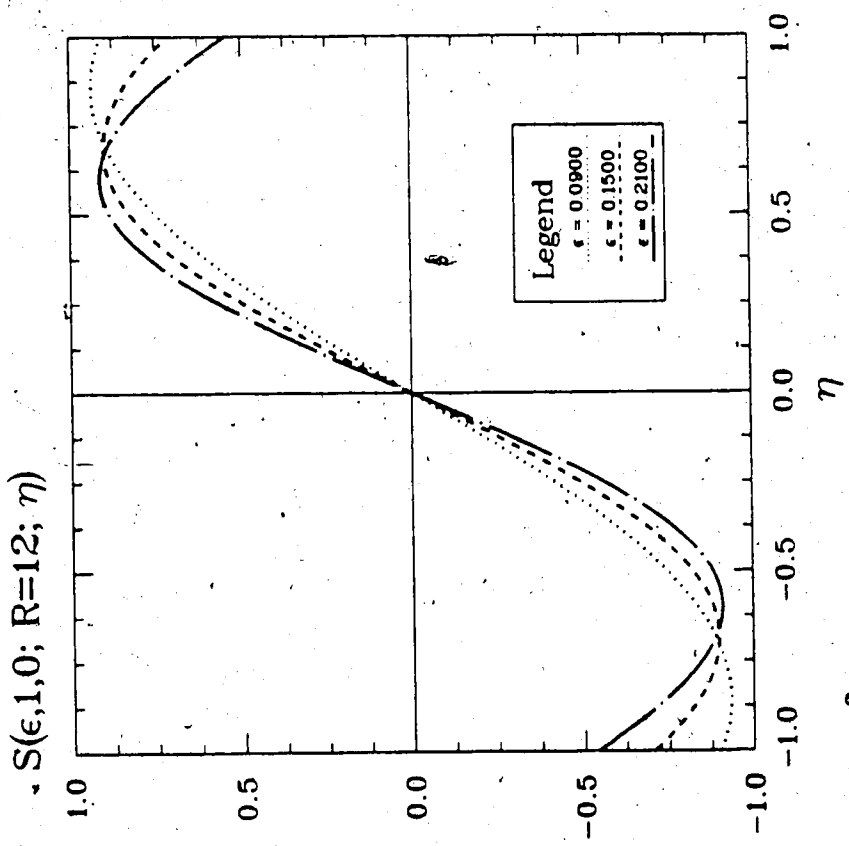
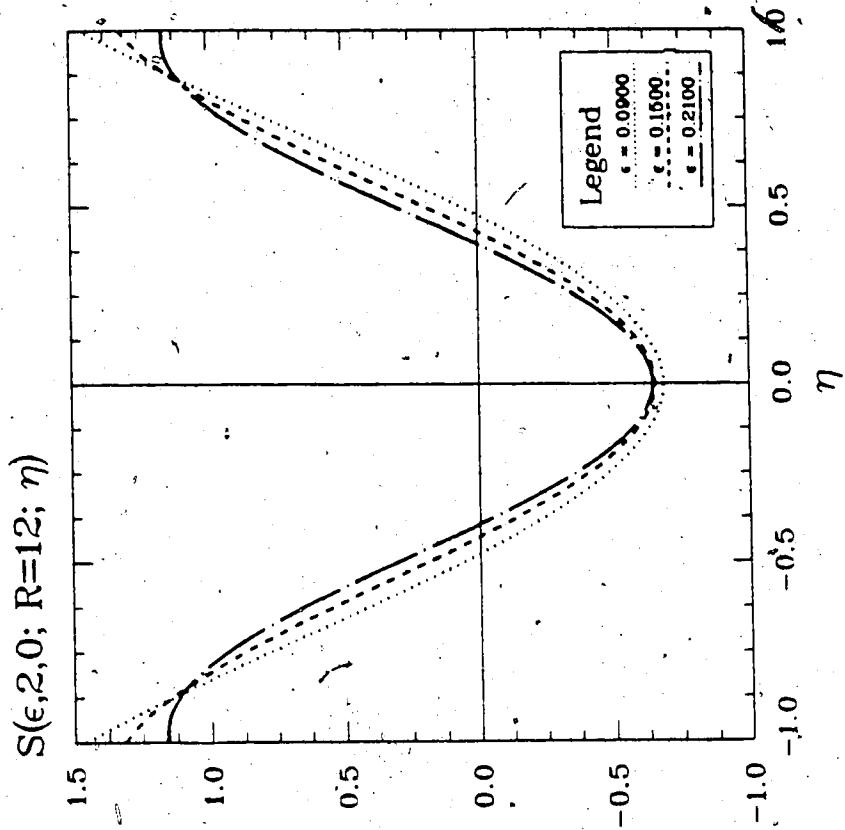


Figure 3 - 13 : Angular Wave Function vs. η

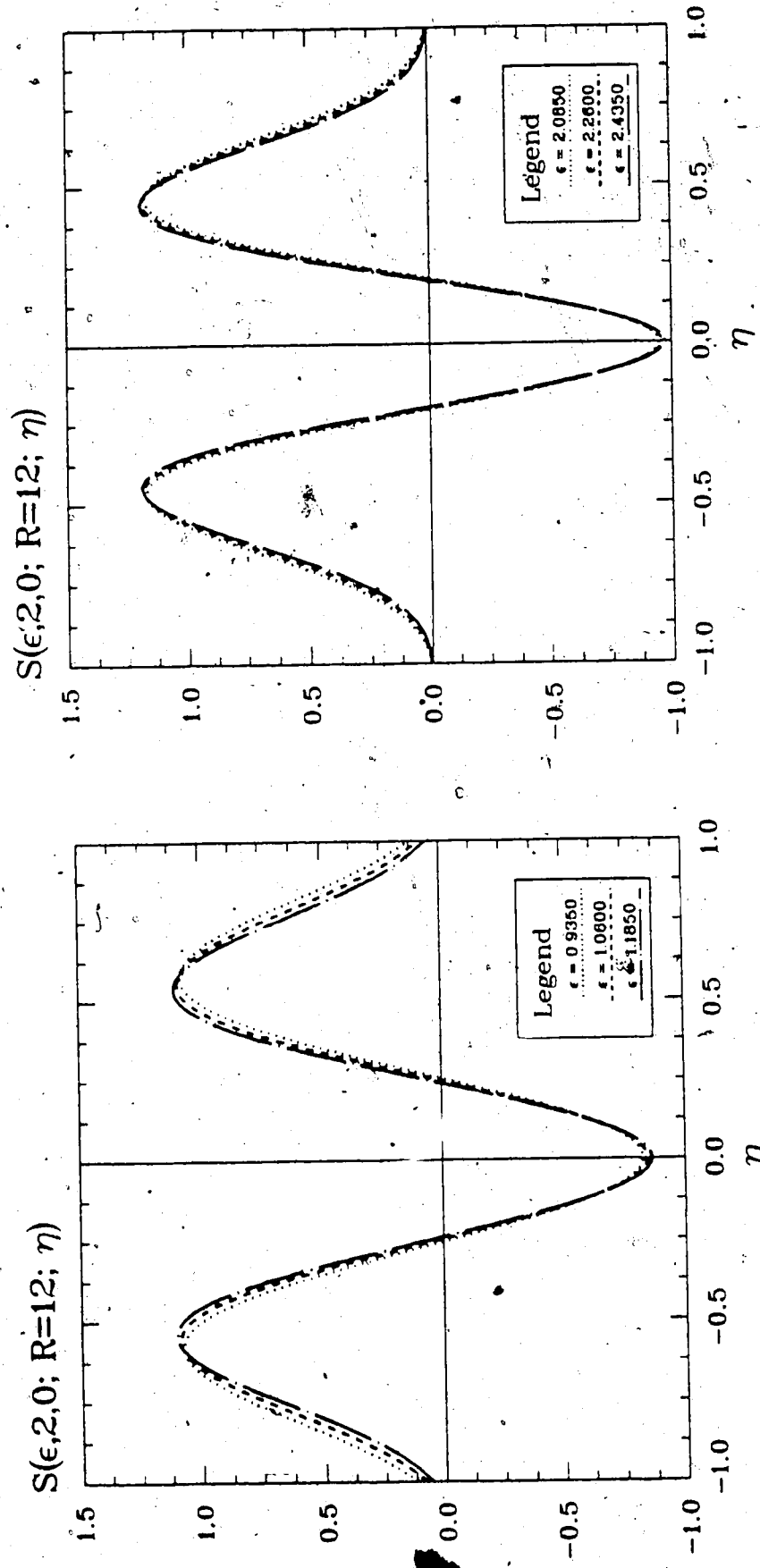
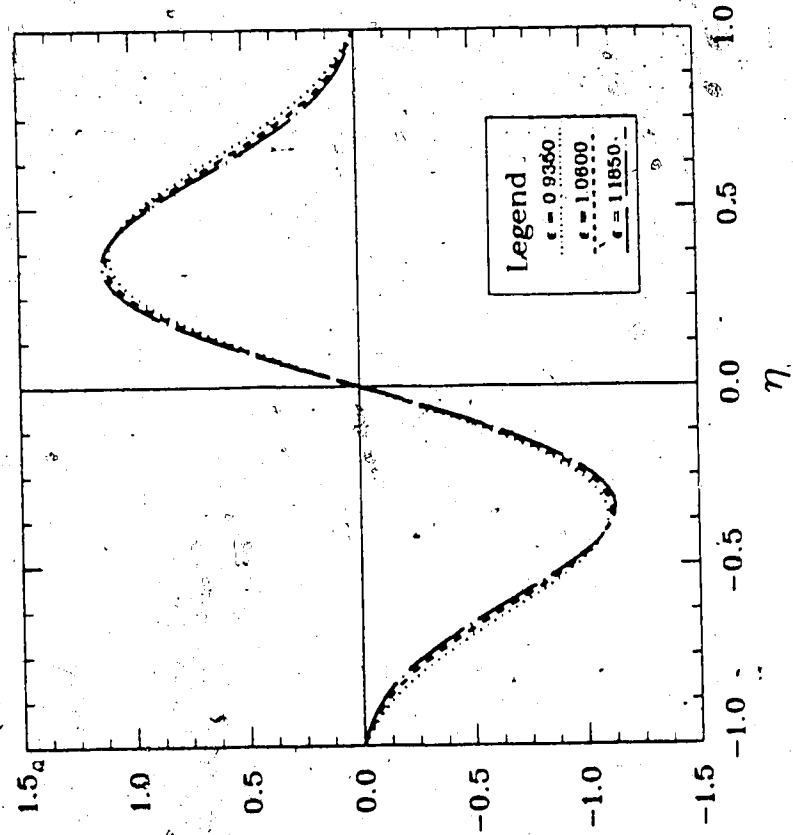


Figure 3 - 14 : Angular Wave Function vs. η

$S(\epsilon, 2, 1; R=12; \eta)$



$S(\epsilon, 2, 2; R=12; \eta)$

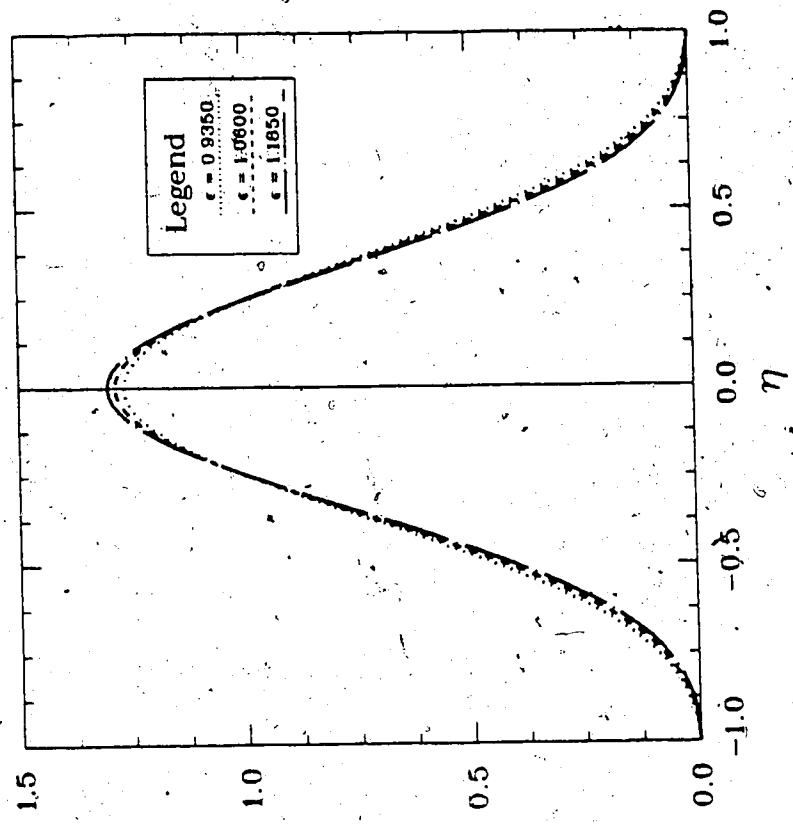
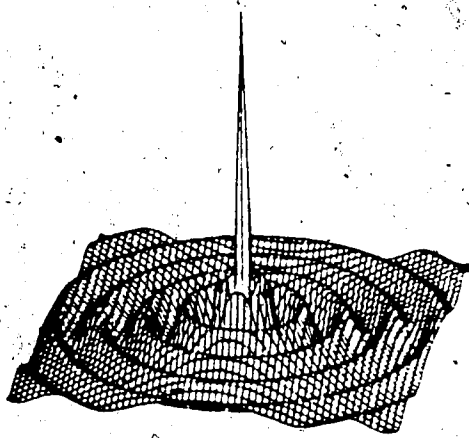
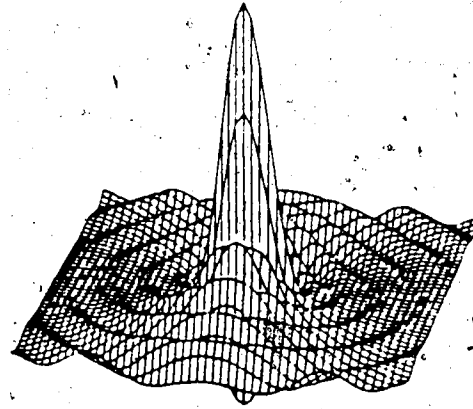


Figure 3 - 15 : Angular Wave Function vs. η

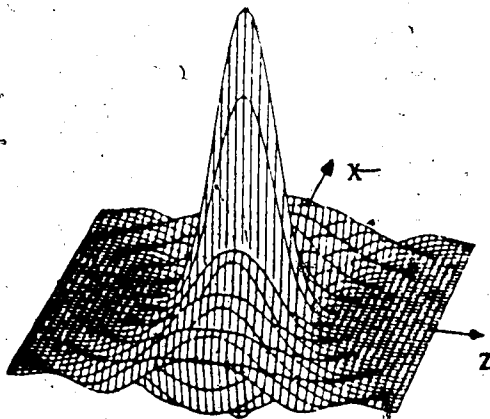
Continuum States



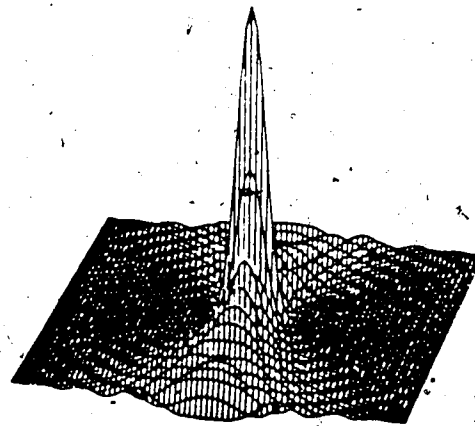
$R = 2.0 \quad \epsilon = 0.15$



$R = 20.0 \quad \epsilon = 0.15$



$R = 40.0 \quad \epsilon = 0.15$

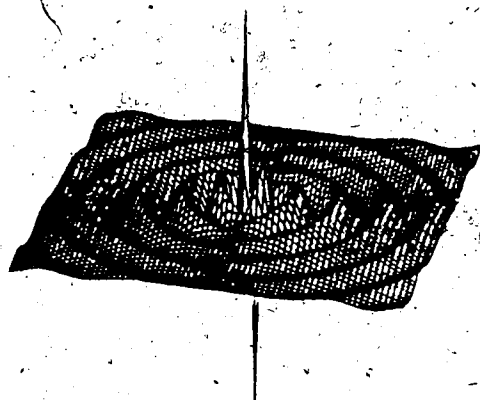
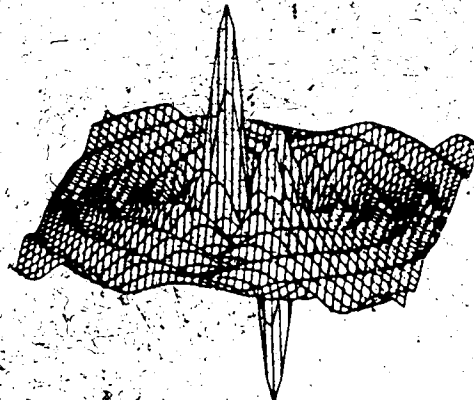
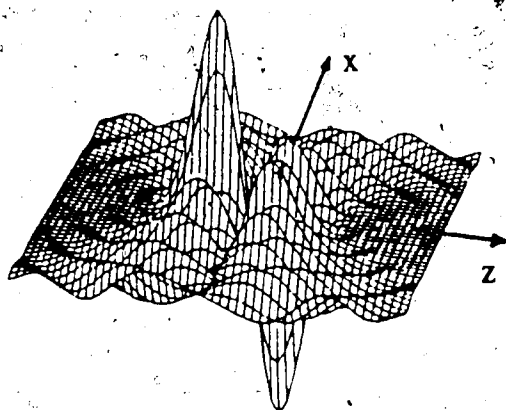
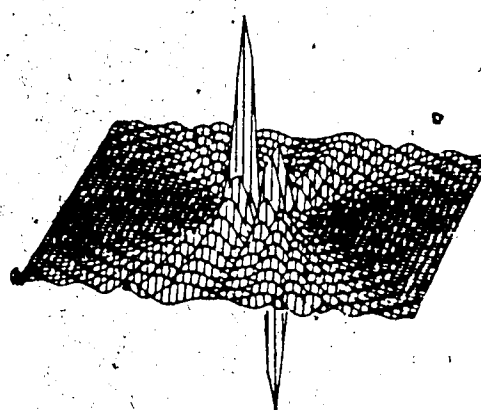


$R = 20.0 \quad \epsilon = 0.825$

$l = 0 \quad m = 0$

Figure 3 - 16 :

Continuum States


 $R = 2.0 \quad \epsilon = 0.15$

 $R = 20.0 \quad \epsilon = 0.15$

 $R = 40.0 \quad \epsilon = 0.15$

 $R = 20.0 \quad \epsilon = 0.825$
 $l = 1 \quad m = 0$
Figure 3 - 17.:

Continuum States

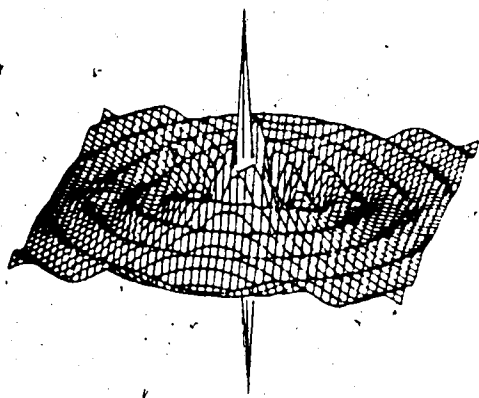
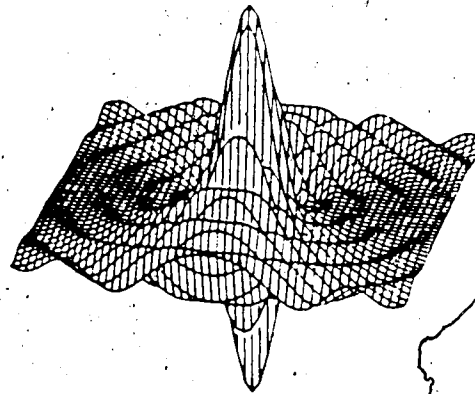
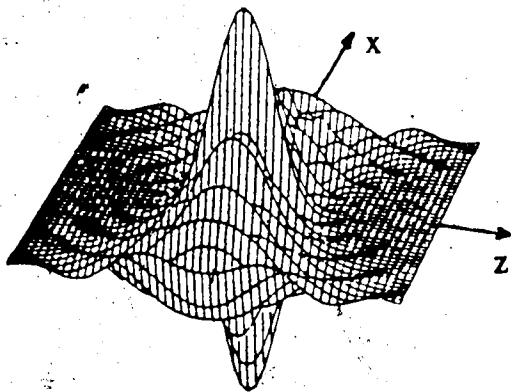
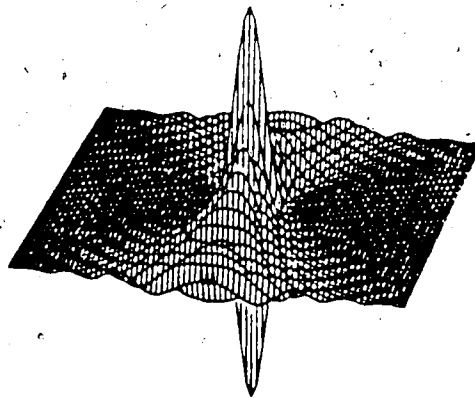
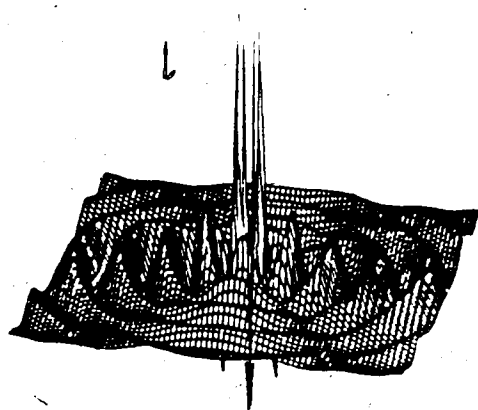
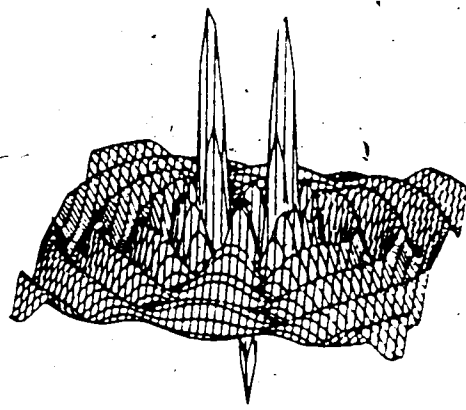
 $R = 2.0 \quad \epsilon = 0.15$  $R = 20.0 \quad \epsilon = 0.15$  $R = 40.0 \quad \epsilon = 0.15$  $R = 20.0 \quad \epsilon = 0.825$ $l = 1 \quad m = 1$

Figure 3 - 18 :

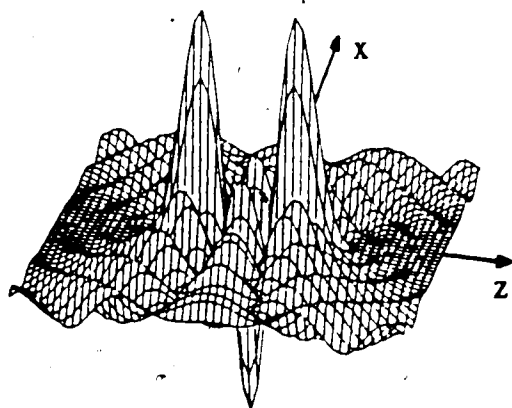
Continuum States



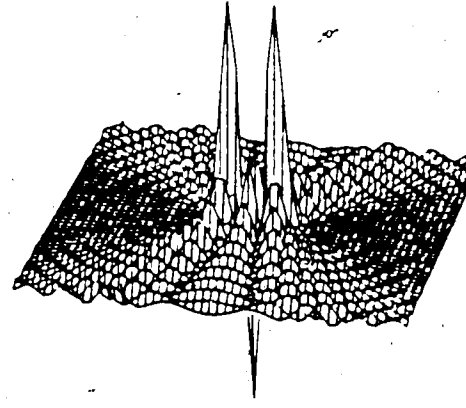
$R = 2.0 \quad \epsilon = 0.15$



$R = 20.0 \quad \epsilon = 0.15$



$R = 40.0 \quad \epsilon = 0.15$



$R = 20.0 \quad \epsilon = 0.825$

$l = 2 \quad m = 0$

Figure 3 - 19 :

Continuum States

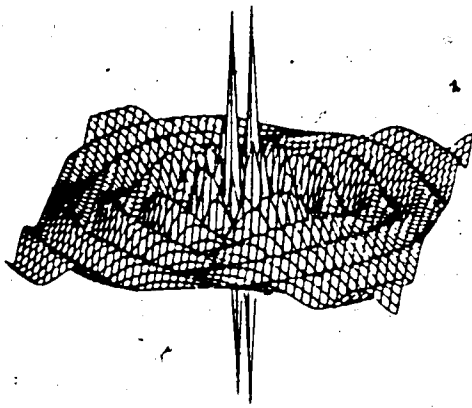
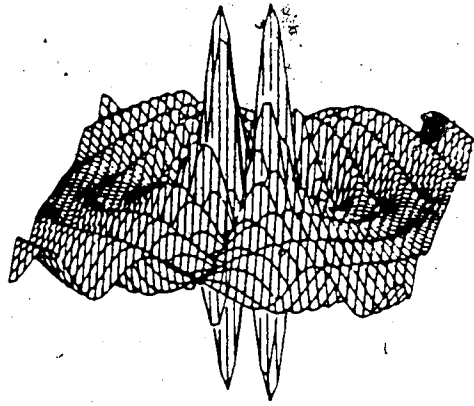
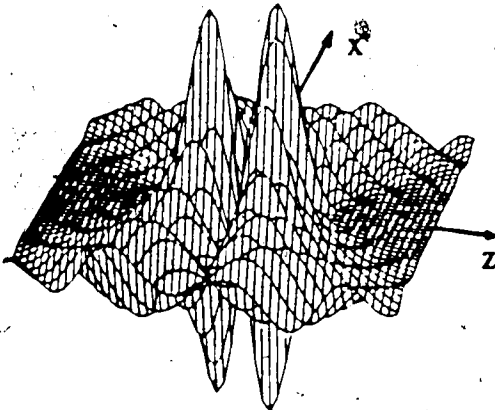
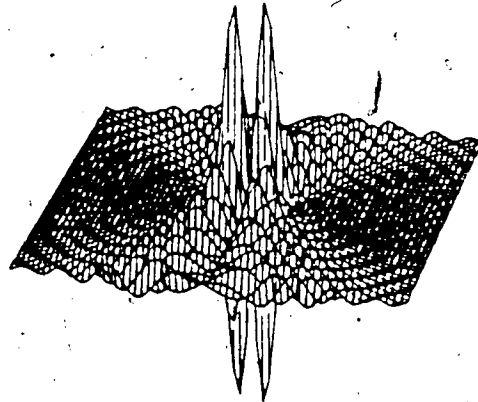
 $R = 2.0 \quad \epsilon = 0.15$  $R = 20.0 \quad \epsilon = 0.15$  $R = 40.0 \quad \epsilon = 0.15$  $R = 20.0 \quad \epsilon = 0.825$ $l = m = 1$

Figure 3 - 20 :

Continuum States

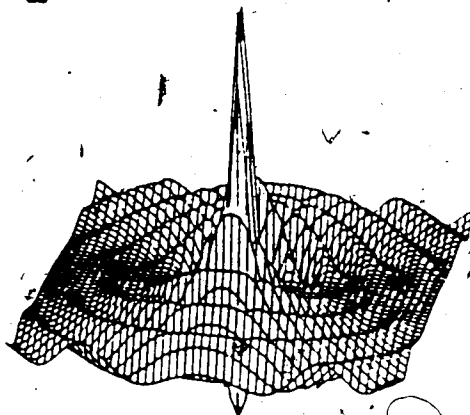
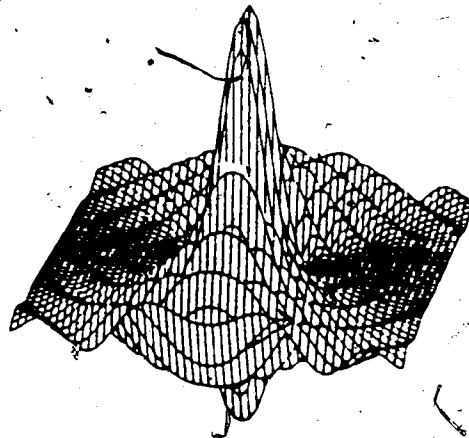
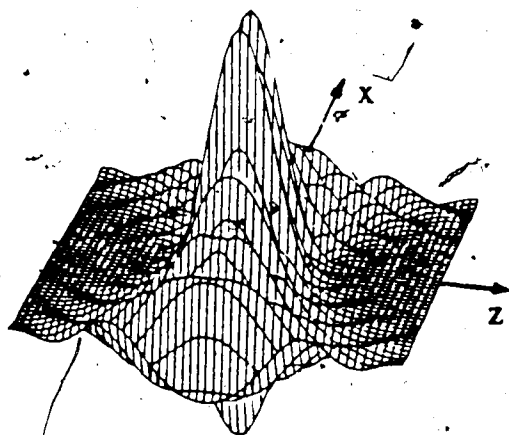
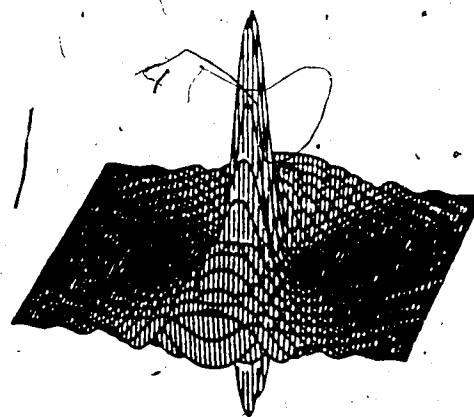
 $R = 2.0 \quad \epsilon = 0.15$  $R = 20.0 \quad \epsilon = 0.15$  $R = 40.0 \quad \epsilon = 0.15$  $R = 20.0 \quad \epsilon = 0.825$ $l = 2 \quad m = 2$

Figure 3 - 21 :

When $c = 0$, one can generate an initial value for P_+ using the Newman-Thorson algorithm [64]. Then following the steps (2)→(5) of section 3.2.7 a point-wise representation for $\chi(\xi)$ can be generated. In this way we have numerically demonstrated the existence of a *slowly varying* P_R even when $c = 0$.

We have fitted P_R up to a maximum absolute error of 1.0×10^{-7} . The number of fitting subintervals ranged from 2 → 10, increasing with decreasing c^2 . The number of parameters required to fit P_R in each subinterval ranged from 5 → 14. On average we can globally represent a total continuum wave function, including the angular part in the form given in equation (3 - 7), with about 90 parameters. This is a non-trivial achievement when the rapidly oscillatory nature of the continuum states is considered.

Due to the growing potential barrier between the two nuclei, the molecular *bound* states become atomic states as $R \rightarrow \infty$. Such a barrier is nonexistent for continuum states and apparently they do not go to simple linear combinations of atomic states with increasing R ; they *remain* centred at the centre of charge of the nuclei which is the location of the saddle point of the molecular electronic potential. Some amplitude enhancement is also seen along the line of "equiforce". For $x < R\sqrt{2}$ this is a ridge of the potential.

It is worth noting that one can generate the *irregular* solution, $\tilde{\chi}(\xi)$, of equation (3 - 4) using the same $P_R(\xi)$ and $\Theta(\xi)$.

4. ADIABATIC WAVE PACKETS

4.1 Introduction

In this chapter we will study the properties of the adiabatic wave packets and propose a systematic way of choosing the *packet widths*, $\{\Delta_j\}$, based on a specification of the size of an "interaction region".

4.2 Definition of Packets

Adiabatic wave packets, ϕ , are defined by

$$\phi(jlm; R; \vec{r}) = \frac{1}{\sqrt{\Delta_j}} \int_{\epsilon_j - \frac{1}{2}\Delta_j}^{\epsilon_j + \frac{1}{2}\Delta_j} d\epsilon \psi(\epsilon lm; R; \vec{r}) \quad (4-1)$$

with

$$\epsilon_1 = \frac{1}{2}\Delta_1 \quad \epsilon_{j+1} = \epsilon_j + \frac{1}{2}(\Delta_{j+1} - \Delta_j) \quad j \geq 1 \quad (4-2)$$

The ψ are the adiabatic continuum states;

$$\psi(\epsilon lm; R; \vec{r}) = \frac{2}{\sqrt{\pi R(\xi^2 - 1)}} \frac{\sin \Theta(\epsilon lm; R; \xi)}{\sqrt{P_R(\epsilon lm; R; \xi)}} S(\epsilon lm; R; \eta) \frac{\exp(im\phi)}{\sqrt{2\pi}} \quad (4-3)$$

and P_R , S and Θ are as defined in Chapter 3.

These wave packets are *orthonormal*; equation (2-9).

4.3 An Approximate Analytical Form

P_R is a slowly varying function of energy (see Chapter 3); hence over a packet width we can approximate

$$\frac{1}{\sqrt{P_R(\epsilon lm; R; \xi)}} \approx \frac{1}{\sqrt{P_R(\epsilon_j lm; R; \xi)}} \quad (4-4)$$

It is reasonable (see Figure 4 - 1) to approximate Θ by

$$\Theta(\epsilon lm; R; \xi) \simeq \Theta(\epsilon_j lm; R; \xi) + \Theta_j^1(lm; R; \xi) (\epsilon - \epsilon_j) \quad (4 - 5)$$

where

$$\Theta_j^1(lm; R; \xi) = \left[\frac{\partial \Theta(\epsilon lm; R; \xi)}{\partial \epsilon} \right]_{\epsilon = \epsilon_j} \quad (4 - 6)$$

The number of nodes of $S(\epsilon lm; R; \eta)$ in the range $-1 < \eta < +1$ is independent of ϵ . Hence we can safely assume that $S(\epsilon lm; R; \eta)$ is a slowly varying function of ϵ (see the plots in Chapter 3) and we write

$$S(\epsilon lm; R; \eta) \simeq S(\epsilon_j lm; R; \eta) \quad (4 - 7)$$

Now, equations (4 - 1), (4 - 3), (4 - 4), (4 - 5) and (4 - 7) give

$$\tilde{\phi}(jlm; R; \bar{r}) \simeq \sqrt{\Delta_j} \frac{\sin\left(\frac{1}{2}\Delta_j \Theta_j^1(lm; R; \xi)\right)}{\left(\frac{1}{2}\Delta_j \Theta_j^1(lm; R; \xi)\right)} \psi(\epsilon_j lm; R; \bar{r}) \quad (4 - 8)$$

The packet state is approximately equal to the adiabatic continuum state at the energy mid-point multiplied by an *envelope* factor, $\sin(x)/x$, and a constant.

$\sin^2(x)/x^2$ is a rapidly decaying function with 90.3% of the area (for $x \geq 0$) within $0 \leq x \leq \pi$.

$\partial \Theta(\epsilon lm; R; \xi) / \partial \epsilon$ is a monotonically increasing function of ξ with

$$\frac{\partial \Theta(\epsilon lm; R; \xi = 1)}{\partial \epsilon} = 0 \quad (4 - 9)$$

(see figure 4-1).

Hence most of the *probability* in a packet state is contained in the prolate spheroidal region $1 \leq \xi \leq \xi_{IR}$ with ξ_{IR} satisfying

$$\frac{1}{2} \Delta_j \Theta_j^1(lm; R; \xi_{IR}) = \pi \quad (4 - 10)$$

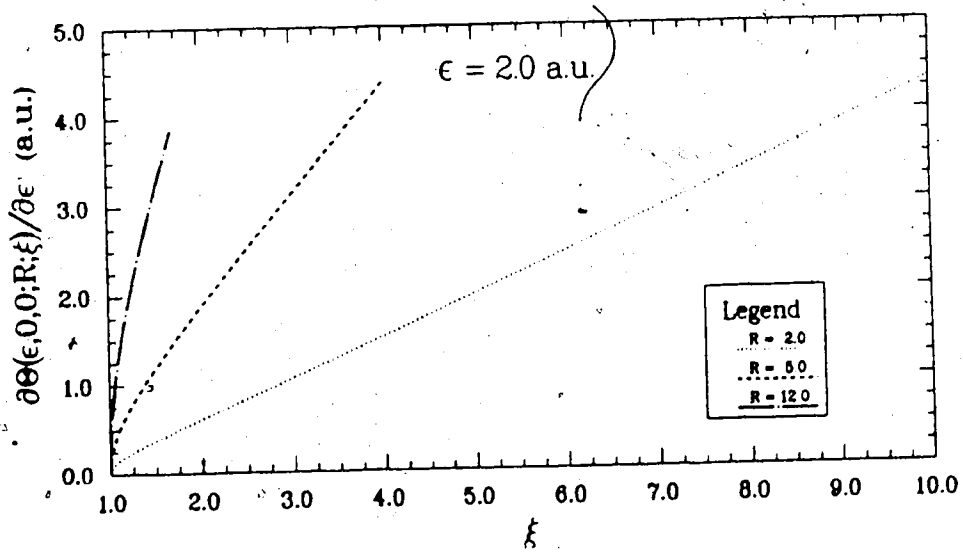
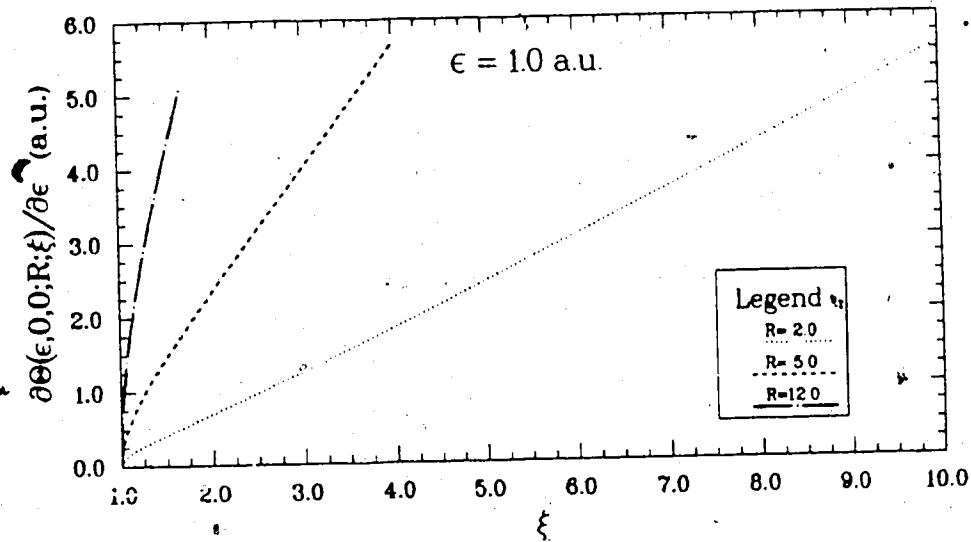
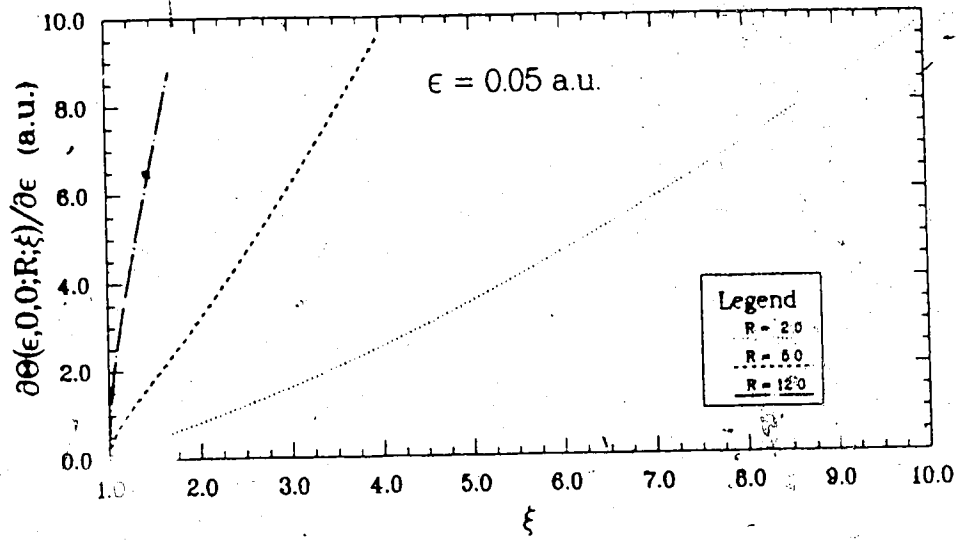


Figure 4 - 1 : $\frac{\partial \theta}{\partial \epsilon}$ vs. ξ

Note that the region of localization of the packet is governed by Θ_j^1 as well as Δ_j .

4.4 A Unique Choice of Packet Widths

Define a prolate spheroidal interaction region with a minor radius a_b and a constant major radius b_b . Then

$$\xi_{IR} = \frac{2b_b}{R} \quad (4-11a)$$

$$a_b = \frac{R}{2} \sqrt{\xi_{IR}^2 - 1} \quad (4-11b)$$

We require Δ_j satisfy the equation (4-10) in addition to equation (4-2). This uniquely defines a set of packet widths, $\{\Delta_j\}$, which guarantees that the packets are well localized within the interaction region.

Several questions must be answered before we accept this "recipe".

- (a) In the theory we assume Δ_j to be independent of R (see Chapter 2). Is this condition satisfied?
- (b) Are Δ_j 's independent of l and m ?

To answer these questions and to calculate Δ_j we numerically study the packet width function, Δ , defined by

$$\Delta(lm; R; b_b; \epsilon) = \frac{2\pi}{\partial\Theta(\epsilon lm; R; \xi_{IR})/\partial\epsilon} \quad (4-12)$$

4.5 Calculation of $\Delta(lm; R; b_b; \epsilon)$

4.5.1 Theory

At a general ξ , by definition

$$\frac{\partial\Theta}{\partial\epsilon} = \Theta^1(\epsilon lm; R; \xi) = \int_1^\xi d\xi \frac{\partial P_R(\epsilon lm; R; \xi)}{\partial\epsilon} = \int_1^\xi d\xi Q_R(\xi) \quad (4-13)$$

The differential equation for Q_R can be obtained by differentiating equation (3 - 14) with respect to ϵ .

$$2Q_+P_+ - i \frac{dQ_+}{d\xi} = W(\xi) \quad (4 - 14)$$

where

$$Q_+ = \frac{\partial P_+}{\partial \epsilon} = Q_R + iQ_I \quad (4 - 15)$$

$$W(\xi) = \frac{1}{(\xi^2 - 1)} \left[\frac{R^2 \xi^2}{2} - \frac{\partial A}{\partial \epsilon} \right] \quad (4 - 16)$$

It can be shown (see Appendix A) that

$$\frac{\partial A}{\partial \epsilon} = \frac{R^2}{2} \int_{-1}^{+1} d\eta \eta^2 S^2(\epsilon l m; R; \eta) \quad (4 - 17)$$

Boundary conditions on Q_+ are obtained from equation (3 - 37).

$$\lim_{\xi \rightarrow \infty} Q_R = \frac{R}{2\sqrt{2\epsilon}} \quad (4 - 18a)$$

$$\lim_{\xi \rightarrow \infty} Q_I = 0 \quad (4 - 18b)$$

Integration of equation (4 - 14) cannot be continued up to $\xi = 1$. Hence, near $\xi = 1$ it is appropriate to use the following forms (deduced from equation (3 - 26) and (3 - 27)).

$$Q_R = \frac{P_R}{\gamma \varrho} \left[\gamma' \varrho - 2P_R (\psi_1 \varphi_1 + (\beta \psi_1 + \gamma \psi_2)(\beta' \psi_1 + \beta \varphi_1 + \gamma' \psi_2 + \gamma \varphi_2)) \right] \quad (4 - 19)$$

$$\frac{\partial \Theta}{\partial \epsilon} = \frac{\varphi_1 - [\beta' \psi_1 + \beta \varphi_1 + \gamma' \psi_2 + \gamma \varphi_2] \tan \Theta}{(\beta \psi_1 + \gamma \psi_2) \sec^2 \Theta} \quad (4 - 20)$$

where $\varphi_j = (\partial \psi_j / \partial \epsilon)$; $j = 1, 2$, $\beta' = (\partial \beta / \partial \epsilon)$ and $\gamma' = (\partial \gamma / \partial \epsilon)$. In deriving equations (4 - 19) and (4 - 20) we have used the fact

$$\frac{\partial \varrho}{\partial \epsilon} = \varphi_2 \frac{d\psi_1}{d\xi} + \psi_2 \frac{d\varphi_1}{d\xi} - \varphi_1 \frac{d\psi_2}{d\xi} - \psi_1 \frac{d\varphi_2}{d\xi} = 0 \quad (4 - 21)$$

In this domain φ_j can be represented by power series which can be obtained by differentiating equations (3 - 28) and (3 - 29) with respect to energy.

Two different iterative schemes can be used to generate P_+ and Q_+ at large ξ . Define the function $h_+(\xi)$ by

$$P_+(\xi) = k(\xi) + h_+(\xi) \quad (4 - 22)$$

with $k^2(\xi)$ given by equation (3 - 12). Substitution in equation (3 - 14) gives

$$h_+(\xi) = \alpha_0(\xi) + \beta_0(\xi)h_+^2(\xi) + \gamma_0(\xi)\frac{dh_+(\xi)}{d\xi} \quad (4 - 23)$$

where

$$\alpha_0 = \frac{i}{2k} \left(\frac{dk}{d\xi} \right) \quad \beta_0 = -\frac{1}{2k} \quad \gamma_0 = \frac{i}{2k} \quad (4 - 24)$$

A general solution to equation (4 - 23) [64] is given by (the asymptotic series)

$$h_+(\xi) \simeq \sum_{j=0}^n \alpha_j(\xi) \quad (4 - 25)$$

with an error of the order of $|\alpha_{n+1}|$ where

$$\alpha_{j+1} = \frac{\beta_j \alpha_j^2 + \gamma_j (d\alpha_j/d\xi)}{1 - 2\alpha_j \beta_j}$$

$$\beta_{j+1} = \frac{\beta_j}{1 - 2\alpha_j \beta_j}$$

$$\gamma_{j+1} = \frac{\gamma_j}{1 - 2\alpha_j \beta_j}$$

It can be shown that

$$\lim_{\xi \rightarrow \infty} \alpha_j = 0 \quad \text{for } j \geq 0$$

Hence, P_+ generated using the series (4 - 25) satisfies the appropriate boundary conditions (equations (3 - 37)).

To obtain an asymptotic series for Q_+ , define κ_0 by

$$Q_+(\xi) = \kappa_0(\xi) + \lambda_0(\xi) \quad (4-26)$$

where

$$\lambda_0(\xi) = \frac{W(\xi)}{2P_+(\xi)} \quad (3-27)$$

Equations (4-14), (4-26) and (4-24) give

$$2P_+(\xi)\kappa_0(\xi) - i \frac{d\kappa_0(\xi)}{d\xi} = i \frac{d\lambda_0(\xi)}{d\xi} \quad (4-28)$$

For $j \geq 0$ define

$$\kappa_j(\xi) = \kappa_{j+1}(\xi) + \lambda_{j+1}(\xi) \quad (4-29)$$

with

$$\lambda_{j+1} = \frac{i}{2P_+} \left(\frac{d\lambda_j}{d\xi} \right) \quad (4-30)$$

Then $\kappa_j(\xi)$ $j \geq 1$ satisfies an equation to (4-28).

Equations (4-26) and (4-29) give

$$Q_+(\xi) = \sum_{j=0}^n \lambda_j(\xi) + \kappa_n(\xi) \quad (4-31)$$

It can be shown that

$$\lim_{\xi \rightarrow \infty} \lambda_0(\xi) = \frac{R}{2\sqrt{2\epsilon}} \quad (4-32a)$$

$$\lim_{\xi \rightarrow \infty} \lambda_j(\xi) = 0 \quad j \geq 1 \quad (4-32b)$$

Then the boundary conditions on Q_+ require that

$$\lim_{\xi \rightarrow \infty} \kappa_n(\xi) = 0$$

Hence equation (4 - 31) gives an asymptotic series and we can approximate

$$Q_+(\xi) \approx \sum_{j=0}^n \lambda_j(\xi) \quad (4 - 33)$$

with an error of the order $|\lambda_{n+1}|$.

4 . 5 . 2 Numerical Method

The method is similar to that described in section 3 . 2 . 7. The differences are as follows.

- (1) $\partial A / \partial \epsilon$ was evaluated using equation (4 - 17).
- (2) Initial values for P_+ and Q_+ were generated at a large enough $\xi (= \xi_m)$ using equations (4 - 22), (4 - 25) and (4 - 33).
- (3) Equations (3 - 14) and (4 - 14) were integrated towards $\xi = 1$ as coupled equations. P_R and Q_R were simultaneously integrated to obtain Θ_T and Θ_T^1 .
- (4) At $\xi = \xi_0$ Q_R was smoothly connected to the form given in equation (4 - 19) to evaluate β' and γ' .

$$\beta' = \frac{B_2 B_5 - B_4 (dB_2/d\xi)}{B_2 (dB_1/d\xi) - B_1 (dB_2/d\xi)}$$

$$\gamma' = \frac{B_1 B_5 - B_4 (dB_1/d\xi)}{B_1 (dB_2/d\xi) - B_2 (dB_1/d\xi)}$$

where

$$B_1 = \psi_1(\beta\psi_1 + \gamma\psi_2)$$

$$B_2 = \psi_2(\beta\psi_1 + \gamma\psi_2) - \frac{\rho}{2P_R}$$

$$B_3 = (\psi_1 + \beta(\beta\psi_1 + \gamma\psi_2))\varphi_1 + \gamma(\beta\psi_1 + \gamma\psi_2)\varphi_2$$

$$B_4 = -\frac{\rho\gamma Q_R}{2P_R^2} - B_3$$

$$B_5 = e\gamma \left(\frac{P_I Q_R}{P_R^2} - \frac{Q_I}{P_R} \right) - \frac{dB_3}{d\xi}$$

(5) At $\xi = \xi_{00}$ in addition to Θ , Θ^1 was evaluated using equation (4 - 20).

(6) Θ_T and Θ_T^1 was adjusted to obtain $\Theta(\xi)$ and $\Theta^1(\xi)$.

4.5.3 Numerical Details

Where applicable, the numerical details are similar to those described in section 3.2.8. In addition one must note the following.

(a) P_+ and Q_+ were evaluated (absolute error 1.0×10^{-7}) at

$$\xi_m = \begin{cases} \xi_L, & \text{if } \epsilon \leq 0.2; \\ \xi_L + 1.5/c, & \text{if } \epsilon > 0.2. \end{cases}$$

where

$$\xi_L = \begin{cases} 10.0/\sqrt{c} + 5.0, & \text{if } l < 2; \\ 10.0/\sqrt{c} + 5.0 + 3(l-1)/\sqrt{2cR}, & \text{if } l \geq 2. \end{cases}$$

Here ϵ , c and R are in atomic units.

(b) Accuracy of φ_1 and φ_2 were monitored by checking the validity of equation (4 - 21).

(c) The study was mainly on states with $l = 0, 1, 2$ with all possible m , $0.0001 < c^2 \leq 200.0 \text{ a.u.}$ and $R \leq 20.0 \text{ a.u.}$

The following checks were done to assess the accuracy/precision of the results.

(i) P_R and Θ were compared with those calculated by the method described in Chapter 3.

(ii) At a number of points (R, ξ) , Θ^1 was compared with an estimate obtained by fitting Θ with a quadratic polynomial in ξ and differentiating it.

(iii) Stability of the results was checked against changes in ξ_m , ξ_0 and ξ_{00} .

4.5.4 Results

A sample of Θ^1 is displayed in Figure 4-1. It is a monotonically increasing function which is quite insensitive to (l, m) .

A representative sample of the results for Δ are in Tables 4-1, 4-2 and 4-3. For a given l value, the dependence of Δ on R becomes stronger with increasing $(l - m)$ and decreasing ϵ and b_b . With increasing b_b , Δ becomes less sensitive to changes in (l, m) .

In particular, for $b_b \geq 40.0$ a.u., $\epsilon \geq 0.05$ a.u. and $R \leq 20.0$ a.u. the maximum deviation of Δ from the average is less than 0.01 a.u. ($< 10\%$); hence to a good approximation one can consider Δ to be independent of R and (l, m) .

Variation of Δ with ϵ and b_b are shown in Figures 4-2 and 4-3. They were calculated using the particular state $l = 0, m = 0$ and $R = 12.0$ a.u..

4.6 Calculation of ϵ_j and Δ_j

ϵ_j is a solution of the equation

$$2 \left(\epsilon - (1 - \delta_{0j-1}) \sum_{q=1}^{j-1} \Delta_q \right) = \Delta(lm; R; b_b; \epsilon) \quad (4-34)$$

This can be solved (for a given b_b) using the graphs in figures 4-2 and the equation (4-2). Table 4-4 is a listing of solutions for $l = 0, m = 0, R = 12.0$ a.u. for a number of b_b values.

4.7 Choice of b_b and the Energy Sampling

The "interaction region" should be large enough to contain all the bound states included in the calculation. A rule of thumb is to use the Bohr radius of the hydrogenic state of the largest principal quantum number of the bound states. For example, if we include all the bound molecular states $n \leq 6$, then b_b must be at

Table 4 - 1 : $\Delta(lm; R; b_b; \epsilon)$ at $b_b = 20.0$.

(All the quantities are in atomic units)

ϵ	(l,m)	(0,0)	(1,0)	(1,1)	(2,0)	(2,1)	(2,2)
	R						
0.05	0.5	0.2390	0.2313	0.2313	0.2190	0.2190	0.2191
0.05	1.0	0.2390	0.2319	0.2314	0.2189	0.2191	0.2192
0.05	3.0	0.2395	0.2376	0.2313	0.2193	0.2211	0.2197
0.05	5.0	0.2402	0.2436	0.2311	0.2276	0.2254	0.2202
0.05	8.0	0.2413	0.2536	0.2312	0.2405	0.2326	0.2210
0.05	12.0	0.2422	0.2680	0.2324	0.2613	0.2430	0.2234
0.05	16.0	0.2436	0.2821	0.2357	0.2885	0.2546	0.2281
0.05	20.0	0.2457	0.2956	0.2424	0.3218	0.2687	0.2365
1.00	0.5	0.5142	0.5049	0.5052	0.4969	0.4970	0.4971
1.00	1.0	0.5142	0.5064	0.5056	0.4963	0.4971	0.4775
1.00	3.0	0.5121	0.5177	0.5058	0.5028	0.5022	0.4993
1.00	5.0	0.5077	0.5197	0.5048	0.5228	0.5078	0.5006
1.00	8.0	0.5054	0.5144	0.5046	0.5280	0.5108	0.5029
1.00	12.0	0.5111	0.5168	0.5110	0.5119	0.5162	0.5107
1.00	16.0	0.5261	0.5304	0.5262	0.5355	0.5204	0.5266
1.00	20.0	0.5520	0.5556	0.5523	0.5595	0.5558	0.5531
2.50	0.5	0.7557	0.7469	0.7474	0.7410	0.7412	0.7415
2.50	1.0	0.7556	0.7494	0.7479	0.7401	0.7416	0.7421
2.50	3.0	0.7506	0.7592	0.7477	0.7563	0.7482	0.7441
2.50	5.0	0.7476	0.7541	0.7469	0.7640	0.7508	0.7454
2.50	8.0	0.7507	0.7542	0.7506	0.7589	0.7538	0.7504
2.50	12.0	0.7655	0.7677	0.7656	0.7703	0.7678	0.7659

Table 4 - 2 : $\Delta(lm; R; b_b; \epsilon)$ at $b_b = 40.0$.

(All the quantities are in atomic units)

ϵ	(l,m)	(0,0)	(1,0)	(1,1)	(2,0)	(2,1)	(2,2)
	R						
0.05	0.5	0.0931	0.0917	0.0917	0.0891	0.0891	0.0891
0.05	1.0	0.0931	0.0917	0.0917	0.0891	0.0891	0.0891
0.05	3.0	0.0932	0.0926	0.0916	0.0892	0.0894	0.0892
0.05	5.0	0.0932	0.0935	0.0915	0.0905	0.0901	0.0892
0.05	8.0	0.0932	0.0949	0.0912	0.0924	0.0911	0.0890
0.05	12.0	0.0928	0.0967	0.0909	0.0953	0.0923	0.0888
0.05	16.0	0.0921	0.0981	0.0905	0.0986	0.0935	0.0887
0.05	20.0	0.0914	0.0989	0.0904	0.1021	0.0939	0.0887
1.00	0.5	0.2426	0.2405	0.2405	0.2385	0.2385	0.2385
1.00	1.0	0.2426	0.2408	0.2406	0.2384	0.2385	0.2386
1.00	3.0	0.2420	0.2432	0.2405	0.2398	0.2396	0.2389
1.00	5.0	0.2407	0.2434	0.2400	0.2441	0.2406	0.2389
1.00	8.0	0.2394	0.2415	0.2392	0.2446	0.2406	0.2387
1.00	12.0	0.2391	0.2404	0.2390	0.2422	0.2402	0.2388
1.00	16.0	0.2398	0.2408	0.2398	0.2420	0.2407	0.2397
1.00	20.0	0.2407	0.2416	0.2415	0.2426	0.2423	0.2415
2.50	0.5	0.3666	0.3645	0.3646	0.3630	0.3631	0.3631
2.50	1.0	0.3660	0.3651	0.3647	0.3628	0.3631	0.3632
2.50	3.0	0.3660	0.3672	0.3645	0.3665	0.3646	0.3635
2.50	5.0	0.3640	0.3656	0.3638	0.3680	0.3647	0.3634
2.50	8.0	0.3636	0.3644	0.3635	0.3656	0.3643	0.3634
2.50	12.0	0.3645	0.3651	0.3645	0.3657	0.3651	0.3645

Table 4 - 3 : $\Delta(lm; R; b_0; \epsilon)$ at $b_0 = 60.0$.

(All the quantities are in atomic units)

ϵ	R	(l,m)					
		(0,0)	(1,0)	(1,1)	(2,0)	(2,1)	(2,2)
0.05	0.5	0.0549	0.0543	0.0543	0.0533	0.0533	0.0533
0.05	1.0	0.0549	0.0543	0.0543	0.0533	0.0533	0.0533
0.05	3.0	0.0549	0.0543	0.0543	0.0533	0.0534	0.0533
0.05	5.0	0.0549	0.0549	0.0542	0.0538	0.0536	0.0533
0.05	8.0	0.0548	0.0554	0.0541	0.0544	0.0540	0.0532
0.05	12.0	0.0546	0.0560	0.0539	0.0554	0.0544	0.0531
0.05	16.0	0.0543	0.0564	0.0537	0.0565	0.0547	0.0529
0.05	20.0	0.0539	0.0565	0.0534	0.0576	0.0548	0.0528
1.00	0.5	0.1580	0.1571	0.1571	0.1562	0.1562	0.1562
1.00	1.0	0.1580	0.1572	0.1571	0.1562	0.1562	0.1563
1.00	3.0	0.1577	0.1583	0.1571	0.1568	0.1567	0.1564
1.00	5.0	0.1576	0.1583	0.1568	0.1586	0.1571	0.1563
1.00	8.0	0.1565	0.1574	0.1564	0.1587	0.1570	0.1561
1.00	12.0	0.1561	0.1567	0.1561	0.1575	0.1566	0.1560
1.00	16.0	0.1561	0.1565	0.1561	0.1571	0.1565	0.1560
1.00	20.0	0.1562	0.1566	0.1562	0.1572	0.1567	0.1564
2.50	0.5	0.2416	0.2406	0.2407	0.2400	0.2400	0.2400
2.50	1.0	0.2415	0.2409	0.2407	0.2399	0.2400	0.2401
2.50	3.0	0.2409	0.2418	0.2406	0.2415	0.2406	0.2402
2.50	5.0	0.2403	0.2410	0.2402	0.2421	0.2406	0.2400
2.50	8.0	0.2400	0.2403	0.2399	0.2409	0.2403	0.2399
2.50	12.0	0.2400	0.2403	0.2400	0.2406	0.2403	0.2400

Figure 4 - 2 : Packet Width vs. Continuum Energy

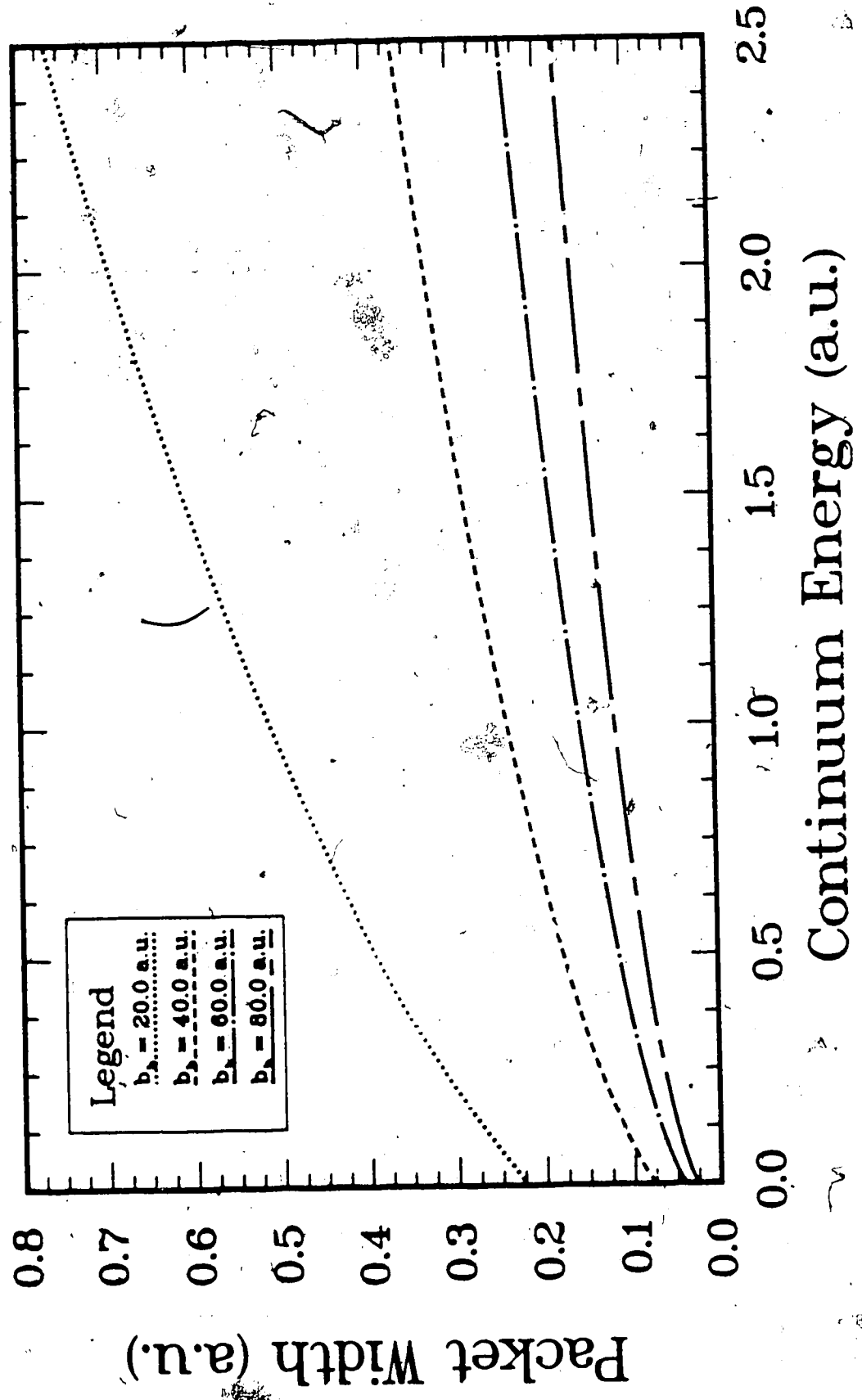


Figure 4 - 3 : Packet Width vs. b_b

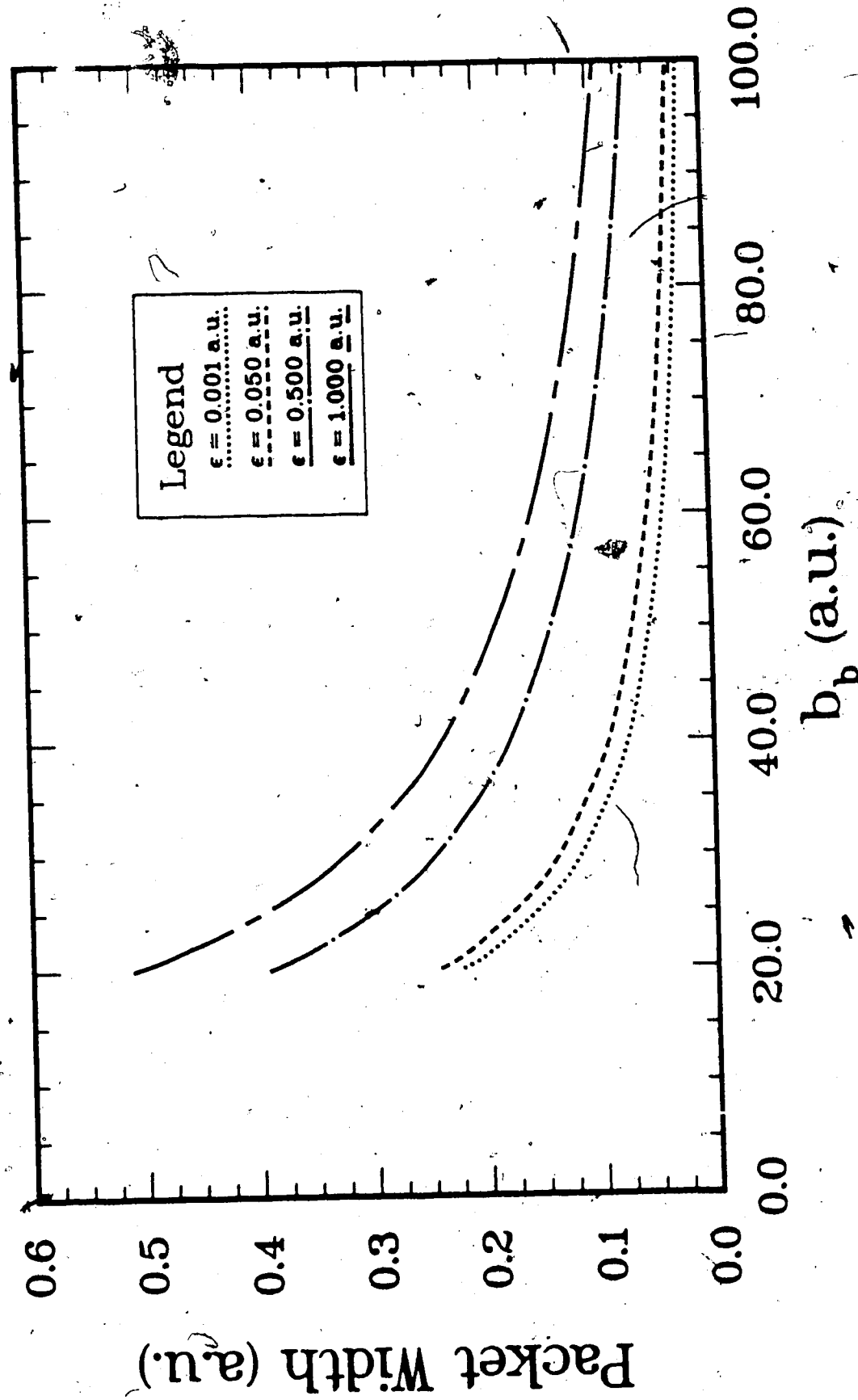


Table 4 - 4 : Energy Sampling. (All quantities are in a.u.)

(Maximum error in ϵ_j is ± 0.0025)

j	$b_b = 40.0$		$b_b = 60.0$		$b_b = 80.0$	
	ϵ_j	Δ_j	ϵ_j	Δ_j	ϵ_j	Δ_j
1	0.0450	0.0900	0.0250	0.0500	0.0150	0.030
2	0.1500	0.1200	0.0800	0.0600	0.0500	0.040
3	0.2825	0.1450	0.1450	0.0700	0.0925	0.045
4	0.4400	0.1700	0.2200	0.0800	0.1400	0.050
5	0.6200	0.1900	0.3075	0.0950	0.1950	0.060
6	0.8250	0.2200	0.4075	0.1050	0.2575	0.065
7	1.0600	0.2500	0.5175	0.1150	0.3250	0.070
8	1.3225	0.2750	0.6400	0.1300	0.3975	0.075
9	1.6100	0.3000	0.7750	0.1400	0.4775	0.085
10	1.9225	0.3250	0.9200	0.1500	0.5650	0.090
11	2.2600	0.3500	1.0750	0.1600	0.6575	0.095
12			1.2400	0.1700	0.7550	0.100
13			1.4175	0.1850	0.8600	0.110
14			1.6075	0.1950	0.9725	0.115
15			1.8075	0.2050	1.0900	0.120
16			2.0175	0.2150	1.2125	0.125
17			2.2375	0.2250	1.3425	0.135
18					1.4800	0.140
19					1.6225	0.145
20					1.7700	0.150
21					1.9250	0.160
22					2.0875	0.165
23					2.2550	0.170

least 36.0 a.u.. For further calculations in this thesis we have taken $b_b = 40.0$ a.u.; the conclusions are generally applicable for $b_b > 40.0$ a.u.

At $b_b = 40.0$ a.u. we observe that the average value of Δ for each ϵ does not deviate much ($< 1\%$) from that at $l = 0$ $m = 0$ $R = 12.0$ a.u.. Hence we take the energy sampling and $\{\Delta_j\}$, independent of R and (l, m) to be that given in Table 4-4.

In Figure 4-4 we have displayed the variation of the first packet energy with the (major) radius of the interaction region. This curve can be fitted accurately (error $< 4\%$ for $30.0 \leq b_b \leq 100.0$ a.u.; $< 0.5\%$ for $100.0 < b_b < 300.0$ a.u.) to the form

$$\epsilon_1 = \zeta \exp(-\varpi(b_b)^\rho)$$

with $\zeta = 3.5916 \times 10^{41}$ $\varpi = 93.2410$ and $\rho = 0.015625$.

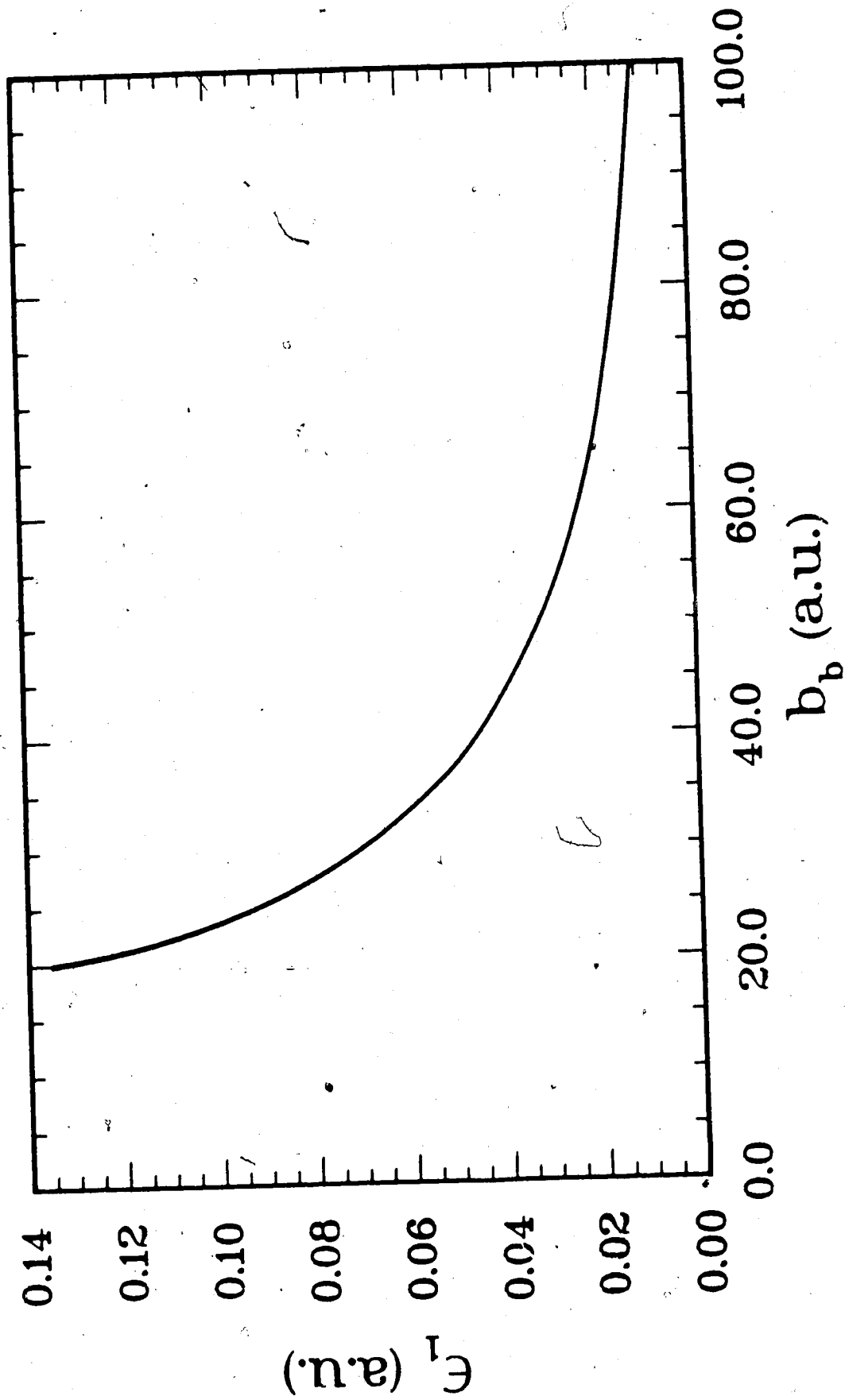
4.8 Explicit Construction of Wave Packets

To verify the properties deduced approximately in section 4.3, wave packets were constructed explicitly using equation (4-4) and the wave functions calculated in Chapter 3. Energy integrations were done using Simpson's rule, 7 energy points per packets kept the absolute error below 1.0×10^{-5} within the interaction region. Relief plots of the wave packets on an 80×80 a.u. grid in the xz -plane are displayed in Figures 4-5 \rightarrow 10. Average packet energies and the internuclear separations are indicated (in a.u.) on each plot.

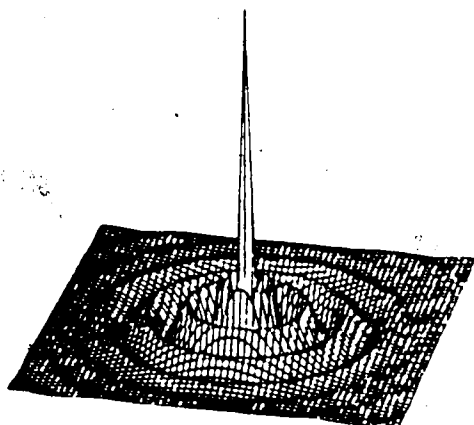
Comparison of these plots with those of the exact continuum states in Chapter 3 clearly reveals the presence of the damping factor in the packets as suggested by the equation (4-8).

4.9 Discussion

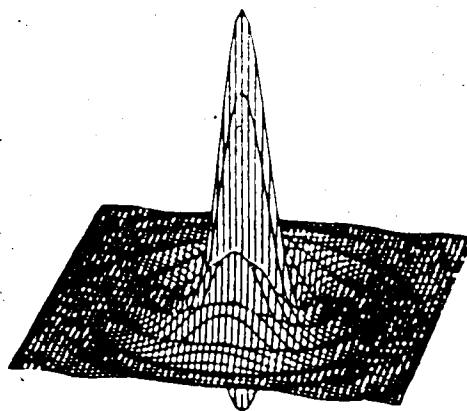
In generating initial values for P_+ and Q_+ we used the asymptotic series given in equations (4-25) and (4-33) rather than the ones given in equation

Figure 4 - 4 : First Packet Energy vs. b_b 

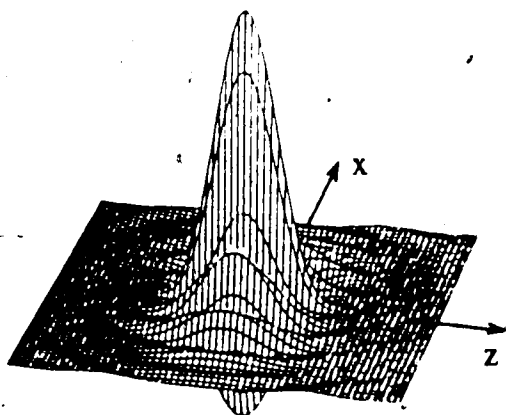
Wave Packets



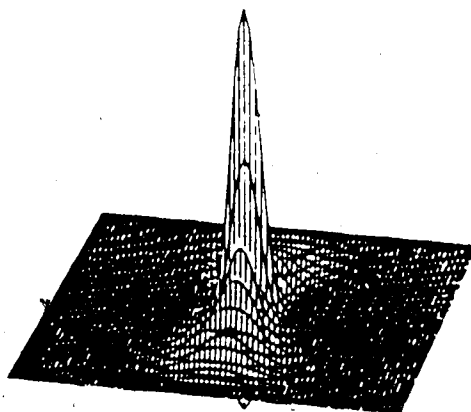
$$R = 2.0 \quad \epsilon_j = 0.15$$



$$R = 20.0 \quad \epsilon_j = 0.15$$



$$R = 40.0 \quad \epsilon_j = 0.15$$

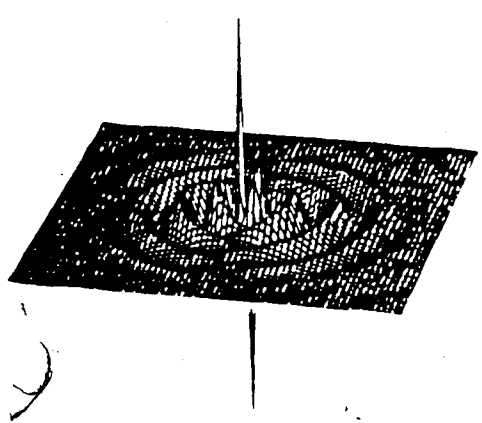


$$R = 20.0 \quad \epsilon_j = 0.825$$

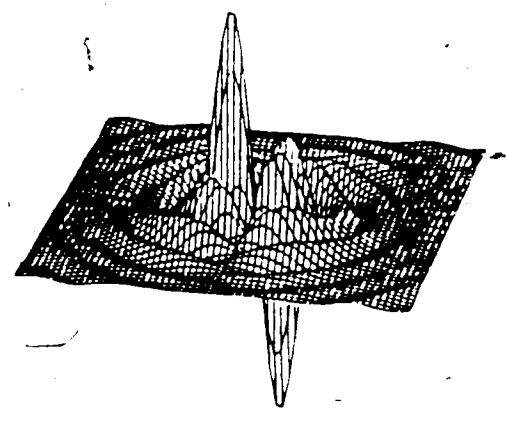
$$l = 0 \quad m = 0$$

Figure 4 - 5 :

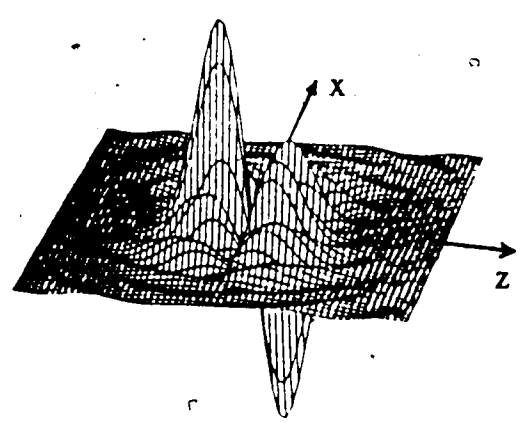
Wave Packets



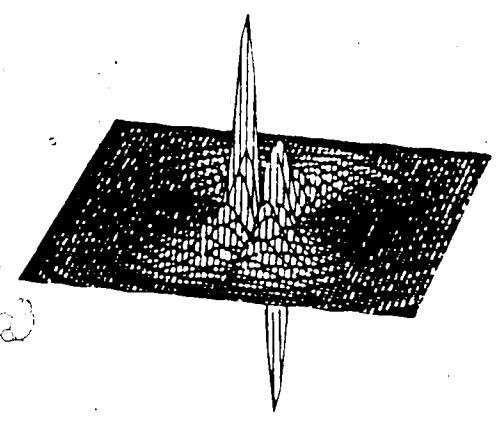
$R = 2.0 \quad \epsilon_j = 0.15$



$R = 20.0 \quad \epsilon_j = 0.15$



$R = 40.0 \quad \epsilon_j = 0.15$

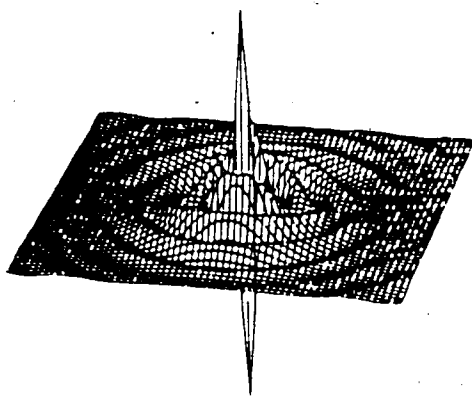


$R = 20.0 \quad \epsilon_j = 0.825$

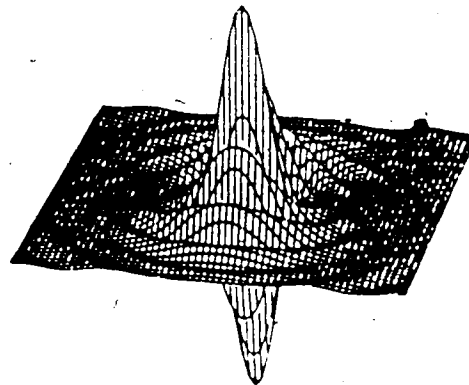
$l = 1 \quad m = 0$

Figure 4 - 6 :

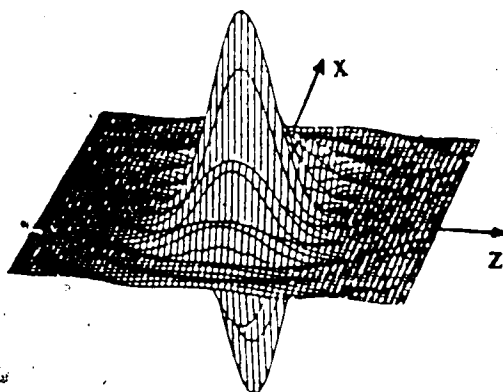
Wave Packets



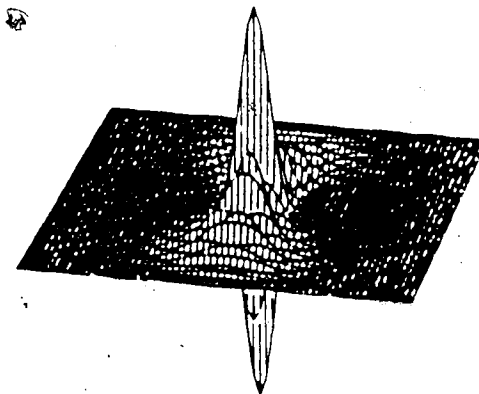
$$R = 2.0 \quad \epsilon_j = 0.15$$



$$R = 20.0 \quad \epsilon_j = 0.15$$



$$R = 40.0 \quad \epsilon_j = 0.15$$

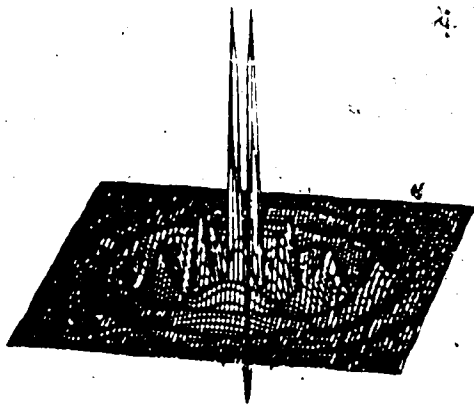


$$R = 20.0 \quad \epsilon_j = 0.825$$

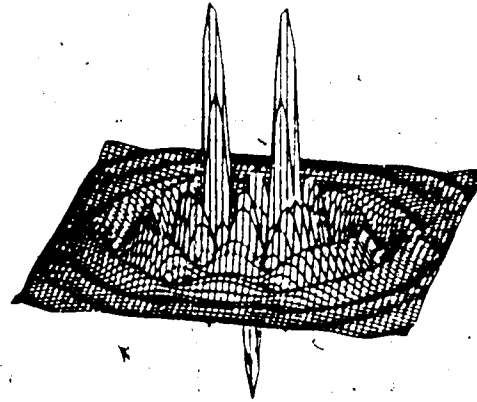
$$l = 1 \quad m = 1$$

Figure 4 - 7 :

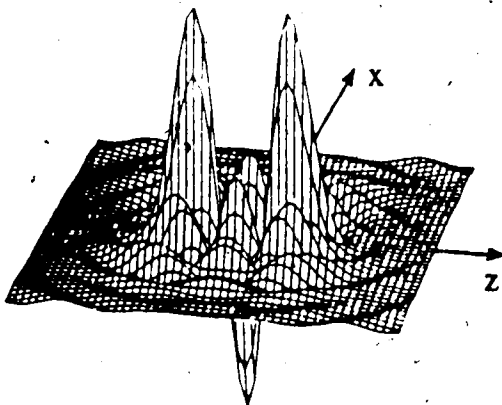
Wave Packets



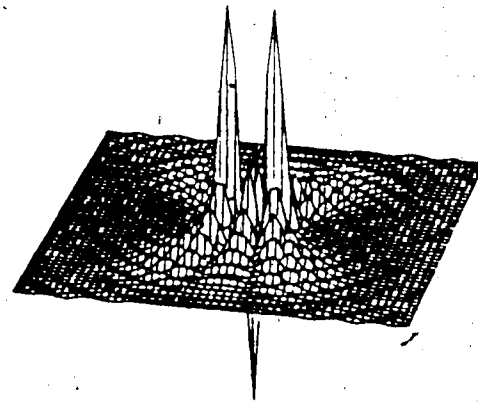
$$R = 2.0 \quad \epsilon_j = 0.15$$



$$R = 20.0 \quad \epsilon_j = 0.15$$



$$R = 40.0 \quad \epsilon_j = 0.15$$

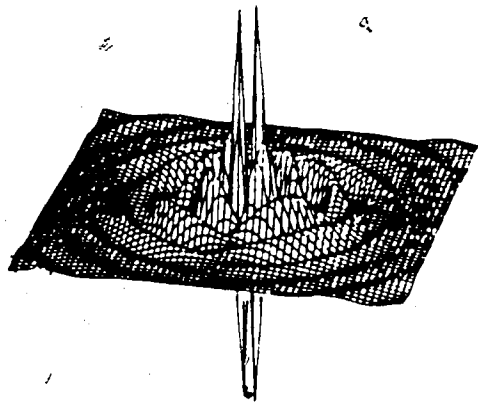


$$R = 20.0 \quad \epsilon_j = 0.825$$

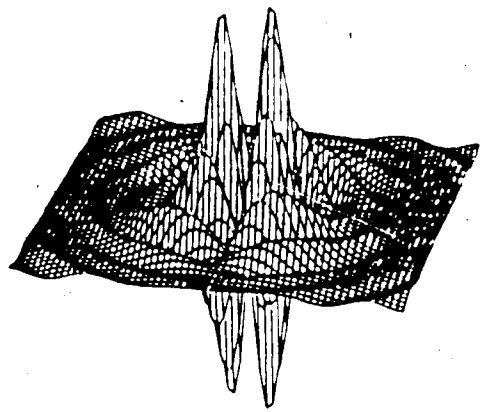
$$l = 2 \quad m = 0$$

Figure 4 - 8 :

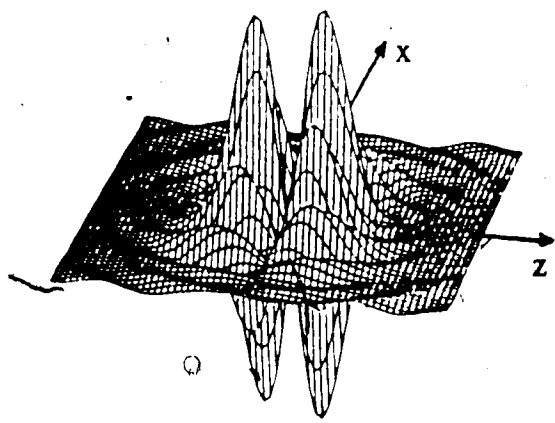
Wave Packets



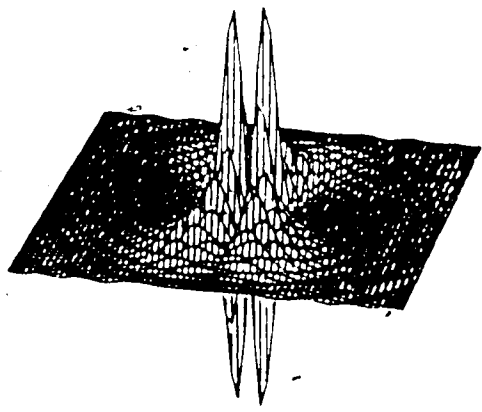
$R = 2.0 \quad \epsilon_j = 0.15$



$R = 20.0 \quad \epsilon_j = 0.15$



$R = 40.0 \quad \epsilon_j = 0.15$

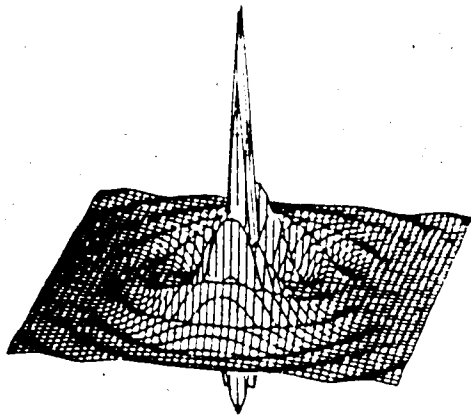


$R = 20.0 \quad \epsilon_j = 0.825$

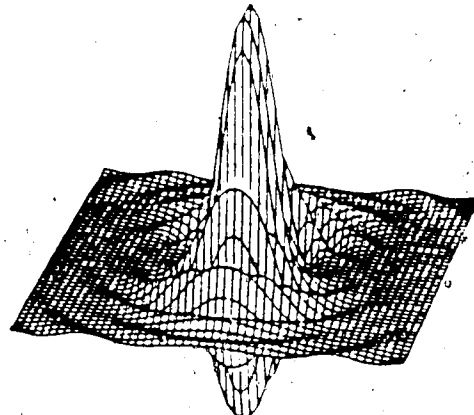
$$l = 2 \quad m = 1$$

Figure 4-9 :

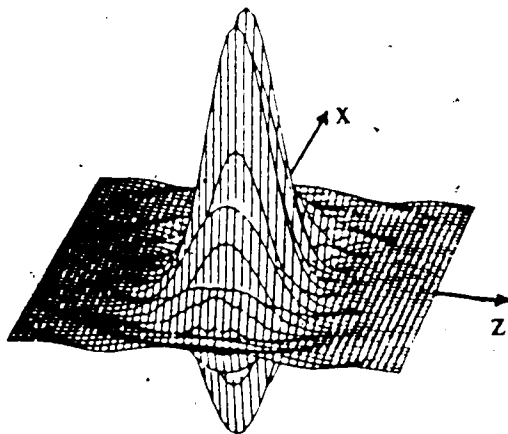
Wave Packets



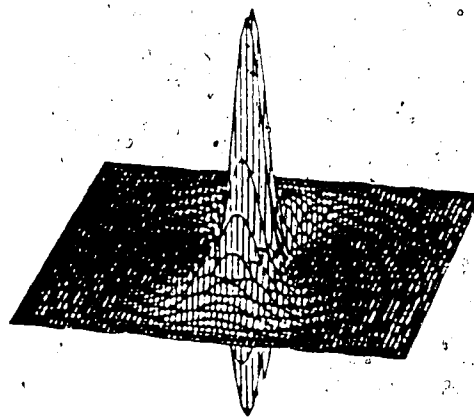
$$R = 2.0 \quad \epsilon_j = 0.15$$



$$R = 20.0 \quad \epsilon_j = 0.15$$



$$R = 40.0 \quad \epsilon_j = 0.15$$



$$R = 20.0 \quad \epsilon_j = 0.825$$

$$l = 2 \quad m = 2$$

Figure 4 - 10 :

(3 - 44) and the one for Q_+ that can be deduced from it, because for small c the latter ones converge at very large ξ_m .

Past calculations [19,20] suggest that $R_0, R_\infty < 20.0 \text{ a.u.}$. Hence we limited our study to the domain $0 < R \leq 20.0 \text{ a.u.}$

Instead of a spherical region we have chosen an ellipsoidal interaction region. In addition the volume changes with R . However for sufficiently large b_b the ellipsoid is almost a sphere. In the case of $b_b = 40.0 \text{ a.u.}$, we have $38.7 \leq a_b \leq 40.0 \text{ a.u.}$ and the change in volume is small ($\simeq 6\%$). Hence we can assume that the packet states are good to describe the ionized electrons within a sphere of radius of about b_b .

Here we have proposed to choose the wave packets in such a way that it covers a certain region of physical space. A consequence of this choice is that only the low energy packets (whose packet widths are small) approximately diagonalize the Hamiltonian. This is in contrast with more traditional ways of choosing pseudostates.

The one-electron-two-centre problem possesses a dynamical symmetry [72] reflected by the fact that the true adiabatic states are eigenfunctions of \hat{A} with the eigenvalue A . In standard notation

$$\hat{A} = \hat{L}^2 - \frac{R^2}{2} (\hat{p}_x^2 + \hat{p}_y^2) + R \left(\frac{Z_A}{r_A} - \frac{Z_B}{r_B} \right)$$

Since A is a slowly varying function of ϵ [30b], packet states at low energy are *approximate eigenfunctions* of \hat{A} ; hence they do not completely destroy the dynamical symmetry. The counterpart of \hat{A} in the atomic case is \hat{L}^2 , where the pseudostates are chosen to be exact \hat{L}^2 -eigenfunctions.

Wave packets are centred at the centre of charge of the nuclei (CCN). As R increases they do not decompose into atomic packet states. Instead they

become relatively more peaked at the CCN and along the line of "equiforce". Low lying molecular bound states go to linear combinations of atomic states. This behavior reduces the overlap between packet and bound states with increasing R . Hence the assumption (Chapter 2) that there are no significant bound \rightarrow packet or packet \rightarrow bound transitions for $R > R_\infty$ is self-consistent with the use of packet states.

Wannier [73] proposed that the double ionization of an atom near threshold takes place in such a way that asymptotically the escaping electrons move in opposite directions keeping the remaining ionic core midway between the electrons. Klar [74] has generalized this idea to any break up of 3-Coulomb particles. He found that this "mechanism" is valid not only at the threshold but also up to a few eV above threshold. Winter and Lin [7] have proposed to extend this energy range up to about 25 keV for proton hydrogen atom collisions. According to this "mechanism" ionization in $H^+ + H$ should take place in such a way that the ionized electron has a higher probability to be found near CCN. The triple centre calculations of Winter and Lin [7] and the classical trajectory Montecarlo calculations of Olson [75] provide evidence in favour of this. Since the adiabatic wave packets have high density about CCN they are appropriate states to describe the ionized electrons.

A consequence of equation (4 - 10) is that if the true continuum state at $\epsilon = \epsilon_j - \frac{1}{2}\Delta_j$ has n nodes within the interaction region, then the state at $\epsilon = \epsilon_j + \frac{1}{2}\Delta_j$ has $n + 2$ nodes. The state at $\epsilon = \epsilon_j$ has $n + 1$ nodes. Because of equation (4 - 8), the j^{th} packet has approximately $n + 1$ nodes which is the average number of nodes of the adiabatic continuum replaced by it. This is a useful feature, especially at higher energies, since it is known [9,76] that the pseudostates obtained using a small number of L^2 -functions (eg. Slater type functions) cannot mimic the highly oscillatory behavior of these continuum states.

5. FORMAL PROPERTIES OF CONTINUUM

NONADIABATIC COUPLINGS

5.1 Introduction

If the heavy particle motion in an ion-atom collision is described by a classical trajectory $\vec{R}(t)$ (for given c.m. energy E and impact parameter b), the electronic system evolves according to the time-dependent Schrödinger equation

$$i\hbar \frac{\partial \Upsilon(\vec{r}, t)}{\partial t} = \hat{h}_e(\vec{r}; \vec{R}(t)) \Upsilon(\vec{r}, t) \quad (5-1)$$

where the electronic Hamiltonian \hat{h}_e depends on time only through its parametric dependence on \vec{R} . If $\Upsilon(\vec{r}, t)$ is expanded in the set of adiabatic eigenstates $|k; \vec{R}(t)\rangle$,

$$\hat{h}_e(\vec{r}; \vec{R}(t)) |k; \vec{R}(t)\rangle = \epsilon_k(R) |k; \vec{R}(t)\rangle \quad (5-2)$$

then the transitions can arise only from *nonadiabatic couplings*¹⁵, whose matrix elements are given by

$$-i\hbar \langle k'; \vec{R}(t) | (\partial/\partial t) |k; \vec{R}(t)\rangle = -i\hbar \vec{v} \cdot \langle k'; \vec{R}(t) | \vec{\nabla}_{\vec{R}} |k; \vec{R}(t)\rangle \quad (5-3)$$

where $\vec{v} \equiv (d\vec{R}/dt)$. (Here $k \equiv (nlm)$ for bound states and $k \equiv (\epsilon lm)$ with $\epsilon_k = \epsilon$ for continuum states) The physical meaning is that transitions result from the finite rates of *deformation* of the adiabatic basis states as the nuclei move on $\vec{R}(t)$; coupling strength is directly proportional to the velocity v .

However, a rigorously correct definition of the nonadiabatic coupling operator and its matrix elements requires careful consideration of several points:

(a) Nonadiabatic couplings must be *gauge - invariant*, i.e. their matrix elements cannot depend on the inertial reference frame used for electron coordinates, and they must also be defined consistently with correct asymptotic boundary conditions for the molecular state channels. These requirements result in "electron translation factor" (ETF) corrections to the nonadiabatic coupling matrix elements. ETF corrections do not directly concern us in this work, so the discussion given in Section 5.3 is a brief survey.

(b) The nonadiabatic coupling operator is not like an ordinary finite-range potential coupling, $\hat{V}(t)$. Its matrix elements between adiabatic continuum states exhibit singularities, which reflect fundamental limitations of an adiabatic description of the continuum. The formal structure and properties of these singularities are the main concern of this chapter. They are derived in detail, using an appropriate generalization of the Hellmann-Feynman relations. Careful attention to this singular structure is needed to form a correct representation of nonadiabatic couplings within the subspace spanned by the adiabatic continuum packet states.

Most previous work on nonadiabatic coupling matrix elements is concerned only with bound-bound or bound-continuum couplings. A representative sample of such work for one-electron-two-nucleus systems can be found in References 30b, 41b, 77 and 78. Since no quasi-bound levels are embedded in the continuum for these systems, all such couplings are non-singular, though individual bound state couplings can exhibit pronounced resonant maxima associated with avoided crossings and other near-degeneracies. Almost no studies of continuum-continuum couplings have been reported (except for a paper by Ponomarev *et al.* [79] whose results we disagree with - cf. Section 5.9 below), and in particular little attention has been given to the structure of the singularities in these couplings.

5.2 Radial and Angular Couplings

The gradient $\vec{\nabla}_{\vec{R}}$ which appears in equation (5-3) for the nonadiabatic couplings is understood to be taken holding electron coordinates \vec{r}' fixed in a non-rotating (space-fixed) reference frame (SFRF). On the other hand the adiabatic eigenfunctions $|k; \vec{R}(t)\rangle$ are normally described in electron coordinates \vec{r} of a molecule-fixed reference frame which rotates with the molecular axis $\vec{R}(t)$. Figure 5-1 depicts the frame rotation connecting these axis systems. The transformation linking $\vec{r} (x, y, z)$ to $\vec{r}' (x', y', z')$ is just

$$\begin{pmatrix} x \\ y \\ z \end{pmatrix} = \begin{pmatrix} \cos \vartheta \cos \varphi & \cos \vartheta \sin \varphi & -\sin \vartheta \\ -\sin \varphi & \cos \varphi & 0 \\ \sin \vartheta \cos \varphi & \sin \vartheta \sin \varphi & \cos \vartheta \end{pmatrix} \begin{pmatrix} x' \\ y' \\ z' \end{pmatrix} \quad (5-4)$$

from which it is easily shown that

$$-i\hbar \left(\frac{\partial}{\partial R} \right)_{\vec{r}'} = -i\hbar \left(\frac{\partial}{\partial R} \right)_{\vec{r}} \quad (5-5a)$$

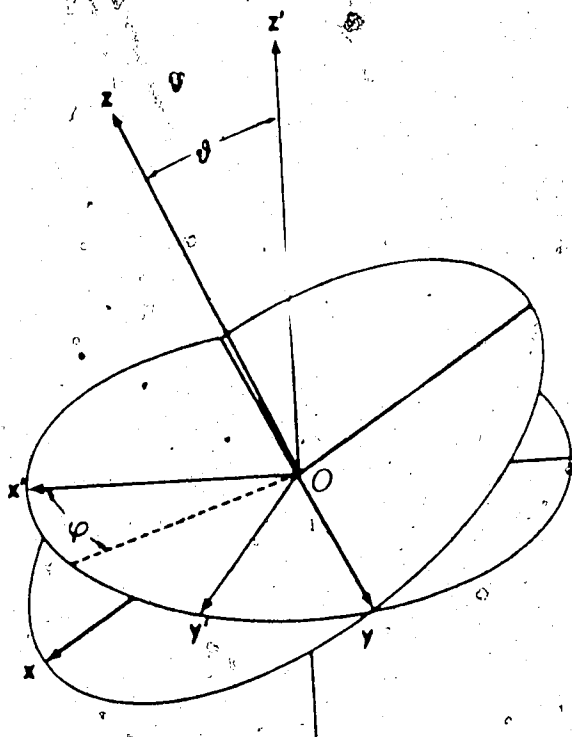
$$-i\hbar \left(\frac{\partial}{\partial \vartheta} \right)_{\vec{r}'} = -i\hbar \left(\frac{\partial}{\partial \vartheta} \right)_{\vec{r}} - \hat{L}_y \quad (5-5b)$$

$$-i\hbar \left(\frac{\partial}{\partial \varphi} \right)_{\vec{r}'} = -i\hbar \left(\frac{\partial}{\partial \varphi} \right)_{\vec{r}} + \sin \vartheta \hat{L}_x - \cos \vartheta \hat{L}_z \quad (5-5c)$$

where \hat{L}_x , \hat{L}_y , \hat{L}_z are the operators for the (molecule-fixed) components of electronic orbital angular momentum.

In a classical trajectory description, the heavy particle motion $\vec{R}(t)$ is confined to a plane, which we take to be the xz -plane. Hence $\varphi = \text{constant} = 0$, $\vec{R}(t)$ is specified by R , ϑ alone, and the instantaneous radial and tangential components of the velocity \vec{v} are $v^R \equiv (dR/dt)$ and $v^\vartheta \equiv R(d\vartheta/dt) = -bv_0/R$, where $\mu v_0^2/2 = E$. Since the adiabatic basis states $|k; \vec{R}(t)\rangle$ depend only upon R

Figure 5 - 1 : Molecule and Space-Fixed reference frames



$$SFRF \equiv Ox'y'z'$$

$$MFRF \equiv Oxyz$$

We obtain *MFRF* as follows. Rotate a reference frame, coincident with *SFRF*, counter clockwise (CCW) by φ about z' . Then rotate it CCW by ϑ about its y -axis. We choose (ϑ, φ) so that \vec{R} is on the z -axis.

in MFRF, the nonadiabatic couplings formally given by equation (5-3) may now be written as

$$\begin{aligned} K_{k'k}(t) &= -i\hbar\vec{v} \cdot \langle k'; \vec{R}(t) | \vec{\nabla}_{\vec{R}} | k; \vec{R}(t) \rangle \\ &= v^R P_{k'k}^R + v^\vartheta P_{k'k}^\vartheta \end{aligned} \quad (5-6)$$

where

$$P_{k'k}^R = -i\hbar \langle k'; R | (\partial/\partial R)_r | k; R \rangle \quad (5-7a)$$

and

$$P_{k'k}^\vartheta = -\frac{1}{R} \langle k'; R | \hat{L}_y | k; R \rangle \quad (5-7b)$$

These are called, respectively, *radial* and *angular* nonadiabatic coupling matrix elements. They are functions of the internuclear separation R .

$P_{k'k}^R$ and $P_{k'k}^\vartheta$ can be calculated entirely within the molecule fixed reference frame where the adiabatic states are functions only of scalar R .

Since the adiabatic eigenstates $|k; R\rangle$ are also eigenfunctions of the figure axis component of angular momentum \hat{L}_z ,

$$\hat{L}_z |k; R\rangle = m\hbar |k; R\rangle \quad (5-8)$$

selection rules hold for the radial and angular coupling matrix elements:

$$\text{For } \textit{radial} \text{ couplings, } m' = m;$$

$$\text{For } \textit{angular} \text{ couplings, } m' = m \pm 1.$$

Since we can write

$$\hat{L}_y = \frac{1}{2i} (\hat{L}_+ - \hat{L}_-)$$

where \hat{L}_\pm are the ladder operators raising and lowering m , it is most convenient to compute coupling matrix elements for \hat{L}_\pm , rather than for \hat{L}_y , with the specific selection rules $m' = m + 1$ for \hat{L}_+ and $m' = m - 1$ for \hat{L}_- .

5.3 Translational Invariance and Translation Factor Corrections

The physical description of a collision offered by the equation (5 - 1) cannot depend on the reference origin chosen for electron coordinates. It follows that the coupling matrix elements defined formally in equation (5 - 3) and elaborated in equations (5 - 6) and (5 - 7) must also be invariant to that choice. However, it is easy to show that computed matrix elements $P_{k'k}^R$ and $P_{k'k}^{\theta}$ given by equations (5 - 7) do not have the required invariance. In this work we find it most convenient to choose the *geometric centre* (GC) as the (conventional) reference origin for electron coordinates \vec{r} . Suppose however that \vec{r}_c are electron coordinates from a new reference origin, displaced along \vec{R} from GC:

$$\vec{r}_c = \vec{r} - c\vec{R}; \quad (c = \text{constant})$$

Then it is easy to show that

$$-i\hbar \langle k'; R | (\partial/\partial R)_{\vec{r}_c} | k; R \rangle = -i\hbar \langle k'; R | (\partial/\partial R)_{\vec{r}} | k; R \rangle + c \langle k'; R | \hat{p}_z | k; R \rangle \quad (5-9a)$$

and

$$-\frac{1}{R} \langle k'; R | \hat{L}_y^c | k; R \rangle = -\frac{1}{R} \langle k'; R | \hat{L}_y^{GC} | k; R \rangle + c \langle k'; R | \hat{p}_x | k; R \rangle \quad (5-9b)$$

where \hat{p}_x , \hat{p}_z are the electronic momentum operators conjugate to x , z and \hat{L}_y^c , \hat{L}_y^{GC} are the angular momentum components referred to the new origin and to GC, respectively.

The inconsistency is resolved by observing that the new origin is *translating* relative to GC, due to the nuclear motion, and that transformation theory requires that wave functions described in the new frame differ from those in the GC frame in a manner representing such relative translation. When the electronic

Hamiltonian \hat{h}_e acts on the transformed wave functions in the new frame of reference, additional coupling terms are generated which exactly compensate for the new terms in equations (5 - 9) and preserve translational invariance of the effective nonadiabatic couplings.

Furthermore, the couplings computed using GC as the reference origin must be defined *correctly*, i.e. in a manner consistent with a correct description of the asymptotic channel wave functions describing the basis states. *This cannot be achieved by using unmodified adiabatic molecular eigenstates of \hat{h}_e .* Consider an electron bound to either nucleus (A or B) as $R \rightarrow \infty$. Seen from the conventional reference origin GC, it is *translating* with the nucleus to which it is bound: that is, the "correct inertial reference origin" for an electron bound to nucleus A is at nucleus A, not GC, and that for an electron bound to nucleus B is B, not GC. *It is impossible to choose any unique "inertial reference frame" for the electron which resolves this problem;* since the nuclei A,B are moving relative to one another with instantaneous velocity \vec{v} , the proper asymptotic inertial reference frames for electrons bound to each are different, and this difference must be accounted for in the definition of the scattering basis functions, even within the classical trajectory description [31,80]. Since the adiabatic Hamiltonian \hat{h}_e contains no information about the *motion* of nuclei, description of such relative translation cannot appear in the eigenstates $|k; R\rangle$ themselves, but must be included as a modifying "electron translation factor" (ETF) in a correct description of the asymptotic channel states. The *asymptotic* definition of these factors is readily found from transformation theory; but the problem is how to modify molecular state basis functions (and the couplings among them) in a *global way* which

- (1) gives the correct asymptotic behavior for wave functions and couplings,

(2) maintains translational invariance of the resulting nonadiabatic couplings, and

(3) forms an effective basis set for convergent close-coupling calculations.

Several solutions for this problem have been proposed. Here we use the formalism of Thorson and Delos [13,31,80]; which is based on the use of *molecular state switching functions*. Several close-coupling calculations using this formulation or closely related scheme have been carried out [19,20,34,81], though none so far have included close-coupling to the continuum. Delos and Thorson show that the most important result of translation factor effects in the description of an ion/atom collision using molecular states is to correct the nonadiabatic coupling matrix elements¹⁶. If GC be chosen (arbitrarily) as the reference origin, then the radial and angular couplings which appear formally in equations (5 - 6) and (5 - 7) are *explicitly defined* by

$$-i\hbar \langle k'; R | (\partial/\partial R) | k; R \rangle = P_{k'k}^R + A_{k'k}^R \quad (5-10a)$$

$$-\frac{1}{R} \langle k'; R | \hat{L}_y | k; R \rangle = P_{k'k}^\vartheta + A_{k'k}^\vartheta \quad (5-10b)$$

where $P_{k'k}^R$ and $P_{k'k}^\vartheta$ are given by equations (5 - 7) with GC as reference origin, and the *ETF correction matrices* A^R , A^ϑ are defined by [31]

$$A_{k'k}^R = \frac{i\hbar}{2} (\epsilon_{k'} - \epsilon_k) \langle k'; R | z f_k(\vec{r}; R) | k; R \rangle \quad (5-11a)$$

and

$$A_{k'k}^\vartheta = \frac{i\hbar}{2} (\epsilon_{k'} - \epsilon_k) \langle k'; R | x f_k(\vec{r}; R) | k; R \rangle \quad (5-11b)$$

where $f_k(\vec{r}; R)$ is the *switching function* for the adiabatic eigenstate $|k; R\rangle$ ¹⁷.

Effectively, the switching function $f_k(\vec{r}; R)$ shifts the electronic reference origin from GC to one which is locally more appropriate. For bound states, the

asymptotically appropriate local origins are the atomic nuclei (A or B) to which the electron is asymptotically bound, and with which it translates uniformly (with respect to GC) as $R \rightarrow \infty$; thus $f_k(\vec{r}; R)$ must satisfy the general asymptotic boundary conditions [31,80]

$$\lim_{R \rightarrow \infty} f_k(\vec{r}; R) = +1 \quad \text{if } |\vec{r}_B| \text{ is finite} \quad (5-12a)$$

$$\lim_{R \rightarrow \infty} f_k(\vec{r}; R) = -1 \quad \text{if } |\vec{r}_A| \text{ is finite} \quad (5-12b)$$

However, the form of $f_k(\vec{r}; R)$ for finite R -values is not fully determined. The efficiency and convergence of close-coupling calculations employing the resulting basis set is a relevant criterion of choice. There is some dispute about whether switching functions need to be state-specific (i.e. different f_k 's for different $|k; R\rangle$'s) or a common switching function can be used for all the adiabatic states. The latter choice is much simpler formally (see references 31,80) and arguments favouring a "universal" choice have been given by Vaaben and Taulbjerg [82]; however, calculations using such a universal choice deal only with total charge transfer cross sections using limited basis sets and continuum couplings or transitions are not considered. More detailed studies show that state-specific switching functions $f_k(\vec{r}; R)$ for each adiabatic state may be derived from several independent considerations [30a,80,83], and the calculations presented in references 20 and 81a show that individual state excitation cross sections are quite sensitive to the detailed choice of switching functions even for fairly large basis sets. From the viewpoint of this study, a key consideration is the dramatic effect of state-specific switching functions on the number and size of couplings to *continuum* states [30a]; in view of the effect of the fact that the same switching functions may be deduced from analytical properties of the adiabatic eigenstates themselves [83], it would appear

that close coupling calculations which include continuum states should employ different $f_k(\vec{r}; R)$ for different $|k; R\rangle$ in spite of some additional formal complications 18,19

This research is not directly concerned with the study of ETF corrections to nonadiabatic couplings, but in conclusion we should make two points which do bear on our objectives:

- (1) We show in this work that the adiabatic continuum packet states which are used to represent the continuum locally are centred on GC (more generally, the centre of positive charge) and not on the atomic centres. The implication is that for these states the GC is the "appropriate reference origin", i.e. there should probably be *no* ETF corrections for continuum-continuum couplings.
- (2) In any case it may be shown that the ETF correction matrix elements are at most *finite* and cannot therefore affect the structure of singularities in nonadiabatic couplings. These arise entirely from the coupling matrices P^R, P^ν , and we restrict our attention to them in the remainder of this chapter.

5.4 Hellmann-Feynman Theorem

If $|k; R\rangle$ are adiabatic eigenfunctions of the Hamiltonian $\hat{h}_e(\vec{r}; \vec{R})$ and ζ is any parametric variable on which both \hat{h}_e and the eigenfunctions $|k; R\rangle$ depend, then the Hellmann-Feynman theorem [84]

$$\langle k'; R | (\partial \hat{h}_e / \partial \zeta) | k; R \rangle = \frac{\partial \epsilon_k}{\partial \zeta} \langle k'; R | k; R \rangle + (\epsilon_k - \epsilon_{k'}) \langle k'; R | (\partial / \partial \zeta) | k; R \rangle \quad (5-13)$$

holds, provided at least one of the eigenfunctions $|k'; R\rangle, |k; R\rangle$ is of L^2 -type. This condition is sufficient to ensure the Hermitian property of \hat{h}_e with respect to

$\langle k'; R |$ and $(\partial/\partial\zeta)|k; R\rangle$,

$$\langle k'; R | \hat{h}_e (\partial/\partial\zeta) | k; R \rangle = \left(\hat{h}_e \langle k'; R | \right) (\partial/\partial\zeta) | k; R \rangle$$

as shown in Appendix D; the derivation of equation (5 - 13) then follows immediately by differentiation of equation (5 - 2). We can apply equation (5 - 14) directly to the computation of *radial* nonadiabatic couplings $P_{k'k}^R$.

$$P_{k'k}^R = -i\hbar \frac{\langle k'; R | (\partial\hat{h}_e/\partial R)_{\bar{r}} | k; R \rangle}{[\epsilon_k(R) - \epsilon_{k'}(R)]} \quad (5 - 14)$$

and indirectly to the *angular* couplings $P_{k'k}^\vartheta$:

$$\begin{aligned} P_{k'k}^\vartheta &= \frac{-i\hbar \langle k'; \vec{R}(t) | (\partial\hat{h}_e/\partial\vartheta)_{\bar{r}} | k; \vec{R}(t) \rangle}{R [\epsilon_k(R) - \epsilon_{k'}(R)]} \\ &= -\frac{1}{R} \frac{\langle k'; R | [\hat{L}_y, \hat{h}_e] | k; R \rangle}{[\epsilon_k(R) - \epsilon_{k'}(R)]} \end{aligned} \quad (5 - 15)$$

as mentioned above it is more convenient to consider the matrix elements of the ladder operators \hat{L}_\pm , for which the corresponding Hellmann-Feynman relation is

$$\langle k'; R | \hat{L}_\pm | k; R \rangle = \frac{\langle k'; R | [\hat{L}_\pm, \hat{h}_e] | k; R \rangle}{[\epsilon_k(R) - \epsilon_{k'}(R)]} \quad (5 - 16)$$

Equations (5 - 14) and (5 - 15) provide efficient means for computing radial and angular adiabatic couplings $P_{k'k}^R$, $P_{k'k}^\vartheta$ between two bound states and also between bound and continuum states.

Equations (5 - 14) and (5 - 15) imply that nonadiabatic couplings may become very large if the states coupled are degenerate. For the one-electron systems we consider, the bound state spectrum lies below the continuum, so this point is not directly pertinent to discrete-continuum couplings. For couplings among two bound states, two cases occur:

(a) *Avoided Crossings.*

Two adiabatic states may have an avoided crossing near some internuclear separation R_x ; the adiabatic eigenvalues $\epsilon_{k'}(R)$, $\epsilon_k(R)$ obey the non-crossing rule [28] but the difference $(\epsilon_k - \epsilon_{k'})$ may become very small near R_x . In these cases the radial coupling matrix element $P_{k'k}^R$ exhibits a pronounced maximum near R_x , with a width and peak height controlled primarily by the energy denominator in equation (5 - 14). Such coupling are resonant but not singular.

(b) *Real Crossings*

Adiabatic eigenstates with different eigenvalues m' , m of the figure axis angular momentum component \hat{L}_z , and, under certain circumstances [28], with $m' = m$, may have *real* crossings, at points R_x where the energy difference between them passes through zero. However, in these cases the corresponding nonadiabatic couplings are *not* singular; the matrix elements in equations (5 - 14) or (5 - 15) may be shown to be *linearly proportional* to the difference $[\epsilon_k(R) - \epsilon_{k'}(R)]$ near R_x so that the corresponding nonadiabatic couplings are smooth, nonresonant functions of R through such crossings.

5.5 Extension of the Hellmann-Feynman Theorem to Continuum States

If matrix elements involving two continuum states are defined appropriately the Hellmann-Feynman relations may be extended to continuum states. In particular

- (1) For two continuum states with different energies $\epsilon_k \neq \epsilon_{k'}$, the analogues

of equations (5 - 14) and (5 - 15) hold, i.e.

$$P_{k'k}^R = -i\hbar \langle k'; R | (\partial/\partial R)_{\bar{r}} | k; R \rangle = -i\hbar \frac{\langle k'; R | (\partial \hat{h}_e / \partial R)_{\bar{r}} | k; R \rangle}{(\epsilon - \epsilon')} \quad (5 - 17)$$

$$P_{k'k}^{\vartheta} = \pm \frac{i\hbar}{2R} \langle k'; R | \hat{L}_{\pm} | k; R \rangle = -i\hbar \frac{\langle k'; R | [\hat{L}_{\pm}, \hat{h}_e] | k; R \rangle}{(\epsilon - \epsilon')} \quad (5 - 18)$$

- (2) The commutator matrix elements appearing in equations (5 - 17) and (5 - 18) are analytic functions of the energies ϵ , ϵ' including $\epsilon = \epsilon'$ (see below).
- (3) When $\epsilon - \epsilon' = 0$, the nonadiabatic coupling matrix elements $P_{k'k}^R$ and $P_{k'k}^{\vartheta}$ are singular. We compute these singularities explicitly and determine their analytic coefficients.
- (4) As implied in equations (5 - 17) and (5 - 18) a connection between the analytic commutator matrix elements for $\epsilon = \epsilon'$ and the analytic coefficients of the singularities in the corresponding nonadiabatic couplings, and we derive these relations.

Calculations of these effects of nonadiabatic couplings among continuum states entail integrations over the continuum energies ϵ , ϵ' . The above results may be summarized by the statement that continuum nonadiabatic couplings have the forms

$$P_{k'k}^R = M_{k'k}^R \delta(\epsilon' - \epsilon) + \mathcal{P} \left[\frac{N_{k'k}^R}{(\epsilon - \epsilon')} \right] \quad (5 - 19a)$$

$$P_{k'k}^{\vartheta} = M_{k'k}^{\vartheta} \delta(\epsilon' - \epsilon) + \mathcal{P} \left[\frac{N_{k'k}^{\vartheta}}{(\epsilon - \epsilon')} \right] \quad (5 - 19b)$$

where $\delta(x)$ is the Dirac delta-function; the symbol \mathcal{P} implies that the Cauchy principal value is to be taken in integrations over energy including the singular point $(\epsilon - \epsilon') = 0$; the analytic coefficients $N_{k'k}^R$, $N_{k'k}^{\vartheta}$ are given by

$$N_{k'k}^R = -i\hbar \langle k'; R | (\partial \hat{h}_e / \partial R)_{\bar{r}} | k; R \rangle \quad (5 - 19c)$$

$$N_{k'k}^{\nu} = \pm \frac{i}{2R} \langle k'; R | [\hat{L}_{\pm}, \hat{h}_e] | k; R \rangle \quad (5-19d)$$

and the analytic strengths $M_{k'k}^R$, $M_{k'k}^{\nu}$ of the singular terms are also directly related to these commutator matrix elements for $\epsilon - \epsilon' = 0$. Such relations may be called "the extended Hellmann-Feynman theorem". In the remainder of this chapter we derive these relations and the associated coefficients explicitly.

5.6 Properties of the Fundamental Integral

Certain improper integrals involving the continuum states do not converge to specific limits. To study the nature of the singularities and to define the matrix elements unambiguously we introduce a *convergence factor* $g(\alpha, \vec{r})$ and interpret the matrix element of an operator \hat{O} as

$$\langle k'; R | \hat{O} | k; R \rangle = \lim_{\alpha \rightarrow 0^+} \int d\vec{r} g(\alpha, \vec{r}) \psi^*(k'; R; \vec{r}) (\hat{O} \psi(k; R; \vec{r})) \quad (5-20)$$

where

$$g(\alpha, \vec{r}) = \exp(-\alpha \xi)$$

Note that the limit $\alpha \rightarrow 0^+$ is taken *after* the spatial integration has been performed.

$g(\alpha, \vec{r})$ can be imagined to provide a confining envelope for the wave functions which is being taken to "infinity" at the end of integration. Then the potentially singular part of a matrix element comes from integrals of the form

$$\int_1^{\infty} d\xi \frac{\exp(-\alpha \xi)}{\xi^n} \cos(\Theta_{\pm}(\xi)) \quad n \geq 0 \quad (5-21a)$$

and/or

$$\int_1^{\infty} d\xi \frac{\exp(-\alpha \xi)}{\xi^n} \sin(\Theta_{\pm}(\xi)) \quad n \geq 0 \quad (5-21b)$$

where

$$\Theta_{\pm}(\xi) = C_{\pm} \xi + \delta_{\pm} \ln(\xi) + \Lambda_{\pm} \quad (5-22a)$$

$$C_{\pm} = c' \pm c \quad \delta_{\pm} = \pm q C_{\pm} / (2c'c) \quad \Lambda_{\pm} = \Lambda' \pm \Lambda \quad (5-22b)$$

Here the parameters c , q and Λ are as defined in Chapter 3.

In the theory we do not have to consider zero energy states; hence $C_+ > 0$ for all cases.

The integrals (5-21) are the real and imaginary parts of the *fundamental* integral

$$\mathcal{F}_n(C_{\pm}, \alpha) = \exp(i\Lambda_{\pm}) \int_1^{\infty} d\xi \xi^{i\delta_{\pm} - n} \exp(-(\alpha - iC_{\pm})\xi) \quad (5-23)$$

\mathcal{F}_n can be expressed in terms of Kummer's U -function whose properties are listed in Chapter 13 of reference 53.

$$\mathcal{F}_n(C_{\pm}, \alpha) = \exp(i\Lambda_{\pm}) \exp(-(\alpha - iC_{\pm})) U(1, 2 - n + i\delta_{\pm}, \alpha - iC_{\pm}) \quad (5-24)$$

In evaluating \mathcal{F}_n at a particular value of C_{\pm} and $\alpha \rightarrow 0^+$ we adopt the following convention: *First* substitute for C_{\pm} in equation (5-24) and *then* take the limit $\alpha \rightarrow 0^+$. This order of operations follows from the fact that in evaluating matrix elements we start with two particular continuum states so that C_{\pm} is determined at the beginning.

In the rest of this section we shall find the behavior and the strengths $\mathcal{F}_n(C_{\pm})$ of any singularities of $\mathcal{F}_n(C_{\pm}, 0^+)$.

(a) $C_+ \neq 0$ and $n \geq 0$:

$$\left| \lim_{\alpha \rightarrow 0^+} \mathcal{F}_n(C_{\pm}, \alpha) \right| < \infty \quad (5-25a)$$

Since \mathcal{F}_n is non-singular,

$$F_n(C_{\pm}) = 0, \quad C_{\pm} \neq 0 \quad (5-25b)$$

(b) $C_- = 0$ and $n \geq 2$:

$$\lim_{\alpha \rightarrow 0^+} \mathcal{F}_n(0, \alpha) = \frac{\exp(i\Lambda_-)}{n-1} \quad (5-26a)$$

Hence

$$F_n(0) = 0, \quad n \geq 2 \quad (5-26b)$$

(c) $C_- = 0$ and $n = 0$:

When $C_- \sim 0$ and $\alpha \sim 0^+$ we have

$$\mathcal{F}_0(c_-, \alpha) = \exp(i\Lambda_-) \exp(-(\alpha - iC_-)) \Gamma(1 + i\delta_-) M(C_-) + K \quad (5-27)$$

where

$$M(C_-) = (\alpha - iC_-)^{-1-i\delta_-} \quad (5-28)$$

$$K = \begin{cases} O(1) & C_- \neq 0 \\ O(|\ln(\alpha - iC_-)|) & C_- = 0 \end{cases} \quad (5-29)$$

Then it follows that

$$\mathcal{F}_0(0, \alpha) \xrightarrow{\alpha \rightarrow 0^+} \left(\frac{1}{\alpha} + \text{const.} \times \ln(\alpha) \right) \exp(i\Lambda_-) \quad (5-30)$$

K has an isolated logarithmic singularity at $C_- = 0$. The strength of this singularity is zero since it has zero area (see Appendix C). To study the singularity in $M(C_-)$ multiply the numerator and the denominator by $(\alpha + iC_-)$ and separate factors

$$M(C_-) = \frac{\alpha(\alpha - iC_-)^{-i\delta_-}}{\alpha^2 + C_-^2} + iC_- \frac{(\alpha - iC_-)^{-i\delta_-}}{\alpha^2 + C_-^2} \quad (5-31)$$

In the limit $C_- = 0$ the second term in equation (5 - 31) vanishes. Since

$$\lim_{\alpha \rightarrow 0^+} \frac{\alpha}{\alpha^2 + C_-^2} = \pi \delta(C_-)$$

we have

$$\begin{aligned} \lim_{\alpha \rightarrow 0^+} M(C_-) &= \pi \delta(C_-) \\ &= \frac{4\pi c}{R^2} \delta(\epsilon' - \epsilon) \end{aligned} \quad (5 - 32)$$

Hence

$$F_0(0) = \frac{4\pi c}{R^2} \exp(i \Lambda_-) \quad (5 - 33)$$

(d) $C_- = 0$ and $n = 1$:

We have

$$F_1(0, \alpha) \xrightarrow{\alpha \rightarrow 0^+} \text{const.} \times \exp(i \Lambda_-) \ln(\alpha) \quad (5 - 34)$$

Then it follows that

$$F_1(0) = 0 \quad (5 - 35)$$

5.6.1 Summary of the Strengths of Singularities

$$F_n(C_{\pm}) = 0 \quad \text{for } n \geq 0 \text{ and } C_{\pm} \neq 0 \quad (5 - 36a)$$

$$F_n(0) = \begin{cases} 0 & n \geq 1 \\ (4\pi c/R^2) \exp(i \Lambda_-) & n = 0 \end{cases} \quad (5 - 36b)$$

5.7 Angular Coupling Matrix Elements

One can easily show that

$$[\hat{h}_e, \hat{L}_{\pm}] = -(\hat{L}_{\pm} V(\vec{r}, R)) \quad (5 - 37)$$

Denote $|k; R\rangle$ by $|\psi_k\rangle$. Then we have

$$\langle g \psi_k | \hat{h}_e \hat{L}_{\pm} - \hat{L}_{\pm} \hat{h}_e | \psi_k \rangle = -\langle g \psi_k | (\hat{L}_{\pm} V) | \psi_k \rangle \quad (5 - 38)$$

where g is the convergence factor which guarantees the Hermiticity of \hat{h}_e (see Appendix D). Hence we have

$$(\epsilon - \epsilon) \langle g \psi_{k'} | \hat{L}_{\pm} | \psi_k \rangle = - \langle g \psi_{k'} | (\hat{L}_{\pm} V) | \psi_k \rangle + Y^{\pm}(\alpha) \quad (5-39)$$

where

$$\begin{aligned} Y^{\pm}(\alpha) &= \frac{\hbar^2}{m_e} \langle (\vec{\nabla}_{\vec{r}} \psi_{k'}) \cdot (\vec{\nabla}_{\vec{r}} g) | \hat{L}_{\pm} \psi_k \rangle + \frac{\hbar^2}{2m_e} \langle \psi_{k'} | (\vec{\nabla}_{\vec{r}}^2 g) | \hat{L}_{\pm} \psi_k \rangle \\ &= \frac{\hbar^3}{m_e} (\alpha Y_1^{\pm}(\alpha) + \alpha^2 Y_2^{\pm}(\alpha)) \end{aligned} \quad (5-40)$$

m_e is the molecular electronic reduced mass; equation (1-3). We study $Y_1^{\pm}(\alpha)$ in detail to explain the mathematical technique used to derive the expressions for angular and radial coupling matrix elements.

In prolate spheroidal coordinates we have

$$\begin{aligned} \vec{\nabla}_{\vec{r}} &= \frac{2}{R} \left[\vec{e}_{\xi} \sqrt{\frac{\xi^2 - 1}{\xi^2 - \eta^2}} \frac{\partial}{\partial \xi} + \vec{e}_{\eta} \sqrt{\frac{1 - \eta^2}{\xi^2 - \eta^2}} \frac{\partial}{\partial \eta} + \frac{\vec{e}_{\phi}}{\sqrt{(\xi^2 - 1)(1 - \eta^2)}} \frac{\partial}{\partial \phi} \right] \\ \vec{\nabla}_{\vec{r}}^2 &= \frac{4}{R^2(\xi^2 - \eta^2)} \left[\frac{\partial}{\partial \xi} (\xi^2 - 1) \frac{\partial}{\partial \xi} + \frac{\partial}{\partial \eta} (1 - \eta^2) \frac{\partial}{\partial \eta} + \frac{(\xi^2 - \eta^2)}{(\xi^2 - 1)(1 - \eta^2)} \frac{\partial^2}{\partial \phi^2} \right] \\ \hat{L}_{\pm} &= \hbar \exp(\pm i \phi) \frac{\sqrt{(\xi^2 - 1)(1 - \eta^2)}}{(\xi^2 - \eta^2)} \left[\frac{i \xi \eta (\xi^2 - \eta^2)}{(\xi^2 - 1)(1 - \eta^2)} \frac{\partial}{\partial \phi} \pm \left(\eta \frac{\partial}{\partial \xi} - \xi \frac{\partial}{\partial \eta} \right) \right] \\ \text{Volume element} = dV &= \frac{R^3}{8} (\xi^2 - \eta^2) d\xi d\eta d\phi \end{aligned}$$

$$\psi_k(\vec{r}) = \frac{\phi_k(\xi)}{\sqrt{\xi^2 - 1}} S_k(\eta) \frac{\exp(im\phi)}{\sqrt{2\pi}}$$

After doing some algebra and integrating over the azimuthal angle we obtain

$$Y_1^{\pm}(\alpha) = \frac{1}{2} R \delta_{m', m \pm 1} \int_{-1}^{+1} d\eta \int_1^{\infty} d\xi [X_1 \mp X_2 \pm X_3 \pm X_4] \exp(-\alpha \xi) \quad (5-41)$$

where

$$X_1 = \frac{m\xi\eta}{\sqrt{(\xi^2-1)(1-\eta^2)}} S_{k'} S_k \frac{d\phi_{k'}}{d\xi} \phi_k \quad (5-42a)$$

$$X_2 = \frac{\eta\sqrt{(\xi^2-1)(1-\eta^2)}}{(\xi^2-\eta^2)} S_{k'} S_k \frac{d\phi_{k'}}{d\xi} \frac{d\phi_k}{d\xi} \quad (5-42b)$$

$$X_3 = \frac{\xi\eta}{(\xi^2-\eta^2)} \sqrt{\frac{1-\eta^2}{\xi^2-1}} S_{k'} S_k \frac{d\phi_{k'}}{d\xi} \phi_k \quad (5-42c)$$

$$X_4 = \frac{\xi\sqrt{(\xi^2-1)(1-\eta^2)}}{(\xi^2-\eta^2)} S_{k'} \frac{dS_k}{d\eta} \frac{d\phi_{k'}}{d\xi} \phi_k \quad (5-42d)$$

When $m' = m \pm 1$, X_i are finite for $-1 \leq \eta \leq +1$ and $+1 < \xi < \infty$. The singularities at $\xi = 1$ are of the form $1/\sqrt{x}$ which is integrable. Hence the possible singularities (in the limit $\alpha \rightarrow 0^+$) come from the infinite range of integration.

Remembering that

$$\phi_k(\xi) \xrightarrow{\xi \rightarrow \infty} \frac{2}{\sqrt{\pi R c}} \sin(c\xi + (q/2) \pi(\xi) + \Lambda)$$

and using the asymptotic forms of X_i we obtain

$$Y_1^\pm(\alpha) = \frac{1}{\pi\sqrt{c'c}} \left[X + m\beta_{-1}^1(k', k) X_1^\infty(\alpha) \mp \beta_1^1(k', k) X_2^\infty(\alpha) \right. \\ \left. \pm \beta_1^1(k', k) X_3^\infty(\alpha) \pm \beta'(k', k) X_4^\infty(\alpha) \right] \quad (5-43)$$

where X is a finite quantity and

$$\beta_j^j(k', k) = \int_{-1}^{+1} d\eta \eta^{j'} (1-\eta^2)^{\frac{1}{2}} S_{k'}(\eta) S_k(\eta) \quad (5-44a)$$

$$\beta'(k', k) = \int_{-1}^{+1} d\eta \sqrt{1-\eta^2} S_{k'}(\eta) \frac{dS_k}{d\eta} \quad (5-44b)$$

$$X_1^\infty(\alpha) = \int_1^\infty d\xi \exp(-\alpha\xi) \left(c' + \frac{q'}{2c'\xi} \right) (\sin \Theta_- + \sin \Theta_+) \quad (5-45a)$$

$$X_2^\infty(\alpha) = \int_1^\infty d\xi \frac{\exp(-\alpha\xi)}{\xi} \left(c' + \frac{q'}{2c'\xi} \right) \left(c + \frac{q}{2c\xi} \right) (\cos \Theta_- + \cos \Theta_+) \quad (5-45b)$$

$$X_3^\infty(\alpha) = \int_1^\infty d\xi \frac{\exp(-\alpha\xi)}{\xi^2} \left(c' + \frac{q'}{2c'\xi} \right) (\sin \Theta_- + \sin \Theta_+) \quad (5-45c)$$

One can study the integrals X_i^∞ using $\mathcal{F}_n(C_\pm, \alpha)$: then we have

$$\lim_{\alpha \rightarrow 0^+} \alpha Y_1^\pm(\alpha) = \begin{cases} 0 & \text{if } c' \neq c \\ (1/\pi) [m \beta_{-1}^1(k', k) \pm \beta'(k', k)] \sin(\Lambda - \Lambda') \delta_{m', m \pm 1} & \text{if } c' = c \end{cases} \quad (5-46a)$$

Using the same method we can prove that the singularities in $Y_2^\pm(\alpha)$ are at most $1/\alpha$. Hence

$$\lim_{\alpha \rightarrow 0^+} \alpha^2 Y_2^\pm(\alpha) = 0 \quad (5-46b)$$

Now equations (5-42b), (5-43) and (5-46) give (remember that when $\epsilon' = \epsilon$, the quantity in the left hand side of equation (5-42b) vanishes)

$$\langle \psi_{k'} | (\hat{L}_\pm V) | \psi_k \rangle = \begin{cases} (\epsilon - \epsilon') \langle \psi_{k'} | \hat{L}_\pm | \psi_k \rangle \delta_{m', m \pm 1} & \text{if } \epsilon' \neq \epsilon \\ \left\{ \left(\frac{\hbar^3}{\pi m_e} \right) (m \beta_{-1}^1(k', k) \pm \beta'(k', k)) \right\} \times \sin(\Lambda - \Lambda') \delta_{m', m \pm 1} & \text{if } \epsilon' = \epsilon \end{cases} \quad (5-47)$$

Note that equation (5-43) gives the angular coupling matrix element when $\epsilon' \neq \epsilon$. When the energies of the two states are the same it gives a (two dimensional) *improper* integral in terms of simpler one dimensional integrals β_{-1}^1 and β' and the phase shift difference.

To obtain the strength of the matrix element when $\epsilon' = \epsilon$, we directly calculate $\langle g \psi_{k'} | \hat{L}_\pm | \psi_k \rangle$ and take the limit $\alpha \rightarrow 0^+$. Using the same techniques and equations (5-36) we obtain

$$\langle \psi_{k'} | \hat{L}_\pm | \psi_k \rangle = -\hbar (m \beta_{-1}^1(k', k) \pm \beta'(k', k)) \cos(\Lambda' - \Lambda) \delta_{m', m \pm 1} \delta(\epsilon' - \epsilon) \quad (5-48)$$

Note that the analytic coefficient of the delta-function part is related to the commutator matrix element appearing in the principal part.

5.7.1 Summary of Continuum State Angular Couplings

$$P_{k'k}^{\mathcal{D}} = \frac{i}{2R} \left(\langle k'; R | \hat{L}_+ | k; R \rangle - \langle k'; R | \hat{L}_- | k; R \rangle \right)$$

$$\langle k'; R | \hat{L}_{\pm} | k; R \rangle = \mathcal{P} \left(\frac{\langle k'; R | (\hat{L}_{\pm} V) | k; R \rangle}{\epsilon - \epsilon'} \delta_{m', m \pm 1} \right)$$

$$- \hbar (m \beta_{-1}^1(k', k \pm 1) \beta(k', k)) \cos(\Lambda' - \Lambda) \delta_{m', m \pm 1} \delta(\epsilon' - \epsilon) \quad (5-49)$$

5.8 Radial Coupling Matrix Elements

One can easily show that

$$\left[\hat{h}_e, \left(\frac{\partial}{\partial R} \right)_{\vec{r}} \right] = - \left(\frac{\partial \hat{h}_e}{\partial R} \right)_{\vec{r}} = - \left(\frac{\partial V}{\partial R} \right)_{\vec{r}}$$

where

$$\left(\frac{\partial}{\partial R} \right)_{\vec{r}} = \left(\frac{\partial}{\partial R} \right)_{\xi, \eta} - \frac{1}{R(\xi^2 - \eta^2)} \left[\xi(\xi^2 - 1) \left(\frac{\partial}{\partial \xi} \right)_{R, \eta} + \eta(1 - \eta^2) \left(\frac{\partial}{\partial \eta} \right)_{R, \xi} \right]$$

Using the same mathematical techniques as in section 5.7 one can derive the following formulae.

$$\langle k'; R | (\partial \hat{h}_e / \partial R)_{\vec{r}} | k; R \rangle = \begin{cases} (\epsilon - \epsilon') \langle k'; R | (\partial / \partial R)_{\vec{r}} | k; R \rangle \delta_{m'm} & \text{if } \epsilon' \neq \epsilon \\ \left\{ \begin{aligned} & \frac{\hbar^2}{\pi m_e} \beta_R(k', k) \sin(\Lambda' - \Lambda) \delta_{m'm} (1 - \delta_{l'l}) \\ & + \frac{\hbar^2}{\pi m_e} \left(\frac{q}{2cR} - \frac{\partial \Lambda}{\partial R} \right) \delta_{m'm} \delta_{l'l} \end{aligned} \right\} & \text{if } \epsilon' = \epsilon \end{cases} \quad (5-50)$$

where

$$\beta_R(k', k) = \int_{-1}^{+1} d\eta S_{k'}(\eta) \left(\frac{\partial S_k(\eta)}{\partial R} \right)_{\eta} \quad (5-51)$$

Also we obtain

$$\begin{aligned} \langle k'; R | (\partial/\partial R)_{\mp} | k; R \rangle = & \mathcal{P} \left[\frac{m_e}{\hbar^2} \langle k'; R | (\partial V/\partial R)_{\mp} | k; R \rangle \right] \delta_{m'm} \\ & + \beta_R(k', k) \cos(\Lambda' - \Lambda) \delta_{m'm} (1 - \delta_{l'l}) \delta(\epsilon' - \epsilon) \end{aligned} \quad (5-52)$$

5.9 Discussion

Some matrix elements of adiabatic continuum states, which are relevant in the quantum mechanical treatment of the Coulomb 3-body problem, have been reported in reference 79. The quantity the authors have represented by $Q_{ss'}^{(+)}$ is the strength of the radial coupling matrix element. Though it appears that their result ($Q_{ss'}^{(+)}$) is general, it is correct *only* when the two continuum states are the same. They have not reported the expressions for \mathcal{P} parts or the angular coupling matrix elements.

In the derivations in reference 79 the authors have neglected the $\ln(\xi)$ term in the asymptotic phase of the radial wave function. It is not justified a priori to drop this term as it becomes arbitrarily large as $\xi \rightarrow \infty$. The mathematical technique developed in this chapter is more rigorous, as is manifested in the derivation of the energy-diagonal part of equations (5 - 43) and (5 - 46). We have numerically confirmed these relations which confirms the validity of the mathematical technique. They also provide critical tests on the computer codes to evaluate $\langle k'; R | (\hat{L}_{\pm}) | k; R \rangle$ and $\langle k'; R | (\partial V/\partial R) | k; R \rangle$.

The equality of the right and the left hand sides of equations (5 - 45) and (5 - 48) is not in the ordinary sense but in the sense of *distributions*; a definite integral of one side is equal to the same integral of the other side.

As in the case of bound states, P_{kk}^R and $P_{k'k}^{\theta}$ for continuum states are strictly *of f-diagonal* and Hermitian.

6. EVALUATION OF NONADIABATIC COUPLING MATRIX

ELEMENTS BETWEEN CONTINUUM STATES

6.1 Introduction

In deriving closed form expressions for the *nonadiabatic propagator* in Chapter 2 we assumed that the numerator of the \mathcal{P} -part and the analytic coefficient of the delta function part of the nonadiabatic coupling matrix elements are *slowly varying* functions of continuum energy so that over a packet width they can be approximated by their values at average packet energies. In this chapter we develop techniques to compute these matrix elements and present results for H_2^+ to prove the validity of this assumption. To our knowledge there are no published values of these matrix elements.

The behavior of the matrix elements as a function of R is also examined; this information is necessary in performing a close-coupling calculation.

One has to calculate the commutator matrix elements, $\langle k'; R | (\hat{L}_\pm V) | k; R \rangle$ and $\langle k'; R | (\partial V / \partial R) | k; R \rangle$. Though the flux ~~with~~ continuum states does not vanish at infinity, the quantities $(\hat{L}_\pm V)$ and $(\partial V / \partial R)$ damp down. Hence these matrix elements can be evaluated accurately by numerical integration provided any singularities at the origin are treated properly.

The integration over the azimuthal angle, ϕ , is done by inspection. Using the power series representation for angular wave functions, the integrals over η is expressed in terms of Gauss Hypergeometric functions, ${}_2F_1$, which can be generated accurately. The remaining integration over ξ is done numerically. The global representation developed in Chapter 3 is used to generate continuum radial wave functions. Throughout this chapter we use atomic units.

6.2 Evaluation of $\langle k'; R | (\hat{L}_{\pm} V) | k; R \rangle$

6.2.1 Derivation of general expressions

In prolate spheroidal coordinate the molecular electronic potential for H_2^+ can be written as

$$V = -\frac{4}{R} \frac{\xi}{(\xi^2 - \eta^2)} \quad (6-1)$$

Then one can show that

$$(\hat{L}_{\pm} V) = \pm \frac{4}{R} \exp(\pm i\phi) \frac{\sqrt{(\xi^2 - 1)(1 - \eta^2)} (\eta^3 + 3\xi^2 \eta)}{(\xi^2 - \eta^2)^3} \quad (6-2)$$

Then it follows that

$$\langle k'; R | (\hat{L}_{\pm} V) | k; R \rangle = \pm \frac{2R}{\pi} (A_0^{\pm}(1, \infty) + 3A_2^{\pm}(1, \infty)) \delta_{k', m \pm 1} \quad (6-3)$$

where

$$A_n^{\pm}(a, b) = \int_a^b d\xi \xi^2 \sqrt{\xi^2 - 1} f_{3-n}^{\pm}(\xi) \left(\frac{\pi R}{4} \chi(k'; R; \xi) \chi(k; R; \xi) \right) \quad n = 0, 2 \quad (6-4)$$

and

$$f_{3-n}^{\pm}(\xi) = \int_{-1}^{+1} d\eta \frac{\sqrt{1 - \eta^2}}{(\xi^2 - \eta^2)^2} \eta^{3-n} S(k'; R; \eta) S(k; R; \eta) \quad (6-5)$$

Use the power series representation, equation (3-7), for the angular wave functions.

$$S(k; R; \eta) = (1 - \eta^2)^{\frac{|m|}{2}} \sum_{i=0}^{\infty} \beta_i(k) \eta^i \quad (6-6)$$

Then f_{3-n}^{\pm} becomes

$$f_{3-n}^{\pm}(\xi) = \frac{1}{\xi^4} \sum_{I=0}^{\infty} C_I K_I^{n \pm}(\xi) \quad (6-7)$$

Where

$$C_I = \sum_{\substack{i,j \\ i+j=I}} \beta_i(k') \beta_j(k) \quad (6-8a)$$

$$K_I^{n\pm}(\xi) = \int_{-1}^{+1} d\eta \frac{\eta^{I+3-n} (1-\eta^2)^{N+1}}{(1-\eta^2/\xi^2)^2} \quad (6-8b)$$

$$2N+1 = |m| + |m \pm 1| \quad (6-8c)$$

$n = 0, 2$; hence $K_I^{n\pm}$ is zero when I is even. To evaluate $K_I^{n\pm}$ when I is odd, change the variable $\eta^2 \rightarrow x$. Then

$$K_I^{n\pm}(\xi) = \int_0^1 dx x^{(I+2-n)/2} (1-x)^{N+1} (1-x/\xi^2)^{-2} \quad (6-9)$$

which can be expressed in closed form in terms of Gauss Hypergeometric function [Chapter 15 of reference 53]. Then one obtains

$$K_I^{n\pm} = \begin{cases} \frac{\Gamma(d)\Gamma(2+N)}{\Gamma(d+2+N)} {}_2F_1(2, d, d+2+N; 1/\xi^2) & \text{when } I \text{ is odd} \\ 0 & \text{when } I \text{ is even} \end{cases} \quad (6-10)$$

$$\text{with } d = \frac{1}{2}(I+4-n) \text{ and } n = 0, 2$$

One can evaluate f_{3-n}^{\pm} at any ξ using equations (6-7) and (6-10).

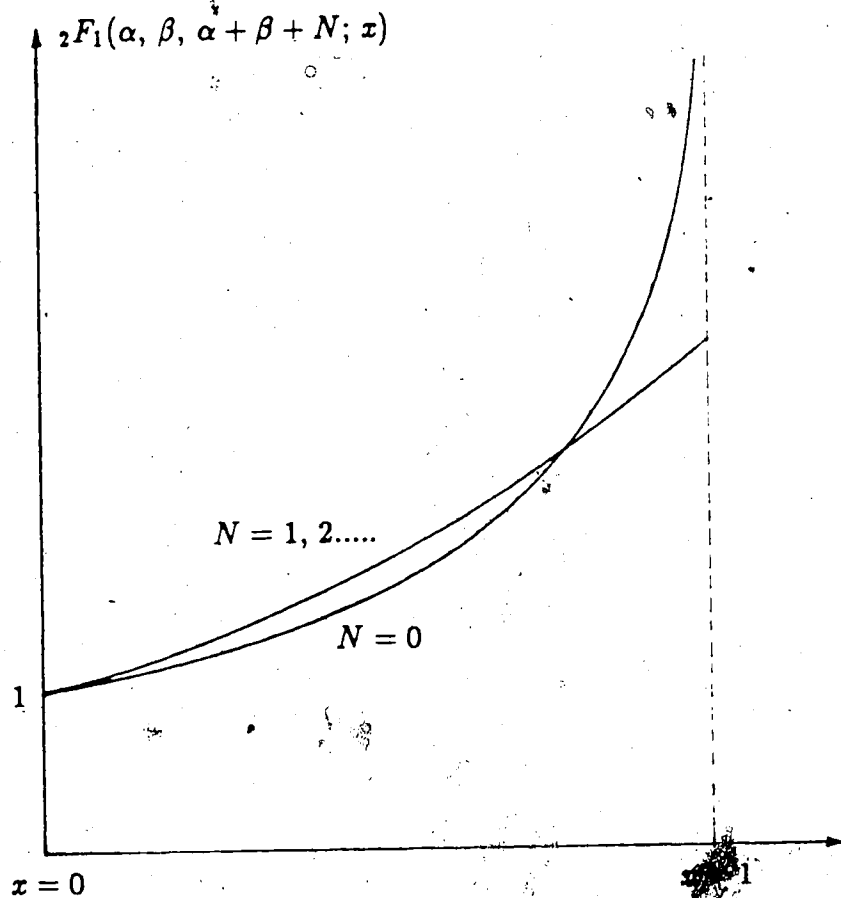
6.2.2 Behavior of the integrand in equation (6-4) near $\xi = 1$

The relevant Gauss Hypergeometric functions have the qualitative forms shown in Figure 6-1. $f_{3-n}^{\pm}(\xi)$ can at most be logarithmically singular ($\ln(\xi-1)$) at $\xi = 1$.

$\chi(k; R; \xi)$ can be expanded in power series (equation (3-28)) near the origin.

$$\chi(k; R; \xi) = T(k) \frac{2}{\sqrt{\pi R}} \frac{(\xi-1)^{|m|/2}}{\sqrt{\xi+1}} \sum_{i=0}^{\infty} a_i(k) (\xi-1)^i \quad (6-11)$$

Figure 6 - 1 : Gauss Hypergeometric Function



The singularity in ${}_2F_1(\alpha, \beta, \alpha + \beta; x)$ at $x = 1$ is of the form $\ln(1 - x)$ (See equation (6 - 19)).

where $T(k)$ is a state dependent constant. Hence the relevant integrand *always* has a factor $(\xi - 1)^{N+\frac{1}{2}}$, $N = 0, 1, 2, \dots$ which will "neutralize" the logarithmic singularity at $\xi = 1$. Hence $A_n^\pm(1, b)$ can be evaluated by direct numerical integration.

6.2.3 An upper-bound to $|A_n^\pm(\xi_\infty, \infty)|$

An upper-bound to $|A_n^\pm(\xi_\infty, \infty)|$ is evaluated here so that one can find a *cutoff* point, $\xi = \xi_\infty$, for the numerical integration such that the result has a given number of significant digits.

It can be shown that

$${}_2F_1(2, d, d + 2 + N; 1/\xi^2) \simeq 1 \quad \text{for } \xi > 10$$

Then

$$f_{3-n}^\pm(\xi) \simeq \frac{D_n}{\xi^4} \quad (6-12)$$

$$D_n = 2 \sum_{I=1}^{\infty} C_I \frac{\Gamma[(I+4-n)/2] \Gamma[2+N]}{\Gamma[N+2+(I+4-n)/2]} \quad (6-13)$$

For sufficiently large ξ we can approximate

$$\sqrt{\xi^2 - 1} \simeq \xi \quad P_R(k; R; \xi) \simeq c$$

Hence

$$\chi(k; R; \xi) \simeq \frac{2}{\sqrt{\pi R c}} \frac{\sin \Theta(k; R; \xi)}{\xi} \quad (6-14)$$

where

$$\Theta(k; R; \xi) = c\xi + (q/2c) \ln(\xi) + \Lambda + G(k; R; \xi) \quad (6-15)$$

The quantities c , q and Λ and, the function G are as defined in Chapter 3. The trigonometric factor in equation (6-4) can now be expanded as

$$\begin{aligned} \sin \Theta(k'; R; \xi) \sin \Theta(k; R; \xi) = & \frac{1}{2} (\cos G_- \cos \Theta_- + \sin G_- \sin \Theta_- \\ & - \cos G_+ \cos \Theta_+ - \sin G_+ \sin \Theta_+) \end{aligned} \quad (6-16)$$

where $G_{\pm} = G(k'; R; \xi) \pm G(k; R; \xi)$ and Θ_{\pm} is as in equation (5 - 22a). Note that

$$\lim_{\xi \rightarrow \infty} G_{\pm} = 0$$

If one chooses ξ_{∞} sufficiently large so that equations (6 - 12) and (6 - 14) are satisfied and $|G_{\pm}| < \pi/2$, then

$$|A_n^{\pm}(\xi_{\infty}, \infty)| < \frac{|D_n|}{2\sqrt{c^*c}} (|X_n^+| + |X_n^-| + |Y_n^+| + |Y_n^-|) \quad (6-17)$$

where

$$\begin{aligned} X_n^{\pm} + iY_n^{\pm} &= \int_{\xi_{\infty}}^{\infty} d\xi \frac{1}{\xi^{5-n}} (\cos \Theta_{\pm} + i \sin \Theta_{\pm}) \\ &= \xi_{\infty}^{i\delta_{\pm} - 4 + n} \exp(i(\Lambda_{\pm} + C_{\pm} \xi_{\infty})) U(1, i\delta_{\pm} - 3 + n, iC_{\pm} \xi_{\infty}) \end{aligned} \quad (6-18)$$

The Kummer's U -function can be generated without much trouble [85].

6.3 Generation of Gauss Hypergeometric Function

Accurate evaluation of ${}_2F_1$ is a major task in evaluating the matrix elements. Three methods are used depending on the range of $x = 1/\xi^2$.

(a) $x_{00} \leq x \leq 1$

A power series representation is used.

$$\begin{aligned} {}_2F_1(\alpha, \beta, \alpha + \beta + j; x) &= (1 - \delta_{j0}) \sum_{i=0}^{j-1} E_{ji} (x-1)^i \\ &\quad + (x-1)^j \sum_{i=0}^{\infty} B_{ji} (A_{ji} - \ln(1-x)) (1-x)^i \end{aligned} \quad (6-19)$$

where

$$A_{j0} = \psi(1) + \psi(j+1) - \psi(\alpha+j) - \psi(\beta+j) \quad (6-20a)$$

$$A_{ji} = A_{j,i-1} + \frac{1}{i} + \frac{1}{j+i} - \frac{1}{\alpha+j+i-1} - \frac{1}{\beta+j+i-1} \quad i \geq 1 \quad (6-20b)$$

The ψ - function is the logarithmic derivative of the Γ -function.

$$\psi(x) = \frac{d(\ln \Gamma(x))}{dx}$$

$$B_{j0} = \frac{\Gamma(\alpha + \beta + j)}{\Gamma(\alpha)\Gamma(\beta)\Gamma(j+1)} \quad (6-21a)$$

$$B_{ji} = B_{j,i-1} \frac{(\alpha + j + i - 1)(\beta + j + i - 1)}{(j+i)^2} \quad i \geq 1 \quad (6-21b)$$

$$E_{j0} = \frac{\Gamma(\alpha + \beta + j)\Gamma(j)}{\Gamma(\alpha + j)\Gamma(\beta + j)} \quad j \geq 1 \quad (6-22a)$$

$$E_{ji} = E_{j,i-1} \frac{(\alpha + j - 1)(\beta + j - 1)}{j(j-i)} \quad j \geq 1, i \geq 1 \quad (6-22b)$$

Note that there is a logarithmic singularity in ${}_2F_1$ at $\xi = 1$ when $j = 0$.

(b) From $x = x_{00}$ to $\xi = \xi_0$

A rational polynomial approximation is used. The relevant subroutine is given in reference 85.

(c) $\xi_0 \leq \xi \leq \xi_\infty$

The Gauss Hypergeometric series is used.

$${}_2F_1(\alpha, \beta, \gamma; x) = \sum_{i=0}^{\infty} G_i x^i \quad (6-23)$$

where

$$G_{i+1} = G_i \frac{(\alpha + i)(\beta + i)}{(\gamma + i)(i + 1)} \quad \text{with } G_0 = 1 \quad (6-24)$$

6.4 Evaluation of $\langle k'; R | (\partial V / \partial R)_T | k; R \rangle$

The techniques used to evaluate $\langle k'; R | (\partial V / \partial R)_T | k; R \rangle$ are quite similar to those described in sections 6.2 and 6.3. except near $\xi = 1$ in the case $m' = m = 0$. This section summarizes the relevant mathematical expressions and outlines their derivation.

Two different forms for $(\partial V/\partial R)_{\bar{r}}$ are used

$$\left(\frac{\partial V}{\partial R}\right)_{\bar{r}} = \frac{4}{R^2} \left[\frac{\xi}{(\xi^2 - \eta^2)} - \frac{\xi^3(\xi^2 - 1)}{(\xi^2 - \eta^2)^3} - \frac{\eta^2 \xi(\xi^2 - 1)}{(\xi^2 - \eta^2)^3} + \frac{2\eta^2 \xi(1 - \eta^2)}{(\xi^2 - \eta^2)^3} \right] \quad (6-25)$$

$$\left(\frac{\partial V}{\partial R}\right)_{\bar{r}} = \frac{4}{R^2} \left[\frac{\xi^3}{(\xi^2 - \eta^2)^3} - \frac{3\xi(\xi^2 - 1)\eta^2}{(\xi^2 - \eta^2)^3} - \frac{\xi\eta^4}{(\xi^2 - \eta^2)^3} \right] \quad (6-26)$$

Define $Y(a,b)$ by

$$Y(a,b) = \frac{\pi R^3}{16} \int_a^b d\xi \left\{ \int_{-1}^{+1} d\eta (\xi^2 - \eta^2) \left(\frac{\partial V}{\partial R}\right)_{\bar{r}} S(k'; R; \eta) S(k; R; \eta) \right. \\ \left. \times \chi(k'; R; \xi) \chi(k; R; \xi) \right\} \quad (6-27)$$

Then

$$\langle k'; R | (\partial V/\partial R)_{\bar{r}} | k; R \rangle = \frac{2}{\pi} (Y(1, \xi_0) + Y(\xi_0, \infty)) \quad (6-28)$$

Using the form given in equation (6-25) near the origin we have

$$Y(1, \xi_0) = Y_1(\xi_0) - Y_2^{(0)}(\xi_0) - Y_2^{(2)}(\xi_0) + 2Y_3(\xi_0) \quad (6-29)$$

where

$$Y_1(\xi_0) = \frac{\pi R}{4} \left[\sum_{I=0}^{\infty} C_I C(I, 0, M) \right] \int_1^{\xi_0} d\xi \xi \chi(k'; R; \xi) \chi(k; R; \xi) \quad (6-30)$$

with

$$C(I, n, M) = \begin{cases} \frac{\Gamma[(I+n+1)/2] \Gamma[1+M]}{\Gamma[(I+n+1)/2 + 1 + M]} & \text{if } I \text{ is even} \\ 0 & \text{if } I \text{ is odd} \end{cases} \quad (6-31)$$

Here $M = |m'| = |m|$.

$$Y_2^{(n)}(\xi_0) = \begin{cases} \frac{\pi R}{4} \int_1^{\xi_0} d\xi \xi^{1-n} F(n; \xi) \chi(k'; R; \xi) \chi(k; R; \xi) & \text{if } M = 0 \\ \frac{\pi R}{4} \int_1^{\xi_0} d\xi \frac{(\xi^2 - 1)}{\xi^{1+n}} f(n, M; \xi) \chi(k'; R; \xi) \chi(k; R; \xi) & \text{if } M \geq 1 \end{cases} \quad (6-32)$$

Here

$$F(n; \xi) = \sum_{I=0}^{\infty} C_I C(I, n, 0) {}_2F_1 \left((I+n+1)/2 - 1, 1, (I+n+1)/2 + 1; 1/\xi^2 \right) \quad (6-33a)$$

$$f(n, M; \xi) = \sum_{I=0}^{\infty} \left\{ C_I C(I, n, M) \times {}_2F_1 \left(2, (I+n+1)/2, (I+n+1)/2 + 1 + M; 1/\xi^2 \right) \right\} \quad (6-33b)$$

$$Y_3(\xi_0) = \frac{\pi R}{4} \int_1^{\xi_0} d\xi \frac{1}{\xi^3} f(2, M+1; \xi) \chi(k'; R; \xi) \chi(k; R; \xi) \quad (6-34)$$

Using equation (6-19) to represent ${}_2F_1$ one can show that the integrands of Y_1 , $Y_2^{(n)}$ and Y_3 are well behaved at $\xi = 1$ when $M \geq 1$; hence they can be evaluated by direct numerical integration. However, the integrand of Y_3 is logarithmically singular at the origin when $M = 0$. We isolate this singularity and perform the integration over it analytically.

Consider the power series representation of χ . Except the first term all the other terms have the factor $(\xi - 1)$ which will "neutralize" the logarithmic singularity in $f(2, 1; \xi)$. One can isolate the "problematic" term as follows.

$$\frac{\pi R}{4} \chi(k'; R; \xi) \chi(k; R; \xi) = \Phi(\xi) + \frac{T}{\xi + 1} \quad (6-35)$$

$$T = T(k') T(k) a_0(k') a_0(k) \quad (6-36)$$

One can isolate the logarithmic singularity in $f(2, 1; \xi)$ using the equation (6 - 19).

$$f(2, 1; \xi) = f_1(2, 1; \xi) + B \ln(\xi - 1) \quad (6 - 37)$$

where

$$B = \sum_{I=0}^{\infty} C_I C(I, 2, 1) B_I \quad (6 - 38a)$$

$$B_I = \frac{1}{2}(I+3) \left[\frac{1}{2}(I+3) + 1 \right] \quad (6 - 38b)$$

$$f_1(2, 1; \xi) = \sum_{I=0}^{\infty} C_I C(I, 2, 1) \left\{ {}_2F_1\left(2, (I+3)/2, (I+3)/2 + 2; 1/\xi^2\right) + B_I \ln(\xi - 1) \right\} \quad (6 - 38c)$$

Then using equations (6 - 34), (6 - 35) and (6 - 37) and, performing the integration over the singular term analytically we obtain for $M = 0$

$$Y_3(1, \xi_0) = \int_1^{\xi_0} d\xi \left[\frac{\pi R}{4} \frac{1}{\xi^3} f_1(2, 1; \xi) \chi(k'; R; \xi) \chi(k; R; \xi) - B \Phi(\xi) \ln(\xi - 1) \right] - B T Y_4(\xi_0) \quad (9 - 39)$$

where

$$Y_4(\xi_0) = \int_1^{\xi_0} d\xi \left\{ \frac{(4\xi + 3)(\xi - 1)[\ln(\xi - 1) - 1]}{\xi^4 (\xi + 1)^2} \right\} + \frac{(\xi_0 - 1)[\ln(\xi_0 - 1) - 1]}{\xi_0^3 (\xi_0 + 1)} \quad (6 - 40)$$

The remaining integrals in equations (6 - 39) and (6 - 40) are done numerically

Note that Y_4 is state independent.

It is more efficient to use the form in equation (6 - 26) to calculate

$Y(\xi_0, \infty)$. Then one obtains

$$Y(\xi_0, \xi_\infty) = \frac{\pi R}{4} \int_{\xi_0}^{\xi_\infty} d\xi \left\{ \left[\frac{1}{\xi} f(0, M; \xi) - \frac{3(\xi^2 - 1)}{\xi^3} f(2, M; \xi) - \frac{1}{\xi^3} f(4, M; \xi) \right] \right. \\ \left. \times \chi(k'; R; \xi) \chi(k; R; \xi) \right\} \quad (6-41)$$

To find ξ_∞ , an upper bound on $|Y(\xi_\infty, \infty)|$ is estimated using the following expression.

$$|Y(\xi_\infty, \infty)| < \frac{1}{2\sqrt{c'c}} \left\{ |f(0, M; 0) - 3f(2, M; 0)| (|X_2^+| + |X_2^-| + |Y_2^+| + |Y_2^-|) \right. \\ \left. + |f(4, M; 0)| (|X_0^+| + |X_0^-| + |Y_0^+| + |Y_0^-|) \right\} \quad (6-42)$$

The first and the last terms in the integrand of (6-41) has singularities of the form $1/(\xi - 1)$ which are nonintegrable; hence it is not suitable to evaluate $Y(1, \xi_0)$. On the other hand the integrands in Y_1 and $Y_2^{(0)}$ damp down as $1/\xi$ as $\xi \rightarrow \infty$ whereas those in equation (6-41) die down faster ($\geq 1/\xi^3$). Hence the latter form more suitable than that in equation (6-30) in evaluating $Y(\xi_0, \xi_\infty)$.

6.5 Numerical Details

- (a) A subroutine in quadruple precision was used to generate ${}_2F_1$ in the domain $x_{00} \leq x \leq 1$ because of the cancellation occurring in the "infinite" summation in equation (6-20).
- (b) The algorithm of Bulirsch and Stoer [86] was used to perform the numerical integrations.
- (c) The parameters were fixed as follows;

$$x_{00} = 0.9 \quad \text{and} \quad \xi_0 = 1.5$$

Program decides the value of ξ_∞ once the number of significant digits in the result is specified.

- (d) The numerical integrator can run into difficulties if two zeros of $\sin \Theta(k'; R; \xi)$ and $\sin \Theta(k; R; \xi)$ become too close to each other. Hence in the domain $\xi_0 \rightarrow \xi_\infty$ the following form was used.

$$\frac{\pi R}{4} \chi(k'; R; \xi) \chi(k; R; \xi) = \frac{1}{2} \left[\cos(\Theta(k'; R; \xi) - \Theta(k; R; \xi)) - \cos(\Theta(k'; R; \xi) + \Theta(k; R; \xi)) \right] / (\xi^2 - 1) \sqrt{P_R(k'; R; \xi) P_R(k; R; \xi)}$$

and each of the \cos -term integrals were done separately (but simultaneously).

- (e) The following checks were done to assess the precision/accuracy of the results.

- (i) Stability of the results against changes in x_0 , ξ_0 and ξ_∞ was examined.
- (ii) It was checked whether the calculated matrix elements satisfy the equations (5-47) and (5-50) when $\epsilon' = \epsilon$. Since the computer codes do not make any important decisions depending on the condition $\epsilon' = \epsilon$, this is a powerful check on the accuracy of the results.

6.6 Analytic Coefficients of the δ -function parts

6.6.1 Angular Couplings

Define the analytic coefficients of the δ -function part of $\langle \hat{L}_+ \rangle$ by $\langle \mathcal{D}^\theta \rangle$.

Then equation (5-49) gives

$$\langle \epsilon' m'; R | \mathcal{D}^\theta | \epsilon l m; R \rangle = -(m \beta_{-1}^1(k', k) + \beta'(k', k)) \cos(\Lambda' - \Lambda) \delta_{m', m+1}. \quad (6-43)$$

Expressing the angular wave functions in power series form and performing the integrals over η analytically we obtain

$$\langle \epsilon l' m'; R | \mathcal{D}^\theta | \epsilon l m; R \rangle = \left[\sum_{i,j=0}^{\infty} \beta_i(k') D_{ij}^\theta \beta_j(k) \right] \cos(\Lambda' - \Lambda) \delta_{m', m+1} \quad (6-44)$$

where

$$D_{ij}^\theta = \begin{cases} \frac{\Gamma[(i+j)/2] \Gamma[M^+]}{\Gamma[(i+j+2)/2 + M^+]} (i \Xi(-m - 1/2) - j \Xi(m + 1/2)) (M^+ - 1) & i + j \text{ odd} \\ 0 & i + j \text{ even} \end{cases} \quad (6-45)$$

with $M^+ = 2 + |m| - \Xi(-m - 1/2)$. $\Xi(x)$ is the unit step function

$$\Xi(x) = \begin{cases} 1 & \text{if } x > 0 \\ 0 & \text{if } x < 0 \end{cases}$$

6.6.2 Radial Coupling

Using equation (5-52) we define

$$\langle \epsilon l' m'; R | \mathcal{D}^R | \epsilon l m; R \rangle = \beta_R(k', k) \cos(\Lambda' - \Lambda) (1 - \delta_{l'l}) \delta_{m', m} \quad (6-46)$$

Using equation (A-15) we can relate β_R to a simple integral over η , which can be performed analytically using the power series representation for angular wave functions.

$$\langle \epsilon l' m'; R | \mathcal{D}^R | \epsilon l m; R \rangle = \frac{\epsilon R}{(A - A')} \left[\sum_{I=0}^{\infty} C_I C(I, 2M) \right] \cos(\Lambda' - \Lambda) (1 - \delta_{l'l}) \delta_{m', m} \quad (6-47)$$

6.7 Results

Calculations were limited to continuum states with $0.005 \leq c^2 \leq 200.0$ a.u., $l = 0, 1, 2$ with all possible m . Most of the matrix elements were evaluated at

the average packet energies corresponding to the energy sampling for an interaction region of radius 40.0 a.u.. Only the matrix elements for \hat{L}_+ were calculated which are related to those of \hat{L}_- by

$$\langle k; R | (\hat{L}_- V) | k'; R \rangle = -\langle k'; R | (\hat{L}_+ V) | k; R \rangle$$

In Figures 6-2 → 5 and Figures 6-6 → 9 we have displayed the matrix elements of $(\hat{L}_+ V)$ and $(\partial V / \partial R)$ as a function of continuum energy at 4 different internuclear separations. We have used the notation

$$(\hat{L}_+ V) = p^\theta \quad (\partial V / \partial R) = p^R$$

Figure 6-10 shows the energy dependence of the analytic coefficients of the δ -function parts. The four curves in each of these graphs belong to the following 4 internuclear separations.

..... $R = 1.0 \text{ a.u.}$
 ----- $R = 3.0 \text{ a.u.}$
 -.-.-.-.- $R = 6.0 \text{ a.u.}$
 _____ $R = 10.0 \text{ a.u.}$

The rest of the figures display the R -dependence of the matrix elements (and the analytic coefficients). In Figures 6-11, 6-13, 6-14 and 6-16 the curves must be identified with the following four continuum energies.

..... $\epsilon'(\text{or } \epsilon) = 0.045 \text{ a.u.}$
 ----- $\epsilon'(\text{or } \epsilon) = 0.150 \text{ a.u.}$
 -.-.-.-.- $\epsilon'(\text{or } \epsilon) = 1.060 \text{ a.u.}$
 _____ $\epsilon'(\text{or } \epsilon) = 2.260 \text{ a.u.}$

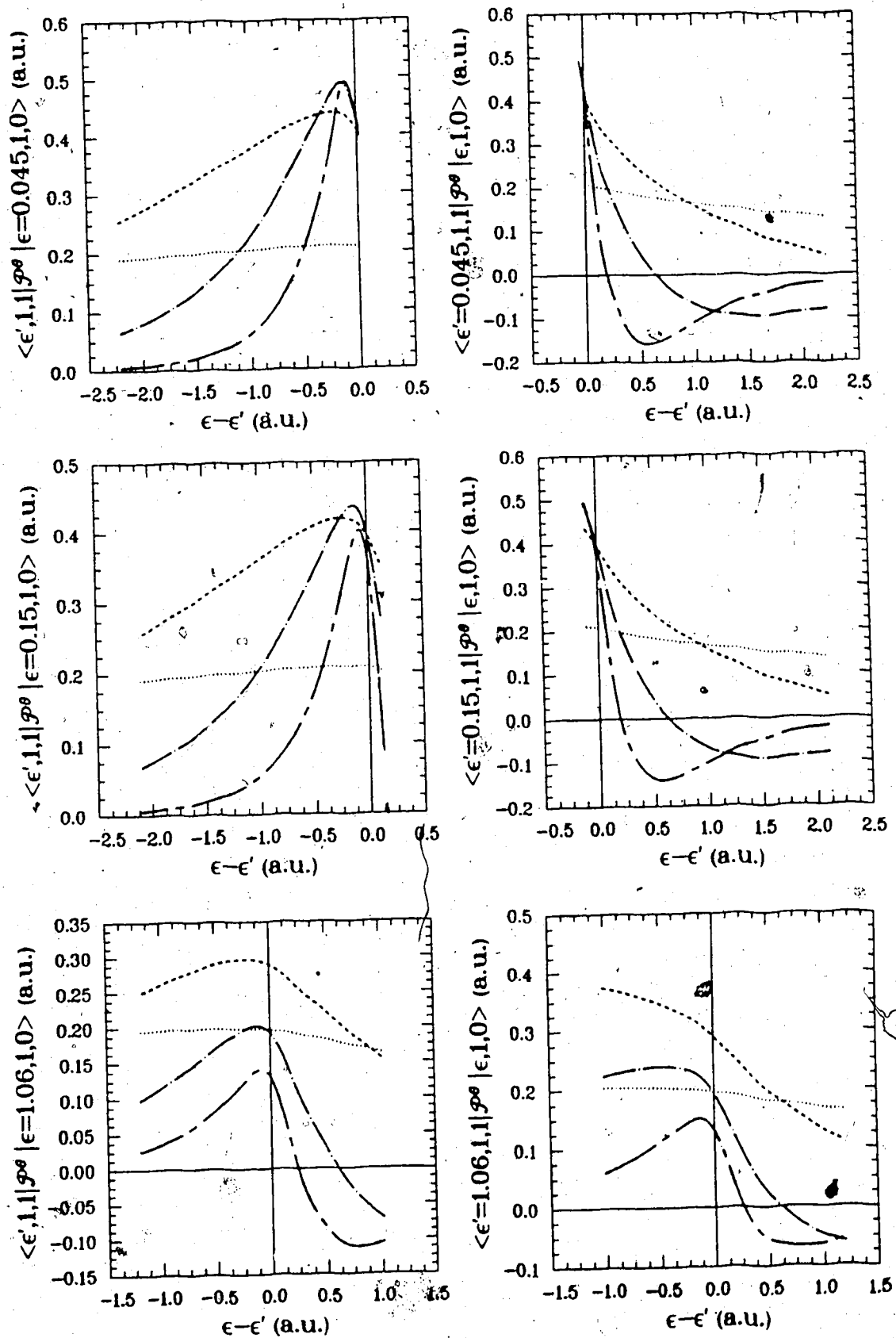


Figure 6 - 2 : $\langle \mathcal{P}^0 \rangle$ vs. Continuum energy

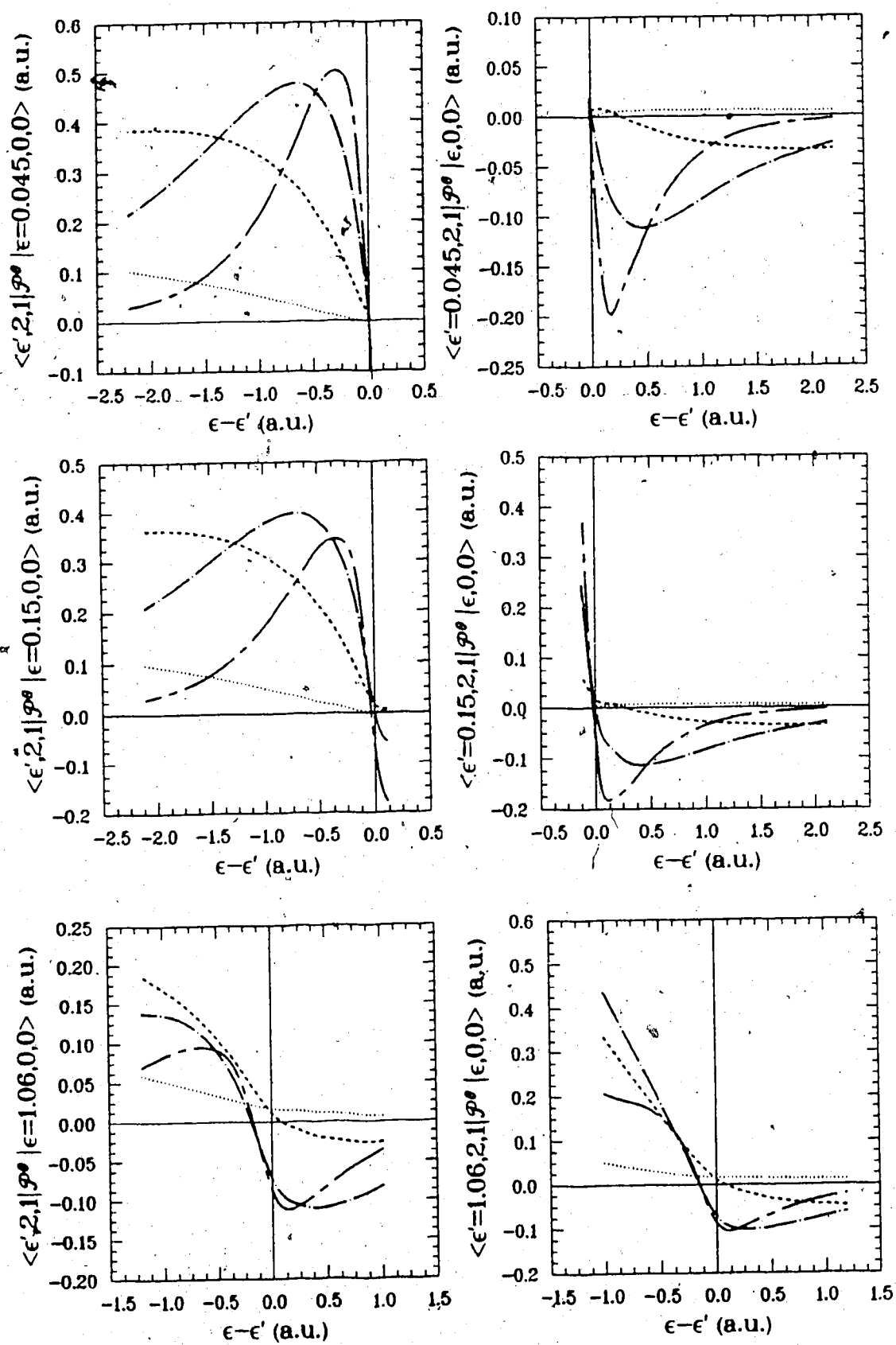


Figure 6 - 3 : $\langle \mathcal{P}^0 \rangle$ vs. Continuum energy

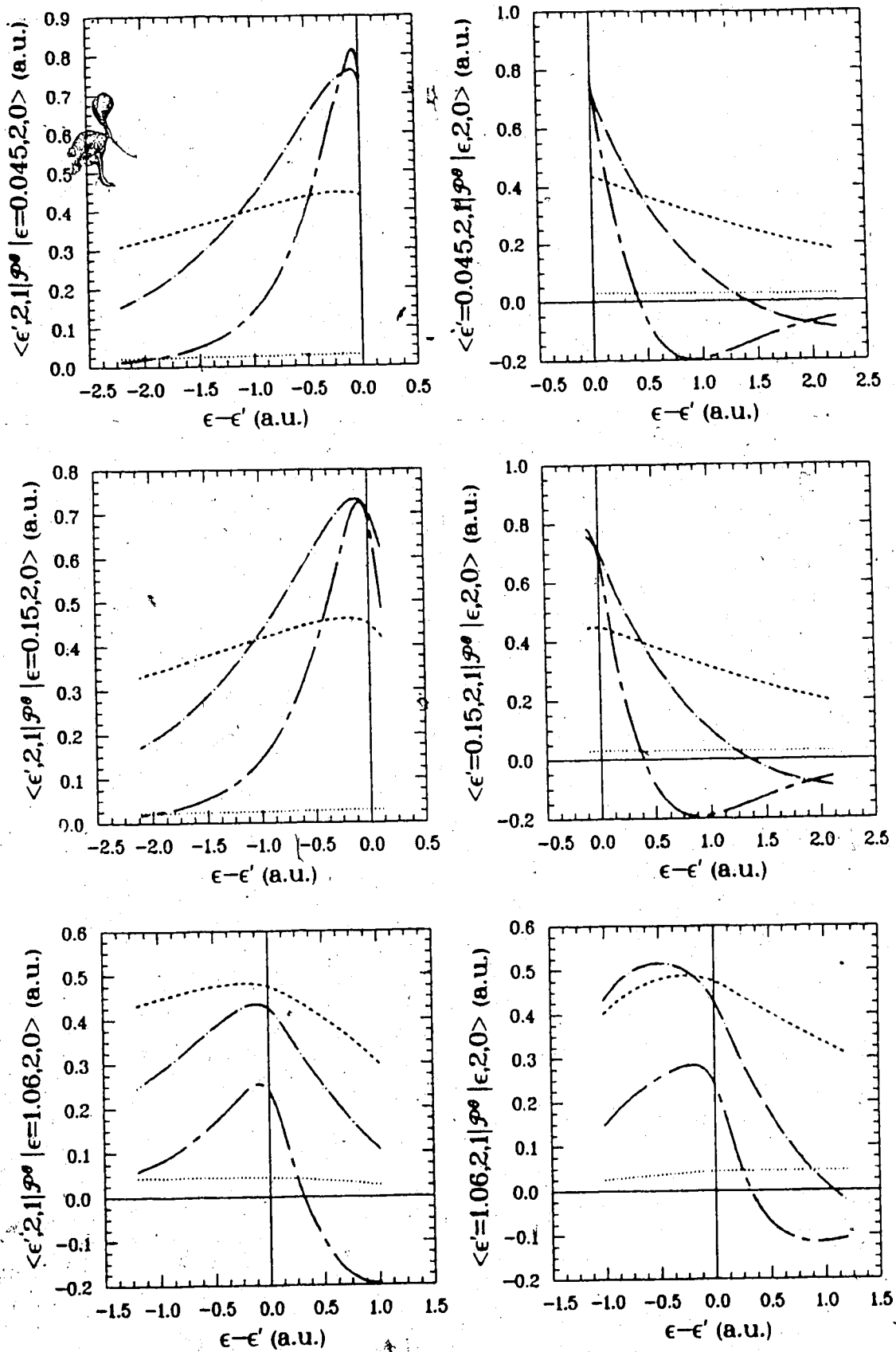


Figure 6 - 4 : $\langle \mathcal{P}^0 \rangle$ vs. Continuum energy

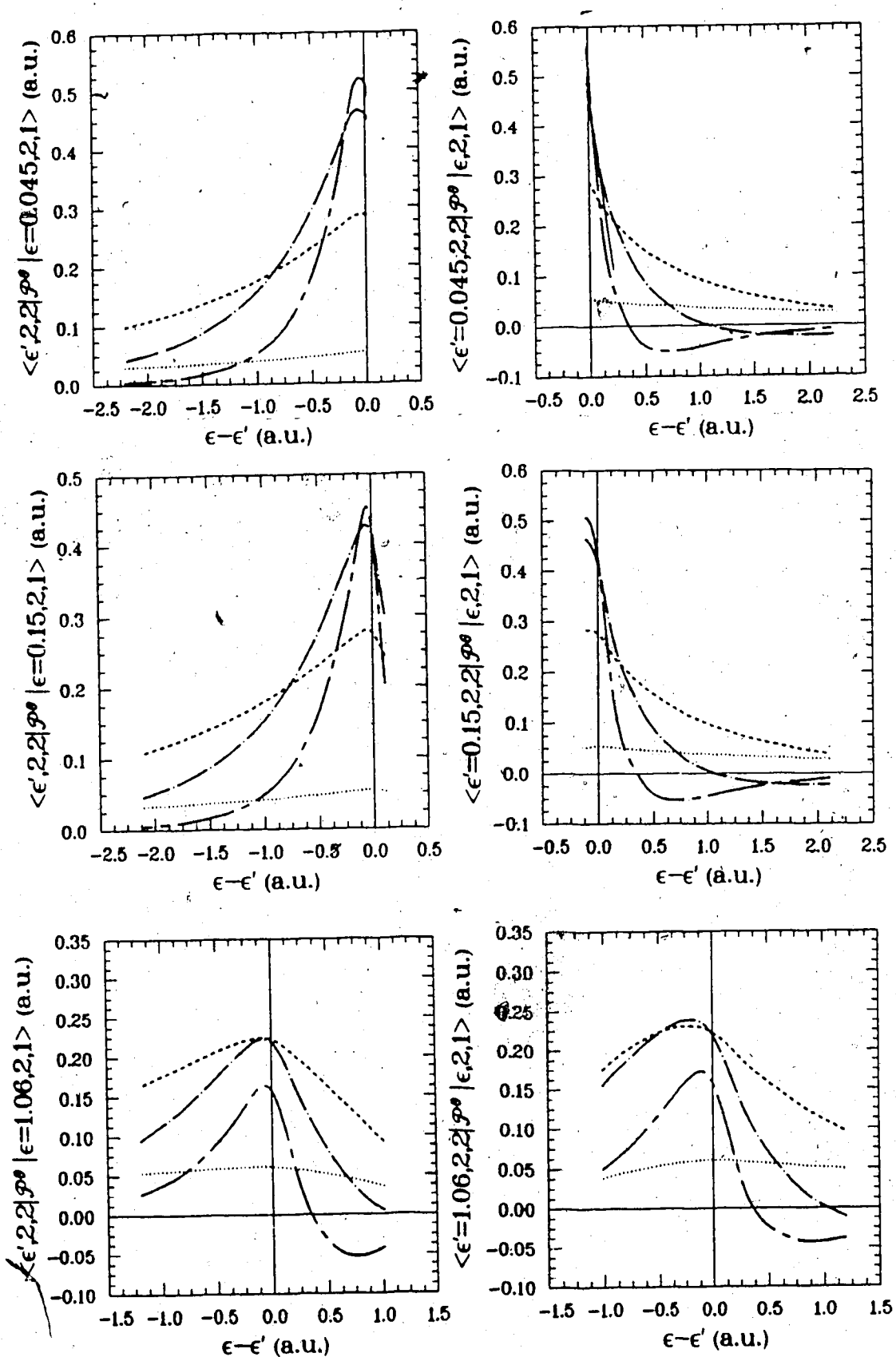


Figure 6 - 5 : $\langle p^0 \rangle$ vs. Continuum energy

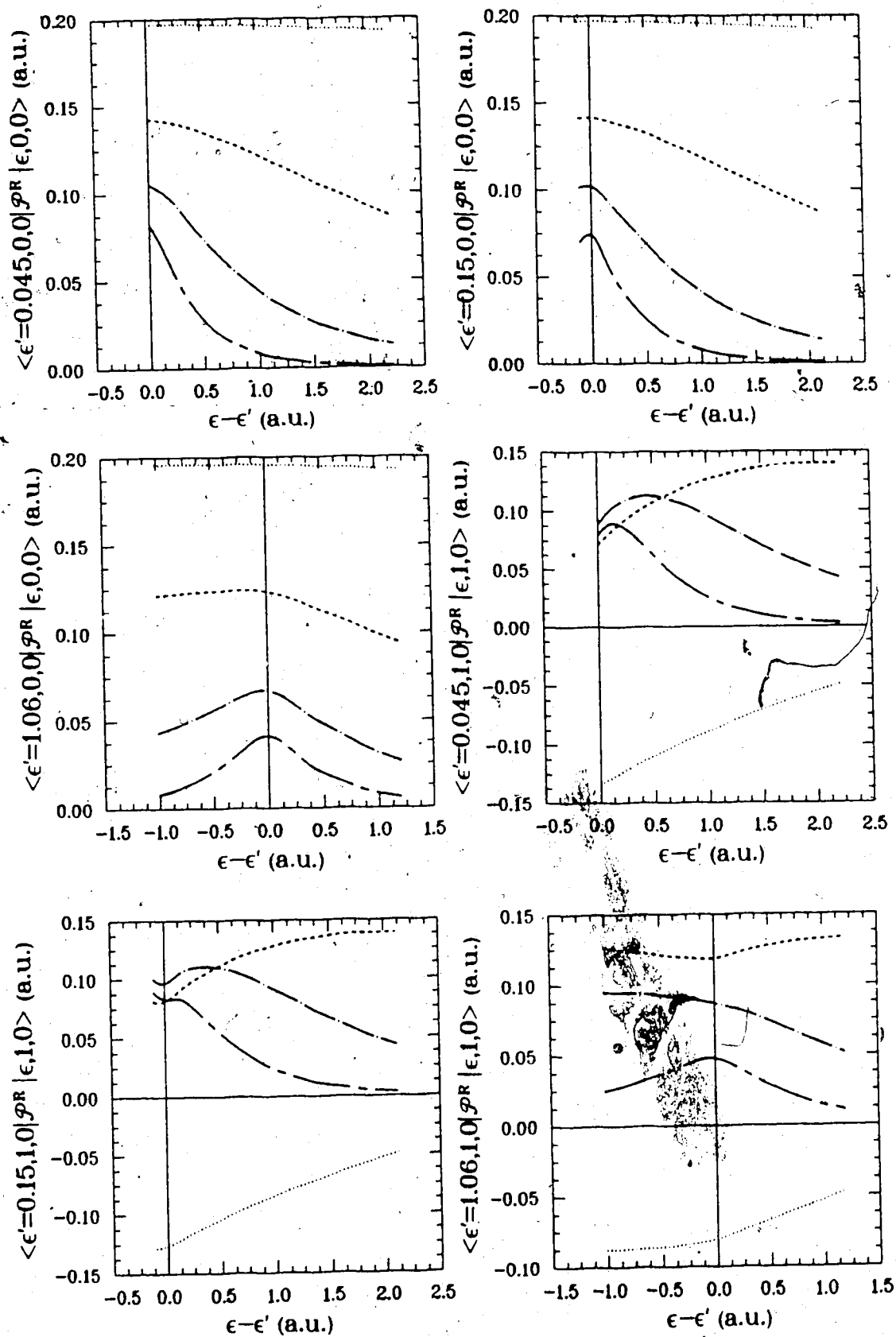


Figure 6 - 6 : $\langle P^R \rangle$ vs. Continuum energy

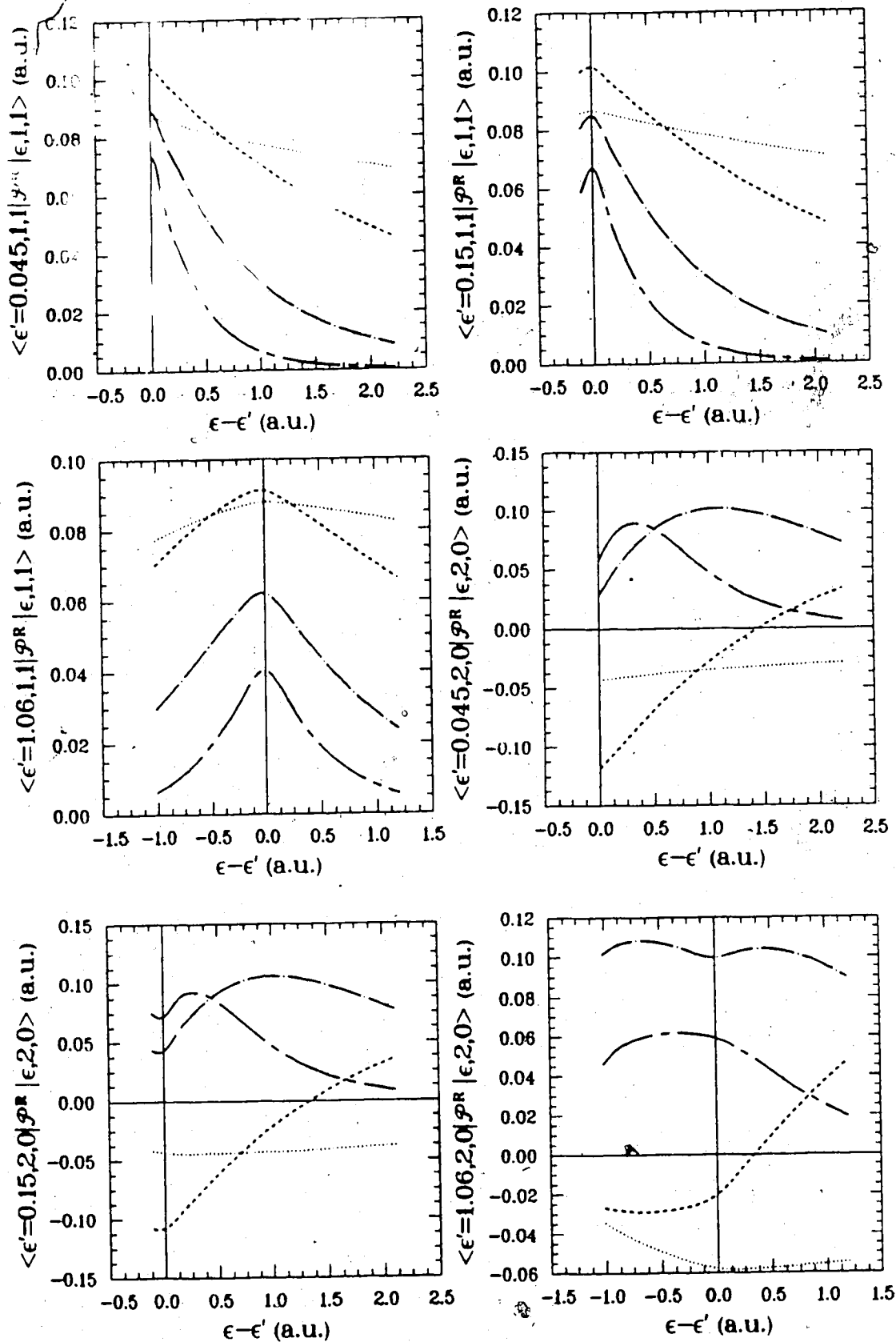


Figure 6 - 7 : $\langle p^R \rangle$ vs. Continuum energy

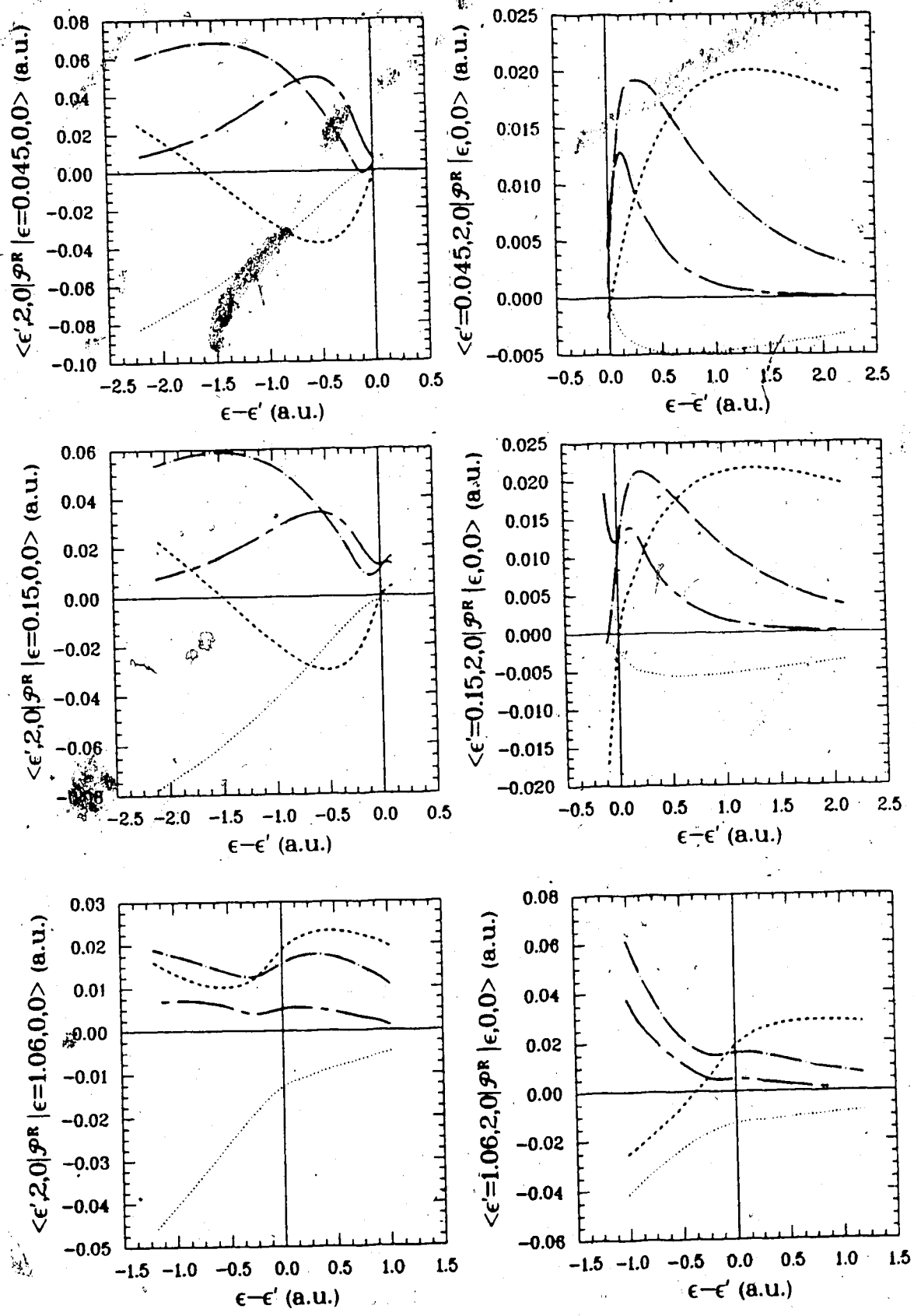


Figure 6 - 8 : $\langle \rho^R \rangle$ vs. Continuum energy

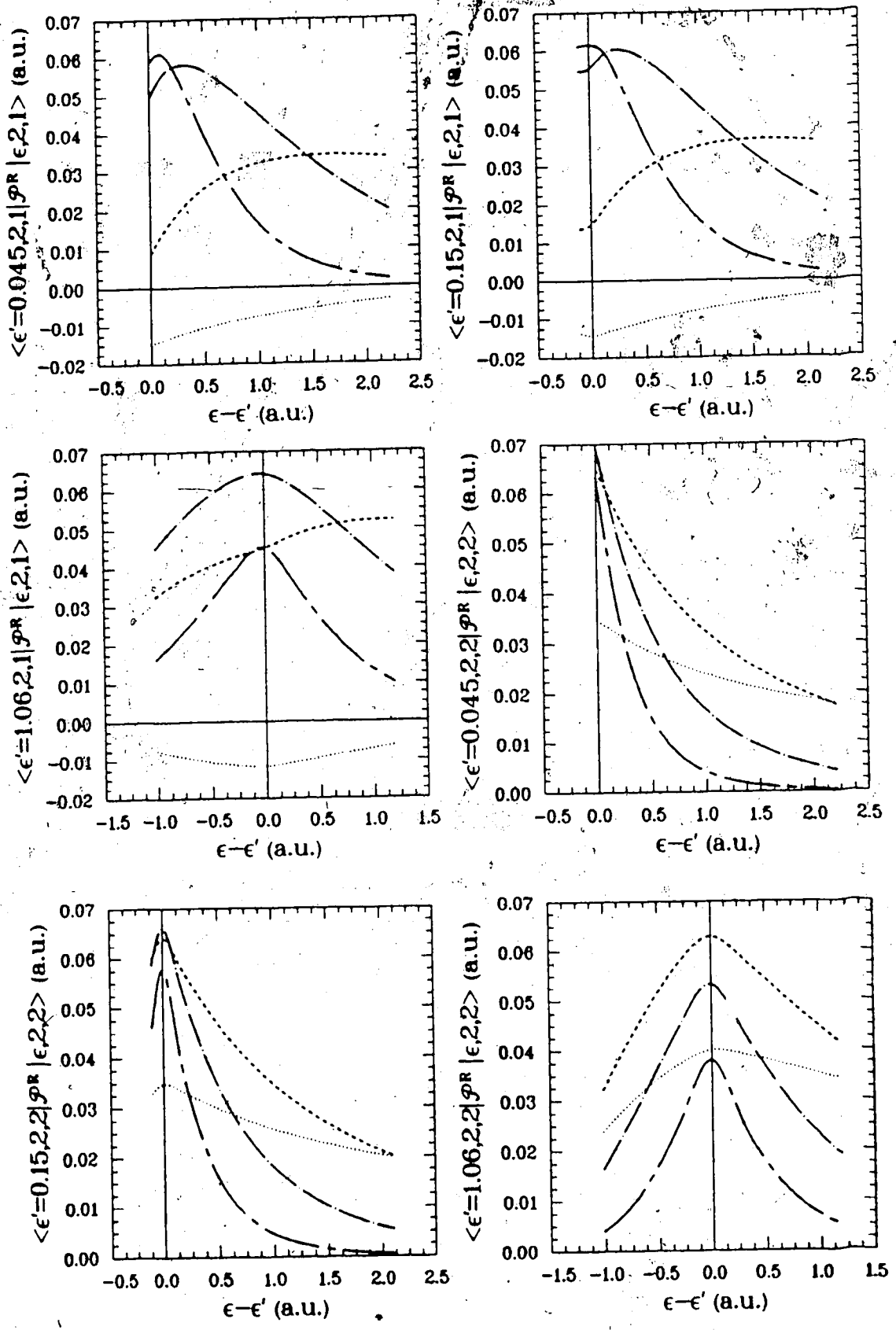


Figure 6 - 9 : $\langle \mathcal{P}^R \rangle$ vs. Continuum energy

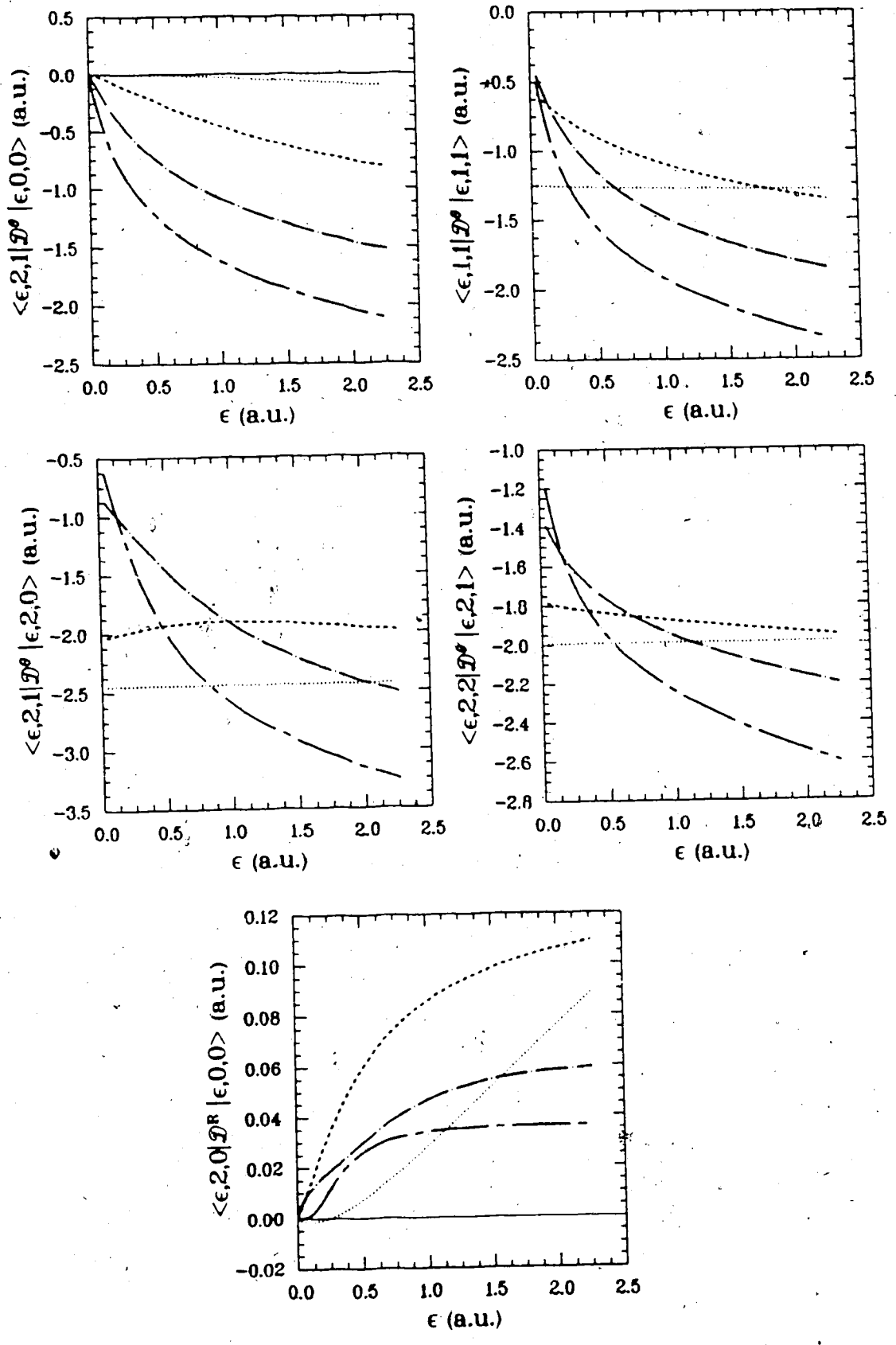
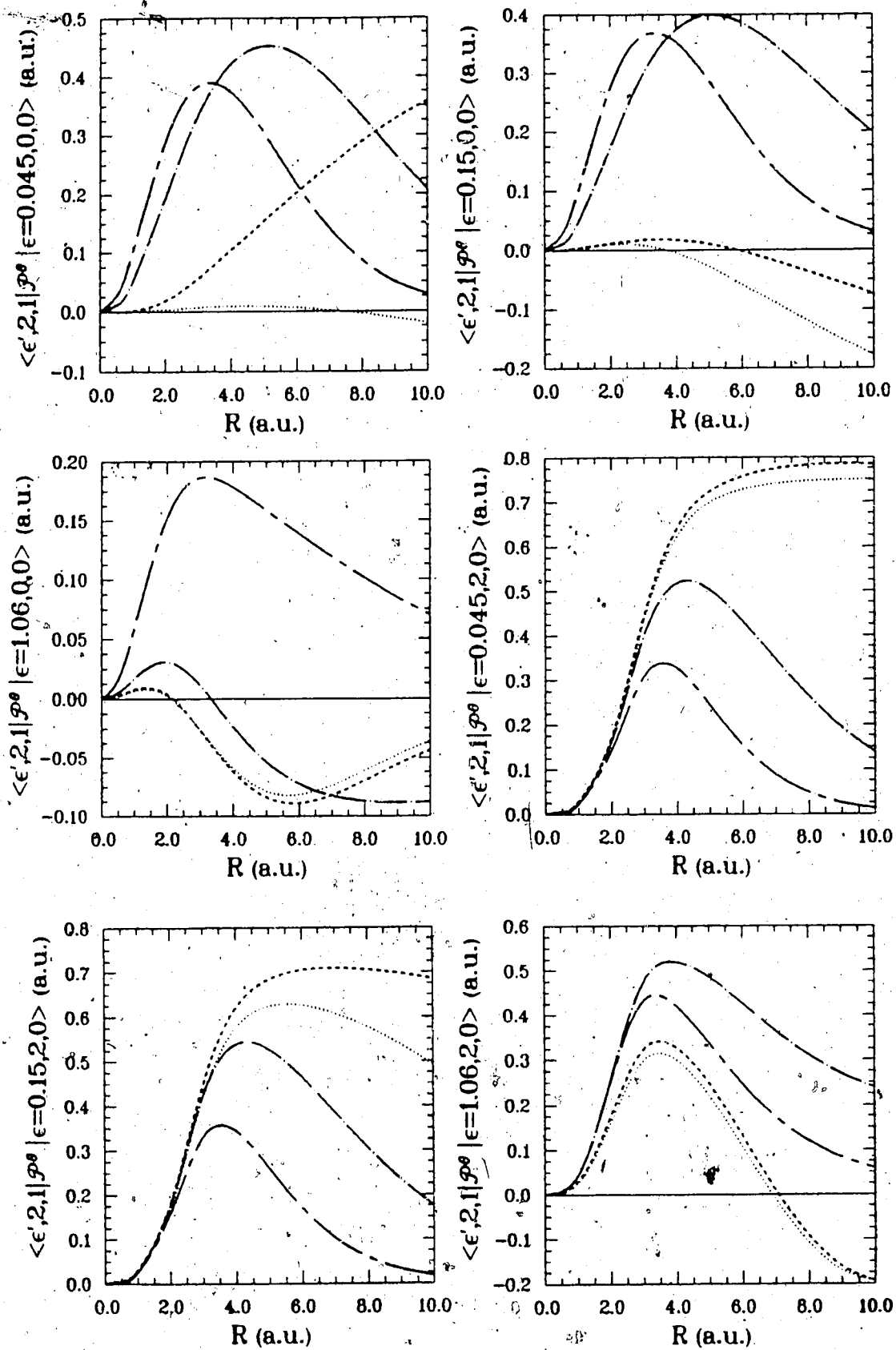


Figure 6 - 10 : $\langle D^0 \rangle$ and $\langle D^R \rangle$ vs. Continuum energy

Figure 6 - 11 : $\langle \rho^0 \rangle$ vs. R

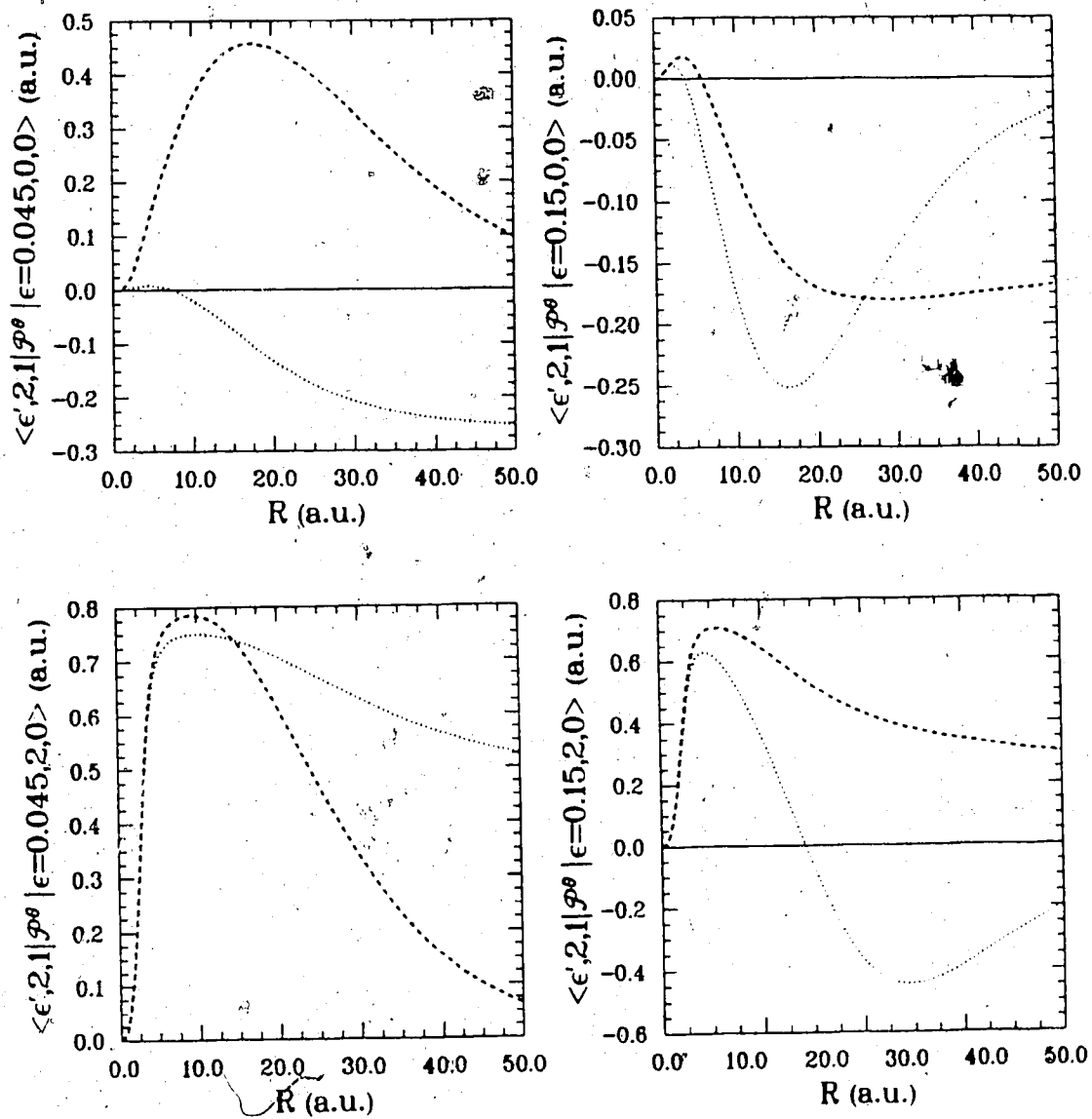
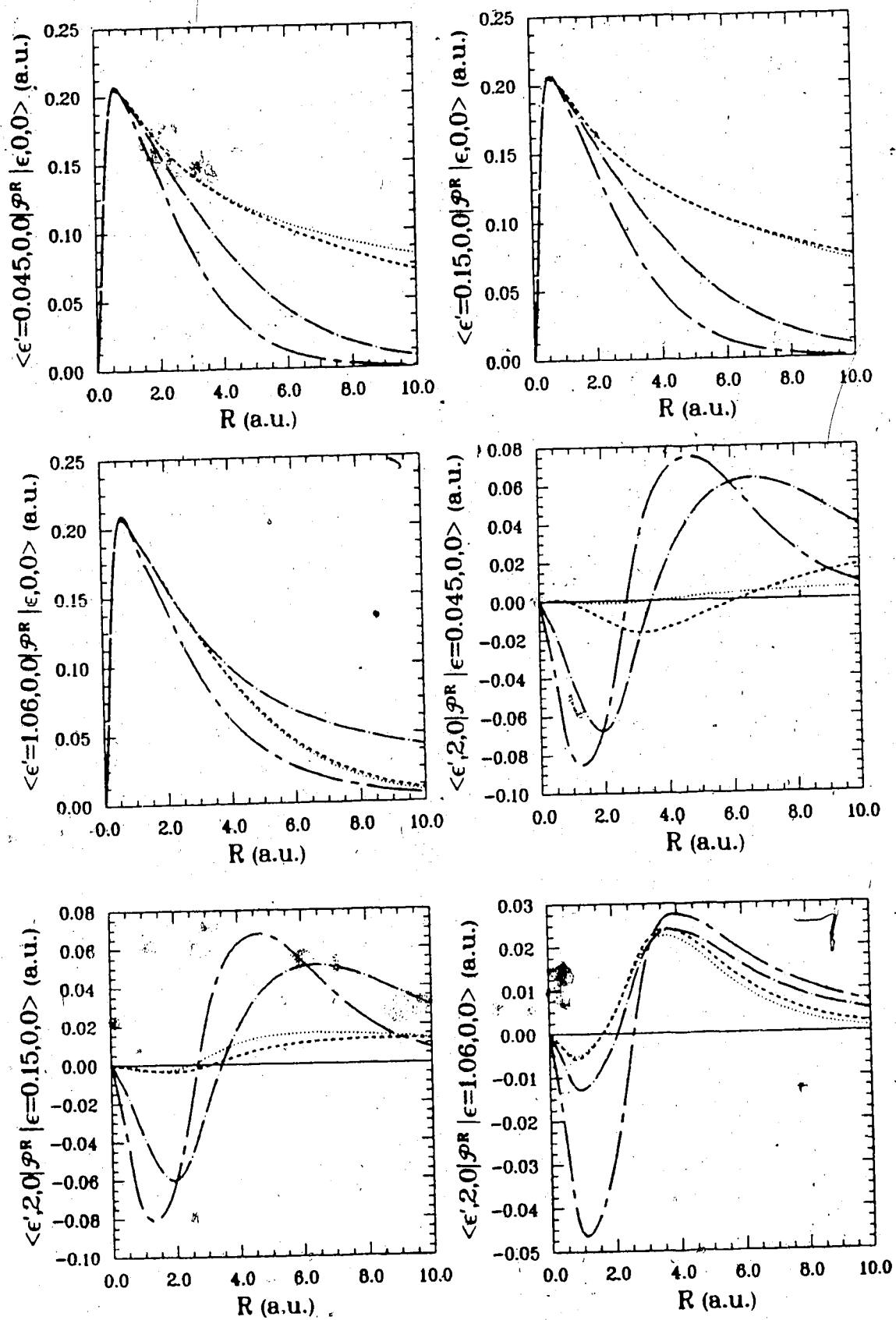
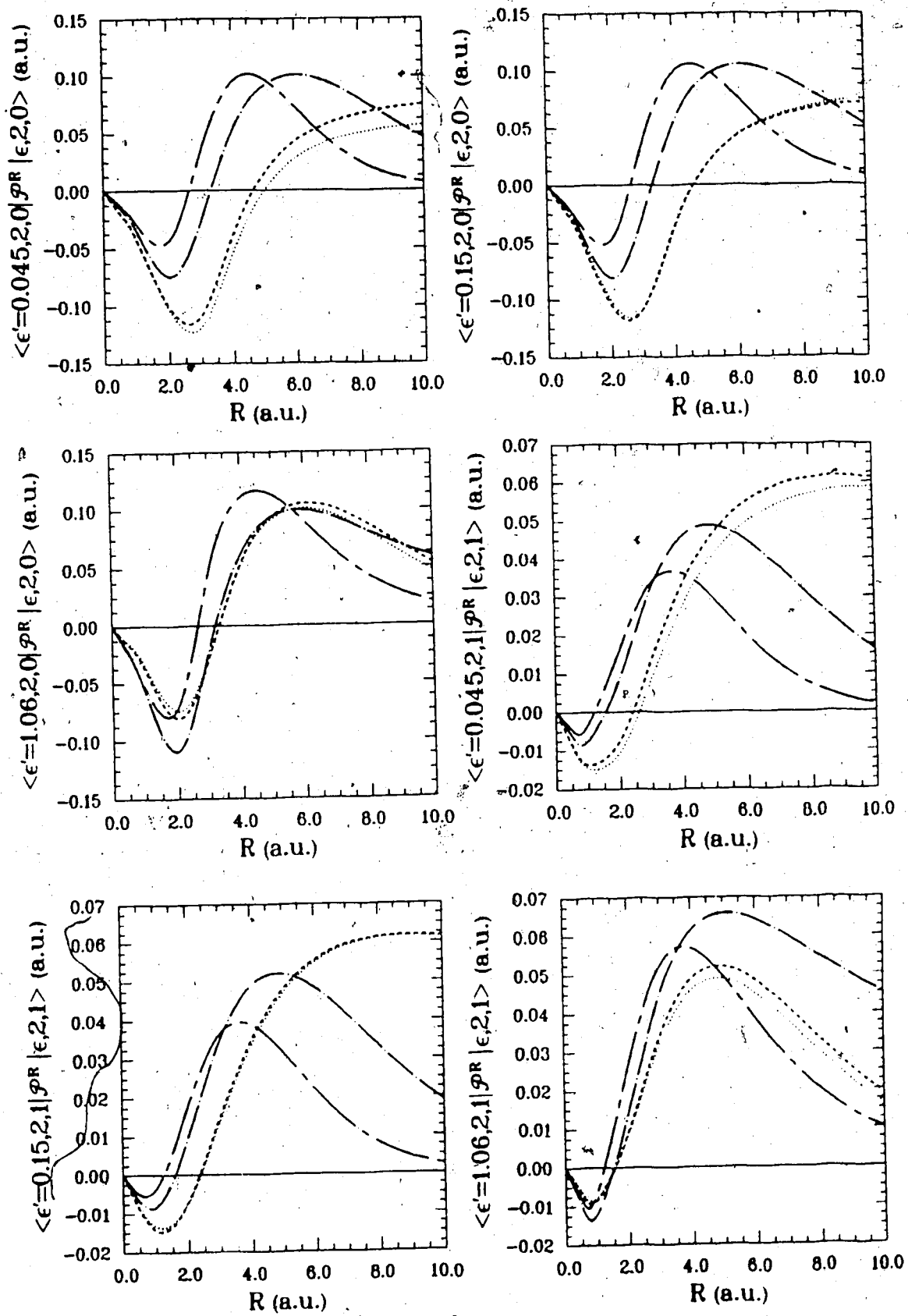
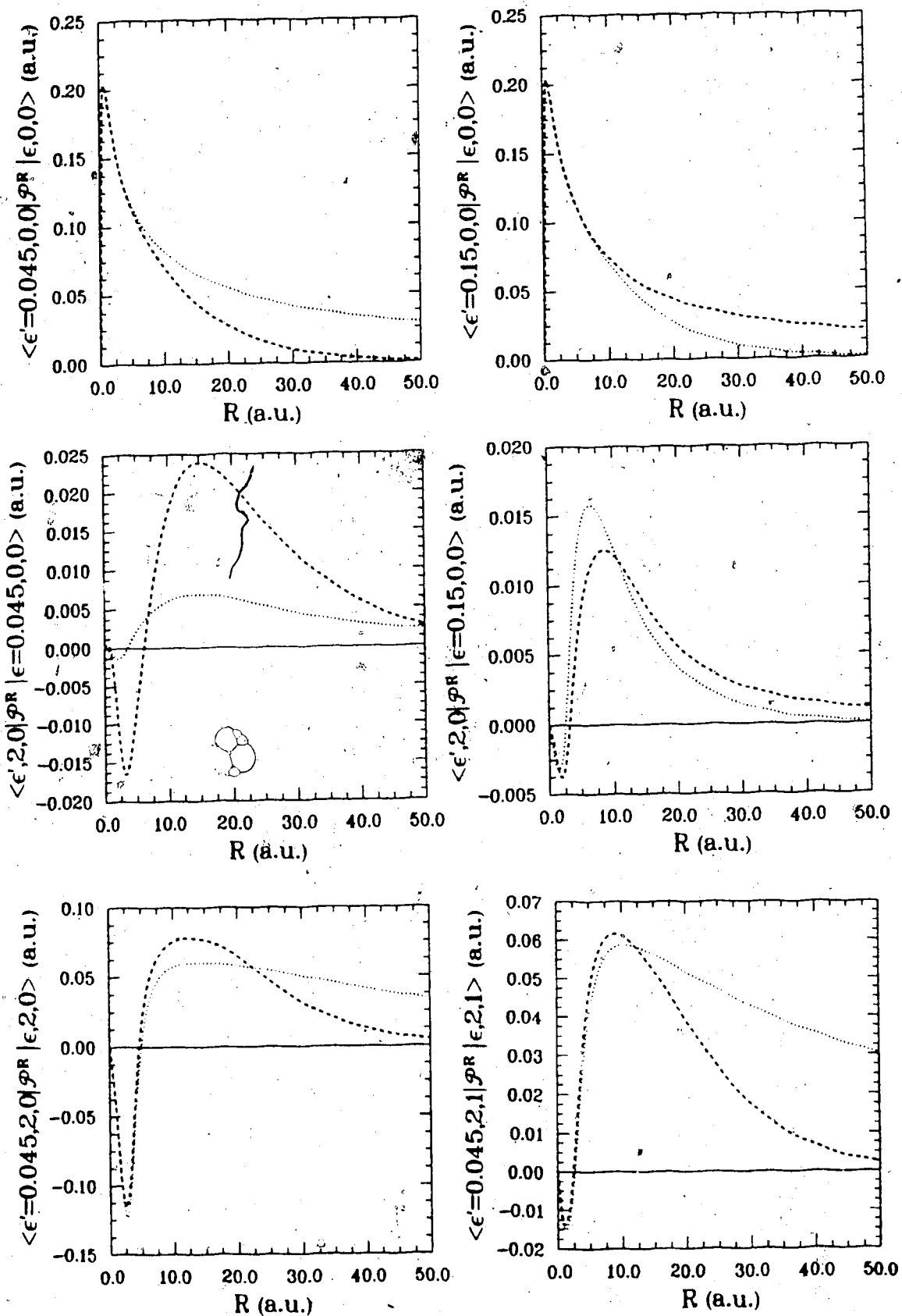


Figure 6 - 12 : $\langle P^{\theta} \rangle$ vs. R

Figure 6 - 13 : $\langle \rho^R \rangle$ vs. R

Figure 6 - vs. R

Figure 6 - 15 : $\langle \rho^R \rangle$ vs. R

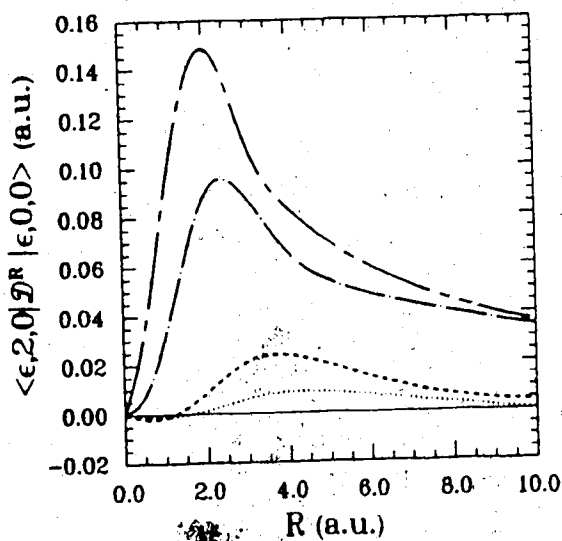
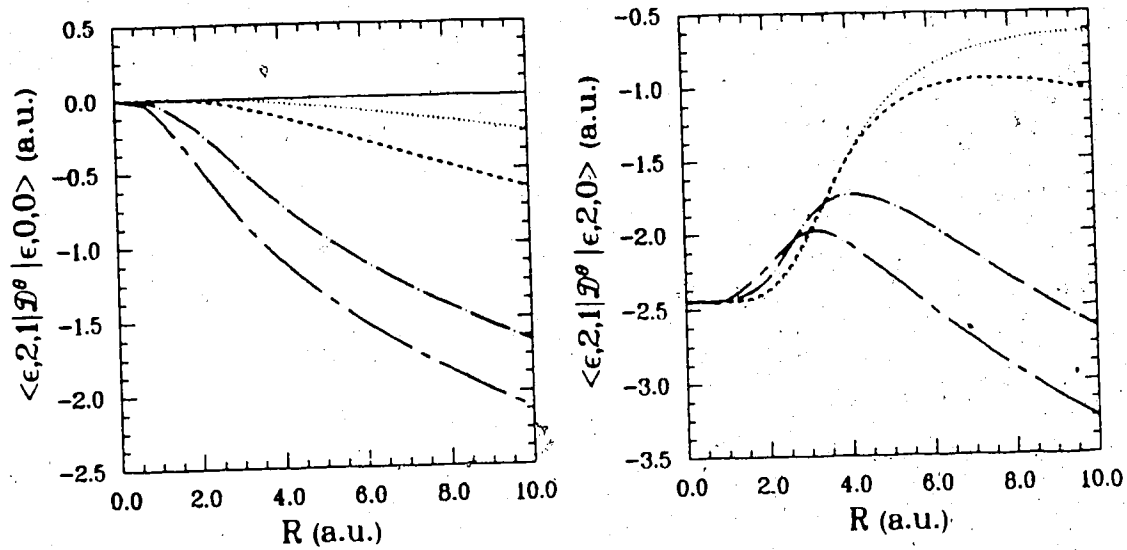


Figure 6 - 16 : $\langle \mathcal{D}^0 \rangle$ and $\langle \mathcal{D}^R \rangle$ vs. R

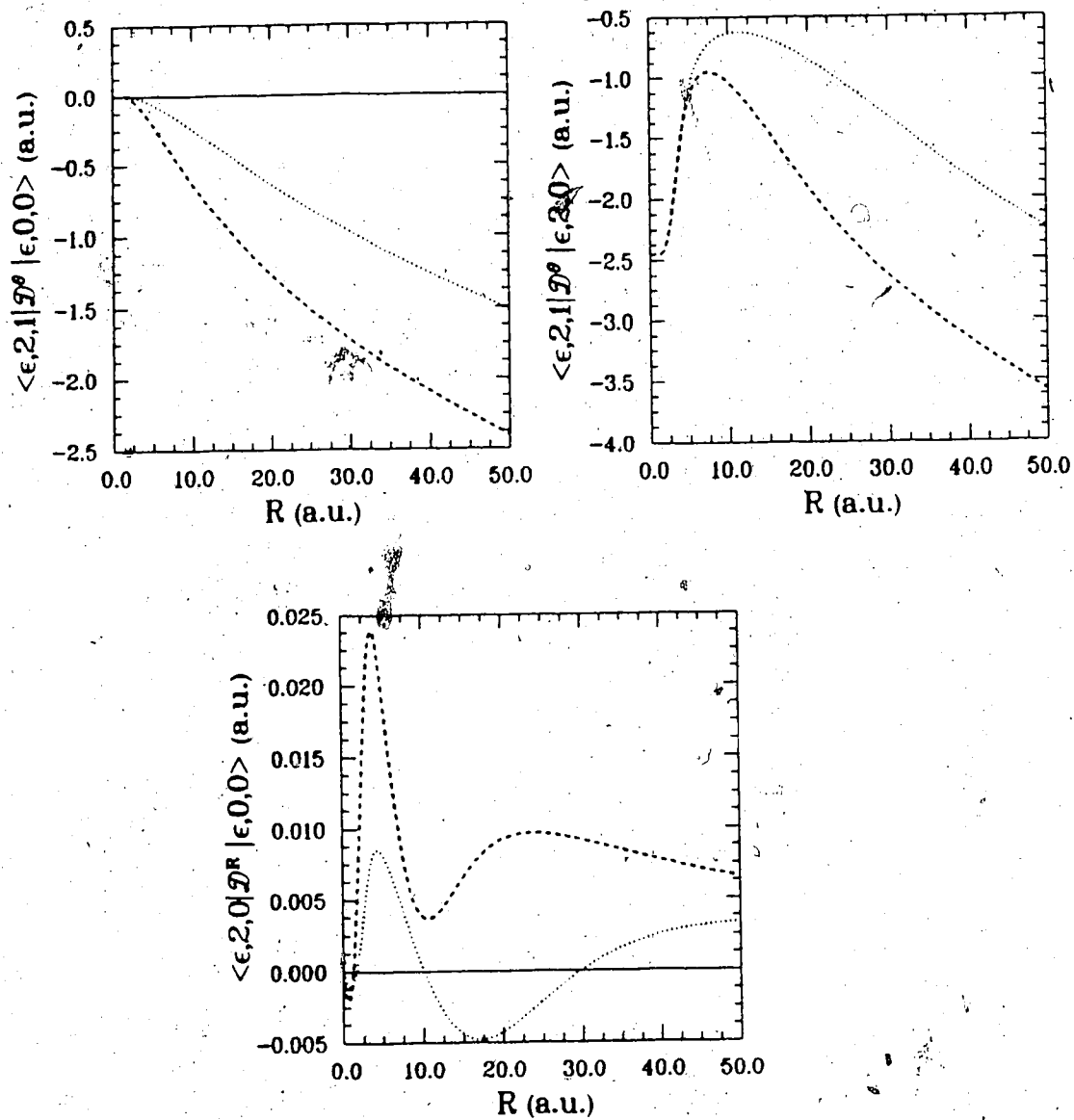


Figure 6 - 17 : $\langle \mathcal{D}^\theta \rangle$ and $\langle \mathcal{D}^R \rangle$ vs. R

In Figures 6 - 12, 6 - 15 and 6 - 17 the curves are as follows.

..... $\epsilon'(or \epsilon) = 0.045 \text{ a.u.}$

----- $\epsilon'(or \epsilon) = 0.150 \text{ a.u.}$

In obtaining the actual angular coupling matrix elements one must multiply the matrix element calculated here by a factor $1/R^2$ which makes the seemingly long range of the angular couplings shorter. In obtaining the actual angular coupling matrix element one must multiply the matrix element calculated here by a factor $1/R^2$ which makes the apparently long range of the angular coupling matrix elements shorter.

6.8 Discussion

As seen in the figures the numerators of the principal parts of the non-adiabatic coupling matrix elements are smooth analytic functions of the continuum energy. In most cases they are sufficiently slowly varying so that over a packet width they can be approximated by their values at the average packet energies. One can go beyond this "constant approximation" by fitting a linear or quadratic polynomial in (ϵ' and ϵ) over packet width and using it in the derivation for \mathcal{G} .

As seen in the figures the qualitative R -dependence of the matrix elements depends on the symmetry of the two states involved. At large R the limiting R -behavior is of the form $\zeta R^\rho \exp(-\varpi R)/(ln R)^\iota$ in every case where this has been attained for an element where ζ , ρ , ϖ and ι are parameters. The range of a matrix element increases with decreasing energy difference.

A relative large portion (say 30-50%) of the computer time spent to evaluate a matrix element is taken up by the integration from $\xi = 1 \rightarrow \xi_0$. This time can be drastically reduced by taking advantage of the power series representations of χ . Then the contribution to the ξ -integral in the range $1 \leq \xi \leq$

a sum of the product of state independent integrals (which have to be done only once) and power series coefficients.

7. SUMMARY

In the classical trajectory formulation of an atomic collision the nuclei are assumed to move in a predetermined classical trajectory which makes the molecular electronic potential time dependent. To describe the electronic dynamics one solves the time dependent Schrödinger equation. In conventional close-coupling formulations, expansion of the electronic wave function in a finite set of square-integrable basis functions and substitution in the Schrödinger equation leads to a set of coupled differential equations for the expansion coefficients (the probability amplitudes of the basis states) which must be solved with some initial condition. *Conservation* of probability within the expansion basis is an important feature of such a calculation. From a practical point of view it is desirable to keep the number of basis functions to a minimum. Physical insight is helpful in achieving this goal. In a *slow* atomic collision one may imagine the collision partners to form a quasi molecule. Hence the set of molecular states forms an appropriate basis to describe such a collision.

However, problems arise if a description of the electronic continuum is required. Conventionally the continuum is described using a finite set of pseudostates, which can represent it at most locally. However, an ionized electron must eventually move to "infinity". Hence the conservation of probability within the finite square-integrable basis is physically unacceptable if ionization is an open channel. In a correct theory one must allow the probability to escape from the (well localized) pseudostates.

Mathematically the defect in the coupled states method described above is the assumption that a *finite* set of square-integrable basis states is complete to describe the electronic wave function over the *infinite* electronic coordinate

space. This can be avoided by abandoning the solution of the full time dependent Schrödinger equation (over all space) and constructing the propagator of the system within the chosen basis set. A derivation of an equation for such a propagator for a one-electron-two-nucleus system is presented in Chapter 2. The derivation is based on the projection of the total propagator of the system onto an entirely discrete molecular basis using a set of physical and mathematical assumptions. The projected propagator describes the time evolution of the collision system within a limited region of physical space, viz. the interaction region, and allows the probability to escape from the pseudostates. Transitions among the basis states are caused by the *non-adiabatic* couplings. This formulation is suitable to describe slow atomic collisions (centre of mass collision energy $< 9 \text{ keV/amu}$).

In this treatment the electronic continuum is described by a set of *molecular wave packets*. They are square-integrable and are linear superpositions of molecular continuum states over certain energy intervals which we call the packet widths. Chapter 4 is a study of these wave packets. We have developed a scheme to calculate the packet widths so that the packets are well localized within the interaction region. A consequence of this scheme is that the number of wave packets required to cover a given continuum energy range increases with the increasing size of the interaction region.

It is shown that the wave packets are centred at the centre of charge of the nuclei and remain molecular in character even at large internuclear separations. Apparently they do not decompose into simple linear combination of atomic wave packets (This behavior is seen in molecular continuum states too. See Chapter 3). This is in sharp contrast to the behavior of molecular bound states which become atomic bound states (or simple linear combinations of them). Recent classical trajectory Monte Carlo calculations and preliminary results of a large scale close-coupling calculation on $\text{H}^+ + \text{H}(1s)$ collision system at low energies have shown

that the ionized electron has a high probability around the centre of charge of the nuclei. Hence the wave packets are appropriate to describe the ionized electron.

Chapter 3 is concerned with the efficient generation of molecular continuum states. The differential equation satisfied by the one-electron-two-nucleus molecular states is separable in prolate spheroidal coordinates. The angular wave function can be generated and stored efficiently in a power series form. We have represented the radial wave function in phase-amplitude form. Generation of the radial wave function in this representation is much more efficient than the direct numerical integration of the radial equation because the amplitude (and the phase) function is a smooth slowly varying function of the radial variable while the radial wave function itself is oscillatory (phase-amplitude representation has some conceptual advantages which has been utilized in Chapter 4). By fitting a simple algebraic function to the amplitude (and phase) we have developed a global representation for the molecular continuum states. This enables efficient and accurate regeneration of these wave functions for non-adiabatic coupling matrix element calculations.

Effective non-adiabatic couplings between two wave packets can be deduced from the non-adiabatic coupling between two molecular continuum states provided the latter has a certain analytical structure. This structure is rigorously established in Chapter 5 by extending the Hellmann-Feynman theorem to molecular continuum states. In Chapter 6 we have numerically evaluated these couplings which can be used with the known bound-bound and bound-continuum couplings to solve the new equation for the projected propagator.

The conceptual and the analytical work presented in this thesis are generally valid for a slow collision of any one-electron-two-nucleus system. The numerical results reported are for the particular system $H^+ + H$.

Further work on applications of the new formulation to the problem of ionization in proton-H-atom collisions, for example, would require as the next step the *solution* of the close-coupled integral equations using the couplings and packet states considered in this thesis. This next stage lies beyond the scope of this thesis, but a few comments about it are appropriate.

- (1) The radius of the "interaction region" (which dictates the selection of packet widths and the resulting choice of basis set to describe the continuum) is not determined and actual calculations to determine stability of the results for various choices would be required. A second, related question is the problem of interpretation associated with the choice of the parameter R_{∞} at which the collision is hypothetically "over" (in the sense that transitions to the continuum from bound states are no longer occurring).
- (2) An alternative interpretation of the formalism would be to select packet widths so small that the interaction region spanned is very large and the associated effects of escape are nearly negligible over a rather long time scale; one could then monitor the evolution of the continuum electrons within the space spanned and learn something about its actual behavior by replacing the decay factors with unity, which leads to the conventional (probability-conserving) close-coupled formulation. Of course the difficulty with such a computation is its enormous cost; the intent of the present formulation is to construct a scheme which can achieve the same results more economically.
- (3) A problem which the close coupling theory described here does not address is the calculation of ionization amplitudes in detail. Solution of close-coupled equations including the packet states and with the escape

effects included would describe the wave function within the interaction region for all times, but give no detailed account of the fate of the escaped amplitudes. The intent of the theory is that a different scheme be used to study subsequent continuum evolution, but we have not considered that question in this thesis.

FOOTNOTES

1. One uses standard potential scattering techniques in treating elastic scattering. See, for example Chapter 8 of reference 1.
2. Apparently the classical trajectory method was first suggested by Mott [27a] in 1931; theoretical justifications for its use came after 1961.
3. In the intermediate energy domain there is a region where neither atomic nor molecular state expansions are clearly preferable. Some recent work has attempted to handle such collisions using a combination of atomic and molecular states [21] or a combination of atomic and united atom states [22], to gather advantages from both types of expansion basis.
4. We should remind the reader that the condition of validity of the classical trajectory description does not necessarily mean that the collision is fast and there is a region where one can use the molecular basis to expand $\Upsilon(\vec{r}, t)$.
5. Molecular states are in one-to-one correspondence with gerade/ungerade combinations of atomic states if $A \equiv B$.
6. Angular coupling is some times called the Coriolis coupling since it can be viewed as the quantum mechanical counterpart of the classical Coriolis interaction.
7. In equations (1 - 12), adiabatic basis functions are expressed in a space-fixed reference frame. Actual calculations are done in a rotating molecular fixed reference frame. This point is discussed more fully in Chapter 5.
8. For homonuclear systems they used a much more complicated formula to construct travelling molecular orbitals.
9. Another problem encountered in these techniques during the integration of the differential equations is the singularities in the potential at the nuclei. Though

not formally quite acceptable, at present it is simply avoided by choosing the space grid so that no points coincide with the nuclei.

10. Sturmian radial functions are the solutions of the hydrogenic radial equation

$$\left(-\frac{\hbar^2}{2m_0} \frac{d}{dr^2} + \frac{l(l+1)}{2m_0 r^2} - \frac{\alpha_{nl}(\epsilon)}{r} \right) S_{nl}(\epsilon; r) = \epsilon S_{nl}(\epsilon; r)$$

but ϵ is an assigned (arbitrary) parameter and $\alpha_{nl}(\epsilon; r)$ is the eigenvalue. They are scaled hydrogenic functions.

$$S_{nl}(\epsilon; r) = \sqrt{\alpha_{nl}(\epsilon; r)} R_{nl}(\alpha_{nl}(\epsilon; r)r)$$

ϵ can be selected to give useful scalings. Sturmians form a complete set and have most of their density in a more compact region than do hydrogenic states.

11. Gallaher *et al.* explicitly calculated and subtracted the oscillatory terms to obtain acceptable cross sections.
12. Recently such Sturmian expansions have been used to study the $\text{He}^{2+} + \text{H}$ and $\text{H}^+ + \text{He}^+$ collisions [37], and $\text{H}^+ + \text{He}^+$ and $\text{H}^+ + \text{Li}^{2+}$ collisions [8].
13. They are L^2 -type functions of the form

$$\left(\frac{2}{R} \right)^{\frac{2}{3}} \exp\left(-\frac{\xi-1}{2a} \right) (\xi^2 - 1) L_n^m \left(\frac{\xi-1}{a} \right) P_l^m(\eta) \cos(m\phi)$$

where (ξ, η, ϕ) are the prolate spheroidal coordinates of \vec{r} , (nlm) are three pseudoquantum numbers, L_n^m are Laguerre polynomials and P_l^m are the associated Legendre polynomials.

14. A similar general solution has been reported in references 67.
15. If a fully quantum mechanical description of the collision is used, time does not appear in the formalism, but it can still be shown that transitions arise from the same formal coupling matrix elements $i\hbar \langle k'; R | \vec{\nabla}_R | k; R \rangle$ (with ETF corrections) as appear here. Cf. for example reference 13.

16. There are other, much smaller effects. If these are of interest, a fully quantum mechanical formalism, along the lines suggested in reference 13, and allowing for different switching functions for different adiabatic states, should be used, since a classical trajectory description entails approximations comparable to the neglect of these effects. Within the classical trajectory approximation, the inclusion of the ETF corrections as indicated here is the main result. (See reference 80 for an extended discussion)
17. This simple form is strictly appropriate only for charge symmetric systems like H_2^+ ($Z_A = Z_B$), where GC coincides with the centre of positive charge. It can be shown [82,83] that in the united-atom limit $R \rightarrow 0$ there should be an additional term which "corrects" the limiting reference origin from GC to the centre of charge.
18. If different $f_k(\vec{r}, R)$ are used for each $\psi_k(\vec{r}, R)$, the basis states become slightly nonorthogonal for increasing collisional velocities and the nonadiabatic couplings \mathbf{P} , \mathbf{A} also exhibit velocity-dependence. Cf. reference 80 for a discussion of the modified formalism (for bound states) in a classical trajectory description. In the calculations of reference 20, it has been shown that effects of such velocity-dependence become significant only for collision energies $E > 7 - 10 \text{ keV/amu}$.
19. Recent preliminary studies by Dr. M. Kimura (private communication), and work currently continuing in this laboratory show that nonadiabatic bound-to-continuum couplings based on the universal switching functions of reference 82 are more numerous, larger and have longer range than those for state-optimized f_k 's, and that continuum-continuum couplings are even more badly behaved (they oscillate vs. R).

BIBLIOGRAPHY

1. B.H.Brandsen, **Atomic Collision Theory**, 2nd edition, The Benjamin Cummings Publishing Company, 1983, Chapters 8 and 10.
2. B.H.Brandsen, *Adv. Atom. Molec. Phys.* **15**, 263, (1979)
3. C.J.Joachain, *NATO ASI Series B, Physics Vol.* **101**, 139 (1983)
4. J.F.Reading and A.L.Ford, *J. Phys.* **B12**, 1367, (1979)
5. Robin Shakeshaft, *Phys. Rev.* **A18**, 1930, (1978)
6. W.Fritsch and C.D.Lin, *Phys. Rev.* **A27**, 3361, (1983)
7. T.G.Winter and C.D.Lin, *Phys. Rev.* **A29**, 3071, (1984)
8. T.G.Winter, *Phys. Rev.* **A33**, 3842, (1986)
9. T.Mukoyama, C.D.Lin and W.Fritsch, *Phys. Rev.* **A32**, 2490, (1985)
10. (a) J.C.Bellum and D.A.Micha, *Phys. Rev.* **A18**, 1435, (1978)
(b) L.R.Relyea and D.A.Micha, *Int. J. Quantum Chemistry* **S13**, 569. (1979)
11. D.A.Micha and R.D.Piacentini, *Phys. Rev.* **A25**, 204, (1982)
12. W.R.Thorson and G.Bandarage, *Phys. Rev.* **A000**, (1987): (In press)
13. J.B.Delos, *Rev. Mod. Phys.* **53**, 287, (1981)
14. (a) M.E.Riley, *Phys. Rev.* **A7**, 626, (1973)
(b) R.E.Turner, *Phys. Rev.* **A26**, 3155, (1982)
15. D.R.Bates and D.S.F.Crothers, *Proc. Roy. Soc. London*, **A315**, 465 (1970)
16. M.H.Mittleman, *Phys. Rev.* **122**, 499, (1961)
17. (a) J.B.Delos, W.R.Thorson and S.K.Knudson, *Phys. Rev.* **A6**, 709, (1972)
(b) J.B.Delos and W.R.Thorson, *Phys. Rev.* **A6**, 720, (1972)
18. S.K.Knudson and W.R.Thorson, *Can. J. Phys.* **48**, 313, (1973)
19. V.SethuRaman, W.R.Thorson and C.F.Lebeda, *Phys. Rev.* **A8**, 1316, (1973)
20. M.Kimura and W.R.Thorson, *Phys. Rev.* **A24**, 1780, (1981)

21. (a) T.G.Winter and N.F.Lane, Phys. Rev. **A31**, 2698, (1985)
(b) M.Kimura and C.D.Lin, Phys. Rev. **A32**, 1357, (1985)
22. T.G.Winter and C.D.Lin, Phys. Rev. **A29**, 567, (1984)
23. A.Messiah, **Quantum Mechanics**, Vol. 2, (Amsterdam; North Holland Publ. Co., 1965) p747
24. H.S.W.Massey, Rep. Prog. Phys. **12**, 248, (1949)
25. (a) W.Lichten, Phys. Rev. **131**, 131, (1967)
(b) R.K.Janev, Adv. Atom. Molecular Phys. **12**, 1 (1976)
26. M.Kimura, Ph.D Thesis, University of Alberta, Edmonton, Canada (1981)
27. (a) N.F.Mott, Proc. Camb. Phil. Soc. **27**, 553, (1933)
(b) N.F.Mott and H.S.W.Massey, **Theory of Atomic Collisions**, 3rd ed. (Oxford; Clarendon Press, 1965) p428
28. J.D.Power, Phil. Trans. Roy. Soc. (London) **A274**, 1246, (1973)
29. H.Rosenthal, Phys. Rev. Lett. **27**, 635, (1971)
30. (a) J.Rankin and W.R.Thorson, Phys. Rev. **A18**, 1990, (1978)
(b) J.Rankin, Ph.D Thesis, University of Alberta, Edmonton Canada (1978)
31. (a) W.R.Thorson and J.B.Delos, Phys. Rev. **A18**, 117, (1978)
(b) W.R.Thorson and J.B.Delos, Phys. Rev. **A18**, 135, (1978)
32. D.R.Bates and R.McCarrol, Proc. Roy. Soc. **A245**, 175, (1958)
33. S.B.Schneiderman and A.Russek, Phys. Rev. **181**, 311, (1969)
34. C.F.Lebeda and W.R.Thorson, Phys. Rev. **A4**, 900, (1971)
35. D.F.Gallher and L.Wilets, Phys. Rev. **169**, 139, (1968)
36. I.M.Cheshire, D.F.Gallaher and A.J.Taylor, J. Phys. **B3**, 813, (1970)
37. T.G.Winter, Phys. Rev. **A25**, 697, (1982)
38. (a) J.H.Weiner and Y.Partom, Phys. Rev. **187**, 1134, (1969)
(b) J.H.Weiner and A.Askar, J. Chem. Phys. **54**, 3534, (1971)

39. (a) N.Grün, A.Mühlhans and W.Scheid, J. Phys. **B15**, 4043, (1982)
- (b) G.Terlecki, N.Grün and W.Scheid, J Phys. **B17**, 3719, (1984)
- (c) K.S.Sandhya Devi, J.D.Garcia and N.H.Kwong, **XIV ICPEAC Invited Papers**, editors D.C.Lorents, W.E.Meyerhof and J.R.Peterson (North Holland publ. Co., 1985) p263
40. M.Horbatsch, J. Phys. **B17**, 2591, (1984)
41. (a) W.R.Thorson and H.Levy II, Phys. Rev. **181**, 232, (1969)
- (b) H.Levy II and W.R.Thorson, Phys. Rev. **181**, 244, (1969)
42. (a) R.D.Taylor and J.B.Delos, Proc. Roy. Soc. **A379**, 179, (1982); *ibid* 209
- (b) T.S.Wang and J.B.Delos, Phys. Rev. **A29**, 542, (1984); *ibid* 552
- (c) M.L.Du and J.B.Delos, Phys. Rev. **A33**, 2294, (1986)
43. (a) R.Shakeshaft, J. Phys. **B8**, 1114, (1975)
- (b) R.Shakeshaft, Phys. Rev. **A14**, 1626, (1976)
44. W.H.Bassichis, J.F.Reading and R.R.Scheerbaum, Phys. Rev. **C11**, 316, (1975)
45. W.Fritch and C.D.Lin, J. Phys. **B15**, 1255, (1982)
46. (a) D.G.M.Anderson, M.J.Antal and M.B.McElroy, J. Phys. **B7**, L118, (1974)
- (b) M.J.Antal, M.B.McElroy and D.G.M.Anderson, J. Phys. **B9**, 1513, (1975)
47. C.D.Lin, T.G.Winter and W.Fritsch, Phys. Rev. **A25**, 2395, (1982)
48. H.J.Lüdde and R.M.Dreizler, J. Phys. **B15**, 2703, (1982)
49. W.P.Reinhardt, Comp. Phys. Communications **17**, 1, (1979)
50. J.F.Reading, A.L.Ford, G.L.Swofford and A.Fitchard, Phys. Rev. **A20**, 130, (1979)
51. (a) W.R.Thorson, Nucl. Instr. and Methods, **214**, 97, (1983)
- (b) W.R.Thorson and J.H.Choi, Phys. Rev. **A30**, 743, (1984)
52. I.S.GradshTEyn and I.M.Ryzhik, **Table of Integrals, Series and Products**, (4th ed, Academic Press, 1980)

53. M. Abramowitz and I. A. Stegun, **Hand-book of Mathematical Functions**, (Dover N.Y)
54. George A. Gibson, **Advanced Calculus**, (Macmillan and Co. Ltd., London 1948) Chapter 12.
55. O. Burran, K. Danske. Videnk. Selsk. Skr. **7**, 14, (1927)
56. D. R. Bates and T. R. Carson, Proc. Roy. Soc. London. **A234**, 207, (1956)
57. E. W. Leaver, J. Math. Phys. **27**, 1238, (1986)
58. L. I. Ponomarev and L. N. Somov, J. Comput. Phys. **20**, 183, (1976)
59. D. R. Bates, U. Opic and G. Poots, Proc. Phys. Soc. **A66**, 1113, (1953)
60. J. Rankin and W. R. Thorson, J. Comput. Phys. **32**, 437, (1979)
61. J. K. Cayford, W. R. Fimple, D. G. Unger and S. P. White, J. Comput. Phys. **16**, 259, (1974)
62. P. T. Greenland and W. Greiner, Theo. Chim. Acta. **42**, 273, (1976)
63. W. E. Milne, Phys. Rev. **35**, 863, (1930)
64. (a) W. I. Newman and W. R. Thorson, Phys. Rev. Lett. **29**, 1350, (1972)
(b) W. I. Newman and W. R. Thorson, Can. J. Phys. **50**, 2997; (1972) and references therein.
65. H. J. Krosh and H. Laurent, J. Phys. **B14**, 4213, (1981)
66. J. A. Wheeler, Phys. Rev. **52**, 1123, (1937)
67. (a) C. J. Eliezer and A. Gray, SIAM J. Appl. Math. **30**, 463, (1946)
(b) J. R. Ray and J. L. Read, J. Math. Phys. **21**, 1583, (1980)
68. E. T. Whittaker and G. N. Watson, **A Course of Modern Analysis**, 4th ed., (Cambridge University Press, 1927) p194
69. D. I. Abramov, A. Ya. Kazakov, L. I. Ponomarev, S. Yu. Somov and L. N. Somov, J. Phys. **B12**, 1761, (1979)
70. P. M. Morse and H. Feshbach, **Methods of Theoretical Physics**, Vol. 1 (McGraw-Hill Book Company, 1953) p437

71. J.A.Richard and F.P.Larkins, J. Phys. B19, 1945, (1986)
72. J.P.Dahl and X.Feng, Theo. Chim. Acta. 66, 261, (1984)
73. G.H.Wannier, Phys. Rev. 90, 817, (1953)
74. H.Klar, Z. Phys. A307, 75, (1982)
75. R.E.Olson, Phys. Rev. A33, 4397, (1986)
76. P.W.Langhoff, **Electron-Molecule and Photon- Molecule Collisions**, Editors T.Rescigno, V.Mckoy and B.Schneider. (Plenum Press, NY, 1979) p. 183.
77. (a) M.P.Faifman, L.I.Ponomarev and S.I.Vinitsky, J. Phys. B9, 2255, (1976)
(b) L.I.Ponomarev, T.P.Puzynina and L.N.Somov, J. Phys. B10, 1335, (1978)
(c) L.I.Ponomarev, T.P.Puzynina and N.F.Truskova, J. Phys. B11, 3861, (1978)
(d) D.I.Abramov, S.Yu.Slavyanov and L.N.Somov, J. Phys. B13, 4717, (1980)
78. F.R.Vukajilovic and N.F.Truskova, Sov. J. Nucl. Phys. 32, 62, (1980)
79. L.I.Ponomarev, S.Yu.Slavyanov and L.N.Somov, J. Phys. B13, 3797, (1980)
80. J.B.Delos and W.R.Thorson, J. Chem. Phys. 70, 1774, (1979)
81. (a) M.Kimura and W.R.Thorson, Phys. Rev. a24, 3019, (1981)
(b) M.Kimura and W.R.Thorson, J. Phys. B16, 1471, (1983)
82. J.Vaaben and K.Taulbjerg, J. Phys. B14, 1815, (1981)
83. W.R.Thorson, M.Kimura, J.H.Choi and S.K.Knudson, Phys. Rev. A24, 1768, (1981)
84. (a) J.C.Slater, **Quantum Theory of molecules and solids**, Vol. 1, (McGraw Hill, NY, 1963) Appendix-2.
(b) Claude Cohen-Tonnoudji, Bernard Diu and Frank Laloe, **Quantum Mechanics**, Vol. 2, (John Wiley and sons, 1969) p 1192.
85. Y.L.Luke, **Algorithms for the Computation of Mathematical Functions**, (Academic Press, N.Y., 1977) p159 and p252

86. R. Bulirsch and J. Stoer. Numer. Math. 8, 1, (1966)

APPENDIX - A

We derive the useful equations (A - 9), (A - 10), (A - 14) and (A - 15) involving integrals over adiabatic continuum angular wave functions (at the same internuclear separation).

The angular wave function satisfies equation (3 - 3):

$$\frac{d}{d\eta} \left[(1 - \eta^2) \frac{dS(\epsilon l' m; R; \eta)}{d\eta} \right] + \left[p\eta - \frac{1}{2} \epsilon R^2 \eta^2 + A_{l'm}(\epsilon, R) - \frac{m^2}{1 - \eta^2} \right] S(\epsilon l' m; R; \eta) = 0 \quad (A - 1)$$

Here $A_{l'm}(\epsilon, R)$ is the same as the separation constant A in Chapter 3.

Since equation (A - 1) is a Sturm-Liouville equation [70], if ϵ , R and m are kept constant, then the bound solutions belonging to different $A_{l'm}(\epsilon, R)$ (i.e. different l) are orthogonal; they are also normalizable.

$$\beta_0(\epsilon l' m; \epsilon l m) = \delta_{l'l} \quad (A - 2)$$

where

$$\beta_n(k'; k) = \int_{-1}^{+1} d\eta \eta^n S(k'; R; \eta) S(k; R; \eta) \quad (A - 3)$$

Define

$$S_\epsilon(\epsilon l m; \eta, R) = \left(\frac{\partial S(\epsilon l m; R; \eta)}{\partial \epsilon} \right)_{\eta, R} \quad (A - 4)$$

$$\beta_\epsilon(k'; k) = \int_{-1}^{+1} d\eta S(k'; R; \eta) S_\epsilon(k; R; \eta) \quad (A - 5)$$

The differential equation satisfied by S_ϵ can be obtained by differentiating equation

(A-1)

$$\frac{d}{d\eta} \left[(1-\eta^2) \frac{dS_\epsilon(\epsilon lm; R; \eta)}{d\eta} \right] + \left[p\eta - \frac{1}{2} \epsilon R^2 \eta^2 + A_{lm}(\epsilon, R) - \frac{m^2}{1-\eta^2} \right] S_\epsilon(\epsilon lm; R; \eta) - \left[\frac{1}{2} R^2 \eta^2 - \frac{\partial A_{lm}(\epsilon, R)}{\partial \epsilon} \right] S(\epsilon lm; R; \eta) = 0 \quad (A-6)$$

The physical angular wave function must be well behaved in energy; hence

$$|S_\epsilon(\epsilon lm; R; \eta = \pm 1)| < \infty \quad (A-7)$$

Multiplying equation (A-1) by S_ϵ and (A-6) by S and subtracting the former from the latter and integrating over η we obtain

$$(A_{lm}(\epsilon, R) - A_{l'm}(\epsilon, R)) \beta_\epsilon(\epsilon l' m; \epsilon lm) - \frac{1}{2} R^2 \beta_2(\epsilon l' m; \epsilon lm) + \frac{\partial A_{lm}(\epsilon, R)}{\partial \epsilon} \beta_0(\epsilon l' m; \epsilon lm) = 0 \quad (A-8)$$

Case 1: $l' = l$

In this case the first term in equation (A-8) vanishes. Then using equation (A-2) we obtain

$$\frac{\partial A_{lm}(\epsilon, R)}{\partial \epsilon} = \frac{1}{2} R^2 \beta_2(\epsilon lm; \epsilon lm) \quad (A-9)$$

Case 2: $l' \neq l$

Using equations (A-2) and (A-8) we obtain

$$\beta_\epsilon(\epsilon l' m; \epsilon lm) = \frac{R^2 \beta_2(\epsilon l' m; \epsilon lm)}{2(A_{lm}(\epsilon, R) - A_{l'm}(\epsilon, R))} \quad (A-10)$$

To derive the other two expressions define

$$S_R(\epsilon lm; R; \eta) = \left(\frac{\partial S(\epsilon lm; R; \eta)}{\partial R} \right)_{\eta, \epsilon} \quad (A-11)$$

$$\beta_R(k'; k) = \int_{-1}^{+1} d\eta S(k'; R; \eta) S_R(k; R; \eta) \quad (A-12)$$

For the physical solution S , S_R must satisfy

$$|S_R(\epsilon l m; R; \eta = \pm 1)| < \infty \quad (A-13)$$

Differentiating equation (A-1) with respect to R and using similar methods as described above we can obtain

$$\frac{\partial A_{lm}(R)}{\partial R} = \epsilon R \beta_2(\epsilon l m; \epsilon l m) - \frac{p}{R} \beta_1(\epsilon l m; \epsilon l m) \quad (A-14)$$

$$\beta_R(\epsilon l' m; \epsilon l m) = \left[\frac{\epsilon R \beta_2(\epsilon l' m; \epsilon l m) - (p/R) \beta_1(\epsilon l' m; \epsilon l m)}{A_{lm}(\epsilon, R) - A_{l'm}(\epsilon, R)} \right] (1 - \delta_{l'l}) \quad (A-15)$$

Once the angular wave functions are calculated in a global representation, β_n can be evaluated readily. Hence one can use equations (A-9), (A-10), (A-14) and (A-15) to calculate $\partial A / \partial \epsilon$, β_ϵ , $\partial A / \partial R$ and β_R .

APPENDIX - B

We derive the useful equation (B - 9) an integral of the radial wave functions (at the same internuclear separation).

Define the auxiliary radial wave function

$$\phi(\epsilon l m; R; \xi) = \sqrt{\xi^2 - 1} \chi(\epsilon l m; R; \xi) \quad (B - 1)$$

Equation (3 - 4) gives

$$\frac{d^2 \phi(\epsilon' l' m; R; \xi)}{d\xi^2} + \frac{1}{\xi^2 - 1} \left[q\xi + (c')^2 \xi^2 - A_{l'm}(\epsilon'; R) + \frac{(1 - m^2)}{\xi^2 - 1} \right] \phi(\epsilon' l' m; R; \xi) = 0 \quad (B - 2)$$

Then we obtain

$$\begin{aligned} \frac{d^2 (g(\xi) \phi(\epsilon l m; R; \xi))}{d\xi^2} &+ \frac{1}{\xi^2 - 1} \left[q\xi + c^2 \xi^2 - A_{lm}(\epsilon, R) + \frac{(1 - m^2)}{\xi^2 - 1} \right] g(\xi) \phi(\epsilon l m; R; \xi) \\ &= 2 \frac{dg(\xi)}{d\xi} \frac{d\phi(\epsilon l m; R; \xi)}{d\xi} + \frac{d^2 g(\xi)}{d\xi^2} \phi(\epsilon l m; R; \xi) \end{aligned} \quad (B - 3)$$

Here g is the convergence factor $\exp(-\alpha \xi)$ described in Chapter 5.

Multiply equation (B - 3) by $\phi(\epsilon' l' m; R; \xi)$ and (B - 2) by $\phi(\epsilon l m; R; \xi)$, subtract the latter from the former, integrate over ξ and take the limit $\alpha \rightarrow 0^+$.

Then

$$\begin{aligned} (c^2 - (c')^2) \gamma_2(\epsilon' l' m; \epsilon l m) - (A_{lm}(\epsilon, R) - A_{l'm}(\epsilon', R)) \gamma_0(\epsilon' l' m; \epsilon l m) \\ = \lambda_1(0^+) + \lambda_2(0^+) \end{aligned} \quad (B - 4)$$

where

$$\gamma_n(k'; k) = \lim_{\alpha \rightarrow 0^+} \int_1^{\infty} d\xi \xi^n \exp(-\alpha \xi) \chi(k'; R; \xi) \chi(k; R; \xi) \quad (B-5)$$

$$\lambda_1(\alpha) = -2\alpha \int_1^{\infty} d\xi \exp(-\alpha \xi) \phi(\epsilon' l' m; R; \xi) \frac{d\phi(\epsilon l m; R; \xi)}{d\xi} \quad (B-6)$$

$$\lambda_2(\alpha) = \alpha^2 \int_1^{\infty} d\xi \exp(-\alpha \xi) \phi(\epsilon' l' m; R; \xi) \phi(\epsilon l m; R; \xi) \quad (B-7)$$

One can study $\lambda_i(\alpha)$ using the techniques developed in Chapter 5. Then

$$\lambda_1(0^+) = \begin{cases} 0 & \text{if } \epsilon' \neq \epsilon \\ -\tilde{a}_1 \tilde{a}_2 \sin(\Lambda' - \Lambda) & \text{if } \epsilon' = \epsilon \end{cases} \quad (B-8a)$$

$$\lambda_2(\alpha) = 0 \quad (B-8b)$$

Here Λ' and Λ are the phase shifts and, \tilde{a}_i are the normalization constants ($= 2/\sqrt{\pi R}$). Hence we have

$$\gamma_0(\epsilon' l' m; \epsilon l m) = \begin{cases} \frac{(\epsilon - \epsilon') R^2 \gamma_2(\epsilon' l' m; \epsilon l m)}{2 (A_{lm}(\epsilon, R) - A_{l'm}(\epsilon', R))} & \text{if } \epsilon' \neq \epsilon \\ \frac{\tilde{a}_1 \tilde{a}_2 \sin(\Lambda' - \Lambda)}{(A_{lm}(\epsilon, R) - A_{l'm}(\epsilon, R))} & \text{if } l' \neq l \text{ and } \epsilon' = \epsilon \end{cases} \quad (B-9)$$

It is worth noting that one can use the second case of equation (B-9) to evaluate the improper integral γ_0 (of an oscillatory integrand) using the relatively easily calculable quantities A and Λ .

APPENDIX - C

We prove that the contribution to an integral coming from a point where the integrand has a logarithmic singularity is zero, viz.

$$X = \lim_{\delta \rightarrow 0^+} \int_{-\delta}^{+\delta} dx f(x) \ln(bx) = 0$$

with $b \neq 0$ and $f(x)$ well behaved at $x = 0$. It is quite straightforward to see that

$$X = f(0) \lim_{\delta \rightarrow 0^+} Y(\delta) \quad (C-1)$$

where

$$Y(\delta) = \int_{-\delta}^{+\delta} dx \ln(bx)$$

By definition of improper integrals

$$Y(\delta) = \lim_{\epsilon_- \rightarrow 0^-} Y_-(\delta) + \lim_{\epsilon_+ \rightarrow 0^+} Y_+(\delta) \quad (C-2)$$

With

$$Y_{\pm}(\delta) = \pm \int_{\epsilon_{\pm}}^{\pm\delta} dx \ln(bx)$$

Integration by parts gives

$$Y_{\pm}(\delta) = \pm (\pm\delta \ln(\pm b\delta) - \epsilon_{\pm} \ln(b\epsilon_{\pm}) \mp \delta + \epsilon_{\pm})$$

We know that

$$\lim_{\alpha \rightarrow 0} \alpha \ln(\alpha) = 0$$

Hence

$$\lim_{\epsilon_{\pm} \rightarrow 0^{\pm}} Y_{\pm}(\delta) = \delta \ln(\pm b\delta) - \delta \quad (C-3)$$

Equations (C - 2) and (C - 3) give

$$= n(\delta) - 2\delta + \delta \ln(-b^2)$$

which gives

$$\lim_{\delta \rightarrow 0^+} Y(\delta) = 0 \quad (C - 4)$$

Hence $X = 0$.

This proves that the area under an isolated logarithmic singularity is zero.

APPENDIX - D

We prove that the conditions

$$\lim_{r \rightarrow \infty} r^2 \psi_j(\vec{r}) = 0 \quad (D-1)$$

and

$$\lim_{r \rightarrow \infty} r \vec{r} \cdot \vec{\nabla}_{\vec{r}} \psi_j(\vec{r}) = 0 \quad (D-2)$$

are *sufficient* to make the one-electron-two-centre Hamiltonian Hermitian with respect to the well behaved functions ψ_i and ψ_j .

We have

$$\hat{h}_e = -\frac{\hbar^2}{2m_e} \vec{\nabla}_{\vec{r}}^2 + V(\vec{r}, R) \quad (D-3)$$

Define

$$X = \frac{2m_e}{\hbar^2} \left(\langle \hat{h}_e \psi_i | \psi_j \rangle - \langle \psi_i | \hat{h}_e \psi_j \rangle \right)$$

Then it follows that

$$X = \int dv \left[\psi_i^* \vec{\nabla}_{\vec{r}}^2 \psi_j - \psi_j \vec{\nabla}_{\vec{r}}^2 \psi_i^* \right] \quad (D-4)$$

Now consider a sphere of radius of "infinite" radius, centred at the origin and transform the *volume* integral (D-4) to a *surface* integral using Gauss' theorem.

$$X = \int_0^\pi d\theta \sin \theta \int_0^{2\pi} d\phi \left\{ \lim_{r \rightarrow \infty} \left[\psi_i^* (r \vec{r} \cdot \vec{\nabla}_{\vec{r}}) \psi_j - (r^2 \psi_j) \hat{r} \cdot \vec{\nabla} \psi_i^* \right] \right\}$$

If equations (D-1) and (D-2) hold, then

$$X = 0$$

Hence the result

$$\langle \hat{h}_e \psi_i | \psi_j \rangle = \langle \psi_i | \hat{h}_e \psi_j \rangle$$

Equations (D - 1) and (D - 2) are satisfied by bound adiabatic states since they die as $\exp(-ar)$. Thus \hat{h}_e is Hermitian with respect to two bound states or a bound and a continuum state. The Hamiltonian may not in general be Hermitian with respect to two continua.

APPENDIX - E

Orthonormality of continuum states (of any Hamiltonian) is usually assumed without proof. Here we rigorously derive the orthonormality relations of one-electron-two-centre continuum states and calculate the normalization constant. The mathematical techniques developed in Chapter 5 are used throughout. We denote $|\epsilon' l' m'; R\rangle$ by $\psi_{k'}$ and $|\epsilon l m; R\rangle$ by ψ_k and work in atomic units.

Azimuthal angular wave functions make two continuum states orthogonal if they have different m quantum numbers. Hence in what follows we consider the case $m' = m$.

Case 1: $\epsilon' \neq \epsilon$ One can easily show that

$$\hat{h}_\epsilon |\psi_k g\rangle = \epsilon \psi_k g - (\vec{\nabla} \psi_k) \cdot (\vec{\nabla} g) - \frac{1}{2} \psi_k (\vec{\nabla}^2 g) \quad (E-1)$$

where g is the convergence factor $\exp(-\alpha \xi)$.

Because \hat{h}_ϵ is Hermitian with respect to $\psi_{k'}$ and $\psi_k g$, multiplication of equation (E-1) on the left by $\langle \psi_{k'} |$ gives

$$(\epsilon' - \epsilon) \langle g \psi_{k'} | \psi_k \rangle = -\langle \psi_{k'} | (\vec{\nabla} \psi_k) \cdot (\vec{\nabla} g) \rangle - \frac{1}{2} \langle \psi_{k'} | \psi_k (\vec{\nabla}^2 g) \rangle \quad (E-2)$$

Expressing $\vec{\nabla}$ and $\vec{\nabla}^2$ in prolate spheroidal coordinates and doing some algebra we obtain

$$(\epsilon' - \epsilon) \langle g \psi_{k'} | \psi_k \rangle = -\frac{1}{4} R \beta_0(\epsilon' l' m; \epsilon l m) (\lambda_1(\alpha) + \lambda_2(\alpha)) \quad (E-3)$$

β_n and λ_i are as defined in equations (A-3), (B-6) and (B-7). In Appendix-B we have proved that $\lambda_i(0^+) = 0$ when $\epsilon' \neq \epsilon$. Hence in the limit $\alpha \rightarrow 0^+$, equation (A-3) gives

$$\langle \psi_{k'} | \psi_k \rangle = 0$$

Hence the continuum states are orthogonal if their energies are different.

Case 2: $\epsilon' = \epsilon (\neq 0)$

Directly integrating $g \psi_{k'}^* \psi_k$ over all space in prolate spheroidal coordinates and taking the limit $\alpha \rightarrow 0^+$ we obtain

$$\langle \psi_{k'} | \psi_k \rangle = \frac{R^3}{8} [\beta_0(\epsilon' l' m; \epsilon l m) \gamma_2(\epsilon' l' m; \epsilon l m) - \beta_2(\epsilon' l' m; \epsilon l m) \gamma_0(\epsilon' l' m; \epsilon l m)] \quad (E-4)$$

γ_n is as defined in equation (B-5).

Subcase 2a: $l' \neq l$

Substitute the values from equations (A-2) and (B-10) in equation (E-4).

$$\langle \psi_{k'} | \psi_k \rangle = \frac{\tilde{a}_1 \tilde{a}_2 \sin(\Lambda' - \Lambda)}{(A_{l'm}(\epsilon, R) - A_{lm}(\epsilon, R))} \beta_2(\epsilon' l' m; \epsilon l m) \quad (E-5)$$

In general $\sin(\Lambda' - \Lambda)$ and β_2 are non-zero. Hence the two continuum states are *non-orthogonal*.

Subcase 2b: $l' = l$

Using the techniques described in Chapter 5 we can easily prove that γ_0 is finite and γ_2 has a $\delta(\epsilon' - \epsilon)$ type singularity. Using equation (5-36b) and remembering that $\beta_0 = 1$ we obtain

$$\langle \psi_{k'} | \psi_k \rangle = \frac{\pi R}{4} \tilde{a}^2 \delta(\epsilon' - \epsilon) \quad (E-6)$$

Now we can set the normalization constant

$$\tilde{a} = \frac{2}{\sqrt{\pi R}} \quad (E-7)$$

so that combining the results of Cases 1, 2a and 2b we obtain

$$\langle \epsilon' l' m'; R | \epsilon l m; R \rangle = \delta(\epsilon' - \epsilon) \delta_{l'l} \delta_{m'm} \quad (E-8)$$

One must be careful in interpreting equation (E - 8). The equality is in the sense of distributions; some of the information is missing at $\epsilon' = \epsilon$. $\langle \psi_{k'} | \psi_k \rangle$ has an isolated "non-zero" when $\epsilon' = \epsilon$, $l' \neq l$ and $m' = m$ which gives no contribution to the distribution of $\langle \psi_{k'} | \psi_k \rangle$ as a function of ϵ' or ϵ .

